

**Scientific Basis for a
Safety Case of Deep
Geological Repositories**

Scientific Basis for a Safety Case of Deep Geological Repositories

Ulrich Noseck
Dirk-Alexander Becker
Thomas Brassler
Christine Fahrenholz
Judith Flügge
Horst-Jürgen Herbert
Alice Ionescu
Klaus-Peter Kröhn
Herbert Kull
Artur Meleshyn
Jörg Mönig
Klaus Röhlig
André Rübel
Tilmann Rothfuchs
Jens Wolf

November 2012

Acknowledgement:

This report was prepared under contract No. 02 E 10548 with the Federal Ministry of Economics and Technology (BMWi).

The work was conducted by the Gesellschaft für Anlagen- und Reaktorsicherheit (GRS) mbH.

The authors are responsible for the content of the report.

Keywords:

Biosphere, Indicator, Natural Analogue, Radioactive Waste, Radionuclide Transport, Safety Assessment, Safety Case

Zusammenfassung

Die in diesem Projekt durchgeführten Arbeiten haben zu verschiedenen Aspekten eines Safety Case einen Beitrag geleistet; speziell zu den Nachweisgrundlagen (Prozessverständnis), zu den Methoden und Strategien zur Entwicklung eines Safety Case, zur Langzeitsicherheitsanalyse und zu zusätzlichen Nachweisen, Analysen und Argumenten, die in einem Safety Case verwendet werden. Laufende nationale und internationale Entwicklungen wurden verfolgt und diskutiert. FuE-Projekte mit Relevanz für die Langzeitsicherheit von Endlagern für radioaktive Abfälle wurden analysiert und bewertet um das Prozessverständnis zu erhöhen. Sofern möglich, wurden neue konzeptuelle Modelle und/oder Parametersätze für die Langzeitsicherheitsanalyse vorgeschlagen.

Die Entwicklungen in anderen Ländern und auf internationaler Ebene wurden verfolgt durch Teilnahme an internationalen Komitees und Arbeitsgruppen speziell der OECD-NEA, wie dem Radioactive Waste Management Committee (RWMC), der Integration Group for the Safety Case (IGSC), dem Clay-Club und dem Salt Club. Die wichtigsten Arbeitsaspekte, Ergebnisse, Strategien und Veröffentlichungen, die in diesen Gruppen in den letzten Jahren erarbeitet wurden, werden in diesem Bericht herausgestellt. Hier sind insbesondere die Statusberichte "State of the art report on methods in safety assessment (MeSA project)", "Indicators in the Safety Case", und das "Guideline document for the development and application of thermodynamic sorption models for safety assessment purposes" zu nennen. Außerdem wurde im Jahr 2012 von der IGSC der Salt Club ins Leben gerufen und die Arbeitsstruktur, sowie Themen und Dauer der ersten Phase festgelegt. Ähnlich wie beim Clay Club ist es Ziel des Salt Clubs, den Informationsaustausch zu fördern sowie unter den Teilnehmern gemeinsame Ansätze und Methoden zu entwickeln, um das Verständnis von Salz als Wirtsf ormation für ein Endlager für wärmeentwickelnde radioaktive Abfälle weiter zu erhöhen.

Eine wichtige internationale Kooperation, die durch dieses Projekt stark gefördert wurde, betrifft die Langzeitsicherheitsanalyse (LZSA). Die IGSC organisierte ein Projekt zur Untersuchung und Dokumentation von Methoden für Langzeitsicherheitsanalysen von geologischen Endlagern für radioaktive Abfälle (MeSA, 2008 – 2011). Ziel des MeSA Projekts war es, Entwicklungen auf dem Gebiet der Langzeitsicherheitsanalyse seit 1991, dem Zeitpunkt des letzten Reviews durch die Performance Assessment Advisory Group (PAAG), zu prüfen, bewerten und zusammenzufassen. Der Bericht zum MeSA-Projekt präsentiert eine umfassende, aktuelle Zusammenfassung zu Methoden

der LZSA, unterstreicht den hohen Grad an internationalem Konsens zu LZSA-Methoden und gibt einen Überblick über die wichtigsten Aspekte und Verwendungszwecke der LZSA. Es unterstreicht im Detail die essentielle Rolle der Sicherheitsanalyse im Safety Case. Aus dem umfangreichen Review resultieren zahlreiche Empfehlungen für zukünftige Arbeiten, wie Überarbeitung der Safety Case Broschüre der NEA, Update und Erweiterung der NEA-FEP-Datenbank, ein gemeinsames Projekt zum Austausch von Informationen und Methoden zur Szenarientwicklung und Erstellung eines Statusberichts zu Sicherheitsindikatoren.

Die letzte Empfehlung wurde bereits während der letzten zwei Jahre unter Federführung der GRS umgesetzt. Das MeSA-Projekt hatte aufgezeigt, dass es während der letzten Jahre wichtige Entwicklungen in der Anwendung von Indikatoren im Safety Case für geologische Endlager gegeben hat. Auf der Grundlage einer Umfrage bei den Mitglieds-Organisationen der IGSC und von nationalen und internationalen Projekten zur Entwicklung und Anwendung von Indikatoren wurde ein NEA-Statusbericht zur Verwendung von Indikatoren im Safety Case erstellt. Eine wichtige Beobachtung ist, dass komplementäre Indikatoren mittlerweile bei der Mehrheit der Verfahrens-Betreiber und Regulierer als eine wichtige Komponente des Safety Case akzeptiert sind. Der Bericht zeigt auch deutlich die vielfältige Anwendung von Indikatoren in einem Safety Case, wie zur Strukturierung des Safety Case, für unterstützende Beweisführungen, zur Erhöhung der Transparenz eines Safety Case, zur Beurteilung der Endlagersicherheit und Konsequenzen unter Heranziehung von Belastungen der natürlichen Umgebung, zur Berücksichtigung unterschiedlicher Zeiträume, zu Ungewissheiten in Dosis und Risiko, zur Untersuchung des Verhaltens von Teilsystemen, zur Beurteilung von Sicherheitsfunktionen, zur Ableitung von Szenarien sowie zur Unterstützung in der Kommunikation des Safety Case. Der Bericht gibt auch Anleitungen zur Verwendung von Indikatoren, speziell für Länder in einem frühen Stadium des Endlagerprogramms.

In einer zweiten Studie zum Thema Indikatoren wurden anhand von Rechnungen für Endlager für wärmeentwickelnde Abfälle in Salz- und in Tonformationen Anwendbarkeit und Nutzen eines Satzes von sechs Indikatoren überprüft, die speziell im Hinblick auf die Sicherheitsfunktion Einschluss relevant sind. Die Studie zeigte für einige Indikatoren deutliche Unterschiede zwischen Salz- und Tonformationen. Speziell Indikatoren, die sich auf Actiniden beziehen, liefern unterschiedliche Werte, da Actiniden aufgrund ihrer starken Sorption an Bentonit und der Tonformation innerhalb einer Millionen Jahre nicht aus dem einschlusswirksamen Gebirgsbereich freigesetzt werden. Bei einem Endlager im Salz werden im Fall eines durchgängigen Transportpfads von den Abfällen

bis zum Rand des einschlusswirksamen Gebirgsbereichs diese Radionuklide freigesetzt, da keine Sorption im Nahbereich des Endlagers und der Salzformation betrachtet wird. Als Fazit wird besonders die Anwendung des Indikators *Radiotoxizität der aus dem einschlusswirksamen Gebirgsbereich freigesetzten Radionuklide* empfohlen. Dieser Indikator entspricht auch dem RGI, der in der Vorläufigen Sicherheitsanalyse Gorleben (VSG) entwickelt wurde. Zudem wird der *Beitrag zur Leistungsdichte aufgrund radioaktiver Strahlung im Porenwasser der Randzone des einschlusswirksamen Gebirgsbereichs* als geeignet angesehen. Der Indikator *Rückhaltung von Schadstoffen im Endlager* wird nur dann als sinnvoll erachtet, wenn er nuklidspezifisch und nicht, wie vorgeschlagen, auf die Gesamtmenge der Radionuklide bezogen wird. Außerdem wäre eine kumulative Darstellung des Indikators interessant. Die Anwendung der Indikatoren *Veränderung der Konzentration der Elemente Uran und Thorium in der Randzone des einschlusswirksamen Gebirgsbereichs* und *Veränderung der Aktivitätskonzentration von Radionukliden im oberflächennahen Grundwasser* wird nicht empfohlen.

Es wurde eine Literaturstudie durchgeführt, um die Relevanz mikrobieller Aktivität für das Langzeitverhalten eines tiefen geologischen Endlagers für wärmeentwickelnde radioaktive Abfälle in Tonstein qualitativ zu bewerten und zu identifizieren, welche sicherheitsrelevanten Prozesse und Eigenschaften durch diese Aktivität möglicherweise beeinflusst werden. In der Analyse wurden acht Eigenschaften ermittelt, die für die Erhaltung der Sicherheitsfunktionen Einschluss und Retardation essentiell sind und durch mikrobielle Prozesse beeinflusst werden können: Quelldruck, spezifische Oberfläche, Kationen- und Anionenaustauschkapazität, Porosität, Permeabilität, Fluiddruck und Plastizität. Wichtige Prozesse, die durch mikrobielle Aktivität beeinflusst werden, sind Reduktion und Auflösung von Tonmineralen, Biofilm-Bildung, Sulfatreduktion und Gasbildung. Diese Studie bildet die Grundlage für die quantitative Ermittlung der durch mikrobielle Prozesse maximal möglichen Effekte auf das Barrierensystem eines Endlagers in einer Tonformation, die in einem zukünftigen Projekt betrachtet werden soll.

Ein weiteres Arbeitspaket hatte die Inventare von Radionukliden und stabilen Elementen in verglasten radioaktiven Abfällen (CSD-V Behälter), die in La Hague produziert und nach Deutschland zurückgeliefert wurden, zum Inhalt. Diese Inventare sind wichtige Eingangsparameter für LZSA. Für einen Teil der Radionuklide und stabilen Elemente stand ein Datensatz von AREVA zur Verfügung, der durch direkte Messung oder durch bekannte Korrelationen zu den gemessenen Radionukliden gewonnen wurde. Dies erlaubte die Verifikation eines Modellansatzes, der auf Daten aus Abbrand- und Aktivierungsrechnungen und Informationen aus dem Wiederaufarbeitungs- und Vergla-

sungsprozess zurückgreift. Nachdem die Anwendbarkeit des Ansatzes geprüft wurde, wurden erfolgreich Mittelwerte, sowie Minimum-, und Maximalwerte für Radionuklidinventare, die langzeitsicherheitsrelevant sind, aber nicht von AREVA angegeben wurden, abgeschätzt. Ein Vergleich mit Inventaren, die von NAGRA für aus La Hague in die Schweiz zurückgelieferte verglaste Abfälle angegeben wurden, zeigt Unterschiede, deren Ursache in einem gemeinsamen Projekt untersucht werden sollte.

Zum Prozess der Bentonit-Wiederaufsättigung wurde der Anwendungsbereich des Strömungsmodells VIPER auf Bentonit-Sand-Mischungen und nicht-isotherme Systeme erweitert. Beide Anwendungen wurden im Rahmen von Benchmark-Experimenten der EBS-Task Force erfolgreich überprüft. Die Anwendung auf Bentonit-Sand-Gemische führte zu einer signifikanten Verbesserung des Rechenprogramms, bei der ein diffusiver Transportprozess des Zwischenschichtwassers implementiert wurde. Der zugehörige Diffusionskoeffizient hängt vom Wassergehalt ab und steigt mit der Menge der Hydratschichten an den Zwischenschichtkationen. Die im Code VIPER verwendete Bilanzgleichung wurde entsprechend einem Doppelkontinuum-Modell erweitert. Das Modell ist in der Lage, die komplexen Wechselwirkungen bei der nicht-isothermen Aufsättigung von Bentonit zu beschreiben. Außerdem wurde ein Laborexperiment begonnen, um den Endzustand bei der nichtisothermen Aufsättigung zu charakterisieren, da die Diskussionen in der EBS-Task Force gezeigt haben, dass es keinen schlüssigen experimentellen Befund zum stationären Zustand am Ende einer nicht-isothermen Aufsättigung gibt. Das Experiment läuft bereits über mehr als zwei Jahre, aber die bisherige Auswertung deutet darauf hin, dass der Endzustand frühestens nach drei Jahren erreicht wird. Daher wird das Experiment weitergeführt.

Als weiterer Themenbereich wurde auch der Einfluss von Klimaänderungen auf Geosphären- und Biosphärenprozesse eines Endlagersystems untersucht. Im vorangegangenen Vorhaben WiGru-5 wurde der Einfluss diskreter Klimazustände studiert. In der jetzigen Arbeit lag der Schwerpunkt auf Klimaübergängen. Für die Geosphäre wurde der Einfluss durch Klimaveränderungen bedingter transienter Fließbedingungen auf den Radionuklidtransport im Fernfeld eines Endlagers zum ersten Mal untersucht. Zeitliche Wechsel von Glazialen und Interglazialen, deren Ausdehnung und Zeitpunkte ihres Auftretens aus schwedischen und finnischen Studien abgeleitet wurden, dienten als Basis für die hier betrachteten zukünftigen Klimaabfolgen. Die Ergebnisse der Strömungsrechnungen für die ausgewählte Klimaabfolge zeigen, dass Strömungsfeld und Salzgehalte zum Endzeitpunkt der Rechnungen nach 251 500 Jahren gut mit denen übereinstimmen, die für ein konstantes Klima berechnet wurden. Das bedeutet, dass

das hydraulische System schnell auf die veränderten Randbedingungen der verschiedenen Klimazustände eines glazialen Zyklus reagiert. Demgegenüber zeigen die Radionuklidtransportrechnungen aber deutliche Unterschiede zwischen transientem und konstantem Strömungsfeld, da der Transport durch die verschiedenen Fließcharakteristika während der einzelnen Klimazustände geprägt wird. Die größten Unterschiede wurde für schwach sorbierende Radionuklide, wie C-14 und I-129 beobachtet, und die geringsten für stark sorbierende Radionuklide wie Zr-93. Generell zeigen die Rechnungen, dass der Einfluss von Klimaübergängen auf Strömung und Radionuklidtransport im Deckgebirge eines Endlagerwirtsgesteins groß sein kann und durch transiente Modellrechnungen in Langzeitsicherheitsanalysen berücksichtigt werden sollte.

Die Auswirkung zukünftiger Klimaänderungen auf Biosphärenmodelle wurde anhand generischer, stilisierter Modelle untersucht. Neun diskrete Klimazustände wurden ausgewählt, um die Vielfalt möglicher Klimazustände, die in den nächsten Millionen Jahren in Norddeutschland auftreten können, abzubilden. Die Bandbreite der Dosiskonversionsfaktoren aus den Rechnungen für die neun diskreten Klimazustände liegt in einer ähnlichen Größenordnung, wie diejenige, die aus Unsicherheitsanalysen basierend auf den generellen Ungewissheiten in Parametern des Biosphärenmodells erhalten wurde. Allerdings sind die hier durchgeführten Unsicherheitsanalysen als eine erste Abschätzung zu betrachten. Weitere Arbeiten zur Ermittlung von Wahrscheinlichkeitsdichteverteilungen für die Parameter und speziell ein Ansatz für die Behandlung von Korrelationen zwischen den Parametern sind notwendig. Die Modelle erlaubten auch Übergänge zwischen Klimazuständen, die speziell im Hinblick auf redox-sensitive Radionuklide von Bedeutung sind, zu berechnen. Die Ergebnisse deuten darauf hin, dass Prozesse, die bei Klimaübergängen auftreten, höhere Strahlenexpositionen bewirken können im Vergleich zu diskreten Klimazuständen. Allerdings werden dabei hohe Anreicherungen redox-sensitiver Radionuklide in Pflanzen (bedingt durch Konzentrationsspitzen in Böden) nicht direkt im Biosphären-Dosiskonversionsfaktor abgebildet, da für viele Radionuklide auch andere Expositionspfade beitragen, die nicht mit der Aufnahme aus dem Boden korrelieren, und damit den Effekt abschwächen.

Der Standort Ruprechtov in der Tschechischen Republik (nahe Karlovy Vary) wurde seit Mitte der neunziger Jahre als natürliches Analogon untersucht. Im südlichen Teil des Untersuchungsgebiets wurde der obertägige Kaolinabbau im Jahr 2006 begonnen. Da die Ton-/Lignitschichten, in denen die als Analogon untersuchten Urananreicherungen auftreten, sich direkt über dem abbauhöffigen Kaolin befinden, erlaubte der Abbau, mit wenigen zusätzlichen Untersuchungen spezielle Fragestellungen zum Analogon zu

beantworten. Ein wichtiges Ergebnis dieser Arbeiten ist, dass alle geologischen Befunde, die während des Kaolinabbaus am Standort Ruprechtov detektiert, analysiert und dokumentiert wurden, sehr gut mit den Modellannahmen übereinstimmen, die aus Bohrlochuntersuchungen in den vorangegangenen Projektphasen entwickelt wurden. Es wurden keine Fakten gefunden, die den Modellannahmen widersprechen. Zusätzlich wurde auch der Einfluss des Kaolinabbaus auf die Urananreicherungen in den Ton-/Lignitschichten untersucht. In Bohrlöchern in direkter Umgebung des Abbaubereiches konnte ein deutlicher Einfluss der Abbauaktivitäten auf den Grundwasserspiegel beobachtet werden. Allerdings zeigten die Grundwasseranalysen einschließlich von in-situ Eh/pH, Elementkonzentrationen und Isotopensignaturen, dass das System geochemisch sehr gut gepuffert ist und kein Oxidationseffekt nachzuweisen ist. Um trotzdem die Auswirkungen einer Oxidation auf die Ton/Lignitschichten zu analysieren, wurde entsprechendes Material mit hohem Urangehalt, das durch den Abbau freigelegt wurde, untersucht. Element- und mineralogische Analysen, Ungleichgewichtszustände in der Uranzerfallsreihe sowie sequentielle Extraktionsuntersuchungen zeigten, dass die Schichten bis in eine Tiefe von 20 cm beeinflusst waren, Pyrite und auch ein Teil des Urans oxidiert war. Zusätzlich zeigte die Untersuchung mit Lysimetern, dass dies zu relativ hohen Urankonzentrationen im Oberflächenwasser führen kann. Anhand der Untersuchungen wurde auch die Stärke der Ungleichgewichtsuntersuchungen der Uranzerfallsreihe, die an der Universität Helsinki während des Projekts weiterentwickelt wurde, bei der Ermittlung von unterschiedlichen Uranphasen und geochemischen Veränderungen in natürlichen Systemen demonstriert.

In einer Vorstudie zu Realisierungsmöglichkeiten für ein virtuelles Untergrundlabor wurden von GRS und Projektpartnern die verschiedenen Anforderungen untersucht. Unter anderem wurde der Import geologischer Daten über die Software openGEO und Daten zur Auslegung des Untertagelabors über CAD Software erfolgreich getestet. Zusätzlich wurden Möglichkeiten zur Visualisierung geologischer Strukturen und von Ergebnissen numerischer Simulationen untersucht. Die dazu verwendeten Daten wurden mit Hilfe von Rechenprogrammen auf Prozessebene auf Basis einfacher Temperaturberechnungen generiert. Fazit dieser Arbeiten war, dass die Ziele der VIRTUS Software Plattform in einem dreijährigen Projekt realisiert werden können.

Preface

The assessment of the long-term safety of a repository for radioactive or hazardous waste and therewith the development of a safety case requires a comprehensive system understanding, a continuous development of the methods of a safety case and capable and qualified numerical tools. The objective of the project “Scientific basis for the assessment of the long-term safety of repositories”, identification number 02 E 10548, was to follow national and international developments in this area, to evaluate research projects, which contribute to knowledge, model approaches and data, and to perform specific investigations to improve the methodologies of the safety case and the long-term safety assessment.

This project, founded by the German Federal Ministry of Economics and Technology (BMWi), was performed in the period from 1st August 2008 to 31st July 2012. The results of the key topics investigated within the project are published in the following reports:

- GRS-264: Grundsatzfragen Hydrogeologie – Workshop der GRS in Zusammenarbeit mit dem PTKA-WTE
- GRS-269: Code Viper: Theory and Current Status
- GRS-291: Microbial Processes Relevant for the Long-Term Performance of Radioactive Waste Repositories in Clays
- GRS- 294: Radionuclide Inventory of Vitrified Waste from Nuclear Fuel Reprocessing: Basic Issues and Current Status in Germany
- GRS- 299: Impact of Different Climates and Climate Transitions on Biosphere Modelling in Long-Term Safety Assessment

The results of the whole project are summarised in the overall final report:

GRS-report 298: Scientific Basis for a Safety Case of Deep Geological Repositories

List of contents

1	Introduction.....	1
2	Safety case and safety assessment	5
2.1	Methods in safety assessment.....	5
2.1.1	Project organisation and working method	6
2.1.2	Project results, conclusions, and recommendations.....	10
2.1.2.1	Safety assessment in the context of the safety case	10
2.1.2.2	Safety assessment and safety case flowcharts	12
2.1.2.3	System description and scenarios	15
2.1.2.4	Modelling strategy.....	21
2.1.2.5	Indicators for safety assessment.....	23
2.1.2.6	Treatment of uncertainties	26
2.1.2.7	Regulatory issues	31
2.1.3	Overall conclusions.....	33
2.1.4	Recommendations and ongoing work.....	34
2.1.5	The project's documentation.....	36
2.1.6	German contributions to MeSA	37
2.2	Current activities on indicators	37
2.3	Applicability of indicators.....	44
2.3.1	Repository in a clay formation.....	49
2.3.1.1	Description of the repository system	49
2.3.1.2	Calculation of indicators.....	57
2.3.2	Repository in a salt formation.....	63
2.3.2.1	Description of the repository system	63
2.3.2.2	Calculation of indicators.....	69
2.3.3	Conclusions	76
2.3.3.1	General conclusions	76

2.3.3.2	Assessment of indicators	78
3	International developments	81
3.1	RWMC.....	81
3.1.1	Recent International Developments	81
3.1.2	Programme of Work (PoW).....	81
3.1.3	Research and Development	82
3.1.3.1	Integration Group for the Safety Case (IGSC).....	82
3.1.3.2	Forum on Stakeholder Confidence (FSC)	83
3.1.3.3	Working Party on Management of Materials from Decommissioning and Dismantling (WPDD).....	83
3.1.3.4	Regulator's Forum (RWMC-RF).....	84
3.1.3.5	R&R Working Group	85
3.1.3.6	RK&M-Project.....	85
3.1.4	Country Trend Analysis.....	86
3.2	IGSC.....	86
3.2.1	Scientific basis.....	86
3.2.1.1	Relevance of gases for the safety case	88
3.2.2	Safety assessment strategy and tools.....	91
3.2.3	Design and implementation	92
3.2.4	Integration and management	93
3.3	NEA Sorption project	94
3.4	Clay-Club.....	98
3.5	Salt-Club.....	102
3.5.1	Foundation of the Salt Club	102
3.5.2	Starting situation.....	104
3.5.3	Proposed activities mission and objectives of the Salt Club:	105
3.5.4	Organizational structure and mode of operation and cooperation	105

3.5.5	The starting work programme	107
3.6	Implementing Geological Disposal-Technology Platform (IGD-TP)	107
4	Selected topics	113
4.1	Microbial Processes Relevant for the Long-Term Performance of Radioactive Waste Repositories in Clays.....	113
4.2	Basic issues for radionuclide inventory of vitrified waste	122
4.3	Repository sealing and closure	129
4.3.1	THERESA.....	129
4.3.2	Workshop Sealing Systems in a Repository for HLW.....	132
4.3.2.1	Workshop Results.....	133
4.3.3	Self-healing backfill.....	135
4.3.3.4	Laboratory experiments and results	137
4.3.3.5	Technical requirements for the construction of seals with SVV	142
4.3.3.6	In-situ-experiments and results	143
4.3.3.7	Long term behavior of SVV seals.....	150
4.3.3.8	Summary and Conclusion.....	152
4.4	New aspects of bentonite re-saturation – Task Force on EBS	153
4.4.1	Bentonite-sand mixtures	153
4.5	Workshop “Grundsatzfragen Hydrogeologie”	166
4.6	Impact of climatic conditions on geosphere modelling	169
4.6.1	Objectives and approach	169
4.6.2	Assessment of long-term climate changes in Sweden and Finland.....	170
4.6.2.1	Investigations of SKB (Sweden) and POSIVA Oy (Finland)	171
4.6.2.2	Summary and results.....	177
4.6.3	Derivation of possible climate changes in Northern Germany	179
4.6.3.1	Model structure.....	182
4.6.3.2	Parameterization.....	186

4.6.3.3	Results	192
4.6.4	Summary	208
4.7	Impact of climate conditions on biosphere modelling	209
4.8	Natural Analogue study Ruprechtov site	220
4.8.1	Impact of mining-related disturbances on the uranium enrichment	220
4.8.2	Verification of the conceptual model	230
4.8.2.1	Background	230
4.8.2.2	Occasion of open-pit mining	231
4.8.2.3	Exemplary geological features of open pit's exposures.....	233
4.8.2.4	Conclusion.....	236
4.8.2.5	Winning of air-influenced soil water	237
4.9	Initiation of the Project VIRTUS (Virtual Underground Research Laboratory in Salt)	240
4.9.1	Preliminary assessment of the chances for a successful realisation of the project objectives	242
4.9.2	Summary and appraisal of the preliminary study	245
5	Summary	247
	References	253
	List of figures.....	271
	List of tables	279

1 Introduction

Within this project strategies and methods to build a safety case for deep geological repositories are further developed. This includes also the scientific fundamentals as a basis of the safety case. In the international framework the methodology of the Safety Case is frequently applied and continuously improved. According to definitions from IAEA and NEA the Safety Case is a compilation of arguments and facts, which describe, quantify and support the safety and the degree of confidence in the safety of the geological repository. The safety of the geological repository should be demonstrated by the safety case. The safety case is the basis for essential decisions during a repository programme. It comprises the results of safety assessments in combination with additional information like multiple lines of evidence and a discussion of robustness and quality of the repository, its design and the quality of all safety assessments including the basic assumptions.

A crucial element of the Safety Case is the long-term safety analysis, i. e. the systematic analysis of the hazards connected with the facility and the capability of site and repository design to ensure the required safety functions and to fulfill the technical claims. Long-term safety analysis requires a powerful and qualified programme package, which contains appropriate hardware and software as well as well trained and experienced modellers performing the model calculations. The calculation tools used within safety cases need to be checked and verified and continuously adapted to the state-of-the-art science and technology. Especially it needs to be applicable to a real repository system. For the assessment of safety a deep process understanding is necessary.

The R&D work performed within this project will contribute to the improvement of process and system understanding as well as to the further development of methods and strategies applied in the safety case. Emphasis was put on the following aspects:

- The current state-of-the-art in long-term safety assessment has been evaluated within a sub project of the Integration Group for the safety case (IGSC) of OECD/NEA. GRS has strongly contributed to this project called Methods for Safety Assessments (MeSA), by leading working groups and with contributions to selected chapters of the NEA state-of-the-art report.
- As an outcome of the MeSA project it was decided to compile the status in the OECD member countries on the use of indicators complementary to dose and risk

in the safety case. GRS played a leading role in drafting and finalizing a state-of-the-art report on indicators. Further the applicability of a specific set of indicators previously proposed in Germany was tested and evaluated for repositories in clay and rock salt formations.

- GRS is involved in several international working groups to follow the state-of-the-art at the international level as well as to introduce results from German R&D into the international discussion. Important working groups are the Radioactive Waste Management Committee (RWMC) of OECD/NEA with the Integration Group for the Safety Case, its subgroups Clay Club and Salt Club and correlated projects like the NEA sorption project.
- The current literature dealing with the role of microbial processes related to repositories in clay formations has been compiled. The potential negative and positive impact of microbes on the long-term integrity of the repository system in clay has been qualitatively evaluated.
- Radionuclide inventories of CSD-V containers received from reprocessing in LA Hague have been evaluated and an updated data set for long-term safety assessment is proposed.
- The non-isothermal re-saturation of bentonite is investigated by specific laboratory experiments accompanied by modelling with the code VIPER. In addition the model was applied to lab and field experiments provided by the EBS task force and all results have been discussed in this international working group.
- The project on self-sealing backfill (SVV) ended in February 2010. However, further long-term observation work at Teutschenthal mine, where the material has been injected and tested in-situ, was performed within the project presented here.
- National workshops have been performed to discuss and document the state-of-the-art of topics relevant for the safety case. Within this project a workshop on fundamental questions on the hydrogeology in sedimentary systems in Northern Germany and a workshop on sealing systems in a repository for HLW were performed.
- The impact of future changes in climate on flow and transport in the geosphere as well on the exposure in the biosphere was further investigated with emphasis on the role of transitions between different discrete climate states.
- With respect to natural analogues some final work has been performed at the analogue site in Ruprechtov, Czech Republic. The kaolin excavation at the site allowed

checking on a larger scale the assumptions for the geological structure used in the conceptual model and the impact of disturbances on the uranium enrichment.

2 Safety case and safety assessment

The methods and strategies used to build a safety case for radioactive waste repositories are continuously further developed on the national and international level. The major projects and developments, where GRS was involved are described in the following.

2.1 Methods in safety assessment

In 1991, the Performance Assessment Advisory Group (PAAG, one of the predecessors of OECD/NEA's Integration Group for the Safety Case IGSC) issued a brochure called "Review of Safety Assessment Methods" /NEA 91/.

"The report has three principal objectives:

- to present a concise, clear, and up-to-date summary of performance assessment method;
- to underline the degree of international consensus on performance assessment activities and methods; and
- to provide an overview of the most important aspects and uses of performance assessment to a non-specialised audience."

Since then, considerable evolution in the field of performance and safety assessment (the distinction between the two terms is not always clear and they are sometimes used interchangeably) took place:

- The concept of the safety case for the demonstration of (long-term) safety of deep disposal facilities was developed /NEA 99/, /NEA 04a/ and found its way into international standards /IAE 04/. National and international regulations have evolved accordingly.
- Numerous safety reports on geological radioactive waste repositories were submitted in the frame of national programmes in order to support decisions within these programmes. These reports, which are often not termed "safety cases" but nevertheless follow the ideas of the safety case concept, contain a variety of safety assessments with much common grounds, but also differences, and new methodological developments.

- Several of these reports underwent national or international peer reviews.
- A considerable number of international projects and activities devoted to the further development of several aspects of methodologies for safety assessments has been carried out /EC 97/, /BAU 00/, /BEX 03/, /EC 09/, /NEA 97/, /NEA 99/, /NEA 04a/, /NEA 08a/, /NEA 09/, /IAE 00/, /IAE 06/.

In light of these substantial developments of the past 20 years, IGSC organised a project examining and documenting Methods for Safety Assessment for long-term safety of geological repositories for disposal of radioactive waste (MeSA, 2008 – 2011). The goals of the MeSA project were to review and summarise developments since 1991 regarding safety assessment methods in order to:

- describe the state-of-the-art,
- discuss the variety of methods and overall approaches, and
- confirm or establish a joint view about what are considered the necessary elements and agreed methods of modern Safety Assessments.

The project was carried out with considerable contribution from several German organisations.

2.1.1 Project organisation and working method

More than 20 individuals from 21 waste management, research, regulatory, and technical support organisations in 11 countries (Tab. 2.1) reviewed the state-of-the-art and identified common grounds and differences of safety assessments undertaken in different countries. The project participants represent all host rocks presently considered for geological disposal, various stages of programme progress, and a variety of regulatory backgrounds. Many programmes with recently submitted, reviewed, or planned safety reports were represented. The factual basis of the project includes these and other safety reports as well as their national and international reviews, national regulations and IAEA safety standards, and the outcomes of various international projects (in particular the NEA INTESC initiative /NEA 09/ and the EU FP 7 project PAMINA /EC 09/).

Tab. 2.1 Countries and organisations represented in MeSA

Country	Organisation	Role
Belgium	Agence fédérale de Contrôle nucléaire / Federaal Agentschap voor Nucleaire Controle (AFCN / FANC)	Regulator
	Organisme National des déchets radioactifs et des matières fissiles enrichies / National instelling voor radioactief afval en verrijkte splijtstoffen (ONDRAF / NIRAS)	Waste management
	Studiecentrum voor Kernenergie / Centre d'Étude de L'Énergie Nucléaire (SCK / CEN)	Research
Canada	Nuclear Waste Management Organisation (NWMO)	Waste management
Czech Republic	Ústav jaderného výzkumu Řež a. s. / Nuclear Research Institute Rez (UJV / NRI)	Technical support organisation / research
Finland	Saario & Riekkola Oy (SRO)	Consultant on behalf of Waste management organisation POSIVA
France	Agence Nationale pour la Gestion des Déchets Radioactifs (ANDRA)	Waste management
Germany	Bundesamt für Strahlenschutz (BfS)	Waste management
	Bundesanstalt für Geowissenschaften und Rohstoffe (BGR)	Research
	Clausthal University of Technology (TUC)	Academia
	Gesellschaft für Anlagen- und Reaktorsicherheit (GRS) mbH	Technical support organisation / research
Japan	Japan Atomic Energy Agency (JAEA)	Waste management
Sweden	Svensk Kärnbränslehantering AB / Swedish Nuclear Fuel and Waste Management Co. (SKB)	Waste management
	Streamflow AB	Consultant
Switzerland	Nationale Genossenschaft für die Lagerung radioaktiver Abfälle (Nagra)	Waste management
	Safety Assessment Management (Switzerland) GmbH (SAM)	Consultant
United Kingdom	Environment Agency	Regulator
	Nuclear Decommissioning Authority (NDA)	Waste management
United States	Sandia National Laboratories (SNL)	Research
	Southwest Research Institute	Research
	U.S. Department of Energy (DoE)	Waste management

The project was carried out in working groups responsible for the following areas:

1. Safety assessment in the context of the safety case
2. Safety assessment and safety case flowcharts
3. System description and scenarios
4. Modelling strategy
5. Indicators for safety assessment
6. Treatment of uncertainties
7. Regulatory issues

These groups exchanged their views and working results via email, phone, and, if necessary, at group meetings. Two of the groups (groups 3 and 5) carried out extensive survey work in their field by means of questionnaires which were answered by MeSA participants.

The whole MeSA project group conducted four workshops:

1. Toulon, France, October 2008:

The project was initiated and its objectives were agreed upon. It was decided that the project had to be carried out in two phases:

A first retrospective phase had to focus on review work with focus on the questions:

- Taking the 1991 brochure as a starting point, what are the most significant and important methodological advances since then?
- What are the implications of the evolving safety case concept on safety assessment methodologies?
- Which issues and challenges depicted in the 1991 brochure are still relevant? Which are obsolete or have been resolved? What new issues have become evident?

A second phase should then aim at achieving consensus on main points and provide further input to an updated brochure on state-of-the-art for safety assessment methods. This brochure should also recommend best practices and recommended elements and procedures for safety assessment.

The workshop was held shortly after the date and close to the venue of the annual meeting of the EU FP 7 project PAMINA which ensured attendance of many PAMINA participants and a strong linkage to this project.

The MeSA working method was defined, responsibilities were assigned and deadlines were agreed upon.

2. Issy-les-Moulineaux, France, May 2009

First working group results (in a number of cases already in the form of reports) were discussed. Cross-cutting issues and linkages between the groups' topics were identified and ways to address them were defined. Advice for the working groups was derived. Preliminary conclusions concerning the topics of the first MeSA Phase were drawn and issues for the second phase were identified.

3. Hohenkammer, Germany, September/October 2009

With the workshop the first MeSA phase was finalised. Reports produced by each working group (so-called "issue papers") were presented and discussed. Advice concerning their further improvements and the handling of linkages and cross-cutting issues was given. A proposal for the second MeSA phase was developed and later approved in November by the IGSC annual session.

Again, the workshop was held shortly after the date and at the venue of the annual meeting of the EU FP 7 project PAMINA.

4. Issy-les-Moulineaux, France, May 2010

This final workshop was open not only to MeSA project participants, but to representatives of all IGSC member organisations. The MeSA "issue papers" were discussed and advice concerning their finalisation and the production of a project synthesis was given. Project conclusions on joint views and differences in methods were derived. In particular, it was concluded that the areas of consensus are sufficiently large to derive a document replacing the 1991 brochure /NEA 91/. This document should consist of the aforementioned synthesis and the seven "issue papers". Recommendations concerning further IGSC work were derived.

In summer 2010, the MeSA synthesis was produced and iterated amongst the project participants. The "issue papers" were finalised and the consistency of the full set of documents was ensured. The project results were then presented to the IGSC annual session which decided on a review by the full IGSC (finalised early in 2011) and publication. The project's recommendations on future work were carried forward to the discussion of IGSC's programme of work.

2.1.2 Project results, conclusions, and recommendations

MeSA reached the conclusion that considerable evolution and advances took place since 1991. Areas with consensus or joint views are sufficiently large to develop a document describing joint views as well as areas in which assessment methodologies vary. This document will consist of a synthesis and a series of reports reflecting the working areas of the project and is meant to replace the 1991 brochure /NEA 91/. In the following, main project conclusions are compiled. For consistency reasons, the language used in the following chapters 3.1 – 3.7 is often the same, or follows closely, the one used in the MeSA reports without explicitly being marked as quotation.

2.1.2.1 Safety assessment in the context of the safety case

Using the definition adopted in the project, a safety assessment is a systematic analysis of the hazards associated with a geologic disposal facility, and the ability of the site and design to provide the safety functions and meet technical requirements. Safety assessment is an essential component of the safety case. From a regulatory perspective, providing the evidence to support the claims made in the safety assessment is just as important as the safety assessment calculations themselves.

Its essential role in the safety case means that aspects of safety assessment relate to numerous elements of the safety case and the dividing line between safety assessment and safety case is not sharply drawn and need not be. What is important is that, firstly, safety assessment forms a central part of the safety case; and secondly, that the results of such assessments must be placed in context and augmented by additional information (i. e., in a safety case) to support decision making.

A given safety case exists in a specific context in terms of the decision being supported and of the site and design information, of the modelling tools and data that are available at that time. Updated safety cases may need to be prepared from the earliest stages of planning at time intervals up until (and sometimes even after) a repository is closed, spanning a period of several decades up to centuries. As investigations continue, data availability increases and the models used for safety assessments are re-evaluated in terms of appropriateness in the context of new information when necessary.

As programmes are implemented it is likely that there will also be differences between what was assumed in earlier safety assessments and what has actually been built and placed in the repository. Deviations from original plans and assumptions need to be identified, evaluated, and in some cases justified. Furthermore, given the long timeframes of repository development and, thus, safety assessment iterations, care must be exercised to preserve key data and the ancillary information that establishes the quality of those data.

There is significant interaction and iteration between safety assessment and other aspects of repository development, notably site characterisation and repository design. In some cases, preliminary safety assessment results are key inputs to guide these activities. In other cases, the results of these activities are key inputs to safety assessment.

One of the most prominent examples of feedback in repository development is the information flow between safety assessment and site characterisation. Preliminary system models are typically developed and used to some extent in the site selection process. Later characterisation of the site selected will then allow refinement of the preliminary modelling to reflect actual field conditions based on the information gained: after all, this is the purpose of site characterisation.

There is also closed-loop feedback between safety assessment and engineered design and barriers of a repository system. In early stages of development, safety assessment results can be utilised in selecting between various options or conceptual designs for disposal. Safety assessment also provides important input to establishing engineered system design requirements.

Safety assessment also provides a means to integrate information and to understand the interactions between various parts of the disposal system or between different sets of requirements. Furthermore, some requirements may compete with one another or imply opposing options. While post-closure safety is a main driver in repository design, operational safety and engineering feasibility are also essential: none can be disregarded in the design of the repository. Safety assessment provides assurance that a change made to solve one problem, such as avoiding the consequences of an uncertainty through a robust design, does not introduce other, potentially more serious problems or uncertainties. Thus, it is clear that safety assessment provides key information to drive research and site characterisation programmes as well as engineering designs and testing. Conversely, these aspects of repository development produce the data

(and interpretations of that data) that support a high quality assessment upon which the quality of the safety assessment depends. Given these links and mutual dependencies, an important aspect of repository planning as well as a sound safety assessment is to ensure clear and effective information flow among the various components of repository development.

2.1.2.2 Safety assessment and safety case flowcharts

Based on a review of approaches to safety assessment followed by various national and international organisations, a generic safety case (Fig. 2.1) and safety assessment flowchart (Fig. 2.2) were developed within MeSA. By means of comparison common features and differences of these various flowcharts were shown.

The proposed higher-level generic safety case and safety assessment strategy flowchart shown in Fig. 2.1 is an illustration of what the main common elements and linkages identified in recent assessment strategies could be. Elements of a safety assessment are shown in Fig. 2.2, focussing on the steps involved in developing the safety case. Labelled arrows show the main flows of information during the course of developing a safety case.

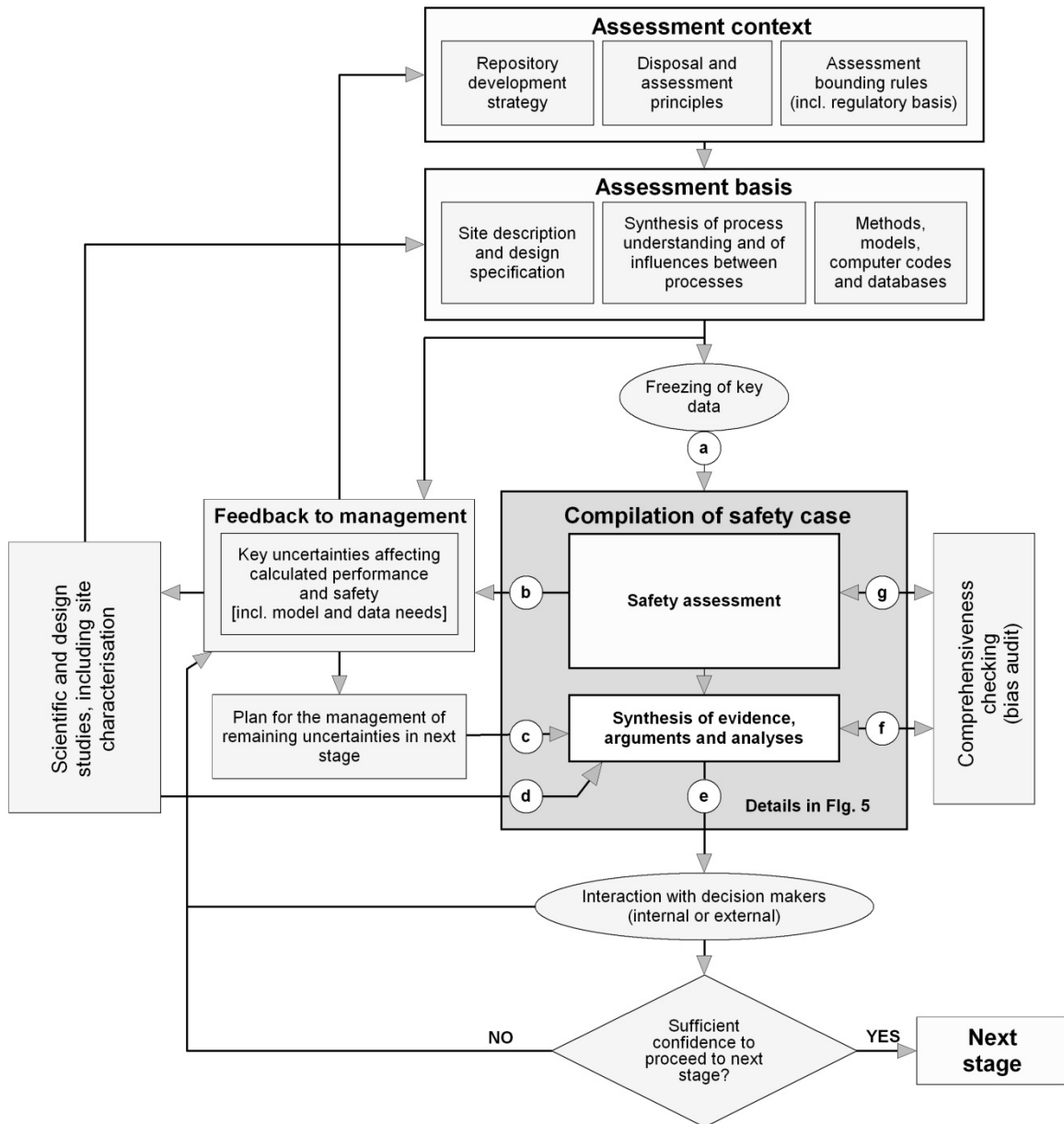


Fig. 2.1 Example of a high-level generic safety case flowchart, showing the key elements and linkages

The arrows labelled with a letter correspond to the arrows labelled with the same letter in Fig. 2.2

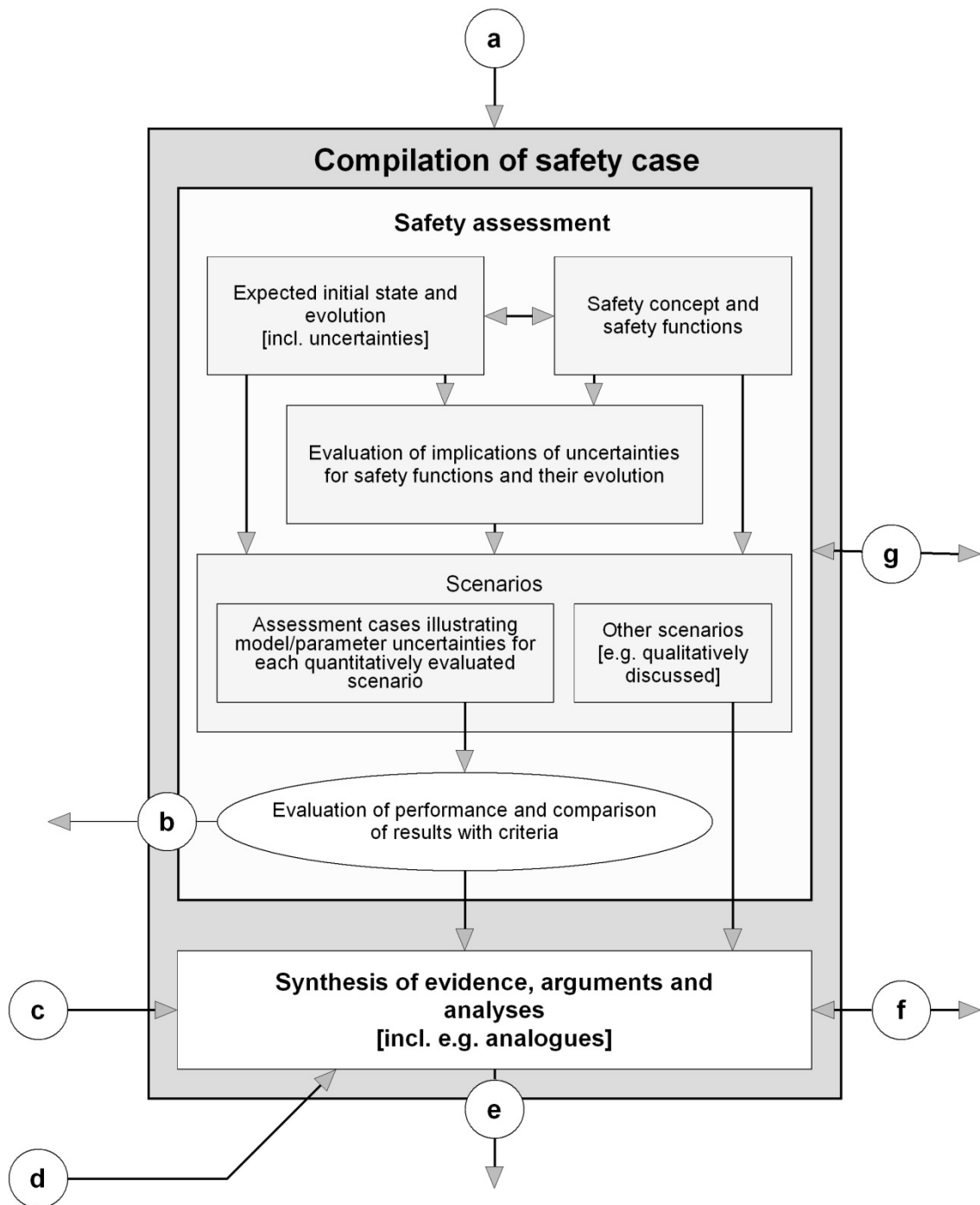


Fig. 2.2 Detailed generic flowchart of the safety assessment component which is included in the compilation of a safety case of the upper level generic flowchart

The labelled arrows correspond to the arrows labelled with the same letter in Fig. 2.1

At a higher level, key assessment activities are “freezing of key data”, comprehensiveness checking, a synthesis of evidence, arguments and analyses, and feedback to programme management. At a more detailed level, safety assessment generally starts

with the development of an integrated description of the expected initial state of the disposal system and of its evolution. The safety concept is developed by describing the roles of the natural and engineered barriers and the safety functions that these are expected to provide in different time frames. This forms the basis for evaluation of the implication of uncertainties in the fulfilment of the safety functions over time, leading to the formulation of scenarios for the evolution of the repository over time and the derivation of related assessment cases. The results of the analyses of scenarios are complemented with arguments, for example, for the quality of the site and design (low impact of detrimental phenomena) and for the validity of model assumptions and boundary conditions from the assessment basis. They are also supplemented with any available independent supporting evidence for safety to place these results into context.

2.1.2.3 System description and scenarios

Scenarios represent specific descriptions of a potential evolution of the repository system from a given initial state. They describe the compilation and arrangement of safety relevant Features, Events and Processes (FEPs) as a fundamental basis for the assessment of post-closure safety which includes assessing the potential consequences on humans and the environment. The development of scenarios for the safety case is of fundamental importance as it constitutes a key element for managing uncertainties. In most regulatory environments, a qualitatively sufficient set of scenarios rather than a “complete” one meets regulatory expectations, as long as this set is comprehensive in the sense that it illustrates or bounds the credible evolutions of the repository system. Completeness in the context of all possible scenarios can easily become an idealistic and impractical goal. To assure a practicable safety assessment expectation, regulators may impose probability cut-offs or provide qualitative guidance on the types of scenarios that need to be considered and those that can be eliminated.

Typically, scenarios are divided into central scenarios aimed at representing the expected evolution(s) of the repository, plus plausible alternative scenarios representing less likely but still plausible repository evolutions, as well as extreme events that are very unlikely. A range of possible future human actions, which may significantly impair the performance of the disposal system, can be envisaged; these are often considered as a specific scenario category. Another category of scenarios, often called “What if” scenarios, can also be considered in which implausible or physically impossible assumptions are adopted in order to help bound or conceptually test the repository ro-

business. Results from such unrealistic calculations need to be properly presented to prevent misinterpretation. They are not predictions of what will happen, they are not even predictions of what can happen, they are only hypothetical mathematical exercises that test robustness.

The perhaps most striking recent development in the area of scenario development, and in safety assessment and safety case building in general is the one “of new conceptual tools such as safety functions, which embody key aspects of performance of the geological disposal system from which can be developed internal requirements that relate the ability of the disposal system to fulfil these functions, thus making more transparent the role of the various components (and their synergies in the disposal concept)” /NEA 09/). At least in some programmes, the role of safety functions goes beyond their use in safety assessments. Rather, they provide a link between activities important for repository development and safety case building.

A related recent development is the one of safety function indicators which are being used as a tool to consider the relevance of phenomena and uncertainties for safety. Such indicators might have the potential for use in the context of host rocks and concepts other than granite and the Swedish KBS-3 concept for which they were developed.

Scenarios are being derived based on the safety concept including the safety functions and taking into account safety-relevant phenomena and uncertainties. In some assessments, scenarios are derived using a bottom-up approach that begins by assessing a range of external events or conditions (e. g. climate change, human intrusion, initial container defect) that may trigger changes in the disposal system or affect its performance. Other programmes or organisations structure the scenario definition using a top-down approach, i. e. identifying first the crucial safety functions and then focussing on what combination of processes and conditions could jeopardise one or more safety functions. Each way, if seen in isolation, has advantages and limitations as explained in the following, and the limitations of each way could or should be compensated by the advantages of the other:

- FEP processing is an effective basis to understand and describe individual safety-relevant features and processes in a system, and also to identify factors that may trigger changes in the disposal system or affect its performance. Furthermore, FEP catalogues and the related process-describing documentation are important bases

for modelling. However purely FEP-based or phenomena-based scenario development has difficulties concerning establishing an objective and formalised methodology and also of ensuring the comprehensiveness of the combinations of FEPs to be considered.

- Safety functions are useful to describe the initial state and evolution of a system in relation to the safety concept. Scenario sets derived from studying (scientific and technologic) uncertainties potentially affecting the safety functions (e. g. barrier performance) are perhaps not necessarily “complete”, but better targeted to, and comprehensive with regard to, safety-relevant issues. However, for providing a sufficient scientific basis concerning the phenomenological knowledge which is needed to establish scenarios with confidence it will also be necessary to take advantage from systematic and comprehensive databases of the underlying thermal, hydraulic, mechanical and chemical (THMC) features and processes.

There is no conflict between a bottom-up or a top-down approach; in fact, they are often used in combination, with one applied as a primary method to identify scenarios, and the other serving as a confirmatory tool. Both are sometimes seen as alternatives, but actually either of them is hard to imagine without the other. A survey undertaken within the MeSA project also showed a tendency to formally link the two in hybrid approaches.

A prerequisite for assessing the future evolution of a repository is the establishment of a system description defining the initial state of the repository, including the waste form, the engineered systems and the site. The subsequent analysis of the evolution of the repository system is an indispensable task in developing a safety assessment. It requires a systematic identification and study of THMC and other (e. g. radiological or biological) processes that could occur in the repository system and affect the evolutions of the site and repository.

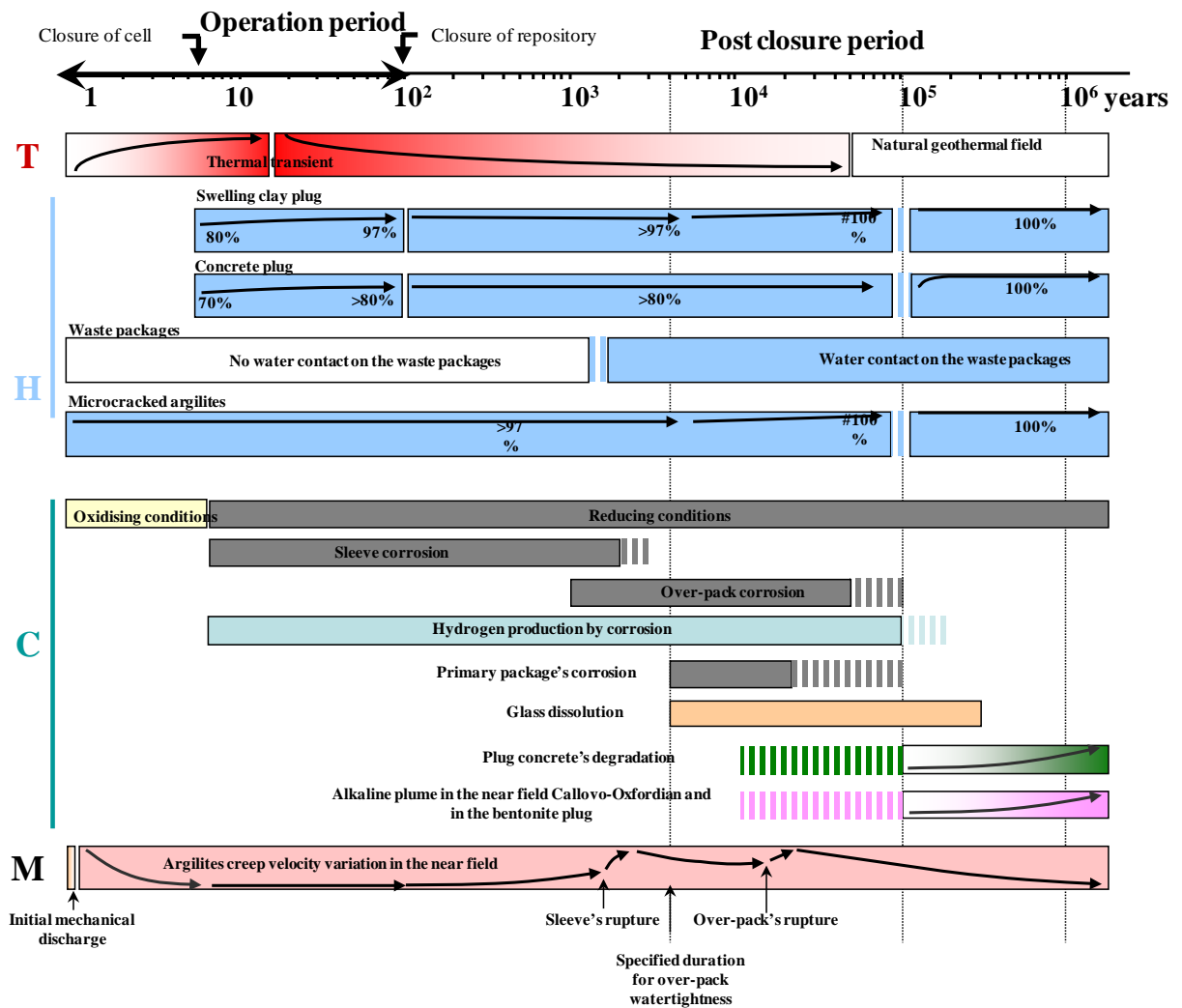
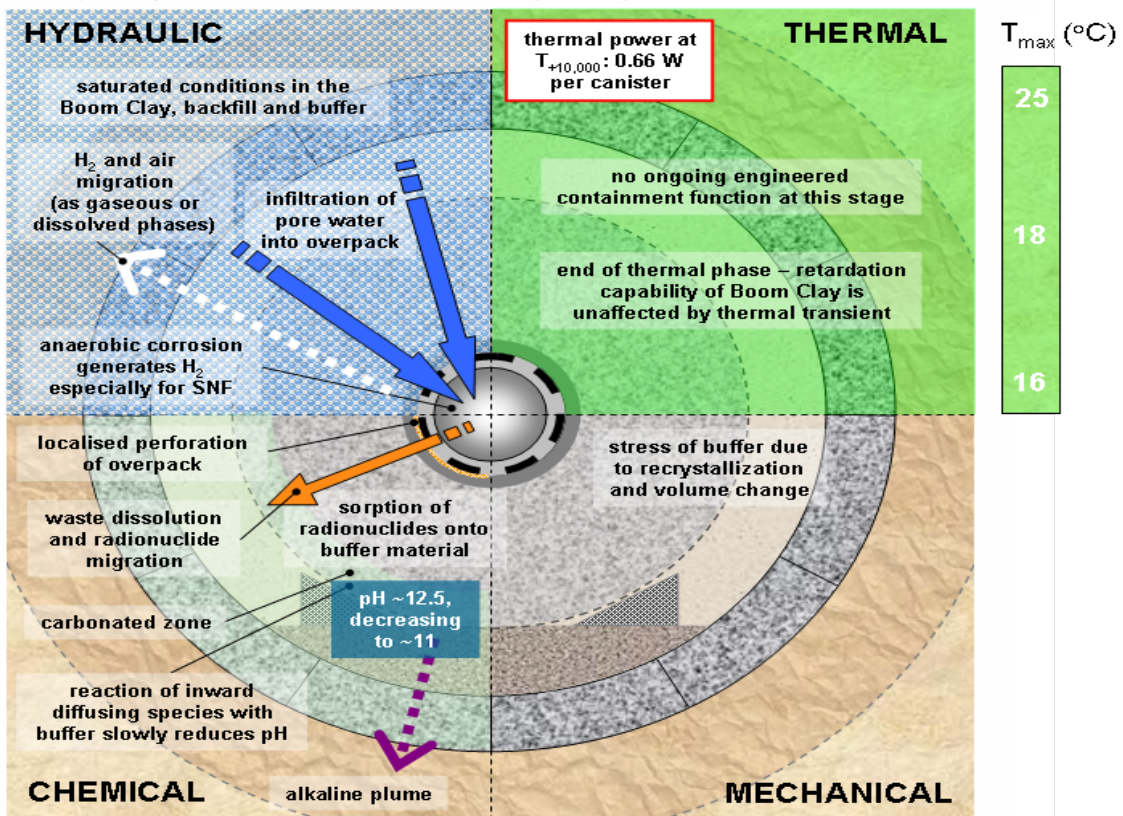


Fig. 2.3 High-level Long-lived Vitrified Waste Modules – Chronological evolution of the THMCGRB processes during the post-closure period /AND 05/

Databases of FEPs developed within specific projects, as well as the NEA FEP database have proved to be valuable tools for describing the system and its potential evolutions, especially for disposal programmes that are in the early stages of repository planning. However, when a programme matures and THMC understanding increases, the knowledge to be managed and documented will go far beyond the capacity of simple FEP records. It will then become necessary to supplement FEP databases with other tools and means of documentation. For example, the understanding and knowledge of THMC processes may be compiled in “process reports”, each one of which will have its own listing of FEPs specific to evaluating one or more processes. In this context, it is important to distinguish between concept-specific FEP catalogues or key safety-relevant phenomena derived from an integrated understanding of the system under consideration, which can have a central role in scenario development, and

the more general NEA FEP database, which is increasingly used for completeness or comprehensiveness checking. Tools for system description include means to address geoscientific issues (geosynthesis, site descriptive models), but also more general tools describing THMC and other phenomena based on discretisation in space and time (story boards, PARS, see Fig. 2.3 and Fig. 2.4). Other, sometimes computer-based tools and methods are in place to address the interaction of phenomena and to identify safety-relevant uncertainties (matrices, diagrams, tree structures).

T_{+10,000} (Initial failure of overpack)



T_{+10,000} (Initial failure of overpack)

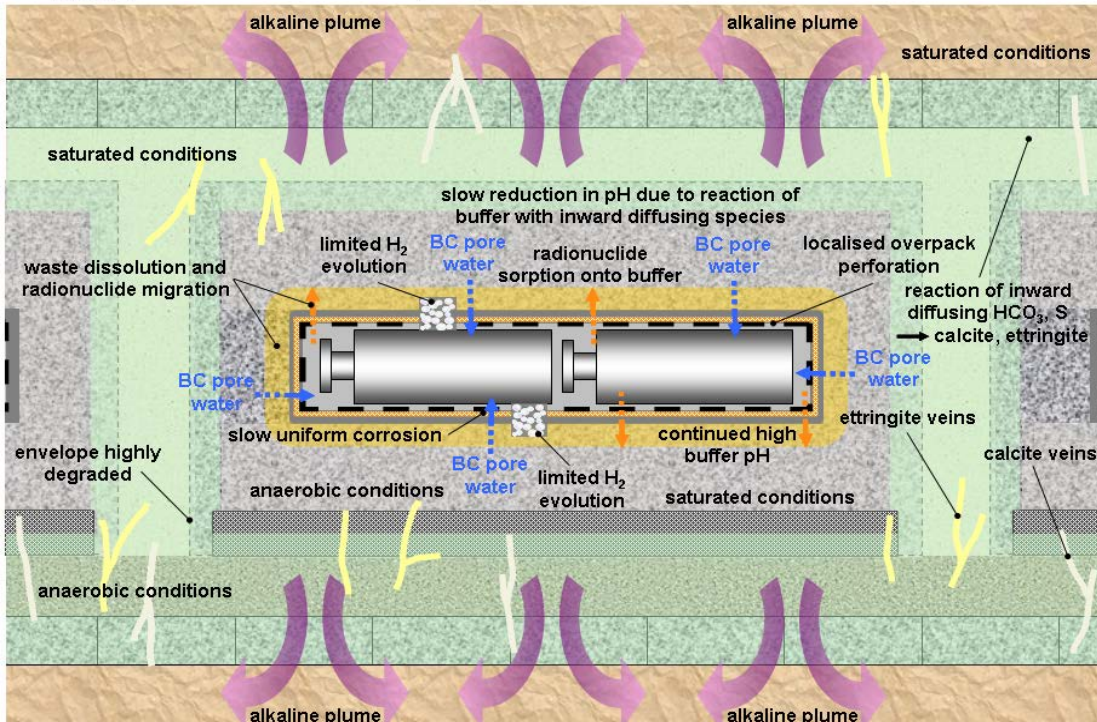


Fig. 2.4 Story boards representing the transverse (top) and longitudinal (bottom) cross section of a disposal tunnel /OND 08/

2.1.2.4 Modelling strategy

An assessment of the performance of a repository can be undertaken by simulation of the potential evolution of the repository system using mathematical or numerical models. Overall, there is wide consensus on the modelling strategies to support safety assessment, and no major areas of disagreement have been identified. Differences exist between countries regarding the extent to which regulations allow simplified handling of the biosphere in the safety assessment.

Process-level models are developed in order to gain a solid understanding of certain aspects of the repository system and to form the basis for conceptual models incorporated into, and parameters used in, system-level models. Process-level models may also help provide justification for simplifications of processes incorporated in system-level models. Over the past 20 years, process-level models have become increasingly important and today such models are increasingly being applied to consider coupled THMC processes, although typically models at this point in time do not consider all of these processes simultaneously. However, there are instances where the processes determining the system's evolution result in little change to the system over time. Modelling such a system has been considered in some instances to be sufficiently straightforward to allow the direct coupling of process models to evaluate the total system.

The central part of the safety assessment is the *integrated or system-level model*, which is used to assess the performance of the disposal system as a whole, leading to a quantitative estimate of potential impact on humans and the environment over the assessment time frame.

Model simplifications are unavoidable; models, no matter how complex, are abstractions of nature. A first type of simplification is introduced when the results of process-level models are converted into system-level model inputs. At this stage, the modeller needs to address which are the essential processes that dominate the system evolution or the performance of the repository system, and on the other hand, which processes can be neglected because they have a negligible (or a limited positive) influence on the performance of the repository system. A second type of simplification can be introduced at the stage of developing numerical models. A third type of simplification is often needed to overcome limitations in the features presently available in computer codes or in the calculation capacity of the computers. Simplifications have important consequences in terms of the level of conservatism and representativeness of the

modelling results. However, as mentioned, there is a clear trend that models are becoming more capable (realistic) due to our improved understanding of the processes and the availability of more powerful computers, and advances in software and numerical methods. In many respects, increased computer power has simply allowed current numerical techniques to be extended to tougher problems by brute force – i. e., allowing the model to be represented with much finer mesh spacing or time steps, and thereby avoiding numerical instability issues. However, there have been notable improvements in the numerical techniques used for discretisation and solvers, which allow for the adaptive refinement of the discretisation and therefore the assessment of more complex models. Another important aspect for safety assessment has been the large improvements in software visualisation methods and graphical user interfaces.

Integrated assessment calculations can be carried out in two principally different ways. A deterministic analysis is a calculation performed with a single set of parameters, and may provide a best estimate, conservative or extreme estimate (e. g. what-if cases) of system performance. In a stochastic or probabilistic analysis, relevant parameters are simultaneously varied to address the range of their uncertainties, constrained, of course, by dependencies or correlations between these parameters. There is an emerging consensus on the use of deterministic and probabilistic approaches. In most safety analyses, deterministic and probabilistic calculations are now seen as complementary and both approaches are applied. Deterministic calculations are more appropriate for detailed calculations and communication purposes. Probabilistic calculations are especially appropriate to deal with parameter uncertainty. Stochastic sensitivity analyses can provide much information on the key parameters controlling the repository system behaviour.

Data gathering and management remains a prerequisite for modelling. Site characterisation, development of the engineered barrier system and associated experiments, and waste characterisation generate large amounts of data, and the traceability of data used in the safety assessment back to these data requires planning. Approaches currently used to help with this include data clearance procedures, site descriptive models, requirements management systems and reference datasets.

Due to the long temporal and large spatial scales involved in geological disposal, a complete comparison between safety assessment model results and experimental measurements cannot be made, but the modelling strategy should include elements of

- independent peer review of the theory, including the conceptual and the mathematical models;
- a software quality assurance process that ensures that software changes are implemented in a formal manner with appropriate review of each step;
- verification that the computer codes accurately implement the mathematical models, i. e. by comparison with analytical solutions;
- benchmarking of new codes against the results of older codes (and the strategy with respect to maintenance of the older codes);
- testing of specific phenomena within the safety assessment model against experimental (laboratory scale) data, field data, natural analogues and/or detailed process models;
- comparison with similar models;
- comparison with field-scale tests that can be conducted within the bounds of underground research laboratories;
- calibration to conditions at a specific site.

The assurance of data and information as well as of model and software development quality is a common theme across national regulatory requirements. In particular, the need for “traceable” and “transparent” links to the source data and references is seen as essential by regulators. It should also be noted that the difficulties associated with system model validation have contributed to the development of the safety case concept, with its emphasis on multiple lines of reasoning.

2.1.2.5 Indicators for safety assessment

The concept of using various types of indicators to complement dose and risk has developed considerably during the last 15 years in national and international projects, and has become internationally accepted. Experience has been gained in international fora such as SPIN, PAMINA, INTESC and various national projects. The early emphasis on

using just dose and risk as safety indicators has been extended, and several types of complementary indicators are now used, most recently safety function indicators. The terminology used for indicators by different organisations is rather inhomogeneous and not consistent between national programmes; identical or very similar concepts are sometimes denoted differently, while in other cases the same term is used with different meanings.

The development of complementary indicators was driven by concern over the inherent uncertainty in estimating potential dose/risk to people in the far-future when climate and human behaviours may be radically different to today. To remove the uncertainty associated with the biosphere exposure pathway, safety assessors have considered other indicators such as the concentrations and fluxes of repository-derived radionuclides that would occur in the geosphere. These indicators may be compared to corresponding concentrations and fluxes of naturally-occurring radionuclides. This approach is still valid, but now forms only one part of the growing suite of complementary indicators that has been proposed and tested. Other indicators relate to the physico-chemical state of barriers (e. g. stress states or swelling pressures of bentonite buffers).

Within the MeSA project, a comprehensive survey concerning indicators being used or applied by organisations represented in MeSA was carried out. As result of this survey, three categories of complementary indicators were defined:

- *concentration and content related indicators*, that provide information on the radionuclide inventory and its distribution within compartments of the repository system and the environment (e. g. total radioactivity content of the wasteform or radiotoxicity concentration in groundwater);
- *flux related indicators*, that provide information on the transport of radionuclides between compartments of the repository system and their release to the accessible environment (e. g. radioactivity flux from the engineered barriers to the geosphere or total integrated radiotoxicity flux from the geosphere to the biosphere over time); and
- *status of barriers related indicators*, that provide information on the functioning and containment capability of the barriers in the repository system (e. g. container life time or buffer swelling pressure).

Another, frequently adopted classification scheme is according to the specific purpose of the indicator (cf. Tab. 2.2). Typical purposes are:

- the quantification of the post-closure safety of the repository in the long term,
- the characterisation and illustration of the performance of the system or subsystems,
- the judgement whether a safety function is fulfilled or not.

Safety indicators give an indication on the safety of the repository and, particularly dose and risk are suitable for comparison with established acceptance criteria. *Performance indicators* are in particular suitable for understanding and evaluating system behaviour. *Safety function indicators* are suitable for evaluating key parts of a repository system in a disaggregated fashion.

Tab. 2.2 Primary and secondary purposes for indicators

Category	Primary Purpose	Secondary Purposes
Safety indicator	Safety statements for the whole system	<ul style="list-style-type: none"> - Performance statement, whole system - Design optimisation - Communication - System understanding
Performance indicator	Performance statements for a system component	<ul style="list-style-type: none"> - Performance statement, whole system - Design optimisation - Communication - System understanding - Site selection
Safety function indicator	Performance statements for a system component	<ul style="list-style-type: none"> - Assessment activity - Design optimisation - Communication - System understanding

Many regulatory systems recognise the potential value of indicators additional to dose and risk but usually without specifying these indicators or their reference values. A reference value is a yardstick against which an indicator can be compared and repository safety and performance evaluated. Reference values for the effective dose rate are usually defined by the regulator. The need for reference values depends, to a large extent, on the purpose of the indicator and the assessment context. For indicators used to make a safety statement, a reference value is essential because, without one, the impact of the repository cannot be judged to be acceptable or not. The same is true for

safety function indicators when they are used to make explicit judgements about the functional performance of the repository. On the other hand, for indicators used to increase understanding of repository behaviour (rather than to judge performance) or to compare between different design options then reference values may not be necessary, although they could still be useful for providing context. The MeSA review of the use of complementary indicators in safety assessments to date shows that the definition of appropriate reference values is the most difficult aspect of their application.

The MeSA review demonstrated a growing use of complementary indicators in a design and engineering context, such as for evaluating the performance of design variants, design optimisation and site selection. This is a relatively new area of interest that was not usually discussed in early reports promoting complementary indicators (see also sections 2.2 and 2.3).

2.1.2.6 Treatment of uncertainties

Uncertainties are, and always will be, associated with assessment results. In the safety case, the connection needs to be made between the key uncertainties that have been identified and the specific measures or actions that will be taken to address them, whether through an R&D programme, repository design studies or bounding safety assessment assumptions. A decision to move to a next step of a repository development is an expression of confidence in the proposed concept and in the findings of the safety assessment (and safety case) despite the existence of uncertainties, some of which will have to be addressed in the next step while others will inevitably remain. A safety case should propose a strategy to address the uncertainties when moving to the next step (Fig. 2.5, Fig. 2.6). Uncertainties can partly be reduced by collecting additional and more accurate data, by design changes, further research, or by additional model development.

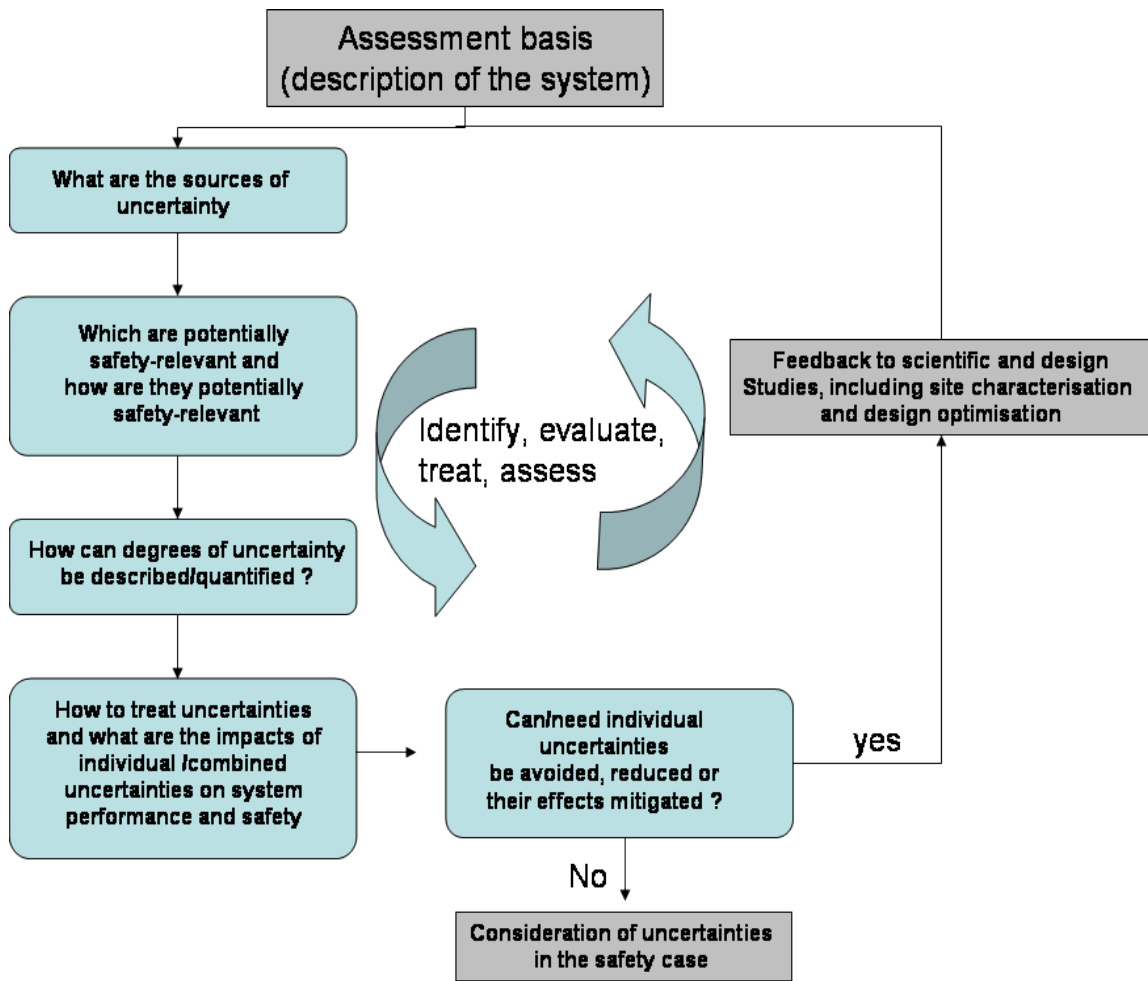


Fig. 2.5 Iterative management of uncertainties (adapted from Figure 6-9 of /POS 09/)

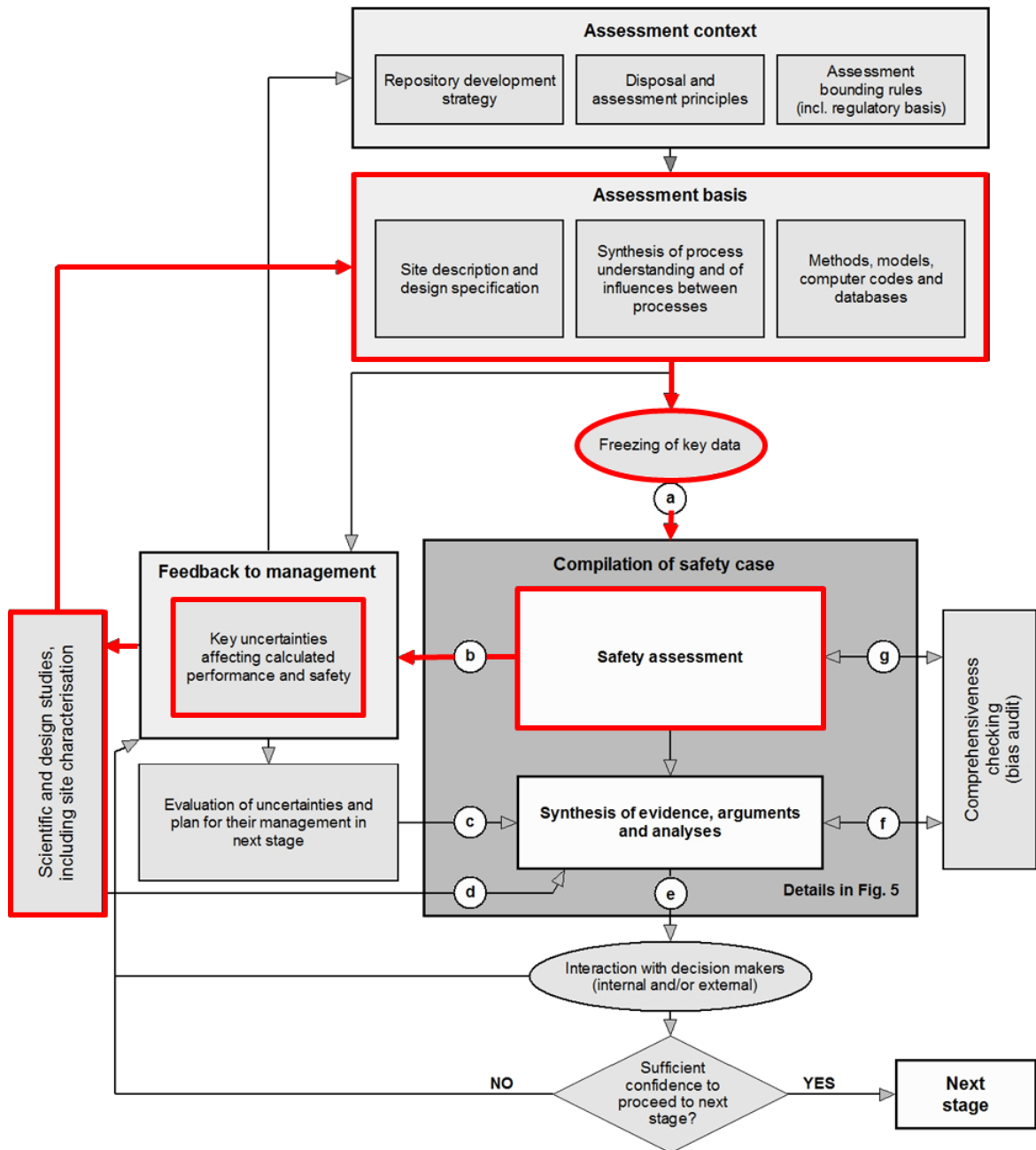


Fig. 2.6 Example of a high-level generic flowchart, showing in red the feedback loop elaborated in Fig. 2.5 (adapted from Fig. 2.1)

Internationally, there is now a consensus on the types and sources of uncertainties in safety assessments, although somewhat different terminology may be used. Typically, the uncertainties considered in safety assessment are classified into scenario uncertainties, model uncertainties, and data and parameter uncertainties. However, all three classes of uncertainties are related to each other, and particular uncertainties can be handled in different ways, such that they might be dealt with in one class or another.

Furthermore, the improved and deeper understanding of the FEPs governing the evolution of a repository considered in recent models, has allowed a more realistic understanding of the repository as compared with earlier, more conservative representations. It has also become possible to represent more of the relevant FEPs and their associated uncertainties from a phenomenological perspective. Following this approach, the phenomenological description of the disposal system and the associated uncertainties can be structured according to key Thermo-Hydro-Mechanical-Chemical (THMC) processes and conditions affecting the evolution of the system. Such descriptions provide the basis for the analysis of uncertainties in the long-term safety of the disposal system and for the subsequent classification of scenario, model and parameter uncertainties as a function of their potential effects on long-term safety.

It is widely recognised that each uncertainty has a specific nature regardless of its classification. In this respect, irreducible (aleatory) and reducible (epistemic) uncertainties can be distinguished. Even though the different nature of uncertainties is generally acknowledged in safety assessments, the distinction between epistemic and aleatory uncertainties is usually not made because many uncertainties are best described and understood to be a result of the interaction of both types.

Strategies for treating uncertainties within the safety assessment are well established. Generally, these fall into one or more of the following five strategies: (1) demonstrating that the uncertainty is not relevant to safety, (2) addressing the uncertainty explicitly, (3) bounding the uncertainty, (4) ruling out the event or process adding to the uncertainty, and (5) using an agreed stylised approach to avoid addressing the uncertainty explicitly.

As integrated safety assessments develop, the assessments themselves are used to identify which areas of uncertainty most need to be reduced in order to increase confidence in the overall assessment results. Uncertainty analysis (analysis about how the uncertainties associated with the different elements of the assessment propagate through it and affect the uncertainty and confidence in the results) and sensitivity analyses (aiming at identifying those input uncertainties which have the greatest impact on the uncertainties of results) are central elements of safety assessments.

Mathematical methods for assessing quantitatively the influence of uncertainties on the calculation end-points are available and are well established. In most safety analyses, deterministic and probabilistic calculations are now seen as complementary, and both

approaches are applied. Probabilistic performance or safety analysis typically consists of two steps. Firstly, a number of runs of the system model are conducted using parameter values sampled at random (or by some other sampling scheme). Secondly, the results are analysed with a combination of any or all of the following techniques:

- correlation and regression methods,
- non-parametric statistical test,
- variance-based methods,
- graphical methods.

In most probabilistic sensitivity analysis studies, linear correlation or regression methods have been applied. These are suitable for systems with a close-to-linear behaviour, and linear regression of rank-transformed data improves the regression model fit for non-linear but still monotonic systems. However, highly non-linear systems and non-monotonic relationships are not amenable to these methods. The drawbacks of the mentioned methods for probabilistic sensitivity analysis can be avoided by applying variance-based sensitivity analysis, which is suitable for non-linear and even non-monotonic systems and yields quantitative results which, in principle, can address not only sensitivities to single input parameters but also to interacting parameter sets. Some methods (e. g. Sobol, FAST) have been applied to repository systems for the first time during recent years. Specific problems have surfaced that are not explicitly addressed in the relevant literature, but which seem to be essential for repository performance models. More research is necessary and planned. The development of new methods is actively pursued.

Regulators expect uncertainties to be identified, to the extent practicable quantitatively characterised or bounded, and their impact on safety clearly articulated in the safety case. Uncertainties which cannot be shown to be irrelevant should be avoided, mitigated or reduced as far as possible e. g. by means of site selection, site characterisation, repository design, and process-oriented research. Uncertainties connected to the assessment results can be placed into an understandable context for evaluation by using multiple lines of evidence. Regulatory requirements in particular govern the extent to which probabilistic safety assessment is used to quantify risks and handle uncertainties.

In order to reduce uncertainties associated with the procedures used for data collection and assessments, regulators often require the application of auditable quality assurance measures to avoid inconsistencies or errors in the data or models, and the use of systematic approaches to prevent methodological mistakes. Following such quality-assurance procedures does not guarantee accurate data or analyses, but it documents that work has been done as described and that activities and results have been reviewed, witnessed or otherwise verified by an observer not directly involved in doing the specific tasks being verified.

2.1.2.7 Regulatory issues

Regulations and regulatory expectations have evolved considerably since the issuing of the NEA brochure on the methodology of safety assessment in 1991. The evolving safety case concept has led to a more sophisticated understanding of the role of safety assessment in the demonstration of repository safety and in the development and optimisation of a disposal system. Regulations nowadays recognise more precisely the implications of the enormous length of the assessment time frame for the demonstration of compliance and for the assessment methodology that should be used. In view of the inherent limitations of assessment methods, the outcomes of the safety assessment are now seen as lines of argumentation which are accompanied by others in order to build confidence in repository safety.

On the national level, several regulations and guidelines for safety assessments have been developed or revised in the NEA member countries during the last decade. On the international level, the ICRP has issued important recommendations with regard to the assessment of compliance with dose and risk constraints. Since 1991, the ICRP publications 77, 81, and 103 /ICR 98a/, /ICR 98b/, /ICR 07/ show a broadening view on the meaning of dose and risk constraints, and on the assessment of compliance for very long time frames. The IAEA safety fundamentals 111-F and SF-1 /IAE 95, /IAE 06/ and the joint convention /IAE 97/ have grounded the general requirement for safety assessments in the framework of radioactive waste disposal. Requirements regarding the methodology of safety assessment (which are not legally binding but represent good practices for national programmes to follow) have been defined in the IAEA standard WS-R-4 /IAE 06/ which will be replaced by more general requirements (DS 354) in the future. More explicit guidance was given in 1999 by the IAEA safety guide WS-G-1.1 /IAE 99/ which is limited to near surface disposal facilities but will be superseded by a

Safety Guide that will also cover deep geological disposal facilities (DS 355). The IAEA has also developed and applied a safety assessment methodology for near surface disposal facilities in the ISAM and ASAM projects, respectively. A common regulatory view on the treatment of uncertainties in safety assessments has been expressed recently by a group of European safety authorities and technical support organisations in the framework of the European Pilot Study /BOD 08/, /VIG 07/.

Regulators expect that the proponent not only assesses compliance with quantitative radiological criteria, but also demonstrates that the repository system is robust and that its possible evolution is well understood. This includes the call for complementary methods to determine the level of protection provided by the repository, e. g. by the use of indicators which are complementary to dose and risk. Also, assurance of data and modelling tool quality, appropriate quality management and transparency and traceability of the assessment process are considered essential.

The regulators themselves have to provide qualitative and quantitative safety criteria and guidance on how to prepare adequate safety cases. The treatment of uncertainties and, in particular, of uncertainties which cannot be quantified, like e. g. those associated to human intrusion, also calls for guidance by the regulator. The specification of guidance on timeframes and timescales for the safety assessment is another important regulatory task. When giving guidance, regulators usually consider how much freedom the proponent needs to optimise the system and to demonstrate that it is safe.

Usually, regulators are responsible for the review of the proponent's safety assessment and safety case. In this context, regulators assess compliance with legislation and regulations and conduct their own assessments in order to gain confidence in the proponent's assessment results and to develop an independent understanding of the system.

It is generally considered beneficial to involve or inform regulators early in the process of developing a safety case in order to promote mutual understanding and to prevent unnecessary work being undertaken. Yet, the regulators still have to keep their independence which is an essential part of the national safety culture and of fundamental importance for the confidence of the stakeholders in the results of the safety case.

2.1.3 Overall conclusions

Key conclusions from the MeSA project include:

- Safety assessment forms a central part of the safety case. However, the results of such assessments must be placed in context and augmented by additional information (i. e., in a safety case) to support decision making.
- Safety assessment provides key information to focus research and site characterisation programmes, as well as engineering design and testing. Conversely, these aspects of repository development produce the data (and interpretations of that data) that support a high quality assessment. Given these links, an important aspect of repository planning is to ensure clear and effective information flow among the various groups and stakeholders involved with repository development.
- Generic safety case and safety assessment flowcharts were developed. At a higher level, key assessment activities are “freezing of key data”, comprehensiveness checking, a synthesis of evidence, arguments and analyses, and feedback to programme management. At a more detailed level, safety assessment generally starts with the development of an integrated description of the expected initial state of the disposal system and of its evolution.
- Scenarios represent specific descriptions of a potential evolution of the repository system from a given initial state. They describe the compilation and arrangement of safety relevant features, events and processes as a fundamental basis for the assessment of post-closure safety which includes assessing the potential consequences on humans and the environment. The development of scenarios for the safety case is of fundamental importance as it constitutes a key element of the management of uncertainties.
- An assessment of the performance of a repository can be undertaken by simulation of the potential evolution of the repository system using mathematical or numerical models. Overall, there is wide consensus on the modelling strategies to support safety assessment, and no major areas of disagreement have been identified. In most safety analyses, deterministic and probabilistic calculations are now seen as complementary, and both approaches are applied.
- The concept of using various types of indicators to complement dose and risk has developed considerably during the last 15 years and has become internationally accepted. However, the terminology used for indicators by different organisations is

rather inhomogeneous and not consistent between national programmes; identical or very similar concepts are sometimes denoted differently, while in other cases the same term is used with different meanings.

- Uncertainties are, and always will be, associated with assessment results. Internationally, there is now a high level of consensus on the types and sources of uncertainties in safety assessments, although somewhat different terminology may be used. Typically, the uncertainties considered in safety assessment are classified into scenario uncertainties, model uncertainties, and data and parameter uncertainties. Strategies for treating uncertainties within the safety assessment are well established.
- Regulations and regulatory expectations have evolved considerably since the issuing of the NEA brochure on the methodology of safety assessment in 1991 and nowadays recognise more clearly the implications of the long assessment time frame for the demonstration of compliance on the assessment methodology that should be used. Regulators expect that the proponent not only assesses compliance with quantitative radiological criteria, but also demonstrates that the repository system is robust and that its possible evolution is well understood. Also, assurance of data and modelling tool quality, appropriate quality management and transparency and traceability of the assessment process are considered essential.

2.1.4 Recommendations and ongoing work

The MeSA project led to several suggestions on areas related to the safety case in which further development work might be conducted. These included:

1. A suggestion to update the NEA brochure on the safety case concept and, in doing so, emphasise more clearly the essential role of safety assessment within in the safety case.
2. A suggestion to update and enhance the NEA database of Features, Events and Processes (FEPs) relevant to safety assessment for geologic disposal.
3. A suggestion to initiate a project that would foster the exchange of information and best practice on scenario development.

4. A suggestion to develop a “state of the art” report on safety indicators in safety assessment, based on further evaluation of responses to a questionnaire survey conducted during the MeSA project.
5. A suggestion to develop guidance on a general scheme for performing sensitivity analyses in safety assessments for geologic disposal systems and interpreting results.
6. A suggestion to develop guidance on when formal approaches to expert judgement and elicitation may be warranted in safety assessment in general, and on disposal system description and scenario development in particular.

These recommendations were, together with the general outcomes of the project, presented to, and discussed by, the IGSC Annual Session in Autumn 2010. Based on decisions of the IGSC, the following activities are presently being carried out:

1. An update of the NEA brochure on the safety case is being prepared by a task group.
2. NEA has performed a survey amongst national organisations about the use of the NEA FEP database. Based on this survey, further work on the NEA FEP database is started (see section 3.2.2).
3. The proposal to establish a project on scenario development was developed further by an IGSC task group and the planned way forward is briefly described in section 3.2.2.
4. A state-of-the-art report on safety indicators in safety assessment, based on further evaluation of responses to a questionnaire survey conducted during the MeSA project, has been developed (see section 2.2).
5. The issue of uncertainty and sensitivity analysis is covered in a Topical Session at the annual IGSC meeting IGSC-14 in 2012.
6. The topic of guidance on formal approaches to expert judgement and elicitation was, as an issue in its own, considered low priority and might be addressed in the framework of the activities on FEPs and scenarios mentioned above as well as of the planned activity on organisational issues.

2.1.5 The project's documentation

J. Andersson, D. Bennett, E. Forinash and K.-J. Röhlrig: Methods for Safety Assessment for Geological Disposal Facilities for Radioactive Waste. Outcomes of the NEA MeSA initiative (synthesis)

A. Van Luik, E. Forinash, and N. Marcos 2011: OECD/NEA project on the Methods of Safety Assessment (MeSA), Issue Paper # 1: "Safety Assessment in Context of the Safety Case"

J. Schneider, L. Bailey, L. Griffault, H. Makino, K.-J. Röhlrig and P.A. Smith 2011: OECD/NEA project on the Methods of Safety Assessment (MeSA), Issue Paper # 2: "Safety Assessment and Safety Case Flowcharts"

K.-J. Röhlrig, L. Griffault, M. Capouet, H. Makino, N. Marcos, P. Smith, A. Vokal, and J. Wollrath, 2011: OECD/NEA project on the Methods of Safety Assessment (MeSA), Issue Paper # 3: "System Description and Scenarios".

P. Gierszewski, L. Bailey, U. Noseck and J. Wollrath 2011: OECD/NEA project on the Methods of Safety Assessment (MeSA), Issue Paper # 4: "Modelling Strategy"

U. Noseck, A. Hedin, J. Marivoet, W. Miller, M. Navarro, K.-J. Röhlrig, A. Vokal and J. Weber 2011: OECD/NEA project on the Methods of Safety Assessment (MeSA), Issue Paper # 5: "Indicators for Safety Assessment"

J. Mönig, L. Bailey, M. Capouet, A. Van Luik and S. D. Sevougian 2011: OECD/NEA project on the Methods of Safety Assessment (MeSA), Issue Paper # 6: "Treatment of Uncertainties"

M. Navarro, D. Ilett, F. Lemy, N. Marcos, B. Sagar and G. Wittmeyer 2011: OECD/NEA project on the Methods of Safety Assessment (MeSA), Issue Paper # 7: "Regulatory Issues"

2.1.6 German contributions to MeSA

German organisations provided considerable contributions to the MeSA project:

- The Bundesamt für Strahlenschutz (BfS) contributed to the work of the groups, and the drafting of the reports no. 3 “System description and scenarios” and 4 “Modelling strategy”.
- The Bundesanstalt für Geowissenschaften und Rohstoffe (BGR) contributed to the work of working group 5 “Indicators for safety assessment”, in particular by funding the evaluation of the review carried out in that group.
- Individuals from Gesellschaft für Anlagen- und Reaktorsicherheit (GRS) mbH contributed by leading the working groups and acting as main authors for the reports no. 5 “Indicators for safety assessment”, 6 “Treatment of uncertainties”, and 7 “Regulatory issues”. The activities in groups no. 5 and 6 were funded by the BMWi project “Wissenschaftliche Grundlagen” (WiGr-6, FKZ 02E10548).
- The Technische Universität Clausthal / Institut für Endlagerforschung (TUC/IELF) chaired and coordinated the whole project. TUC employees were leading the working group and acting as main authors for the report no. 3 “System description and scenarios” and contributed to the work of the groups, and the drafting of the reports no. 2 “Safety assessment and safety case flowcharts” and 5 “Indicators for safety assessment”. Its work was funded by the BMWi project “Wissenschaftliche Grundlagen” (WiGr-6, FKZ 02E10548).

2.2 Current activities on indicators

The last several years have seen a number of important developments in the use of indicators in safety cases for geological disposal. The NEA has reviewed these developments within the scope of its Methods for Safety Assessment (MeSA) project. The review began by evaluating relevant aspects of previous NEA initiatives into safety cases, in particular the International Experience in Safety Cases (INTESC), Long-Term Safety Criteria (LTSC) and Timescales initiatives, as well as key publications from other international agencies such as the IAEA and EC. That evaluation confirmed the growing international interest in the subject but also highlighted a clear lack of consistency in the terminology, characteristics and methods of application of the indicators used by different organisations. To understand the situation better, a questionnaire was

developed that included a number of questions grouped under the headings of (i) regulatory context and guidance, (ii) status of repository development programme, (iii) use of complementary indicators, and (iv) areas of uncertainty and future development. The Indicators Questionnaire was circulated to implementing and research organisations as well as regulatory agencies participating in the Integration Group for the Safety Case (IGSC)¹, and twenty one separate responses were received that covered a range of experiences from developing assessment programmes just beginning to consider how to use indicators, to mature programmes that have already performed detailed site-specific assessments.

Together with the outcomes from comparable international work, in particular relevant IAEA Technical Reports and the EC's SPIN and PAMINA Project reports /BEC 03/, /BEC 09/ the responses to the Indicators Questionnaire provided the primary source material for the NEA Status Report "Indicators for the safety case" /MIL 12/. In the following a summary of the status report is provided.

The main purpose of the Status Report is to increase awareness and understanding of the potential applications of indicators in the safety case, and provide support for further development in the area. Some guidance on the possible use of indicators is given but it is not the objective to seek to propose a 'standard' approach or terminology. This would be neither sensible nor possible given the differences in national regulations concerning their requirements for how indicators should be applied. For the sake of clarity, however, the report makes a distinction between primary and complementary indicators. A *primary indicator* (typically annual dose or risk) is one that is compared to a legally or regulatory defined radiological constraint, whilst all other indicators that may be used in a safety case are referred to in this report as *complementary indicators*.

The Status Report is intended to be useful to anyone engaged in the planning, preparation and review of safety cases for radioactive waste repositories. It is, however, focussed on providing advice to developers of deep geological repositories with programmes at an early stage of development (e. g. pre-site selection), rather than those that are more mature and which have already defined their assessment methodologies and end-points. The report may also be useful to regulators and those engaged in peer review of safety assessments, particularly in regimes where regulators may choose to

¹ More details can be found in section 3.2

stipulate the use of specific indicators in addition to dose or risk in formal safety cases that are submitted to them.

The first important observation that was made from the responses to the Indicators Questionnaire is that complementary indicators are now accepted by the majority of implementers and regulators as an important component of a safety case. This is a markedly different position from a decade ago, when the potential for complementary indicators was still under investigation. This shift in approach is consistent with the development of safety cases using multiple lines of reasoning which require the mechanics of repository evolution to be understood at the sub-system or process level.

Whilst there is almost universal acceptance of the potential benefits of using complementary indicators, there are significant differences in the types of indicators that are used or proposed, and the methods for their application in safety cases. Over 100 separate indicators were reported in the responses to the Indicators Questionnaire, illustrating their growing relevance within assessment programmes. On inspection, however, many of the reported indicators are shown to be broadly the same or variants of each other, but they are often differently named, described or categorised. In simple terms, the most commonly reported indicators fall into three main groups, as follows:

- *'Content and concentration'* related indicators, such as:
 - Radioactivity/toxicity concentration in the waste form
 - Radioactivity/toxicity concentration in the engineered barrier system components
 - Radioactivity/toxicity concentration in the geosphere (particularly in groundwater)
 - Radioactivity/toxicity concentration in the biosphere (particularly in surface waters)
 - Inventory of radionuclides in a part of the repository system
 - Power density in groundwater
- *'Flux'* related indicators, such as:
 - Radioactivity/toxicity flux from the engineered barriers to the geosphere
 - Radioactivity/toxicity flux from the geosphere to the biosphere
 - Integrated radioactivity/toxicity flux from the geosphere to the biosphere
 - Radionuclide molar flow (mass over the assessment period)
- *'Status of barriers'* related indicators, such as:

- Groundwater age
- Container lifetime
- Transport times through the engineered barrier system components and the geosphere
- State of stress in the near-field rock (containment zone)
- Swelling pressure (buffer and backfill)
- Ionic strength (geosphere groundwater)

The grouping shown above has been derived within the scope of developing the Status Report, based on the types of indicators reported to have been used to date. This simple grouping is considered to be useful because it does not suggest any relative importance or hierarchy between the various indicators that may be used in a safety case. Many (but not all) organisations, however, make a distinction between *safety indicators* and *performance indicators*, following the recommendations of the IAEA made in 2003 /IAE 03a/.

In very broad terms, a safety indicator provides a measure of the overall safety of the entire repository system. Safety indicators are usually compared with quantities, known as *reference values*, which represent some minimum measure of safety that is generally considered to be acceptable. At the simplest level, calculated repository releases may be compared with the abundances of naturally occurring radionuclides measured in the rocks and groundwaters at the repository site, on the basis that the natural environment is generally considered to be safe. The approach can be refined by making more specific comparisons between particular transport pathways (e. g. groundwater discharge), and abundances can be defined for either concentrations or fluxes of all radionuclides or just for specific nuclides of interest. The approach is also suited for comparing chemotoxic hazard associated with repository releases and natural systems.

A difficulty with the use of safety indicators lies in the derivation of appropriate reference values. There are a small number of universally applicable reference values that may be used in all safety cases, such as internationally agreed drinking water standards /WHO 11/. There is a trend, however, towards using site-specific reference values, such as local or regional groundwater concentrations, because these are often considered to provide the most relevant situational context. Several national repository development organisations anticipate deriving site-specific reference values from characterisation studies, once sites have been chosen.

In comparison to a safety indicator, a performance indicator provides a measure of the behaviour of an individual repository component or sub-system. For this reason, performance indicators are usually more concept or site-specific than safety indicators. Multiple performance indicators may be applied in a safety case and they could be used to evaluate performance of the disposal system barrier-by-barrier, and to determine what redundancy and performance 'head room' is available in the repository design. Various performance indicators have been used or proposed, and they typically relate to such things as the containment times provided by individual barriers or the migration rate (flux) of radionuclides across them.

One newly identified potential application of performance indicators is their use in site selection and design optimisation. Performance indicators allow the relative containment provided by different host rocks, geological environments and engineered barrier materials to be quantified and compared to each other in a structured manner. They may, therefore, be used to select and optimise the design in dependence of the subsurface conditions (e. g. the best buffer material given known groundwater composition), and to ensure the overall cost and effort for constructing the repository are not excessive.

Performance indicators may be compared with independent quantities, known as *indicator criteria*, although these are not available for all performance indicators. Where they are available, indicator criteria may be derived from independent modelling, laboratory studies or, occasionally, natural analogue studies (e. g. to provide a measure of long-term metal corrosion rates).

More recently, a number of organisations have begun to define explicit safety functions for some individual repository components. It is possible to derive indicators from these safety functions, sometimes called *safety function indicators*, which are measurable or calculable properties that indicate the extent to which the system components achieve their safety function. For example, a metal waste canister may be assigned the safety function of 'physical containment' in which case an appropriate safety function indicator may be the redox condition of the groundwater because, if it is too oxidising, the metal may corrode rapidly causing it to lose its containment function. Safety function indicators are usually compared with indicator criteria which define the quantitative limits (maximum or minimum conditions) that are the boundary conditions under which the matching safety function may be maintained. These will generally be derived from independent studies.

It is clear that safety function indicators have quite a lot in common with performance indicators in so far as they both relate to the evaluation of system components and sub-systems. The key difference between them lies in the requirement for a safety function indicator to be compared with a corresponding indicator criterion, whereas a performance indicator not always has a matching criterion for comparison. Given their similarity, safety function indicators can be considered as a special case and application of performance indicators.

The concept of safety function indicators has been developed further by SKB in its recent safety cases for spent fuel disposal in Sweden, in which safety function indicators were used to identify scenarios and to derive calculation cases for the safety assessment. In SKB's methodology, when an assessment showed that a safety function indicator may not achieve its matching indicator criterion, then additional calculations were performed to evaluate the consequences of the associated safety function being lost.

Although many organisations stated in their responses to the Indicators Questionnaire that they do explicitly categorise indicators as either safety, performance or safety function indicators, several other organisations deliberately do not apply any defined categorisation scheme and prefer to use more general terminology that does not suggest any hierarchy amongst the complementary indicators they use. This is due, in part, to differences in the regulatory regimes and safety assessment methodologies adopted in different countries.

There is increasing recognition of complementary indicators within national regulations. In many countries, the regulatory regimes are non-prescriptive and complementary indicators are featured in non-statutory guidance documents but, nonetheless, the language used in them often makes it evident that the regulator has a strong expectation that the repository developer *will* use complementary indicators to support their safety case, even if there is no formal requirement in law to do so. At the present time, however, new regulations have been produced in final or draft form in several countries (e. g. Finland, Germany) and these include formal requirements to use complementary indicators, although these regulations vary considerably in how the regulator expects them to be applied. These variations are driven, in part, by differences in the repository design and safety concepts in each country. For example, the Finnish regulations are expressed in terms of maximum allowable concentrations of repository releases in groundwater (a form of safety indicator), whereas the German regulations are ex-

pressed in terms of the functional requirements for the containment providing rock zone (a form of performance indicator or safety function indicator).

Irrespective of what classification scheme or terminology may be adopted, it is clear that complementary indicators may have multiple but related applications within a safety case. Those identified from the responses to the Indicators Questionnaire include:

- supporting the safety case structure and applying multiple lines of reasoning;
- increasing the transparency of safety case arguments;
- assessment of repository safety and presenting impacts in the content of the natural environment;
- assessment of repository safety in different timeframes;
- addressing uncertainty in dose and risk calculations;
- assessment of sub-system performance;
- assessment of safety functions;
- scenario identification; and
- helping with communication, especially to non-technical audiences.

Not all of these applications are appropriate in all circumstances. Whilst it is recommended that complementary indicators should feature in all safety cases, the safety case developer is encouraged to give careful thought to choosing and applying appropriate indicators so that they are consistent with:

- the regulatory context;
- the assessment context;
- the assessment methodology;
- the stage in the repository development programmes; and
- the intended audiences for the safety case.

In the Status Report, examples are provided of the many different indicators that have been proposed, including their methods of application, intended to be useful to programmes beginning to consider applying them in their own safety cases.

In addition to choosing appropriate indicators, the way in which they are presented in a safety case is also important. One of the primary drivers behind the use of complementary indicators is that they can offset some of the drawbacks associated with the calculation of dose and risk. In particular, assumptions to be made about the future human behaviour can be avoided; they allow the performance of the repository to be disaggregated rather than presented as a single parameter (e. g. dose) thus enabling the performance and safety functions of individual barriers to be assessed; and they provide site-specific context to repository releases and so can be more readily comprehended by non-technical audiences.

Of these points, the first is perhaps the most important and this has led several national regulators to require repository developers to place greater emphasis on complementary indicators in far-future assessment times, beyond the period when radiation exposure to humans can be reliably assessed, and especially after significant climate change may have occurred. When presenting indicators in a safety case, therefore, there is significant benefit to be gained from using different indicators in different assessment timeframes, so that the advantages of one can clearly be seen to be balancing the disadvantages associated with another. In this way, using a suite of different indicators will help to address uncertainty and to increase confidence in the safety case.

In the coming years, it is likely that further developments in the use of complementary indicators will occur, particularly in the context of safety cases produced to support repository siting and implementation decisions. The Status Report presents 'best case' examples of how indicators may be used in safety cases but does not propose that a standardised approach to their application should be promoted. One of the strengths of complementary indicators is that they can be applied flexibly in safety cases to provide a number of benefits, and to align with the particular circumstances at the time.

2.3 Applicability of indicators

For the reasons discussed in section 1.1, there has been a move on the one hand to use indicators that are complementary to dose and risk and on the other hand to apply indicators that are derived from safety functions. An important safety function of repositories for the final disposal of radioactive waste is to isolate and contain the waste to ensure long-term safety of people and protection of the environment. There are many different designs for repositories but containment is generally provided by the geologi-

cal and a series of engineered barriers. For example, in the German Safety Requirements Governing the Final Disposal of Heat-Generating Radioactive Waste /BMU 10/ containment refers to a safety function of the repository system which is characterised by the fact that the radioactive waste is contained inside a defined rock zone, in such a way that it essentially remains at the site of emplacement, and at best, minimal defined quantities of material are able to leave that rock zone. An important element of this approach is the definition of the rock zone, which in conjunction with the technical seals, e. g. shaft seals or backfill, ensure containment of the waste. This rock zone is called containment providing rock zone (CRZ)².

One approach to define a set of indicators that is especially directed to the safety function containment is provided by /BAL 07/. The proposed indicators comprise the dose³ and five complementary indicators:

- Proportion of the cumulative released quantity of substance over the safety case period: The first proposed indicator is the ratio of the total released radionuclide quantity from the CRZ to the initially emplaced total amount of radionuclides. This definition implies that this indicator cannot have a direct safety statement, since it does not assess the radiological consequences of the released radionuclides. Nevertheless this indicator can be used to illustrate the quantities of radionuclides released from the CRZ and how small the percentage of released radionuclides is in comparison with the emplaced inventory. The yardstick proposed by /BAL 07/ requires that less than 0.01 mol-% of the total radionuclide inventory is released within the assessment period of 10^6 y.
- Concentrations of released U and Th in the porewater at the CRZ boundary: The idea of this indicator is to illustrate what quantities of uranium and thorium are released from the CRZ and how small the percentage of the released quantities is in comparison with naturally occurring uranium and thorium. Therefore, the concentration of all released radionuclides of uranium and thorium is used for the comparison to the natural concentration of these elements. The yardsticks are 1 µg/l for uranium, and 0.1 µg/l for thorium /BAL 07/.

² The German regulations denote this zone as the 'isolating rock zone' but to be consistent with the content of this report the term 'containment providing rock zone' is used instead to illustrate that it refers to the safety function of 'containment'.

³ In the following sections denoted as effective individual dose.

- Contribution to power density in the porewater at the CRZ boundary: Starting point for the calculation of this safety indicator is the calculated activity concentration in the groundwater at the boundary of the CRZ. Actually, it can be the activity concentration in any subsystem of the repository system, but it is proposed in /BAL 07/ to use the power density in the porewater and in the soil matrix in the deeper aquifer system. Here, the indicator is calculated from the activity concentration in the porewater without considering the power density coming from radionuclides in the soil matrix, since no data for the matrix are available. The calculation of the power density is carried out with a simple weighting scheme by multiplying the activity concentration of every radionuclide [Bq/m³] in the porewater at the boundary of the CRZ with its decay energy. This operation yields a power density p (power per volume, [MeV/(s·m³)]).

$$p = \sum_{\text{all nuclides } n} c_n E_n \quad (2.1)$$

with the activity concentration c_n [Bq/m³] of radionuclide n in groundwater and the corresponding decay energies E_n [MeV], given in Tab. 2.12.

The indicator contribution to the power density in groundwater is independent of any specific biological species. It is an aggregation over all radionuclides and can be seen as a yardstick for the impact on biota in general. It is difficult to derive a yardstick for the power density in the porewater and in the soil matrix of a deeper groundwater system. /BAL 07/ estimated a value of 100 MeV/(s·m³) for the power density in claystone⁴. For, the upper groundwater above the salt dome Gorleben /BEC 09/ derived a natural value of about 75 MeV/(s·m³).

- Contribution to radiotoxicity in groundwater: The contribution to radiotoxicity in groundwater is calculated from the radionuclide flux s_n through the boundary of the CRZ. This flux is distributed in a virtual water body used by a group of humans. The virtual water body comprises the annual water consumption of this group. As a reference a group of 30 humans with an annual water consumption w of 15,000 m³ is used for the calculation. To assess the radiological consequences of the radionuclide concentrations in this water body, the same dose conversion factors D_n are applied as for the calculation of the individual dose.

⁴ In /BAL 07/ a value of 0.1 MeV/l is given. Since the indicator is called power density we applied the unit MeV/(s·m³).

$$r = \sum_{\text{all nuclides } n} \frac{s_n D_n}{W} \quad (2.2)$$

The yardstick should be a small percentage of the average natural background radiation. In /BAL 07/ a yardstick of 0.1 mSv/a is proposed.

- Radionuclide concentration in the usable water near the surface: For radionuclides, that are part of natural waters, it is possible to compare the natural concentrations with the concentrations released from the repository into these waters. Therefore /BAL 07/ proposes limits for naturally occurring radionuclides (U-238, U-234, Ra-226, Pb-210, U-235, Th-228, Th-230 and Th-232), which can be used for such kind of comparisons. The yardsticks are as follows
 - U-238: 1,58 Bq/m³
 - U-234: 1,83 Bq/m³
 - Ra-226: 0,48 Bq/m³
 - Pb-210: 0,57 Bq/m³
 - U-235: 0,1 Bq/m³
 - Th-228: 0,01 Bq/m³
 - Th-230: 0,2 Bq/m³
 - Th-232 0,05 Bq/m³
- Effective individual dose: The effective dose rate to exposed individuals is the main indicator internationally accepted for assessing the safety of a repository system. In many countries the regulatory authorities have established regulatory limits for this indicator. For example, the limit for the effective dose rate in Germany is 0.3 mSv/a, which is derived from the regulation §47 StrlSchV /AVV 12/. This limit was chosen since it represents a small proportion relative to the natural background radiation doses. The average natural background radiation in Germany is in the range of 2 to 3 mSv/a /BMU 07/. According to the German Safety Requirements /BMU 10/, evidence must be provided that for probable developments through the release of radionuclides from the emplaced radioactive waste, an additional effective dose in the range of only 10 micro Sieverts per year can occur for individuals. Individuals with today's life expectancy and with a lifetime of exposure are to be considered.

Following transport through geosphere, contaminants reach the upper aquifer. From here, a fraction of 15 000 m³/y of the contaminated water is pumped through a well and used for human and livestock consumption, and irrigation. For the conversion of the radionuclide activity in the upper aquifer to the effective dose rate the following exposition pathways are included (the dose conversion factors, see Tab. 2.12):

- consumption of contaminated drinking water,
- consumption of fish from contaminated ponds,
- consumption of plants irrigated with contaminated water,
- consumption of milk and meat from cattle, which were watered and fed with contaminated fodder and
- exposure due to habitation on the contaminated land.

In the following subsections, these six indicators are tested and evaluated regarding their usefulness indicating containment for a generic repository system in a clay and a salt formation. For salt a generic repository system in a salt dome in Northern Germany is used. The applied system is based on the case developed in the context of the research project ISIBEL /BUH 08/. The generic repository system in a clay formation in Northern Germany was developed in the research project TONI /RUE 07/. Both projects were carried out independently and differ in some fundamental aspects, e. g. the emplaced inventory (the clay case considers only spent fuel, whereas the salt case considers spent fuel and reprocessed waste). Therefore, the calculations cannot be used to compare both generic sites. Another important reason for the incomparability of both systems is that the calculation case for clay formation represents an evolution without unexpected events whereas the repository system in salt represents an evolution with some unexpected events, especially the instantaneous failure of all containers. Due to the uncertainty in crushed salt compaction it is assumed that compacted crushed salt keeps a residual effective porosity for the whole assessment period.

The different properties of the repository systems in clay and salt are also important for the release out of the CRZ: In clay it is assumed that the radionuclides are released over the whole area of the CRZ, whereas in salt the impermeable salt allows only a release via the shaft (Fig. 2.7). This has a tremendous effect on the indicators that are used to compare concentrations or dependent quantities calculated directly at the CRZ

boundary (concentration of released U and Th and contribution to the power density in the porewater at the CRZ boundary; see also discussion in section 2.3.3).

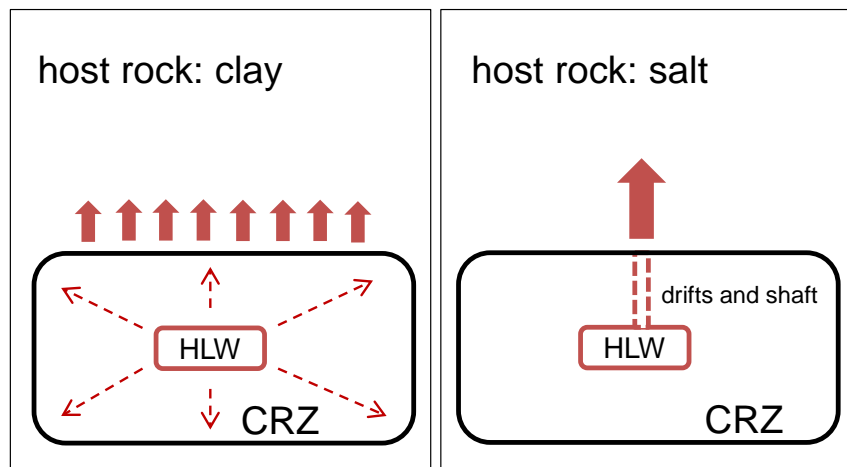


Fig. 2.7 Schematic illustration for the release of radionuclides out of the CRZ for a repository in clay and rock salt, respectively

2.3.1 Repository in a clay formation

2.3.1.1 Description of the repository system

The basis of the layout of the generic repository system used in this report was developed in /RUE 07/ and /RUE 10/ for a repository in a clay formation in the Lower Cretaceous formation in Northern Germany. Fig. 2.8 shows the different compartments of this repository system that are distinguished for the calculation of the indicators. The blue arrows represent the locations in the repository system, where the indicators are calculated.

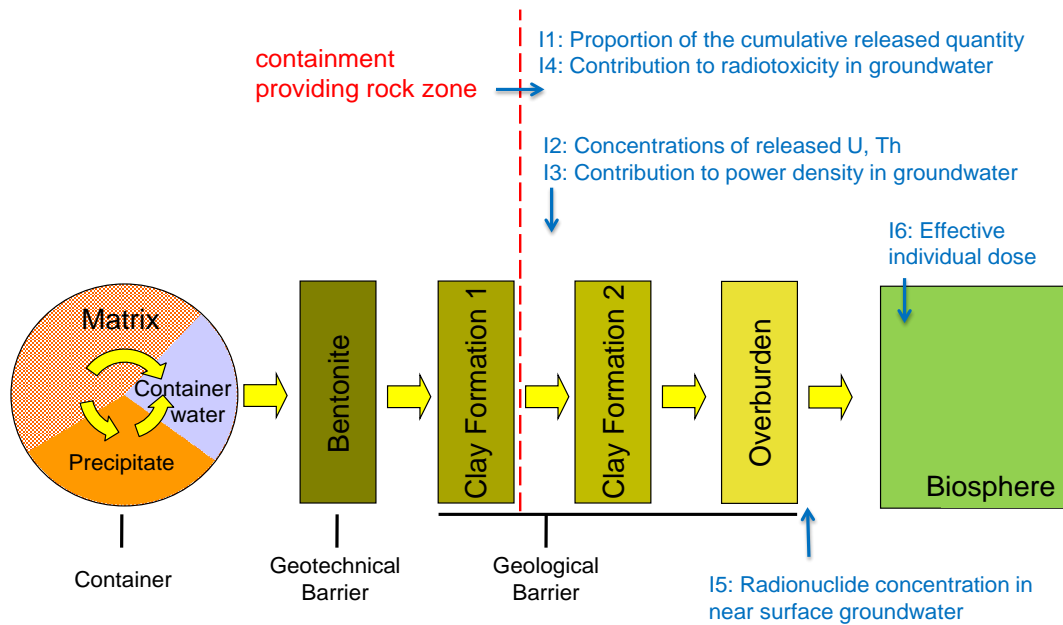


Fig. 2.8 Compartments of the generic repository system and the locations of the CRZ and the indicator assessment (I1-I6)

The different compartments are:

- **Container (Matrix, container water, precipitate):** The containers are stored in vertical boreholes holding five containers each. In order to avoid exceedance of the critical temperature of 100 °C a borehole distance of 47 m was calculated for geometry with five containers in each borehole. The cavity around the containers is back-filled with bentonite. It is assumed that before any containers corrode, the bentonite and those parts of the host rock formation that were desaturated during the construction of the repository are re-saturated and all pathways in the bentonite and the excavation-disturbed zone (EDZ) are closed by the swelling process. As soon as the first containers fail, radionuclides are mobilised from the waste matrix and dissolved in the water volume inside the container. Part of the radionuclides precipitate again due to solubility limits. The matrix represents the non-mobilised radionuclides in the spent fuel matrix. The precipitate represents nuclides that were mobilised from the matrix, but are precipitated since solubility limits are reached. The concentration of radionuclides in the container water is the source for further transport processes.
- **Bentonite:** It is assumed that the mobilised radionuclides are exclusively transported by diffusion through the bentonite. The transport length for diffusion in the bentonite depends on the location of the container within the borehole. The minimum

value is 10 m, which is used for the calculations. During the transport process the radionuclides are retained by sorption.

- Clay Formation 1: The transport distance in this formation is derived from the general geological settings of lower-cretaceous clay formations in Northern Germany under the assumption that the repository is located exactly in the middle of a clay formation that has a thickness of 160 m. The boundary of the CRZ is located between clay formation 1 and clay formation 2. The radionuclides are transported only by diffusion through both clay formations.
- Clay Formation 2: The second clay formation is considered as low-permeable barrier with an additional thickness of 250 m which is a representative value for Northern Germany.
- Overburden: The overburden consists of a sequence of aquifers representative for Northern Germany. The length of the transport pathway through the overburden was derived in /BUE 85/. For the radionuclide transport outside the clay formations advection, dispersion, dilution and sorption are taken into account.
- Biosphere: When a contamination of groundwater occurs, the population is exposed to radiation, if it uses the groundwater as drinking water or for foodstuff production.

For the modelling of the radionuclide transport the EMOS module CLAYPOS is used. CLAYPOS simulates a single waste container/borehole for high level waste in low-permeable media. It is based on a one-dimensional geometry. For the modelling of the transport in the overburden the module CHETLIN is used. The transport lengths in the different compartments are summarized in Tab. 2.3. The radioactive decay is taken into account in the whole domain.

Tab. 2.3 Transport lengths [m] in the repository system and EMOS module applied for calculation

Parameter	EMOS	Value
Transport length bentonite	Claypos	10
Transport length clay formation 1	Claypos	80
Transport length clay formation 2	Claypos	250
Transport length overburden	Chetlin	9,394

2.3.1.1.1 Container

For the calculations of the indicators, 5350 containers with spent fuel are regarded. The radionuclide inventory is given in Tab. 2.13. The container is of the type BSK3 made from steel and its geometry is given in Tab. 2.4. Due to the corrosion of the steel by the saline porewater of the clay the container is failing after some time. It is further assumed that the container will collapse under the rock pressure if half of the thickness of the container wall is corroded and a container life-time of 2,500 years was derived. Conservatively, it is further assumed that all containers in the repository fail at the same time.

Tab. 2.4 BSK container data

Parameter	Unit	Value
Length	m	4.90
Diameter	m	0.43
Wall thickness	m	0.05
Void volume	m ³	0.30
Life-time	a	2,500
Container per borehole	[-]	5

The radionuclides are contained in three different components of the fuel and the radionuclides are released from these compartments with different rates. The following three different components are considered; the

- gas space from which the nuclides are released instantaneously after container failure, which is therefore also called instant release fraction,
- metal parts of the fuel element from which mainly activation products are released within several hundreds of years and
- fuel matrix from which the radionuclides are released very slowly over a period of several hundreds of thousands of years.

After the container has failed, the radionuclides are released from the spent fuel. The release rates from the different components are given in Tab. 2.5. The distribution of the elements on the three components in the fuel is given in Tab. 2.6 in per cent of the total inventory. After the radionuclides are released from the fuel they are dissolved in the water volume inside the container. Some radionuclides may be precipitated if they reach their solubility limits within the container volume. Data for the solubility limit for each element (Tab. 2.7) is taken from the Reference Case (pH = 7.25, Eh = -194 mV) for Opalinus Clay /NAG 02/.

Tab. 2.5 Mobilisation rates for different fuel components

Parameter	Unit	Metal parts	Fuel matrix	IRF
Mobilisation rate	[a ⁻¹]	3.6·10 ⁻³	1·10 ⁻⁶	instantaneous

Tab. 2.6 Relative inventory in the different fuel fractions

Element	Unit	Metal parts	Fuel matrix	IRF
C	[%]	72.20	26.41	1.39
Cl	[%]	0	94	6
Co, Ni, Mo, Nb	[%]	99.5	0.47	0.03
Sn	[%]	0	98	2
I, Se	[%]	0	97	3
Cs	[%]	0	96	4
Sr, Sm, Pb	[%]	0	99.9	0.1
Zr	[%]	9.4	86.07	4.53
Tc	[%]	0.1	99.89	0.01
Pd, Cm, Am, Pu, Pa, U, Th, Ac, Np, Ra	[%]	0	99.99	0.01

Tab. 2.7 Solubility limits in [mol/l], “high” denotes no solubility limit

Element	Solubility limit	Element	Solubility limit	Element	Solubility limit
C	high	Mo	1·10 ⁻⁶	Th	7·10 ⁻⁷
Cl	high	Tc	4·10 ⁻⁹	Pa	1·10 ⁻⁸
Co	high	Sn	1·10 ⁻⁸	U	3·10 ⁻⁹
Ca	1·10 ⁻²	I	high	Np	5·10 ⁻⁹
Ni	3·10 ⁻⁵	Cs	high	Pu	5·10 ⁻⁸
Se	5·10 ⁻⁹	Sm	5·10 ⁻⁷	Am	1·10 ⁻⁶
Sr	2·10 ⁻⁵	Pb	2·10 ⁻⁶	Cm	1·10 ⁻⁶
Zr	2·10 ⁻⁹	Ra	2·10 ⁻¹¹		
Nb	3·10 ⁻⁵	Ac	1·10 ⁻⁶		

2.3.1.1.2 Bentonite

As described above, a distance of 10 m is assumed for the transport length in the bentonite. Transport is modelled by diffusion. In addition, the retention by linear sorption according to the Henry isotherm is considered. It is assumed that the drifts are filled with bentonite with a dry density of $\rho = 2,760 \text{ kg/m}^3$. The data for the element-specific transport parameter values (Tab. 2.8) were taken from the Reference Case (pH = 7.25, Eh = -194 mV) for the Opalinus Clay /NAG 02/. The sorption values are given in Tab. 2.8. The effective diffusion coefficient is assumed to be $3 \cdot 10^{-12} \text{ m}^2/\text{s}$ for the elements Cl, Se, Mo, and I occurring in anionic form and $2 \cdot 10^{-10} \text{ m}^2/\text{s}$ for all other elements. In the same way the porosity for Cl, Se, Mo, and I is assumed to be 0.05, whereas 0.36 is se-

lected for all other elements. The pore diffusion coefficient needed as input value for CLAYPOS can be calculated from the effective diffusion coefficient by division by the porosity.

Tab. 2.8 Sorption values [m^3/kg] for the bentonite

Element	Sorption value [m^3/kg]	Element	Sorption value [m^3/kg]	Element	Sorption value [m^3/kg]
C ⁵	0	Mo	0	U	40
Cl	0	Tc	60	Th	60
Ni	0.2	Sn	800	Ra	0.002
Co	0	I	0.0005	Am	20
Se	0	Cs	0.1	Np	60
Sr	0.003	Sm	4	Pb	7
Zr	80	Cm	20	Pa	5
Nb	30	Pu	20	Ac	20

2.3.1.1.3 Clay formations

The diffusive transport length in clay formation 1 is 80 m, in clay formation 2 it is 250 m. No advection is considered in the calculations, therefore no data about the hydraulic gradient and hydraulic permeability of the host rock is given. The density of the clay is $\rho = 2,520 \text{ kg/m}^3$. All other values for the element-specific transport parameter values for the clay formations were taken from the Reference Case (pH = 7.25, Eh = -194 mV) for the Opalinus Clay /NAG 02/. The effective diffusion coefficient is assumed to be $1 \cdot 10^{-12} \text{ m}^2/\text{s}$ for the elements Cl, Se, Mo, and I occurring in anionic form and $1 \cdot 10^{-11} \text{ m}^2/\text{s}$ for all other elements. A porosity of 0.06 is selected for Cl, Se, Mo, and I, whereas 0.12 is used for all other elements. The sorption values are listed in Tab. 2.9.

Tab. 2.9 Sorption values [m^3/kg] for the clay formations

Element	Sorption value	Element	Sorption value	Element	Sorption value
C	0	Mo	0.01	U	20
Cl	0	Tc	50	Th	50
Ni	0.9	Sn	100	Ra	0.0007
Co	0.4	I	0.00003	Am	10
Se	0	Cs	0.5	Np	50
Sr	0.001	Sm	50	Pb	2
Zr	10	Cm	10	Pa	5
Nb	4	Pu	20	Ac	10

⁵ As conservative assumption it was assumed in this study that all C-14 is in organic form, resulting in lower retention parameters.

2.3.1.1.4 Overburden

For the radionuclide transport outside the clay formations advection, dispersion and dilution (Tab. 2.10), sorption (Tab. 2.11) and radioactive decay are taken into account. The parameter values for the aquifer are based on investigations of overlying rocks of salt domes in Northern Germany /BUE 85/. The geological formation along the migration pathway is modelled as a homogeneous medium (porosity 0.2) with an average width of 820 m and a thickness of 45 m /CAD 88/. With a pore velocity of about 6.5 m/a, the resulting natural groundwater flow is 48,000 m³/a.

Tab. 2.10 Transport parameters in the overburden

Parameter	Unit	Value
Natural groundwater flow	m ³ /a	48,000
Dispersion length	m	65
Diffusion coefficient	m ² /a	0.03
Porosity	m	0.2
Rock density	kg/m ³	2,500

Tab. 2.11 Sorption values in [m³/kg] for the overburden

Element	Sorption value	Element	Sorption value	Element	Sorption value
C	0.005	Mo	0.001	Cm	1
Cl	0	Tc	0.007	Ra	0.0009
Co	0.005	Sn	0.2	Ac	0.04
Ni	0.01	I	0.0005	Pa	1
Se	0.0003	Cs	0.001	U	0.02
Sr	0.0005	Sm	1	Th	0.3
Zr	0.1	Pb	0.04	Np	0.03
Nb	0.1	Am	1	Pu	1

2.3.1.1.5 Biosphere

The potential radiation exposure of a grown-up individual was calculated with the module EXCON using dose conversion factors (Tab. 2.12).

Tab. 2.12 Dose conversion factors and decay energies according to /FIR 99/ and /WEA 86/

For daughter nuclides, not calculated, the decay energies are added to the decay energy of the mother nuclide, see /BEC 09/

Nuclide	Dose conversion factor [(Sv/a)/(Bq/m ³)]	Decay energy [MeV]	Nuclide	Dose conversion factor [(Sv/a)/(Bq/m ³)]	Decay energy [MeV]
C-14	$4.6 \cdot 10^{-8}$	0.156	Am-241	$8.0 \cdot 10^{-7}$	5.638
Cl-36	$3.5 \cdot 10^{-8}$	0.709	Np-237	$4.7 \cdot 10^{-6}$	4.959
Co-60	$3.9 \cdot 10^{-6}$	2.824	U-233	$3.9 \cdot 10^{-6}$	4.909
Ni-59	$4.9 \cdot 10^{-9}$	1.072	Pa-233	$8.8 \cdot 10^{-9}$	0.572
Ni-63	$1.1 \cdot 10^{-9}$	0.065	Th-229	$1.7 \cdot 10^{-5}$	5.168
Se-79	$3.4 \cdot 10^{-7}$	0.151	Ra-225	$1.1 \cdot 10^{-7}$	0.357
Sr-90	$1.8 \cdot 10^{-7}$	0.546	Ac-225	$3.7 \cdot 10^{-8}$	5.953
Zr-93	$3.7 \cdot 10^{-8}$	0.091	Pu-242	$9.4 \cdot 10^{-7}$	4.983
Nb-94	$3.1 \cdot 10^{-6}$	2.04	Am-242	$7.6 \cdot 10^{-7}$	0.665
Mo-93	$3.2 \cdot 10^{-7}$	0.405	Pu-238	$7.5 \cdot 10^{-7}$	5.593
Tc-99	$8.8 \cdot 10^{-9}$	0.294	U-238	$7.1 \cdot 10^{-7}$	4.27
Sn-126	$1.6 \cdot 10^{-5}$	0.380	Th-234	$4.8 \cdot 10^{-9}$	0.273
I-129	$5.6 \cdot 10^{-7}$	0.194	U-234	$1.4 \cdot 10^{-6}$	4.856
Cs-135	$5.7 \cdot 10^{-8}$	0.269	Th-230	$3.7 \cdot 10^{-5}$	4.770
Cs-137	$9.5 \cdot 10^{-7}$	1.176	Ra-226	$3.0 \cdot 10^{-5}$	4.871
Sm-151	$3.2 \cdot 10^{-10}$	0.077	Pb-210	$2.3 \cdot 10^{-6}$	0.064
Cm-244	$3.8 \cdot 10^{-7}$	5.902	Po-210	$4.9 \cdot 10^{-6}$	5.407
Pu-240	$9.6 \cdot 10^{-7}$	5.255	Am-243	$2.0 \cdot 10^{-6}$	5.438
U-236	$5.6 \cdot 10^{-7}$	4.572	Pu-239	$9.8 \cdot 10^{-7}$	5.244
Th-232	$1.1 \cdot 10^{-4}$	4.081	U-235	$3.3 \cdot 10^{-6}$	4.679
Ra-228	$2.4 \cdot 10^{-6}$	0.046	Pa-231	$4.0 \cdot 10^{-5}$	5.149
U-232	$5.4 \cdot 10^{-6}$	5.414	Ac-227	$1.0 \cdot 10^{-5}$	0.045
Th-228	$1.3 \cdot 10^{-6}$	5.520	Th-227	$1.9 \cdot 10^{-8}$	6.146
Cm-245	$1.4 \cdot 10^{-6}$	5.623	Ra-223	$1.1 \cdot 10^{-7}$	5.979
Pu-241	$1.8 \cdot 10^{-8}$	0.021			

2.3.1.2 Calculation of indicators

2.3.1.2.1 Proportion of the cumulative released quantity of substance over the safety case period

The first proposed indicator is the ratio of the total released radionuclide quantity from the CRZ to the initially emplaced total amount of radionuclides. For the considered repository system, those radionuclides are taken into account that are released from clay formation 1. Tab. 2.13 gives the released fraction for all radionuclides after one million years. The initially inventory of the containers is taken from /RUE 07/. In contrast to the according table in /RUE 07/, an interim storage time of 30 years was taken into account yielding some differences for some short-lived radionuclides, e. g. Co-60. For the half-life of Se-79, $1.1 \cdot 10^6$ years is used. It has been revised several times. Recent investigations show that it is probably only 295 000 years /JOE 10/. To be conservative, the higher value has been used in safety assessments until now.

The result of the calculation show, that only five radionuclides are released from the CRZ: C-14, Cl-36, Se-79, I-129 and Cs-135. The calculated value for Cs-135 is de facto a zero emission and can be neglected. In order to improve the informative value of this indicator, the cumulative release of the four radionuclides is illustrated over time in Fig. 2.9. Although the safety relevant time period for a safety assessment is one million years, a longer period of time is shown. This is due to the fact, that some of the curves show interesting details even beyond that period of time. To reflect that this period is normally not regarded in long-term safety assessments, the background is shaded for times later than one million years.

Tab. 2.13 Inventory data years after end of operational phase and the released quantities after 10⁶ years

Radionuclide	Half-life [a]	Inventory container [Bq]	Inventory total [Bq]	Inventory total [mol]	Released at CRZ after 10 ⁶ a [mol]	Relation Released / total Inventory [-]
C-14	5.730·10 ³	3.013·10 ¹⁰	1.612·10 ¹⁴	6.982·10 ¹	2.21·10 ⁻¹⁰	3.17·10 ⁻¹²
Cl-36	3.000·10 ⁵	5.493·10 ⁸	2.939·10 ¹²	6.666·10 ¹	2.85·10 ⁻⁵	4.28·10 ⁻⁷
Ni-59	7.500·10 ⁴	9.623·10 ¹⁰	5.148·10 ¹⁴	2.919·10 ³	-	-
Co-60	5.272·10 ⁰	1.178·10 ¹³	6.303·10 ¹⁶	2.512·10 ¹	-	-
Ni-63	1.000·10 ²	1.193·10 ¹³	6.385·10 ¹⁶	4.827·10 ²	-	-
Se-79	1.100·10 ⁶	2.796·10 ¹⁰	1.496·10 ¹⁴	1.244·10 ⁴	7.93·10 ⁻⁵	6.37·10 ⁻⁹
Sr-90	2.864·10 ¹	2.314·10 ¹⁵	1.238·10 ¹⁹	2.681·10 ⁴	-	-
Zr-93	1.500·10 ⁶	1.341·10 ¹¹	7.174·10 ¹⁴	8.136·10 ⁴	-	-
Nb-94	2.000·10 ⁴	9.975·10 ⁴	5.337·10 ⁸	8.189·10 ⁻⁴	-	-
Mo-93	3.500·10 ³	7.121·10 ⁷	3.809·10 ¹¹	1.008·10 ⁻¹	-	-
Tc-99	2.100·10 ⁵	4.065·10 ¹¹	2.175·10 ¹⁵	3.453·10 ⁴	-	-
Sn-126	2.345·10 ⁵	4.964·10 ¹⁰	2.656·10 ¹⁴	4.708·10 ⁴	-	-
I-129	1.570·10 ⁷	3.222·10 ⁹	1.724·10 ¹³	2.046·10 ⁴	3.38·10 ⁻⁵	1.65·10 ⁻⁹
Cs-135	2.000·10 ⁶	3.482·10 ¹⁰	1.863·10 ¹⁴	2.817·10 ⁴	1.80·10 ⁻³³	6.39·10 ⁻³⁸
Cs-137	3.017·10 ¹	3.994·10 ¹⁵	2.137·10 ¹⁹	4.874·10 ⁴	-	-
Sm-151	9.300·10 ¹	9.408·10 ¹³	5.034·10 ¹⁷	3.539·10 ³	-	-
Cm-244	1,810·10 ¹	4.183·10 ¹⁴	2.238·10 ¹⁸	3.062·10 ³	-	-
Pu-240	6.563·10 ³	8.276·10 ¹³	4.428·10 ¹⁷	2.197·10 ⁵	-	-
U-236	2.342·10 ⁷	1.352·10 ¹⁰	7.235·10 ¹³	1.281·10 ⁵	-	-
Th-232	1.41·10 ¹⁰	2.143·10 ¹	1.147·10 ⁵	1.218·10 ⁻¹	-	-
Ra-228	5.750·10 ⁰	1.568·10 ¹	8.390·10 ⁴	3.65·10 ⁻¹¹	-	-
Cm-245	8.500·10 ³	3.479·10 ¹¹	1.861·10 ¹⁵	1.196·10 ³	-	-
Pu-241	1.435·10 ¹	5.279·10 ¹⁵	2.824·10 ¹⁹	3.064·10 ⁴	-	-
Am-241	4.322·10 ²	5.972·10 ¹⁴	3.195·10 ¹⁸	1.044·10 ⁵	-	-
Np-237	2.144·10 ⁶	2.468·10 ¹⁰	1.320·10 ¹⁴	2.140·10 ⁴	-	-
U-233	1.592·10 ⁵	6.357·10 ⁶	3.401·10 ¹⁰	5.019·10 ⁻¹	-	-
Th-229	7.880·10 ³	2.221·10 ⁴	1.188·10 ⁸	7.078·10 ⁻⁵	-	-
Pu-242	3.750·10 ⁵	6.036·10 ¹¹	3.229·10 ¹⁵	9.155·10 ⁴	-	-
Am-242	1.410·10 ³	2.925·10 ¹¹	1.565·10 ¹⁵	1.668·10 ²	-	-
Pu-238	8.774·10 ¹	4.058·10 ¹⁴	2.171·10 ¹⁸	1.440·10 ⁴	-	-
U-238	4.468·10 ⁹	1.953·10 ¹⁰	1.045·10 ¹⁴	3.529·10 ⁷	-	-
U-234	2.455·10 ⁵	9.091·10 ¹⁰	4.864·10 ¹⁴	9.027·10 ³	-	-
Th-230	7.540·10 ⁴	2.077·10 ⁷	1.111·10 ¹¹	6.334·10 ⁻¹	-	-
Ra-226	1.600·10 ³	1.303·10 ⁵	6.969·10 ⁸	8.430·10 ⁻⁵	-	-
Pb-210	2.230·10 ¹	3.197·10 ⁴	1.711·10 ⁸	2.884·10 ⁻⁷	-	-
Cm-243	2.910·10 ¹	8.989·10 ¹¹	4.809·10 ¹⁵	1.058·10 ¹	-	-
Am-243	7.370·10 ³	5.730·10 ¹²	3.065·10 ¹⁶	1.708·10 ⁴	-	-
Pu-239	2.411·10 ⁴	3.464·10 ¹³	1.853·10 ¹⁷	3.378·10 ⁵	-	-
U-235	7.038·10 ⁸	7.978·10 ⁸	4.268·10 ¹²	2.271·10 ⁵	-	-
Pa-231	3.276·10 ⁴	2.771·10 ⁶	1.482·10 ¹⁰	3.671·10 ⁻²	-	-
Ac-227	2.177·10 ¹	1.234·10 ⁶	6.605·10 ⁹	1.087·10 ⁻⁵	-	-
Total		1.325·10 ¹⁶	7.090·10 ¹⁹	3.676·10 ⁷	1.42·10 ⁻⁴	3.85·10 ⁻¹²

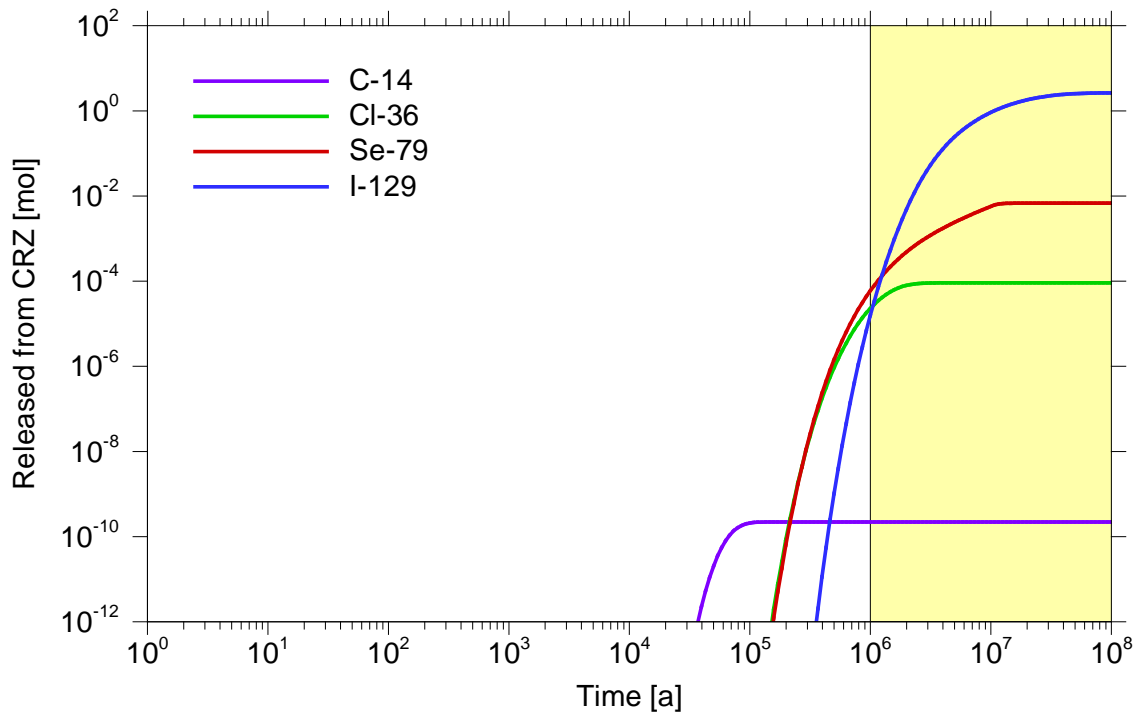


Fig. 2.9 The cumulative released quantities from the CRZ

Tab. 2.13 and Fig. 2.9 illustrate that the released quantities are only a small fraction of the emplaced waste. The relation of released to total inventory for the considered repository after one million years is $3.85 \cdot 10^{-12}$. As stated above, this does not indicate the potential health hazard of the released radionuclides.

Although the cumulated released quantities increase by several orders of magnitude within the next ten million years after the assessment period, the overall value is 2.64 mol, which is still far below the yardstick of 0.01 mol-% of $3.676 \cdot 10^7$ mol. The reason is that the waste from spent fuel elements in large parts consists of uranium, which is strongly sorbed in the bentonite and the clay formation 1 and not released out of the CRZ.

2.3.1.2.2 Concentrations of released uranium and thorium in the porewater at the CRZ boundary

According to the results given in Tab. 2.13, only C-14, Cl-36, Se-79 and I-129 are released from the CRZ. Even after 10^8 years no actinides are released due to the low solubilities of their species in reducing conditions and the high sorption values of the bentonite and the clay formation 1. This shows the high retardation capacity of the clay barriers towards strong sorbing actinides.

2.3.1.2.3 Contribution to power density in the porewater at the CRZ boundary

The indicator illustrates the contribution to the natural power density by the released radionuclides. Starting point for the calculation of this safety indicator is the calculated activity concentration in the groundwater at the boundary of the CRZ. Actually, it can be the activity concentration in any subsystem of the repository system, but it is proposed in /BAL 07/ to use the power density in the porewater and in the soil matrix in the deeper aquifer system. The calculation of the power density is carried out with a simple weighting scheme by multiplying the activity concentration of every radionuclide [Bq/m³] in the outer rim of porewater of clay formation 1 with its decay energy. This operation yields a power density p (power per volume, [MeV/(s·m³)]). The decay energies applied to calculate the power density are derived in /BEC 09/. Tab. 2.12 gives the decay parameters for the four considered radionuclides, which are released from the CRZ.

For a repository system in a clay formation, where only radionuclides are released with low β -decay energies, the contribution to power density is only a small percentage of the natural power density in porewater, which is dominated by the isotopes of Uranium and Thorium and their daughter nuclides (mostly α -decay with about 50 times higher decay energies).

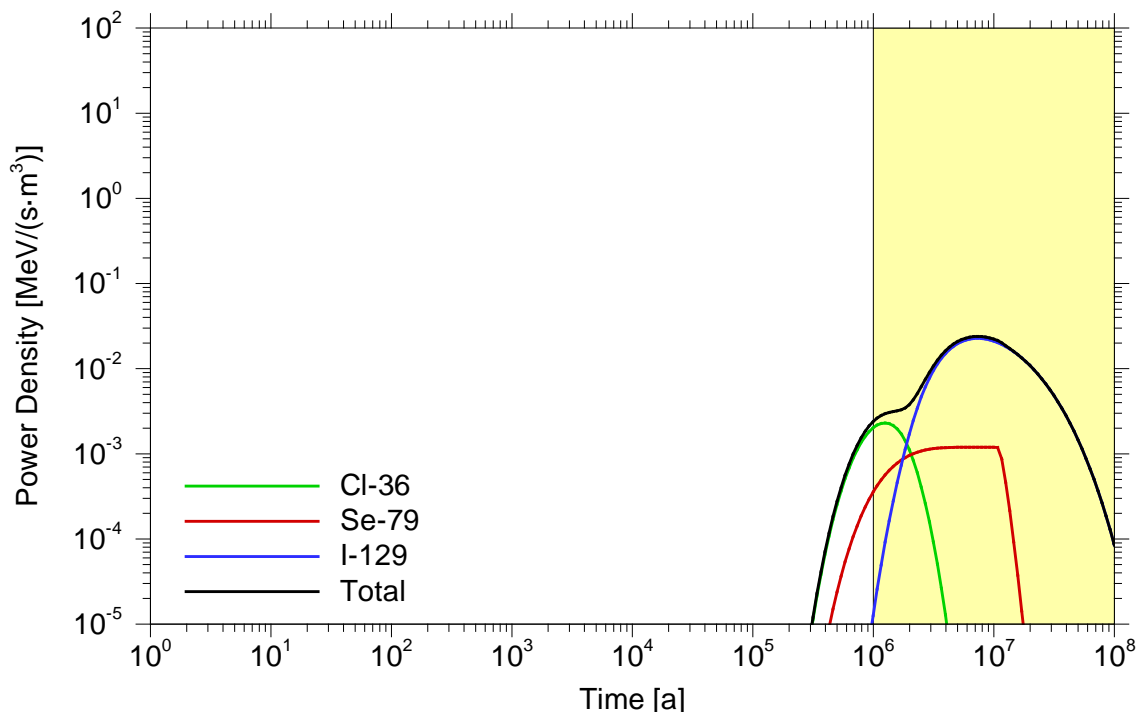


Fig. 2.10 The contribution to power density in porewater at the CRZ boundary

Fig. 2.10 shows the temporal evolution of the power density caused by radionuclides released from the repository. The dominating radionuclides are Cl-36 and I-129. The relatively high decay energy of Cl-36 amplifies its peak compared to calculations with ingestion dose coefficients or dose conversion factors. The maximum value of the calculated power density is $0.0026 \text{ MeV}/(\text{s}\cdot\text{m}^3)$ at one million years and is dominated by Cl-36. The highest calculated value is $0.024 \text{ MeV}/(\text{s}\cdot\text{m}^3)$ after about seven million years and is dominated by I-129.

2.3.1.2.4 Contribution to radiotoxicity in groundwater

The contribution to radiotoxicity in groundwater is calculated from the radionuclide flux through the boundary of the CRZ. This flux flows in a virtual water body used by a group of humans. The virtual water body comprises the annual water consumption of this group (see section 2.3). To assess the radiological consequences of the radionuclide concentrations in this water body the same dose conversion factors are applied as for the calculation of the individual dose (see Tab. 2.12).

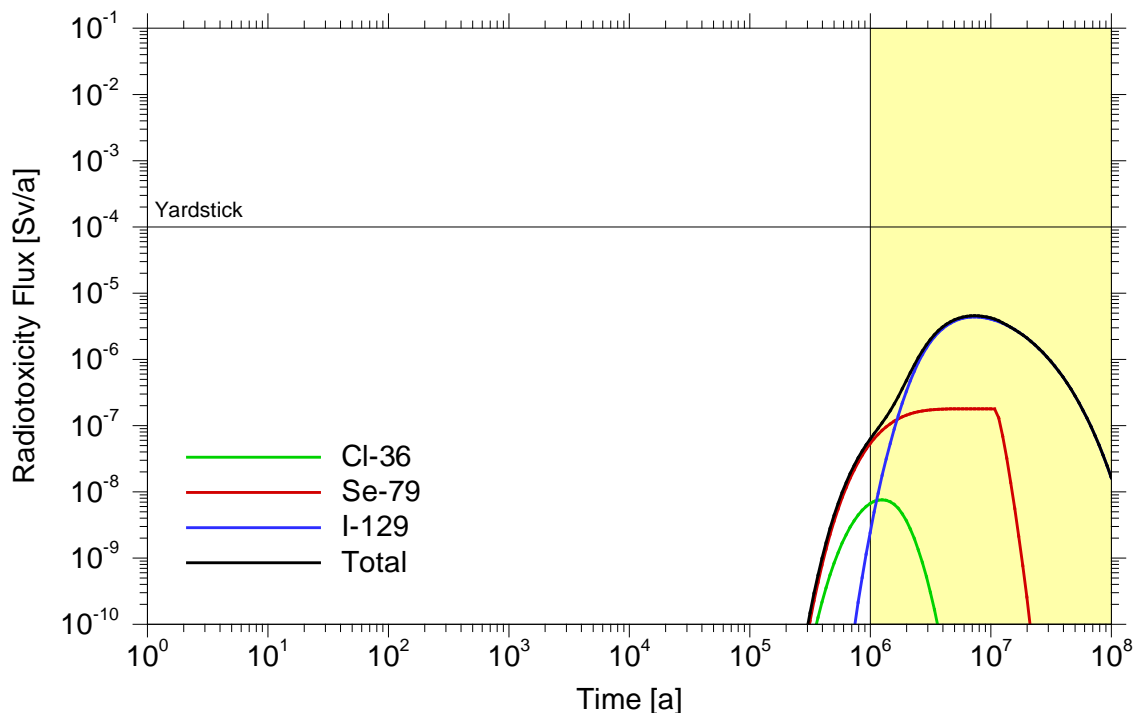


Fig. 2.11 The contribution to radiotoxicity at the CRZ

Fig. 2.11 illustrates that within 10^6 years the contribution to radiotoxicity is dominated by Se-79. The highest value is at 10^6 years with a radiotoxicity flux of about 10^{-7} Sv/a . At

later times the radiotoxicity flux is dominated by I-129. The highest value is at $7.3 \cdot 10^6$ years with a peak value of $4.4 \cdot 10^{-6}$ Sv/a.

2.3.1.2.5 Radionuclide concentration in the usable water near the surface

Only C-14, Cl-36, Se-79 and I-129 are released from the CRZ. For none of these radionuclides reference values in /BAL 07/ are given. Even after 10^8 years no actinides are released due to the low solubilities of their species in reducing conditions and the high sorption values of the bentonite and the clay formation 1. This shows the high retardation capacity of the clay barriers towards strong sorbing actinides.

2.3.1.2.6 Effective individual dose

Fig. 2.12 illustrates that for the considered repository system no additional effective dose occurs in one million years. The only radionuclide, which is released to the biosphere, is I-129 with a maximum dose of $3.5 \cdot 10^{-8}$ Sv/a. The low indicator value is due to the very long transport time in the compartment clay formation 2 with a thickness of 250 m. During transport of more than 10^7 years, the concentrations of Cl-36 and Se-79 are reduced by several orders of magnitude due to radioactive decay.

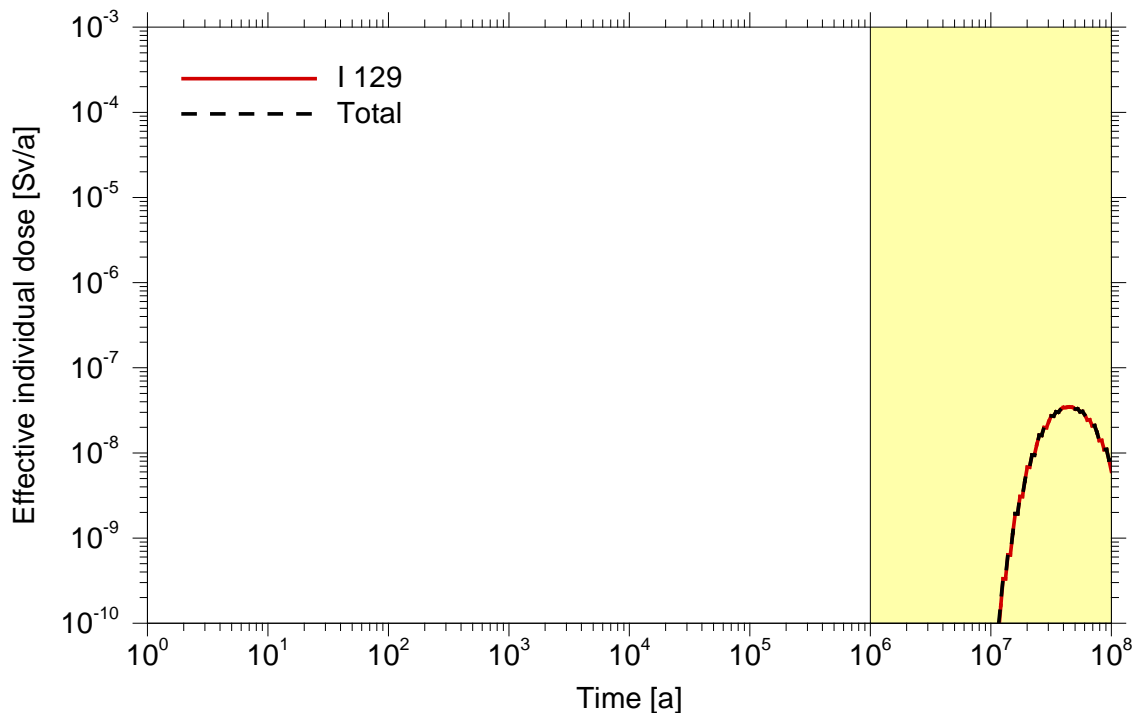


Fig. 2.12 The effective individual dose in the biosphere

2.3.2 Repository in a salt formation

2.3.2.1 Description of the repository system

The applied layout for the salt case is a variant of the disposal concept introduced in the ISIBEL project /BUH 08a/, which was developed for a repository in a salt dome with a sedimentary coverage of about 300 m in Northern Germany. The differences against this concept are referring to:

- The waste storage capacity: the repository was enlarged, to accommodate all the radioactive waste (spent fuel and reprocessed waste) arising in Germany.
- The repository layout: plugs of crushed salt instead of borehole sealings.

The repository concept comprises emplacement fields for different types of waste in different parts of the mine. The compartment structure used is shown in Fig. 2.13. It contains the following compartments:

- Repository: The repository is located in a depth of 870 m below surface (disposal level) in a homogeneous rock salt layer within the salt dome. The structure of the repository model consists of an access shaft, a central field and two access drifts, which connect the central field with a horizontal network of transfer drifts. Drift seals are located between the central field and the access drifts. From the inner transfer drifts boreholes are drilled to a depth of 300 m, 290 m are intended for emplacing the waste canister and 10 m for a plug. In the applied concept crushed salt is applied for backfilling of all open spaces and for the borehole plug.
- Overburden: The overburden consists of a sequence of aquifers typical for Northern Germany.
- Biosphere: When a contamination of groundwater occurs, the population is exposed to radiation, if it uses the groundwater as drinking water or for foodstuff production.

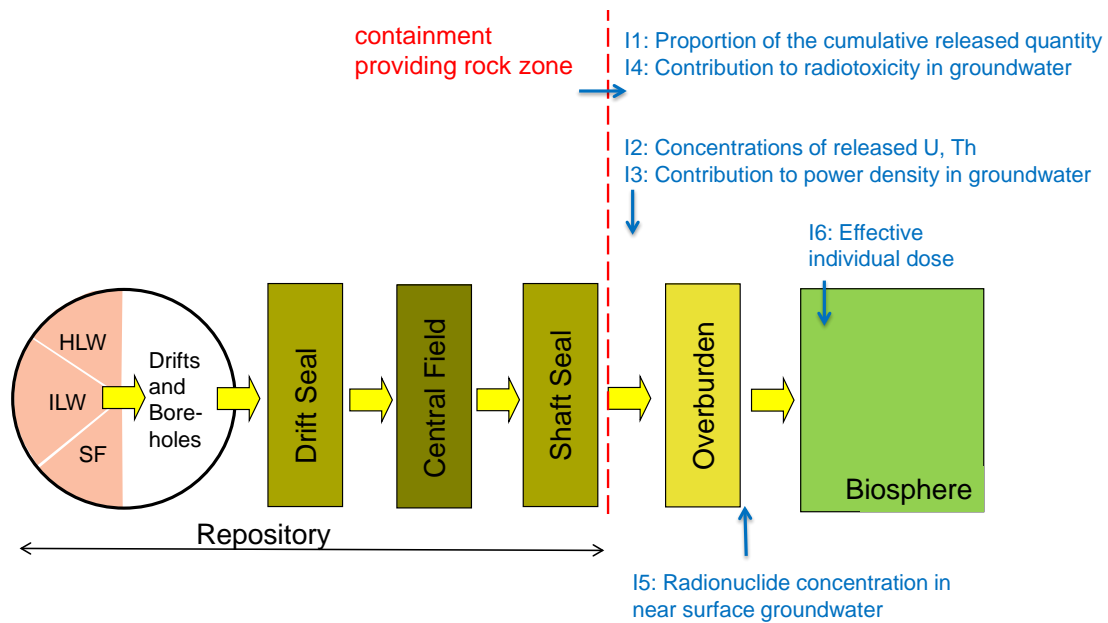


Fig. 2.13 Compartments of the generic repository system and the locations of the CRZ and the indicator assessment (I1-I6)

The strategy of the safety concept is the containment of the emplaced waste by the tight and long-term stable rock salt formation. The main engineered barriers, which prevent water ingress in the repository, are the shaft seal and the drift seals. The function of these engineered barriers is to reseal the disturbed salt formation after the construction of the repository.

For the simulation of the radionuclide transport in the different compartments the EMOS modules LOPOS, CHETLIN and EXCON/EXMAS were used. For the calculation of the indicators, it is assumed that the crushed salt in the backfill and the borehole plug are compacting down to a porosity of 1 %. This porosity then remains for the whole assessment period. The initial permeability of 10^{-18} m^2 of the shaft and the drift seals remains unchanged for 1000 years, and afterwards it increases by four orders of magnitude.

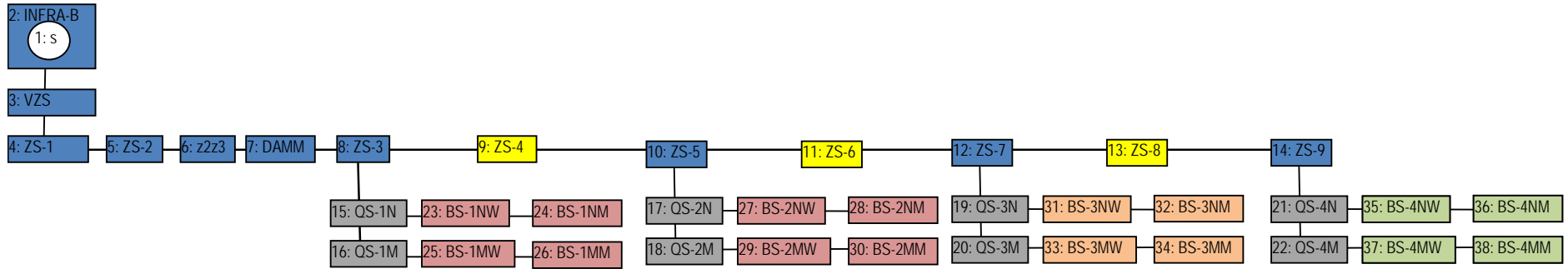
2.3.2.1.1 Repository

The repository is able to emplace the total waste volumes of HLW, which are expected to accumulate in Germany /BUH 08b/. Considered types of waste are spent fuel rods (SF), vitrified waste (HLW) and compacted constituents of spent fuel elements (ILW). The corresponding containers are thin-walled canisters (type BSK 3) for SF with a

length of 4.98 m and a radius of 0.22 m, HLW canisters (type CSD-V, length = 1.34 m, radius = 0.22 m) and ILW canisters (type CSD-C, same geometry as CSD-V). Altogether 6,960 SF canisters, 3,225 HLW canisters and 7,455 ILW canisters are emplaced in the conceptual repository. The inventories are given in Tab. 2.14.

The failure of the canisters starts as soon as brine flows into a borehole with emplaced waste. For all canister types a uniformly distributed canister lifetime is assumed in the range between 0 and 10 years. The release from the waste matrix starts immediately after failure of the canister. Different mobilisation rates are used for the three types of waste. The corresponding mobilisation approaches for SF, HLW and ILW are discussed in /BUH 08/. All further project relevant general input data related to the modelling of the repository are given in Tab. 2.15.

The mobilised radionuclides are dissolved in the available water volume of the borehole. The radionuclides may precipitate if they reach their solubility limits within this water volume. Conservative solubility limits (see Tab. 2.16) are used for the mobilisation process. Neither temporal change nor spatial differences in chemical conditions are considered. Sorption is disregarded for the radionuclide transport in the repository. The contaminant transport in the repository (the drifts and the central field) is not influenced by solubility limits.



Disposal galleries:

	Spent Fuel (SF)
	High-level waste (HAW)
	Intermediate-level waste (ILW)

Fig. 2.14 Plane view of the repository concept

The vertical disposal boreholes drilled in the floor of the disposal drifts are not shown. Flank galleries in blue. Connecting drifts in yellow. Access drifts in grey

Tab. 2.14 Radionuclide inventory /BUH 08b/

Nuclide	Half life [a]	SF [Bq/can.]	HLW [Bq/can.]	ILW [Bq/can.]	Total [Bq]	Total [mol]
C-14	$5.730 \cdot 10^3$	$7.37 \cdot 10^{10}$	-	$1.4 \cdot 10^{10}$	$6.17 \cdot 10^{14}$	$2.67 \cdot 10^2$
Cl-36	$3.000 \cdot 10^5$	$9.77 \cdot 10^{08}$	-	-	$6.80 \cdot 10^{12}$	$1.54 \cdot 10^2$
Co-60	$5.272 \cdot 10^0$	$1.63 \cdot 10^{15}$	$3.32 \cdot 10^{13}$	$7.71 \cdot 10^{13}$	$1.21 \cdot 10^{19}$	$4.81 \cdot 10^3$
Ni-59	$7.500 \cdot 10^4$	$8.14 \cdot 10^{11}$	$7.00 \cdot 10^{07}$	-	$5.66 \cdot 10^{15}$	$3.21 \cdot 10^4$
Ni-63	$1.000 \cdot 10^2$	$1.16 \cdot 10^{14}$	$9.50 \cdot 10^{09}$	$2.71 \cdot 10^{13}$	$1.01 \cdot 10^{18}$	$7.61 \cdot 10^3$
Se-79	$1.100 \cdot 10^6$	$2.98 \cdot 10^{10}$	$1.72 \cdot 10^{10}$	$5.51 \cdot 10^{07}$	$2.63 \cdot 10^{14}$	$2.19 \cdot 10^4$
Sr-90	$2.864 \cdot 10^1$	$5.99 \cdot 10^{15}$	$3.23 \cdot 10^{15}$	$1.40 \cdot 10^{13}$	$5.22 \cdot 10^{19}$	$1.13 \cdot 10^5$
Zr-93	$1.500 \cdot 10^6$	$1.58 \cdot 10^{11}$	$8.92 \cdot 10^{10}$	$8.60 \cdot 10^{09}$	$1.45 \cdot 10^{15}$	$1.65 \cdot 10^5$
Nb-94	$2.000 \cdot 10^4$	$1.36 \cdot 10^{11}$	$8.18 \cdot 10^{06}$	-	$9.47 \cdot 10^{14}$	$1.43 \cdot 10^3$
Mo-93	$3.500 \cdot 10^3$	$6.95 \cdot 10^{09}$	$6.47 \cdot 10^{06}$	-	$4.84 \cdot 10^{13}$	$1.28 \cdot 10^1$
Tc-99	$2.100 \cdot 10^5$	$1.04 \cdot 10^{12}$	$6.19 \cdot 10^{11}$	$2.31 \cdot 10^{09}$	$9.22 \cdot 10^{15}$	$1.46 \cdot 10^5$
Pd-107	$6.500 \cdot 10^6$	$8.33 \cdot 10^{09}$	$4.65 \cdot 10^{09}$	-	$7.30 \cdot 10^{13}$	$3.59 \cdot 10^4$
Sn-126	$2.345 \cdot 10^5$	$4.47 \cdot 10^{10}$	$2.43 \cdot 10^{10}$	$1.51 \cdot 10^{06}$	$3.89 \cdot 10^{14}$	$6.90 \cdot 10^3$
I-129	$1.570 \cdot 10^7$	$2.44 \cdot 10^{09}$	$1.65 \cdot 10^{04}$	$5.31 \cdot 10^{06}$	$1.70 \cdot 10^{13}$	$2.02 \cdot 10^4$
Cs-135	$2.000 \cdot 10^6$	$2.45 \cdot 10^{10}$	$1.62 \cdot 10^{10}$	$7.11 \cdot 10^{07}$	$2.23 \cdot 10^{14}$	$3.37 \cdot 10^4$
Cs-137	$3.017 \cdot 10^1$	$8.60 \cdot 10^{15}$	$4.67 \cdot 10^{15}$	$1.51 \cdot 10^{13}$	$7.50 \cdot 10^{19}$	$1.71 \cdot 10^5$
Sm-151	$9.300 \cdot 10^1$	$2.00 \cdot 10^{13}$	$1.53 \cdot 10^{13}$	$6.00 \cdot 10^{10}$	$1.89 \cdot 10^{17}$	$1.33 \cdot 10^3$
Th-series						
Pu-244	$8.000 \cdot 10^7$	$6.95 \cdot 10^{04}$	$1.12 \cdot 10^{02}$	-	$4.84 \cdot 10^{08}$	$2.93 \cdot 10^0$
Cm-244	$1.810 \cdot 10^1$	$3.46 \cdot 10^{14}$	$1.13 \cdot 10^{14}$	$9.51 \cdot 10^{10}$	$2.77 \cdot 10^{18}$	$3.79 \cdot 10^3$
Pu-240	$6.563 \cdot 10^3$	$3.83 \cdot 10^{13}$	$7.61 \cdot 10^{10}$	$5.20 \cdot 10^{10}$	$2.67 \cdot 10^{17}$	$1.33 \cdot 10^5$
U-236	$2.342 \cdot 10^7$	$1.91 \cdot 10^{10}$	$6.63 \cdot 10^{07}$	-	$1.33 \cdot 10^{14}$	$2.35 \cdot 10^5$
Th-232	$1.41 \cdot 10^{10}$	$2.10 \cdot 10^{00}$	$5.65 \cdot 10^{00}$	-	$3.28 \cdot 10^{04}$	$3.49 \cdot 10^{-2}$
U-232	$6.890 \cdot 10^1$	$1.24 \cdot 10^{09}$	$1.11 \cdot 10^{07}$	-	$8.65 \cdot 10^{12}$	$3.76 \cdot 10^{-3}$
Np-series						
Cm-245	$8.500 \cdot 10^3$	$2.72 \cdot 10^{10}$	$1.11 \cdot 10^{10}$	-	$2.25 \cdot 10^{14}$	$1.45 \cdot 10^2$
Pu-241	$1.435 \cdot 10^1$	$9.27 \cdot 10^{15}$	$1.27 \cdot 10^{13}$	$1.00 \cdot 10^{13}$	$6.47 \cdot 10^{19}$	$7.01 \cdot 10^4$
Am-241	$4.322 \cdot 10^2$	$1.03 \cdot 10^{13}$	$6.20 \cdot 10^{13}$	$3.51 \cdot 10^{10}$	$2.72 \cdot 10^{17}$	$8.89 \cdot 10^3$
Np-237	$2.144 \cdot 10^6$	$2.63 \cdot 10^{10}$	$1.66 \cdot 10^{10}$	$7.20 \cdot 10^{06}$	$2.37 \cdot 10^{14}$	$3.83 \cdot 10^4$
U-233	$1.592 \cdot 10^5$	$4.12 \cdot 10^{06}$	$1.83 \cdot 10^{04}$	-	$2.87 \cdot 10^{10}$	$3.46 \cdot 10^{-1}$
Th-229	$7.880 \cdot 10^3$	$1.27 \cdot 10^{04}$	$6.63 \cdot 10^{03}$	-	$9.08 \cdot 10^{08}$	$5.41 \cdot 10^{-4}$
U-series						
Cm-246	$4.730 \cdot 10^3$	$6.81 \cdot 10^{10}$	$2.27 \cdot 10^{10}$	-	$5.47 \cdot 10^{14}$	$1.96 \cdot 10^2$
Pu-242	$3.750 \cdot 10^5$	$1.84 \cdot 10^{11}$	$3.08 \cdot 10^{08}$	$2.80 \cdot 10^{08}$	$1.29 \cdot 10^{15}$	$3.64 \cdot 10^4$
Am-242	$1.410 \cdot 10^2$	$3.06 \cdot 10^{11}$	$1.55 \cdot 10^{11}$	-	$2.63 \cdot 10^{15}$	$2.80 \cdot 10^1$
U-238	$4.468 \cdot 10^9$	$1.86 \cdot 10^{10}$	$6.67 \cdot 10^{07}$	-	$1.30 \cdot 10^{14}$	$4.37 \cdot 10^7$
Pu-238	$8.774 \cdot 10^1$	$2.61 \cdot 10^{14}$	$4.28 \cdot 10^{11}$	$4.71 \cdot 10^{11}$	$1.82 \cdot 10^{18}$	$1.21 \cdot 10^4$
U-234	$2.455 \cdot 10^5$	$4.97 \cdot 10^{10}$	$2.10 \cdot 10^{08}$	-	$3.46 \cdot 10^{14}$	$6.43 \cdot 10^3$
Th-230	$7.540 \cdot 10^4$	$9.61 \cdot 10^{05}$	$3.17 \cdot 10^{06}$	-	$1.69 \cdot 10^{10}$	$9.63 \cdot 10^{-2}$
Ra-226	$1.600 \cdot 10^3$	$1.27 \cdot 10^{03}$	$6.25 \cdot 10^{03}$	-	$2.90 \cdot 10^{07}$	$3.50 \cdot 10^{-6}$
Ac-series						
Am-243	$7.370 \cdot 10^3$	$2.13 \cdot 10^{12}$	$1.05 \cdot 10^{12}$	$3.51 \cdot 10^{08}$	$1.82 \cdot 10^{16}$	$1.02 \cdot 10^4$
Pu-239	$2.411 \cdot 10^4$	$2.10 \cdot 10^{13}$	$4.54 \cdot 10^{10}$	$3.00 \cdot 10^{10}$	$1.47 \cdot 10^{17}$	$2.67 \cdot 10^5$
U-235	$7.038 \cdot 10^8$	$7.77 \cdot 10^{08}$	$3.51 \cdot 10^{06}$	-	$5.42 \cdot 10^{12}$	$2.88 \cdot 10^5$
Pa-231	$3.276 \cdot 10^4$	$1.98 \cdot 10^{06}$	$1.22 \cdot 10^{06}$	-	$1.78 \cdot 10^{10}$	$4.40 \cdot 10^{-2}$

Tab. 2.15 General data for the modelling of the repository

Parameter	Dimension	Value
Average rock density	kg/m ³	2,300
Average fluid density	kg/m ³	1,200
Depth of repository (= reference level)	m b. s.	870
Rock temperature (reference level)	K	310
Geothermal gradient	K/m	0.03
Rock pressure (reference level)	MPa	18
Hydrostatic pressure (reference level)	MPa	10
Reference convergence rate	1/a	0.01
Initial permeability of the seals	m ²	10 ⁻¹⁸
Permeability of the seals after 10 ³ a	m ²	10 ⁻¹⁴
Lifetime of shaft seal	a	1000
Permeability of the shaft seal (after expiration of lifetime)	m ²	10 ⁻¹⁴
Initial plug porosity	-	0.3
Initial backfilling porosity	-	0.3
Final backfilling porosity	-	0.01

Tab. 2.16 Solubility limits in the emplacement areas [mol/m³]

Element	Solubility limits	Element	Solubility limits
C	1.0·10 ⁻¹	I	5.0·10 ⁻³
Cl	5.0·10 ⁻³	Cs	5.0·10 ⁻³
Co	5.0·10 ⁻³	Sm	1.0·10 ⁻¹
Ni	1.0·10 ⁻¹	Eu	5.0·10 ⁻³
Se	1.0·10 ⁻¹	Pb	5.0·10 ⁻³
Rb	5.0·10 ⁻³	Ra	1.0·10 ⁻³
Sr	1.0·10 ⁰	Th	1.0·10 ⁻³
Zr	1.0·10 ⁻¹	Pa	1.0·10 ⁻³
Cd	5.0·10 ⁻³	U	1.0·10 ⁻¹
Nb	1.0·10 ⁻¹	Np	1.0·10 ⁻²
Mo	1.0·10 ⁻¹	Pu	1.0·10 ⁻³
Tc	1.0·10 ⁻¹	Am	1.0·10 ⁻²
Pd	1.0·10 ⁻¹	Cm	1.0·10 ⁻²
Sn	1.0·10 ⁻¹		

2.3.2.1.2 Overburden

see section 2.3.1.1.4.

2.3.2.1.3 Biosphere

see section 2.3.1.1.5

2.3.2.2 Calculation of indicators

2.3.2.2.1 Proportion of the cumulative released quantity of substance over the safety case period

This indicator requires a comparison of the initially emplaced amount of radionuclides to the released quantities from the CRZ to. For the considered repository system the radionuclides are taken into account, which are released from the shaft seal. The initially inventory of the containers in Tab. 2.17 considers an interim storage time of 30 years. Therefore there are some differences for some short-lived radionuclides, e. g. Co-60, in comparison to Tab. 2.14.

Tab. 2.17 illustrates that the released quantities are only a small fraction of the emplaced waste. The relation of released to total inventory for the considered repository after one million years is $8.48 \cdot 10^{-10}$. The most important contributions stem from the mobile long-living radionuclides I-129 and Cs-135. As stated above, this does not indicate the potential health hazard of the released radionuclides.

Tab. 2.17 Inventory data after end of operational phase and released quantities after 10⁶ years

Nuclide	Half-life [a]	Inventory total [Bq]	Inventory total [mol]	Released 10 ⁶ a [mol]	Relation [-]
C-14	5.73 · 10 ³	6.15 · 10 ¹⁴	2.67 · 10 ²	-	-
Cl-36	3.00 · 10 ⁵	6.80 · 10 ¹²	1.54 · 10 ²	1.90 · 10 ⁻⁵	1.23 · 10 ⁻⁷
Co-60	5.27 · 10 ⁰	2.33 · 10 ¹⁷	9.30 · 10 ¹	-	-
Ni-59	7.50 · 10 ⁴	5.66 · 10 ¹⁵	3.21 · 10 ⁴	3.70 · 10 ⁻⁶	1.15 · 10 ⁻¹⁰
Ni-63	1.00 · 10 ²	8.17 · 10 ¹⁷	6.17 · 10 ³	-	-
Se-79	1.10 · 10 ⁶	2.63 · 10 ¹⁴	2.19 · 10 ⁴	4.50 · 10 ⁻⁴	2.06 · 10 ⁻⁸
Sr-90	2.86 · 10 ¹	2.53 · 10 ¹⁹	5.47 · 10 ⁴	-	-
Zr-93	1.50 · 10 ⁶	1.45 · 10 ¹⁹	1.65 · 10 ⁵	4.95 · 10 ⁻⁶	3.01 · 10 ⁻¹¹
Nb-94	2.00 · 10 ⁴	9.46 · 10 ¹⁴	1.43 · 10 ³	-	-
Mo-93	3.50 · 10 ³	4.81 · 10 ¹³	1.27 · 10 ¹	-	-
Tc-99	2.10 · 10 ⁵	9.22 · 10 ¹⁵	1.46 · 10 ⁵	9.10 · 10 ⁻⁵	6.23 · 10 ⁻¹⁰
Pd-107	6.50 · 10 ⁶	7.30 · 10 ¹³	3.58 · 10 ⁴	6.24 · 10 ⁻⁴	1.74 · 10 ⁻⁸
Sn-126	2.35 · 10 ⁵	3.89 · 10 ¹⁴	6.90 · 10 ³	1.11 · 10 ⁻⁴	1.61 · 10 ⁻⁸
I-129	1.57 · 10 ⁷	1.70 · 10 ¹³	2.01 · 10 ⁴	1.84 · 10 ⁻²	9.11 · 10 ⁻⁷
Cs-135	2.00 · 10 ⁶	2.23 · 10 ¹⁴	3.37 · 10 ⁴	1.81 · 10 ⁻²	5.38 · 10 ⁻⁷
Cs-137	3.02 · 10 ¹	3.77 · 10 ¹⁹	8.58 · 10 ⁴	-	-
Sm-151	9.30 · 10 ¹	1.51 · 10 ¹⁷	1.06 · 10 ³	-	-
Pu-244	8.00 · 10 ⁷	4.84 · 10 ⁸	2.93 · 10 ⁰	-	-
Cm-244	1.81 · 10 ¹	8.79 · 10 ¹⁷	1.20 · 10 ³	-	-
Pu-240	6.56 · 10 ³	2.72 · 10 ¹⁷	1.35 · 10 ⁵	-	-
U-236	2.34 · 10 ⁷	1.33 · 10 ¹⁴	2.36 · 10 ⁵	5.34 · 10 ⁻⁶	2.27 · 10 ⁻¹¹
Th-232	1.41 · 10 ¹⁰	2.30 · 10 ⁵	2.44 · 10 ⁻¹	3.04 · 10 ⁻⁶	1.25 · 10 ⁻⁵
U-232	6.89 · 10 ¹	6.39 · 10 ¹²	3.33 · 10 ⁻²	-	-
Cm-245	8.50 · 10 ³	2.25 · 10 ¹⁴	1.44 · 10 ²	-	-
Pu-241	1.44 · 10 ¹	1.52 · 10 ¹⁹	1.65 · 10 ⁴	-	-
Am-241	4.32 · 10 ²	1.85 · 10 ¹⁸	6.05 · 10 ⁴	-	-
Np-237	2.14 · 10 ⁶	2.49 · 10 ¹⁴	4.03 · 10 ⁴	5.45 · 10 ⁻⁵	1.35 · 10 ⁻⁹
U-233	1.59 · 10 ⁵	6.02 · 10 ¹⁰	7.24 · 10 ⁻¹	3.93 · 10 ⁻⁶	5.42 · 10 ⁻⁶
Th-229	7.88 · 10 ³	1.02 · 10 ⁹	6.09 · 10 ⁻⁴	1.01 · 10 ⁻⁷	1.65 · 10 ⁻⁴
Cm-246	4.73 · 10 ³	5.45 · 10 ¹⁴	1.95 · 10 ²	-	-
Pu-242	3.75 · 10 ⁵	1.29 · 10 ¹⁵	3.64 · 10 ⁴	2.01 · 10 ⁻⁶	5.51 · 10 ⁻¹¹
Am-242	1.41 · 10 ²	2.27 · 10 ¹⁵	2.42 · 10 ¹	-	-
U-238	4.47 · 10 ⁹	1.30 · 10 ¹⁴	4.37 · 10 ⁷	6.57 · 10 ⁻⁴	1.50 · 10 ⁻¹¹
Pu-238	8.77 · 10 ¹	1.44 · 10 ¹⁸	9.53 · 10 ³	-	-
U-234	2.46 · 10 ⁵	4.84 · 10 ¹⁴	8.97 · 10 ³	-	-
Th-230	7.54 · 10 ⁴	1.32 · 10 ¹¹	7.52 · 10 ⁻¹	-	-
Ra-226	1.60 · 10 ³	9.52 · 10 ⁸	1.15 · 10 ⁻⁴	-	-
Am-243	7.37 · 10 ³	1.82 · 10 ¹⁶	1.01 · 10 ⁴	-	-
Pu-239	2.41 · 10 ⁴	1.46 · 10 ¹⁷	2.67 · 10 ⁵	-	-
U-235	7.04 · 10 ⁸	5.42 · 10 ¹²	2.88 · 10 ⁵	9.90 · 10 ⁻⁶	3.44 · 10 ⁻¹¹
Pa-231	3.28 · 10 ⁴	2.12 · 10 ¹⁰	5.24 · 10 ⁻²	-	-
Total		8.40 · 10 ¹⁹	4.54 · 10 ⁷	3.85 · 10 ⁻²	8.48 · 10 ⁻¹⁰

2.3.2.2.2 Concentrations of released uranium and thorium in the porewater at the CRZ boundary

This indicator monitors the change of uranium and thorium concentrations in the geosphere.

Since at very long times the convergence process is completed, radionuclide transport in the repository is dominated by diffusion. A significant uranium release occurs very late, but the overall elemental concentration of Uranium exceeds the yardstick of 1 $\mu\text{g/l}$ (Fig. 2.15). The concentration is dominated by U-238. Although the safety relevant time period for a safety assessment is one million years, a longer period of time is shown. This is due to the fact, that some of the curves show interesting details even beyond that period of time. To reflect that this period is normally not regarded in long-term safety assessments, the background is shaded for times later than one million years.

Similar result is yielded for thorium, even though for the assessment period the concentration does not cross the yardstick (Fig. 2.16). Here, the concentration is dominated by Th-232. The concentrations at the repository exit do not take into account the dilution in the aquifer; it is the concentration that is given in the boundary segment in the repository model (shaft, segment s:1 in Fig. 2.14).

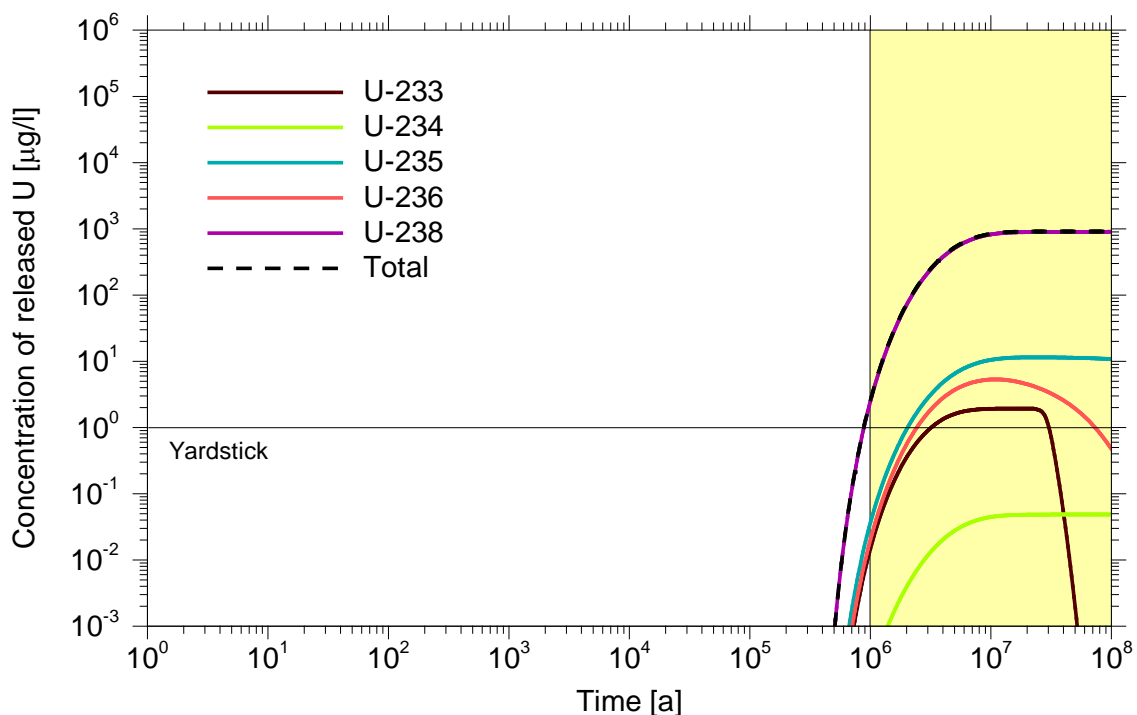


Fig. 2.15 Elemental concentrations of released uranium from the repository

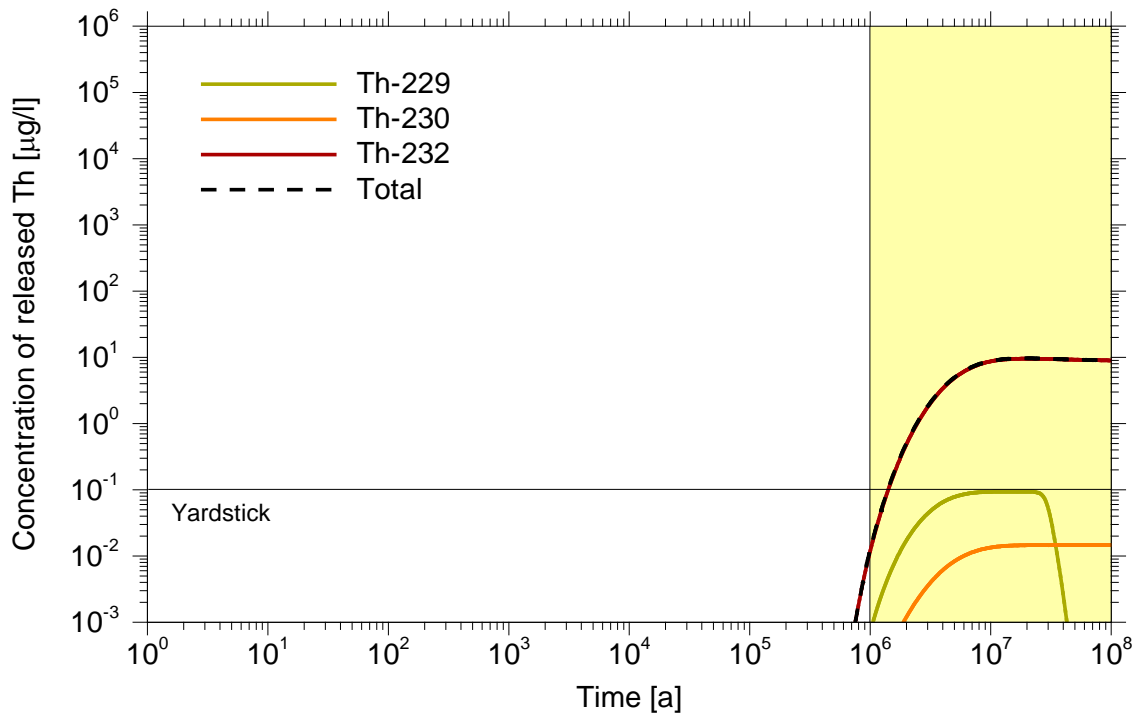


Fig. 2.16 Elemental concentrations of released thorium from the repository

2.3.2.2.3 Contribution to power density in porewater at the CRZ boundary

The calculated power density and the main contributors are shown in Fig. 2.17. The maximum value of the calculated power density within the assessment period is $1.2 \cdot 10^6$ MeV/(s·m³) at one million years and is dominated by Cs-135 and Sn-126. The highest calculated value is $1.0 \cdot 10^8$ MeV/(s·m³) after about five million years. The main contributions at that time are due to Cs-135, U-233 and I-129.

The high power densities are caused by the fact that the porewater volume in the repository is very low at time frames of 10^6 years and later, since the convergence process is completed and all void volumes in the repository have been reduced to very low values and that no sorption is assumed. Therefore, the concentration of dissolved radionuclides in the disposal area is distributed in the whole repository by diffusion after 10^6 years and later causing high concentrations in the repository.

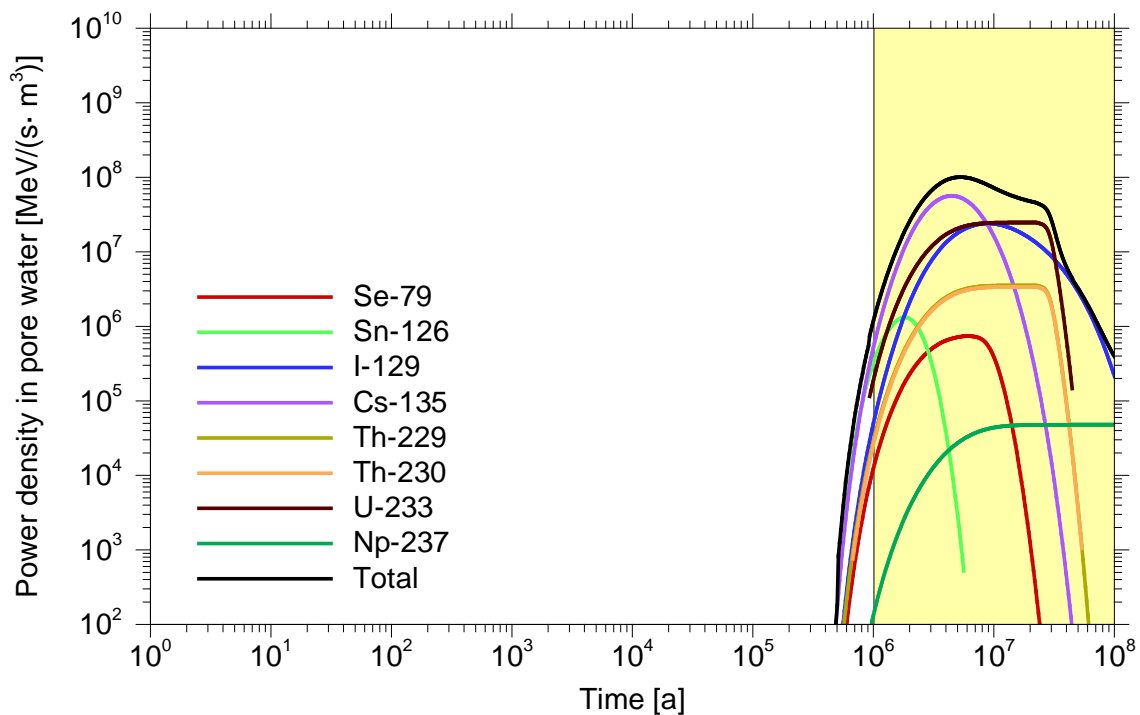


Fig. 2.17 The contribution to power density in groundwater at the CRZ

2.3.2.2.4 Contribution to radiotoxicity in groundwater

The contribution to radiotoxicity in groundwater is calculated from the radionuclide flux through the boundary of the CRZ. This flux flows in a virtual water body used by a group of humans. The virtual water body comprises the annual water consumption of this group (see section 2.3). To assess the radiological consequences of the radionuclide concentrations in this water body the same dose conversion factors are applied as for the calculation of the individual dose (see Tab. 2.12).

Fig. 2.18 illustrates that within 10^6 years the contribution to radiotoxicity is dominated by Sn-126, mainly caused by its very high dose conversion coefficient. The highest value within the assessment period of 10^6 years is a radiotoxicity flux of about $6.3 \cdot 10^{-8}$ Sv/a. At later times the radiotoxicity flux is dominated by I-129 with the highest value at $8.2 \cdot 10^6$ years of $3.5 \cdot 10^{-6}$ Sv/a. Additional important contributors are long-lived nuclides with high dose conversion factors (Cs-135, Th-229).

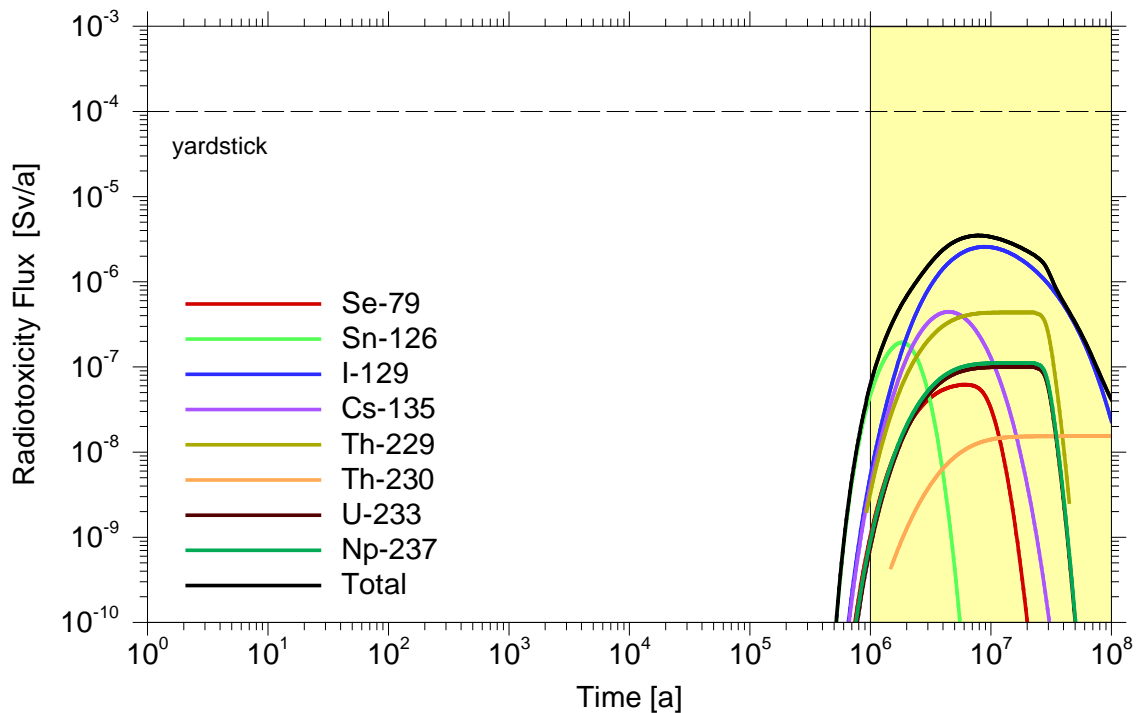


Fig. 2.18 The contribution to radiotoxicity at the CRZ

2.3.2.2.5 Radionuclides concentrations in the near-surface water

The aim of this indicator is to monitor the change of ambient concentrations of the naturally occurring radionuclides. All naturally occurring radionuclides are several orders of magnitude below the nuclide-specific yardsticks proposed by /BAL 07/, see Fig. 2.19. Within the uranium decay chain the isotopes U-238 and U-234 are in radioactive equilibrium. Concentrations of Pb-210, Ra-226 and Th-230 are higher or lower, respectively, due to different K_d -values in the overburden.

Within the thorium decay chain the isotopes Th-232 and Th-228 are in radioactive equilibrium.

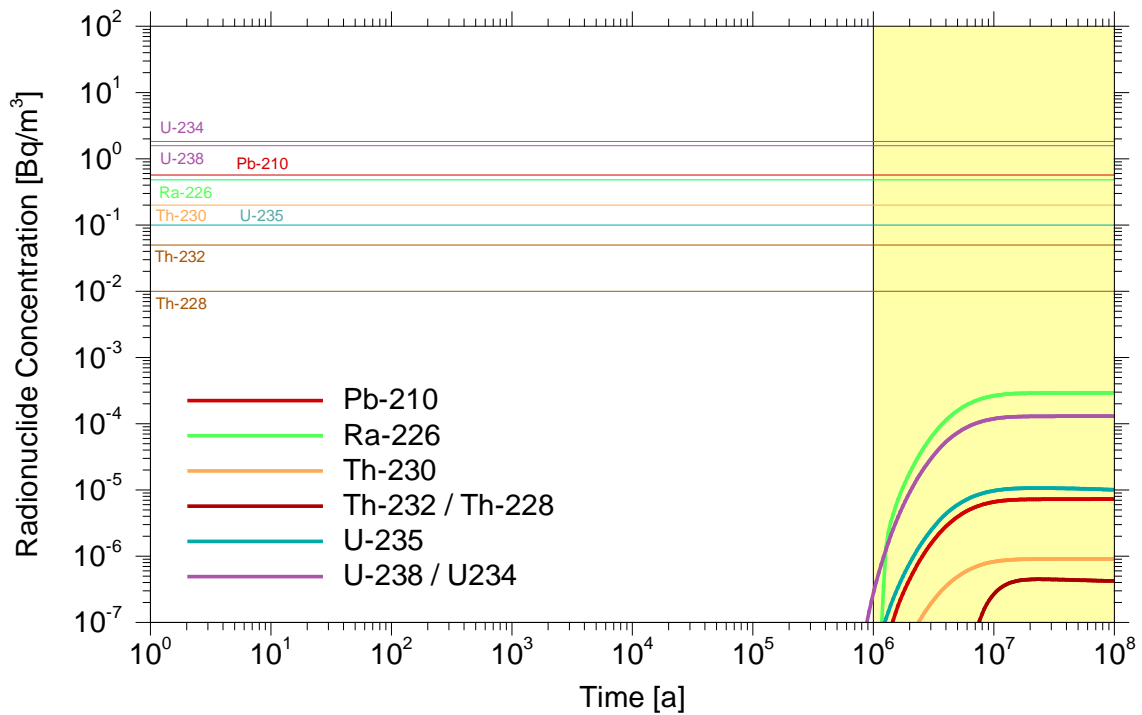


Fig. 2.19 Naturally-occurring radionuclide concentrations in the near-surface water

2.3.2.2.6 Effective dose rate

Fig. 2.20 illustrates that for the considered repository system only a small additional effective dose occurs in one million years. The highest value within the assessment period is at 10^6 years with a dose of about $2.0 \cdot 10^{-8}$ Sv/a. The effective dose rate is dominated by Sn-126. At later times the dose is dominated by I-129 with the highest value at $8.2 \cdot 10^6$ years of $1.1 \cdot 10^{-6}$ Sv/a. Additional important contributors are long-lived nuclides with high dose conversion factors (Cs-135, Th-229)

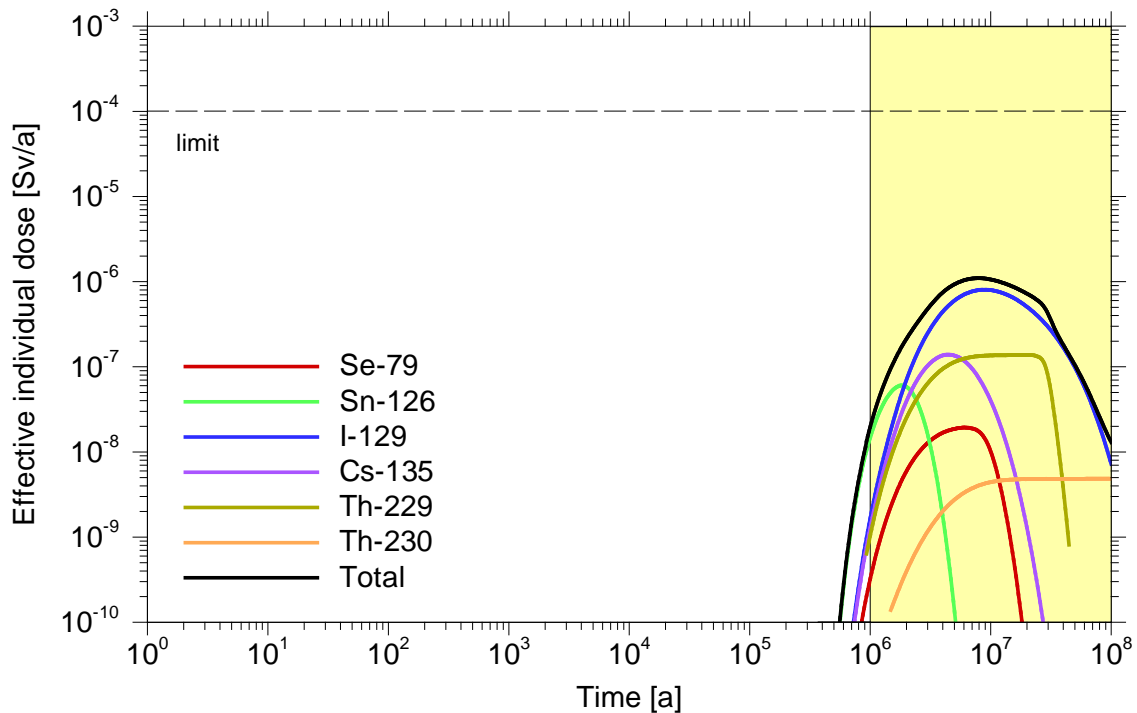


Fig. 2.20 Effective individual dose [Sv/a], and main contributors to dose

2.3.3 Conclusions

2.3.3.1 General conclusions

With respect to indicators there has been a move during the last decade to use indicators that are complementary to dose and risk and to apply indicators that are derived from safety functions. Here, a set of indicators that is especially directed to the safety function containment provided by /BAL 07/ has been calculated for a repository in a clay formation, and for a repository in a salt formation. Each of the indicators has been assessed regarding its applicability. The proposed indicators comprise the dose⁶ and the five complementary indicators

- proportion of the cumulative released quantity of substance over the safety case period,
- concentration of released uranium and thorium in the porewater at the CRZ boundary,

⁶ In the following sections denoted as effective individual dose

- contribution to power density in porewater at the CRZ boundary,
- contribution to radiotoxicity in groundwater,
- radionuclide concentration in the usable water near the surface.

Concerning the results for the clay formation the evaluation of the indicators is restricted in so far, that none of the natural occurring radionuclides are released from the containment providing rock zone within the assessment time frame of one million years and even not after 100 million years, which is due to the slow transport by diffusion and high sorption values of the actinides. This regards particularly the indicator concentration of released U and Th, but also impacts the contribution to the power density, since none of the alpha-emitting radionuclides with high decay energies occur. For the calculation case considered here only the four most mobile radionuclides C-14, Cl-36, Se-79 and I-129 contribute to the indicators. All the indicators calculated are below the proposed yardsticks.

For the calculation case applied for a repository in rock salt additional radionuclides play a role, since no sorption is considered during transport through the repository. This concerns the actinides but is also shown by significant contributions of e. g. Sn-126 dominating the radiotoxicity flux and the effective individual dose within the assessment period of one million years.

This study reveals one important aspect that has to be considered when applying indicators for comparing concentrations or dependent quantities calculated directly at the CRZ boundary, e. g. *concentrations of released U and Th in the porewater* or *contribution to power density in the porewater*. For such indicators it is of crucial importance, whether the radionuclides are released over the whole area of the CRZ boundary as in the case of a repository in clay or only via a small section of this area as for a repository in rock salt (see Fig. 2.7). As a consequence, the value for rock salt is several orders of magnitude higher than in the case of the clay formation, whereas the indicators radiotoxicity flux and the effective individual dose, which are calculated after dilution in surface near aquifers and allow a statement about safety, are within a similar range of magnitude for both formations and clearly below the yardsticks. Therefore, maximum information for such indicators is received, when they are calculated for both, (i) referred to the area, over which they are released and (ii) referred to the total area of the rim of the CRZ boundary. This aspect was also discussed in the project VERSI (VER-

gleichende Sicherheitsanalysen), where one of the indicators considered there is normalized to a defined area /RES 10/.

2.3.3.2 Assessment of indicators

In the following the five tested indicators used complementary to dose are evaluated:

The indicator *proportion of the cumulative released quantity of substance over the safety case period* is a performance indicator. The yardstick proposed for this indicator is fulfilled. Since for this indicator the total amount of all radionuclides in mol is the basis, for a repository containing spent fuel, the release of U-238 is of crucial importance, since its inventory in SF elements is more than 2 orders of magnitude higher than the amount of each other radionuclide. Therefore, this indicator is not sensitive enough to judge the relevance of the release of nuclides other than U-238. It would be a very useful indicator, if it is considered nuclide-specific. Further a cumulative representation would be interesting, particularly to illustrate the retardation capacity, e. g. Fig. 2.9. This indicator is applicable to both formations, clay and rock salt. The indicator is recommended, if defined nuclide-specific.

The indicator *concentration of released uranium and thorium in the porewater at the CRZ boundary* is a performance indicator. Considering the radionuclide flow out of the CRZ the natural radionuclides, particularly of uranium and thorium, are not that relevant. Most of the radionuclides released out of the CRZ are not natural radionuclides or occur in only extremely low concentrations in natural waters (e. g. C-14, Cl-36). Further, this is an indicator for strongly sorbing radionuclides, namely the actinides U and Th. Such indicators are not sensitive for repositories in clay formations, where they always deliver a value of 0. If the indicator *proportion of the cumulative released quantity of substance over the safety case period* will be considered as nuclide specific, it can be applied to illustrate the retardation capacity of the CRZ. According to this the indicator *concentration of released uranium and thorium in the porewater at the CRZ boundary* does not deliver additional information. It is not recommended for further use.

The indicator *contribution to power density in porewater at the CRZ boundary* is a performance indicator. It is clearly not related to safety, since it is only based on physical quantities. Therefore, it is not dependent on any biosphere or near surface processes and is not covered with the uncertainties existing for these processes. On the other

hand it is difficult to derive a yardstick for this indicator, which is of course not necessarily needed for a performance indicator. As discussed above for this indicator it is important to define, whether an average value normalized to the area of the CRZ boundary or the maximum value referred to the fraction of the surface, where the radionuclides are released is applied. We would recommend both applications of the indicator. The maximum value is strongly dependent from the repository formation or concept and allows the identification of different kind of releases, as observed for repositories in clay and rock salt.

The indicator *contribution to radiotoxicity in groundwater* is a safety indicator. If an appropriate calculation scheme and an accepted yardstick are applied for the calculation of this indicator (for example by a given scheme from the regulator) this indicator gives a strong argument for the safety of the repository system independent of the barrier function of geological formations outside the CRZ. The indicator is independent from the repository formation or concept and is recommended for application. The fundamental idea of this indicator is the basis for the simplified long-term radiological statement in the German Safety Requirements /BMU 10/.

The indicator *radionuclide concentration in the usable water near the surface* represents a performance indicator in the proposed form. As discussed above the value of the proposed indicator is limited, since most of the radionuclides, released from the CRZ are not the naturally occurring radionuclides proposed for this indicator. Therefore, it would be much more useful to consider the whole spectrum of released radionuclides and compare its radiotoxicity concentration with the radiotoxicity concentration of natural radionuclides. However, this indicator is well known, usually denoted as radiotoxicity concentration and used in national and international studies /BEC 03/, /BEC 09/. Therefore, the indicator *radionuclide concentration in the usable water near the surface* as proposed here is not recommended for further use.

3 International developments

3.1 RWMC

The Radioactive Waste Management Committee (RWMC) is an international committee made up of senior representatives from regulatory authorities, radioactive waste management agencies policy making bodies and research and development institutions. Its purpose is to foster international co-operation in the management of radioactive waste and radioactive materials amongst the OECD member countries. The main tasks of the RWMC are to constitute a forum for the exchange of information and experience on waste management policies and practices in NEA Member countries, to review the state-of-the-art in the field of radioactive waste and materials management, and to conduct international peer review of national activities in the field of radioactive waste management, such as R&D programmes, safety assessments, specific regulations. The NEA's 50th anniversary celebration took place in October 2008.

3.1.1 Recent International Developments

During RWMC-45 (March 2012) it was reported that the OECD membership will continue to enlarge. New candidate countries include Russia, Estonia, Israel, and Chile. These countries are on a path to accession within 3 to 5 years. Russia is an observer since 2008. Significant progress has been until 2012 regarding its membership with NEA. Poland became a full OECD/NEA member in 2010 and Slovenia in 2011. Romania is seeking observer status with OECD/NEA. A Memorandum of Understanding and broad co-operation agreement is still being explored with China.

3.1.2 Programme of Work (PoW)

During RWMC-45 in 2012 NEA's bureau members gave an overview of the actual PoW including RWMC's activities and publications during the past year. Highlights included the dialogue with the ICRP in the area of disposal safety; the elaboration of the RWMC strategic plan /NEA 11a/; the RWMC collective statement on "National Commitment - Local and Regional Involvement" and participation in the organization of the conference in Toronto in September 2012 /ICR 12/; the flyer on the waste management profession; the collective statement /NEA 11b/ and vision for the project on preservation of records,

knowledge & memory /NEA 11c/, the finalization of the reversibility & retrievability project / and completion of the documentation /NEA 11d/; and peer reviews in Belgium and Sweden.

3.1.3 Research and Development

The RWMC's Steering Committee has released a statement on Qualified Human Resources. Amongst the messages of this statement is the point that international research programmes and co-operations represent a good avenue to address lack of resources. In this spirit, RWMC still supports the following international working groups:

- the Integrated Group of the Safety Case (IGSC)
- the Forum on Stakeholder Confidence (FSC)
- the Working Party on Decommissioning and Dismantling (WPDD).

During RWMC-45 it was repeated that the RWMC has a vibrant and effective pool of human resources and expertise to call upon in these groups.

3.1.3.1 Integration Group for the Safety Case (IGSC)

IGSC activities covered a wide range, on matters related to the scientific basis for design and analysis, safety assessment strategy and tools, design and implementation, and integration and management. Current trends include an increasing focus on practical information as member countries approach licensing and construction, on knowledge consolidation and management, and continuing work aimed at strengthening safety cases.

At the 13th IGSC meeting in October 2011, the proposal to establish a "Co-operative Project of IGSC on Safe Disposal of Long-lived and Heat generating Radioactive waste in a Deep Geological Repository in Rock salt" was presented to the IGSC. The IGSC endorsed the foundation of the Salt Club and approved the proposed working approach, work topics, and duration of the start-up phase. Similar to the Clay Club, which celebrated its 20th anniversary in 2010, the Salt Club is intended to promote the exchange of information and shared approaches and methods to develop and document an understanding of salt formations as a host rock for a high-level waste repository.

During its 45th meeting the RWMC explained that it was pleased with the IGSC's Programme of Work. The Committee supports the point of helping the national programmes collaborate on issues of operational safety and industrialization of disposal. Further details on the work of IGSC can be found in section 3.2.

3.1.3.2 Forum on Stakeholder Confidence (FSC)

The FSC facilitates the sharing of experience in addressing the societal dimension of radioactive waste management. It explores means of ensuring an effective dialogue with the public with a view to strengthening confidence in the decision-making processes. The time when exchanges between waste management institutions and civil society were confined to rigid mechanisms is coming to a close. A more complex interaction now involves players at national, regional and local levels. A broader, more realistic view of decision making is taking shape. The FSC contributes to these trends. The FSC celebrated its 10th anniversary in Sept. 2010.

The most recent event of the FSC was the 8th National Workshop and Community Visit in in Östhammar/Sweden May 2011 addressing experience and history of the Swedish programme. A synthesis is provided in /NEA 12c/.

3.1.3.3 Working Party on Management of Materials from Decommissioning and Dismantling (WPDD)

The WPDD provides a focus for the analysis of decommissioning policy, strategy and regulation, including the related issues of management of materials, release of sites and buildings from regulatory control and the associated cost estimation and funding. Beyond policy and strategy considerations, the WPDD also reviews practical considerations for implementation such as techniques for characterization of materials, for decontamination and for dismantling.

Recent projects of the WPDD have included work on management of large components from decommissioning, analysis of R&D and innovation needs for decommissioning, radiological characterization, and the ongoing work of the Decommissioning Cost Estimation Group. Plans for future work include the areas of knowledge and record management, and remediation following accidents. RWMC-45 briefly described the

continuing progress of work in the Cooperative Programme for Decommissioning (CPD), which has now been active for over 30 years.

3.1.3.4 Regulator's Forum (RWMC-RF)

The regulator members of the RWMC also participate in a separate Forum (RWMC RF) through which they discuss and report on topics of specific regulatory interest and which determines, where appropriate, how such issues are progressed within the full Committee.

Actually, involvement of ICRP members and other RP-expert for further dialogue on long-term radiological criteria of rad waste disposal is in the focus of the forum. During the 13th meeting (March 2010) exposures from repositories in very long time frames were discussed.

There was general agreement that calculated doses are effective doses, which are, in the long term, a measure only of potential effects under assumed conditions and therefore not a direct indicator of health effects. Some regulators do treat calculated doses as a fairly direct measure of future health risk, whereas others consider that in the long term they provide only a context, or an indicator that needs to be supplemented by other indicators. During RWMC-43 in March 2010 the current position in ICRP was highlighted presenting the ICRP viewpoint on interpreting radiological protection principles and criteria for geological disposal. Radiation protection is based on a combination of science, values and experience. Detriment is an indicator of risk, whereas effective dose is an indicator of exposure.

The key evolution from ICRP-60 to ICRP-103 has been the abandonment of the distinction between practices and interventions, which has been replaced by recognition of three types of exposure situations: planned, emergency and existing. The basic principles of justification, optimization and limitation of exposure apply similarly to all three situations, but with different suggested criteria.

An ICRP Task Group has been formed to prepare a new ICRP publication that will describe how the recommendations of ICRP 103 apply to the geological disposal of long-lived solid radioactive waste. This publication will update and replace ICRP-77 and ICRP-81.

3.1.3.5 R&R Working Group

The working group met twice during 2009, in June and December, and another meeting in June 2010, followed by the conference in Reims in December 2010. During RWMC44 there was general satisfaction expressed with the outcomes of the project. It was felt that the final report represents a good synthesis of current thinking on the topic. It was however suggested that an executive summary should be added to the report. In RWMC45, March 2012 it was stated that the R&R project is now fully documented /NEA 11d/.

Following that, regulatory questions raised in the Reims conference were reviewed in the form of a seed document for further discussion in the RF. The RF took part in a survey as part of the RK&M project (see below), and the RF has recommended that the survey be opened to all members of the RWMC.

3.1.3.6 RK&M-Project

At the 2009 meeting, RWMC members were very positive on starting an initiative on long-term memory. Two documents were issued in 2011, the Vision Document /NEA 11b/ and the Collective Statement /NEA 11c/. Star of the project was approved in 2011. The project is planned to run for three years from now through the beginning of 2014. Changes will be made to the vision document and collective statement according to comments received. During RWMC-45 (March 2012) a progress report on the RK&M-project was presented. The project involves representatives from 12 countries, the IAEA and the EC. After RWMC approval, a project web site was set up, three surveys have been conducted, and a bibliography has been assembled and a preliminary analysis conducted. The bibliography will be refined and a more detailed analysis will be performed. At the first project workshop in October 2011, several areas for further investigation were identified, among them the relationships among regulation, licensing and RK&M; assumptions about future capabilities; the relationship between RK&M and safeguards; and the role of national archives vis-à-vis RK&M preservation for radioactive waste management. A picture is emerging that a combination of institutional and cultural mechanisms is needed, keeping in mind the dual tracks of informing succeeding generations in the near term and the more distant future. A project work plan has been developed, including two workshops in 2012 and aiming towards a menu-driven document in 2014 as the main project deliverable.

3.1.4 Country Trend Analysis

At RWMC-45 a presentation summarizing major trends and challenges in the member countries was given by Mr. Molnár from Hungary. He noted efforts in a few countries related to establishment and development of national plans, and work on legislation and regulatory frameworks. Among the trends noted were changes in policy in some countries following Fukushima, as well as implications for design of spent fuel management facilities. International developments including the Joint Convention, the EC Directive on waste management, increasing use of IAEA safety standards, and the increased use of international peer review are all contributing to improvements in safety overall. Challenges noted include the need for provisions for dealing with mixed HLW from accidents, decommissioning of damaged facilities and remediation of contaminated areas. It was also noted that the RWMC continues to be responsive to its members in relation to identified trends and challenges.

3.2 IGSC

The mission of the Integration Group for the Safety Case (IGSC) is to assist member countries to develop effective safety cases supported by robust scientific technical basis. In addition to the technical aspects in all developmental stages of repository implementation, the group also provides a platform for international dialogues between safety experts to address strategic and policy aspects of repository development.

IGSC activities foster consensus on best practices and advance the development of innovative approaches used in all stages of repository implementation. Activities are organized in the thematic framework of the scientific basis, safety assessment strategy and tools, repository design and implementation and safety case integration and management.

3.2.1 Scientific basis

The Scientific Basis activities of the IGSC examine important scientific and technical issues for the development and integration of safety cases. Activities in this field are designed to address the question: "What do we know?"

Important activities within the last years were the NEA sorption project, phase III (see section 3.3), activities in the clay club (section 3.4) and salt club (section 3.5), the workshop on cementitious materials, the thermodynamic database NEA-TDB, and gas migration.

The disposal of long-lived radioactive wastes requires the evolution and interactions of cementitious materials with other repository components, host rocks and ground water to be well understood. In 2009, the NEA IGSC organized a workshop to assess current understanding on the use of cementitious materials in radioactive waste disposal. The workshop was designed to consider issues relevant to the post-closure safety of radioactive waste disposal, but also to address some related operational issues such as cementitious barrier emplacement. The proceedings of the workshop are available in the report /NEA 12d/.

The overall objective of the NEA TDB project is to make available a comprehensive, internally consistent, internationally recognized and quality-assured chemical thermodynamic database of selected chemical elements. This database should meet the specialized modelling requirements for safety assessments of radioactive waste disposal. High priority is assigned to the critical review of relevant data for inorganic compounds and complexes containing the actinides. Data on other elements present in radioactive waste are also critically reviewed as well as compounds and complexes of the previously considered elements with selected organic ligands. The work which was performed in phase IV and is currently started in phase V of the project is focused on inorganic species and compounds of Sn, Fe and Mo. Further, work on ancillary data, i. e. relevant species and compounds to describe the aqueous chemistry of Al and Si, and the inorganic compounds and species of I, B, Mg, Ca, Sr and Ba is done. In addition work on three state-of-the-art reports on the topics cements, high ionic strength systems and extrapolation to high temperatures has been initiated. The reports "Inorganic species and compounds of Sn" and "Inorganic species and compounds of Fe (vol. 1)" are announced to be published in December 2012. The review reports of the inorganic species and compounds of Mo, the inorganic species and compounds of Fe (vol. 2) and the ancillary data will be finalized in 2014.

3.2.1.1 Relevance of gases for the safety case

This topic was dealt with in the topical session at the 13th IGSC meeting. Aims of the topical session were to gain understanding of the strategies (e. g. in terms of R&D, feasibility, optimization) put in place in national programmes to address the issues and in particular the irreducible uncertainties associated to gas generation and migration. Therefore, information on work in national programmes was gathered by addressing the following key questions:

1. What are the regulatory requirements and what are their impacts?
2. What is the relevance of the gases for the long-term safety?
3. How are gases and the related uncertainties considered in the latest SA?
4. What are the remaining process uncertainties?
5. What is the strategy that has been put in place to treat the remaining issues?
6. Where do the organizations see potential to lower conservatism in the description of the gas pathway?
7. What multiple lines of arguments do you use to address the issue of gases in the safety case?
8. What are the strategic choices for the future?

Presentations from eight countries addressing the issue for the three main host formations clay, granite and rock salt as well as a presentation about the on-going EC project FORGE were given. The major results are summarized in the following.

In the post closure phase of a deep geological repository for radioactive waste, significant quantities of gases may be generated. The most important gas generating process is anaerobic metal corrosion. Additionally, degradation of organic matter by bacterial activity (mainly important for intermediate level waste and low-level waste (ILW and LLW) repositories) and water radiolysis contribute to gas formation. Non-radioactive gases can be important because of potential pressure related impacts on the engineered barrier system and geological host formation, and their role as carrier gas for transporting radioactive gases.

Besides the large amount of non-radioactive gases, small amounts of radioactive gases are also generated and can have direct radiological consequences. Due to an usual-

ly large initial inventory and a longer half-life, ^{14}C if present in (or converted to) gas form can be of safety relevance depending on its degree of conversion to methane and the period of confinement in the geological repository before it reaches the biosphere. Depending on the concept and scenario, in some studies a fraction of volatile ^{129}I is considered to be released from the waste (see e. g. Sect.3). Radon presents a specific case as it will be continuously formed by radioactive decay of parent nuclides during the containment period but also afterwards, when parent nuclides migrate throughout the barrier system. Radon is also particularly studied in the framework of operational safety. Noble gases and tritium are not an issue for the long-term safety due to their short-life time.

Mitigating these various processes presents the designer with a possible conflict of goals. While radioactive gases are subject to the strategy of the system providing isolation and containment, the non-radioactive gases may need to be dissipated to minimize the pressure build-up in the repository system. Consequently a sound safety strategy addressing these issues, and a body of robust arguments, are needed to support a post-closure safety case in order to give an adequate level of confidence that gas generation is not an issue likely to compromise the safety of a deep disposal system. Gas production might also influence geochemical conditions in the near field and/or the host formation in different ways. A potential positive effect is lower dissolution rate of spent fuel due to even more reducing conditions imposed by the presence of hydrogen gas. A potential negative effect is higher solubility of actinides due to the lower pH conditions imposed by the presence of CO_2 gas.

Investigations of gas generation and transport in this context were initiated more than 15 years ago. However, high level waste management program R&D priorities were originally focused on aqueous solute transport, THM (Thermo Hydraulic Mechanic) and/or DZ (Disturbed Zone) processes. In the last decade, as knowledge on these topics reached a mature state and new tools became available (modelling, process visualization), and as deep disposal of ILW has gained attention, the gas issue has come to the foreground of waste management organization and regulatory development programs. For example, this topic was identified at a strategic level by the 2007 IGSC, as a concerted research project in 2009 with the European Commission's (EC's) FORGE project (www.forgeproject.org). It is in this context that IGSC revisits the state-of-the-art regarding this issue based on recent safety cases and studies. Since gas generation issues are not the same in different geologic media, this position paper addresses clay, salt and granite host-rocks individually.

Revisiting the current state of the national WMO's programs reveals clearly that the nature of the gas issue depends on the type of waste, the repository concept and the type of host formation. Recent works have shown that the state of knowledge is different from one host-rock to the other. Likewise, the corresponding requirements and constraints on repository design can differ. Consequently the positions for each host formation are summarized hereafter:

In clay where a gas build-up might be expected, simplified bounding calculations and/or robust arguments suggest that gas production and transport should not compromise the safety of the disposal system. However, uncertainties regarding the understanding of gas behavior beyond the well-known diffusive process remain too large to be only accounted for conservatively to the risk of reducing confidence in the performance of the system. A noticeable trend during the last decade indicates that gas aspects are now more often integrated in the system concept design earlier in the R&D program and treated on the same level as other safety relevant issues.

For a repository in salt host rock, the dry conditions expected in the normal evolution result in only a low amount of gases to be generated. In general, no impact on safety is expected to result from the gas production. However, this should not be taken to mean understanding gas behavior is not required, e. g. Germany requires due to strict regulations (especially with regard to confinement in the host rock) that the gas issue has to be studied more closely. Unless research is performed that allows one to rule out a potential release of radioactive gases from the repository, detailed repository concept modelling will be necessary in the long-term safety assessment. Regarding this, some open questions remain on the level of process understanding currently covered by pessimistic assumptions. Design optimizations, including dedicated gas storage capacities, could be considered to further decrease potential consequences of gas generation.

The concept of disposal in copper canisters in a granitic host rock, as proposed e. g. in Sweden and Finland, presents a different situation and has, to a large extent, neutralized the potential safety issue raised by gas generation. The copper canisters are highly resistant to corrosion in the conditions expected to prevail in the repository near field in the long term. Even if the copper is perforated, reducing conditions will favor low corrosion rates for the cast iron insert, and hence low rates of generation of hydrogen gas as a corrosion product. Furthermore, the bentonite buffer surrounding the canisters allows gas to migrate through pathways that will eventually re-seal once gas generation

ceases and the presence of fractures in the host rock means that gas reaching the buffer-rock interface can readily be dissipated without the build-up of potentially damaging gas pressures in the near field.

3.2.2 Safety assessment strategy and tools

IGSC activities in the field of Assessment Strategy and Tool evaluate effective assessment tools and strategies in developing and integrating a safety case. Activities in this area are designed to answer the question of “how do we use what we know to demonstrate safety?”

A very important topic in this framework is the project Methods for Safety Assessment (MeSA), which is described in detail in section 2.1. A second relevant topic dealt with the use of complementary indicators to dose and risk in the safety case. This work is described in detail in section 2.2. Then, two new initiatives are just started concerning the NEA FEP database and the topic scenario development.

The FEP (Features, Events and Processes) database for Geologic Disposal of Radioactive Waste was first published in 2000 by the NEA. The database, originally consisted of a set of project-specific FEP (PFEP) from 8 national programmes mapped to the NEA international FEP list (IFEP), and was updated in 2006 to include additional project-specific databases. Since then the declining role of the NEA FEP database was recognized as national programmes tend to use other approaches to support their safety analyses. A survey of the IGSC amongst the IGSC member organizations showed that the database is nearly only used as a tool for checking completeness. It was also noted in the MeSA project that the NEA FEP database may not be up-to-date as more detailed PFEPs have been developed in some advanced repository programmes. Nevertheless, the MeSA project concluded that an enhanced NEA FEP database would be valuable to all programmes, especially those at early stages, and would represent a knowledge transfer from more advanced programmes to less advanced ones. Therefore an initiative was started to update the list of project-specific FEP (PFEP) databases by including all published FEPs from national programmes, and extract PFEP lists from safety assessment and R&D reports of organizations that do not use formal FEPs. Further it is intended to re-establish the NEA FEP database using current software tools.

Scenario development: Scenario development methods mainly evolved in national programmes since a workshop on the topic held in 1999. The more recent developments were documented in the NEA INTESC initiative /NEA 09/ and the EC PAMINA project /EUR 09/. However, both of these projects were meant to address the issue. As the role of the IGSC is to foster exchange of information on subjects related to safety cases, the IGSC has approved a project on scenario development. The main objectives of this project are to review the tools and methods used, as well as to identify commonalities and contribute to their transferability. More specifically, the following areas have been proposed to be further developed:

- Derivation scenarios using safety functions;
- The categories of scenarios (including human intrusion). Also to consider the associated uncertainties at various stages of repository development;
- The relationship between scenarios and calculation cases;
- The analysis of similarities and differences of the developed scenarios, taking into account of the similar FEPs
- The externalization of expert judgements used in scenario development

It is the aim to arrange an international workshop in 2013. In advance a questionnaire will be sent out to collect inputs from national programmes. This information will be used as basis for the workshop discussion. In particular the questionnaire should provide a clear overview of the progress that has been made since 1999, provide a clear overview of the feedback and lessons learned from application practices for scenario development in safety cases, provide a state of art report to support discussions within the framework of a workshop, and identify areas in which further co-operation at the international level is desirable.

3.2.3 Design and implementation

Design and Implementation activities of the Integration Group for the Safety Case (IGSC) focus on “how to achieve safety in practice?” Here, the overall EBS project, jointly sponsored by the NEA and the European Commission (EC), was designed to develop greater understanding of how to achieve the necessary integration for the successful design, testing, modelling and performance assessment of EBS for deep underground disposal of radioactive waste. The series of workshops addressed in se-

quence the various stages of the design and optimization cycle for EBS. A brochure has been developed to summarize topics and conclusions of the full series of four EBS workshops, drawing on updated examples from national programmes. The final report was published by EC in 2010 as a joint NEA-EC report entitled: The Joint EBS EC/NEA Engineered Barrier System Project: Synthesis Report (EBSSYN) /EUR 10/.

3.2.4 Integration and management

Integration and Management activities of the Integration Group for the Safety Case (IGSC) are designed to address the issue of “how to synthesize knowledge and build confidence in safety.” Current work under this topic regards an update of the brochure Post closure safety case /NEA 04a/. As an outcome of the MeSA project an update of the brochure was proposed, emphasising more clearly the essential role of safety assessment within in the safety case (see section 2.1.4). The new version, containing all the new developments from international projects and national safety cases, will be published in 2013.

Two safety case peer reviews by international review teams (IRT) under the aegis of NEA have been finalized in 2012, namely for the safety case of the surface disposal facility for low-level waste in Belgium /NEA 12e/ and for the Swedish study SR-Site for a HLW repository at Forsmark site /NEA 12f/. The main objective of the peer review for the Belgian study was to provide a statement from an international perspective on the credibility and robustness of key aspects of the safety case produced by ONDRAF/NIRAS. It should help to ensure that its future license application will be in line with international best practice, and to provide the observers of the review process with an overview of the work from ONDRAF/NIRAS in preparation of the license application. The second review was performed for the safety study “Long-term safety for the final repository for spent nuclear fuel at Forsmark” produced by SKB. The purpose of this review was to help the Swedish government, the public and relevant organizations by providing an international reference about the maturity of SKB’s spent fuel disposal programme vis-à-vis the best practice of long-term disposal safety and radiation protection. Accordingly, the terms of reference for the review indicates that the peer review should provide the Swedish government with a statement, from an international perspective, on the sufficiency and credibility of SKB’s post-closure radiological safety case for the licensing decision at hand. In developing such statement, the IRT was asked to refer to international best practice in specific areas, namely: presentation of

safety arguments, safety assessment methods, completeness, handling of remaining issues, selection of site and disposal method, and feasibility.

3.3 NEA Sorption project

The OECD/NEA Sorption Project was launched to study the potential of chemical thermodynamic models for improving representation of sorption phenomena in the long-term safety analysis of radioactive waste repositories. Phase II of the NEA sorption project showed the potential value of the TSM approach in simulating sorption data for a range of radionuclides and geochemical conditions. This outcome was clearly significant for PA applications. However, it also highlighted that the same sorption data could be modelled in a number of different ways, and there was a lack of clear guidance on the appropriate methods of model development.

Hence, after finalisation of NEA sorption project phase II, it was proposed to develop and publish a guiding document regarding the development and use of thermodynamic sorption models within the framework of PA/safety case building. It was the intention that in such a document the critical issues are treated in a way that will facilitate communication with waste management organisations as well as regulatory authorities. Phase III of the NEA Sorption Project was started in November 2007 and ended in April 2010.

The development of the guideline document was performed by a technical direction team (TDT) which was supported by external experts. A management board was following and steering the work. GRS as member of the management board contributed in discussions on the structure of the report and reviewing the final sections. The final comments were given in November 2010 and the report was published in 2011 under the title "NEA Sorption Project Phase III: Thermodynamic sorption modelling in support of radioactive waste disposal safety cases. A guideline document". All the details can be found in /NEA 11/. The major outcomes are briefly summarized in the following.

Firstly, it need to be clearly stated that TSMs can be used to analyse only sorption phenomena that are governed by surface complexation and ion exchange. To construct or apply a TSM in a meaningful way within a PA or safety case context, several requirements must be addressed.

The following four general considerations are important to be addressed in the beginning /NEA 11/:

- *Model purpose*: This needs to be clearly defined at the outset of any TSM development, as it influences the choice of systems to be considered as well as the type of TSM and overall modelling approach to be used. It might range from general scoping calculations in a very early phase of a disposal programme over the development of TSMs, which are aiming to explain mechanistic or macroscopic aspects of radionuclide sorption to support confidence building in the safety case, to predictive applications for calculating K_d values to be used or estimate uncertainties in performance assessment.
- *Geochemical conditions*: A very fundamental and important prerequisite is a well-constrained geochemistry in terms of both porewater and major mineral phases. How well this can be achieved depends on the complexity of the system, the accessibility of the solid and liquid phases for sampling, the appropriateness of the sampling and characterisation programme, and the quality and detail of geochemical modelling. Here it is critical to appreciate the possible complexity of conditions and the degree to which they can be constrained based on geochemical modelling and sampling/analyses.
- *Thermodynamic databases* of sufficient quality and completeness need to be available to describe the chemistry of a system with regard to all aqueous species and solid phases, i. e. the major components and radionuclides.
- *Measurements of sorption data* of sufficient quality are needed to parameterise and/or to test the model quality and applicability. The amount of sorption data which needs to be accumulated depends strongly on the model purpose and the complexity and geochemical characteristics of the system. It also must be clarified whether the processes of surface sorption included in a TSM are sufficient for describing all observable effects of RN retention, or whether additional, non-sorption processes need to be considered.

These general considerations are important to develop an adequate acquisition programme for sorption data and TSM parameterization. For such an acquisition programme modelling and experiments should be carried out in complementary, since modelling might indicate additional experimental needs. Initially, the key system parameters like the pH, concentration of aqueous components, and the characteristics of the solid should be determined, followed by aqueous geochemical speciation computa-

tions and the experimental determination of a first set of sorption values. It is then important to create a comprehensive RN sorption data set including as a minimum the dependence on pH, ionic strength, RN concentration, carbonate, and major competing cations.

When it comes to the development of a specific TSM model, strategies are given in the report. If a complex material need to be considered it is often valuable to start with a simple system, since it might help to understand the fundamental sorption processes. Sorption on single mineral phases might also later on be used to describe the sorption on the complex material, particularly when specific minerals dominate the sorption process. For complex materials it also need to be decided, whether a Component Additivity (CA) or General Composite (GC) modelling approach (or some type of mixed approach) can be followed. In a CA approach, it may be possible to apply and test the ability of existing TSMs to describe and explain the experimental data. In a GC approach, parameterization of a new TSM on the basis of the obtained sorption data may be attempted.

For the concrete development of the TSM model the following advices are given. Postulated surface reactions should be chemically plausible. Ideally, they will be supported by spectroscopic information. Standard methods are available to estimate site density, surface protolysis behaviour, EDL parameters, etc. Appropriate methods should be used for each parameter relevant to the system being studied. Certain limitations and experimental choices within these techniques must be recognised, as these can be a source of inconsistent results. The data should be fitted using a numerical optimisation routine with an appropriate choice for representation of sorption. All used parameters should be checked for consistency with the state of knowledge concerning their reasonable range. Parameter values based solely on data fitting are inherently uncertain. Extrapolations to chemical conditions different from those of TSM parameterisation are associated with a high uncertainty. Extensions to other, but similar, substrates are often possible, but need to be done carefully. Interpolation within the parameter range considered in model parameterisation is expected to be more robust. Uncertainty/sensitivity analyses may help to identify those parameters having the greatest influence on calculated K_d , as well as those that are insignificant. Finally, the quality of a sorption model can be assessed against the following characteristics:

- an appropriate level of complexity;
- documented and traceable decisions;

- internal consistency;
- limitations on the number of adjustable parameter values;
- an adequate fit to a comprehensive calibration data-set;
- capability of fitting independent data sets.

In conclusion, phase III of the sorption project has not specified a single 'preferred' modelling sequence that can be applied in a recommended optimum approach, but it has shown that modelling can proceed in a systematic and defensible way, by following some key recommendations, in particular:

- The objective of the modelling exercise should be carefully defined at the outset.
- The key decision points in the modelling process at which critical modelling choices must be made should be clearly identified.
- The range of choices can be reduced and decisions justified by reference to key pieces of experimental or theoretical evidence, and by chemical reasoning. The key evidence used to derive the model should be documented.
- The modelling should utilise a suitable consultative and iterative model development process, during which it is tested as much as practicable.
- Confidence in the resulting models can be increased by a decision-making rationale aimed at maintaining consistency with available evidence and by the documentation of key decisions.

Whereas it is still a challenging task to develop and apply an appropriate TSM for a specific case, the present guideline report delivers the essentials to solve this task, namely the basic strategies and tools, but it also provides key references and discussions regarding the required input parameters. At the same time, there are on-going efforts within the scientific community to increase the knowledge about TSMs as well as to extend the base of available experimental data and TSM parameters in terms of broadening their scope and improving their quality.

3.4 Clay-Club

The Clay Club promotes the exchange of information and shared approaches and methods in the OECD member countries to develop and document an understanding of clay media as a host rock for a repository. The Clay Club provides advice to the IGSC on major and emerging issues related to the understanding of the characterization, evolution, modelling and performance of argillaceous media. In particular, the Clay Club addresses recommendations, trends, and information gaps concerning issues such as:

- the understanding (and development of associated conceptual models) of argillaceous rocks through site characterization and expert evaluation, including both field and laboratory work on key issues;
- the quality (characterization, understanding and conceptualization capability) and limitations of the information that is available;
- performance assessment and supporting models, including model abstraction and simplification as well as the traceability of related data and information;
- links and potential knowledge transfer between the understanding of clay as a host material and its use in engineered barrier systems of geological repositories.
- relevant progress in R&D on clay materials in other fields or industries, such as petroleum exploration and CO₂ sequestration.

During the last years the clay club has published two major reports on two co-operation projects, which have been finalized:

- Natural Tracer Profiles Across Argillaceous Formations. The CLAYTRAC Project. /NEA 09a/,
- Self-sealing of Fractures in Argillaceous Formations in the Context of Geological Disposal of Radioactive Waste. Review and Synthesis. /NEA 10/.

The water flow, solute transport and mechanical properties of clay are largely determined by the microstructure, the spatial arrangement of the solids and the pore water chemistry. Examples include anion accessible porosity and macroscopic membrane effects (chemical osmosis, hyperfiltration), geomechanical properties and the characteristics of two-phase flow properties, which are (relevant for gas transport. At the actual

level of knowledge, there is a strong need to reach the nanoscale description of the phenomena observed at a more macroscopic scale. However, based on the scale of individual clay-minerals and pore sizes, for most of the imaging techniques this resolution is a clear challenge. Therefore, clay club initiated a workshop which was intended to give inter alia a discussion platform on:

- The current state-of-the-art of different spectroscopic and microscopic methods,
- new development in order to address the above mentioned knowledge gaps in clays, and
- the perception of the interplay between geometry and electrostatics of experimentalists and molecular / Monte Carlo modelling groups providing valuable information on a lattice.

The international workshop “Clay under Nano- Microscopic resolution” took place from 6-8 September 2011 in Karlsruhe, Germany. It was structured in three main sessions

- Chemical Information under high spatial resolution,
- Pore structure and connectivity,
- Water and ion mobility, and
- Upscaling and implementation in model approaches.

In the first session on chemical information and high spatial resolution it was re-confirmed that nano-scale chemical analyses are needed in the clay, because the clay minerals are very small particles. The phenomena that are studied have to be looked at such scales as short term experiments although a repository time scale is much longer than the experimental scale. It has to be kept in mind that the mainly low reactivity rates are observed in the clays and this leads a very narrow altered zone. What is the claimed gain of the high resolution techniques through the presentations is that high resolution data thanks to very sensitive method that can observe surface analysis at atomic scales information. This enables a better description and consequently deeper comprehension on phenomena and processes as e. g. identification of neo-formed clay minerals after glass alteration. New ways of data interpretation and modelling are explained to analyze new correlations or distribution maps such as bounds between organic matter and metallic ligands.

Lastly, some future issues on this topic were presented:

- How to improve resolution, accuracy and representativity of data and how to avoid artifact and over-interpretation.
- How to evaluate pathway in the sample.
- Data treatment to make better correlations/distributions. The segmentation and noise filtration is sometimes time-consuming and leads data loss.
- Time evolution and real time acquisition (4D).
- How to link chemical information and physical mass transport information.
- How to put chemical data to models at different scales.
- Update the strategy for use of chemical data and reconsider it through the workshop every several years.

In the second session on pore structure and connectivity all talks were mainly about studies using Broad Ion Beam and Scanning Laser Microscopy to increase the understanding on the pore structure on the SEM scale. For the application of these methods polishing of the material is a prerequisite, which requires complex work. Normally K or Ar ion beams are used to polish the samples in order to reduce artifacts, which are expensive techniques. Therefore, further improvement is necessary to avoid artifacts during the preparation of the samples. Important issues and lessons learned are the following:

- For microstructural characterization the processing technique for the samples and as well the reporting of the conditions for preparation have to be improved.
- Freezing, high pressure fast freezing and impregnation protocols minimize damages.
- Important questions are
 - what are representative areas/volumes to study,
 - how are data at different scales bridged by multi-method approach, and
 - how are the connectivity and pores in different minerals evaluated in the clay matrix?
- Correction of measured pore size distribution data is necessary.

- Correlation with independent methods (BET-N₂ and Hg-porosimetry) is necessary.
- Handling large amounts of data is crucial.
- Different physics are taking place at different scales.

In the third session on water and ion mobility the discussion was focused on the issue that for full understanding of chemical phenomena a look at the interfaces under high spatial resolution is needed. This is, basically, why we want to see local molecular structure information at the reaction front that is any kinds of the precipitation or the dissolution reaction. This study is a notable example as using information obtained on classical tomography (structural properties), μ XRF, μ XRD, μ LA-ICP-MS, chemical tomography (chemical properties) and neutron studies (fluid properties). Furthermore, macroscopic results for random walk simulations on realistic porous media can be directly compared with chemical tomography for the process understanding. It should be noted that this experiment works for Cs due to very high concentration. On the other hand, other elements affected by their solubility limits and caused the precipitation may not be applicable.

The fourth session on up-scaling and implementation in model approaches was focused on diffusion of water at different time and space scale. One presentation highlighted the approach using neutron scattering diffusion for studying water diffusion. The presented experiment is still ongoing and it would be too early to make a conclusion. In a second presentation, it was highly recommended to show some photographs or figures, especially for the laminar flow profile across a pore in the clay. It could play with double layer thickness adding salinity and also could play by changing the hydraulic gradient. These should be understood as one of the most interesting knowledge from nano/microscopic experts. It was concluded that the molecular modelling may have an unexploited potential to bridge the scale gaps and to obtain mechanistic process understanding at the scale of interesting physics.

Since an additional progress in this field is expected in the next three years a second workshop of this type is planned for 2014/2015. The information and data derived from such analysis or experimental systems would contribute to the demonstration of the long term safety in the safety case. In this context, the integration between the rad waste studies and pure scientific nano/microscopic studies, and up-scaling from the molecular dynamics analysis to meet to geological disposal were remarked.

As another topic for future work an update on the Clay Club Catalogue is intended. The first version has not been used very often as an input for site descriptive models or PA over the world. This is because the current version is relatively outdated and the compiled data are mixed a wide range of qualities. Using both the Clay Club Catalogue of Characteristics (CCC) and the FEPCAT database, the update will include a selected group of clay formations that have been extensively studied and are well-characterized. It is proposed that the update would include the preparation of a focused report highlighting key attributes and characteristics of argillaceous sediments considered favorable for the long-term passive containment and isolation of nuclear waste, and a vetted database (to be included as an addendum to the report). Specifically, emphasis should be placed on the knowledge of geosphere properties and their spatial distribution, coupled with understanding of the behavior in the geologic past and future. Key goals of the proposed report are as follows:

- To provide a comparable database of selected physical and chemical properties (e. g., geochemical, hydrogeological and geomechanical) representative for clay-rich sedimentary formations investigated during the last decade with respect to disposal of radioactive waste.
- To emphasize the breadth and scope of unique international knowledge and experience associated with the characterization of argillaceous rocks for long-term radioactive waste management purposes.
- To highlight key features and attributes of argillaceous formations, which are relevant for establishing a geosynthesis and Safety Case for a deep geological repository.

3.5 Salt-Club

3.5.1 Foundation of the Salt Club

In the scientific community worldwide it is accepted that deep geological disposal is the appropriate way to dispose of spent/used fuel elements, high-level radioactive waste, and other, especially long-lived radioactive waste safely and securely for long times /NEA 08/. The geological formations that can host deep geological repositories include argillaceous rocks, crystalline rocks, and rock salt.

An advanced scientific and geotechnical understanding of rock salt as an appropriate geological material to host repositories has been accumulated by the dedicated research carried out by a number of countries favoring this material in the latter half of the 20th century.

The area of repository development for long-lived waste is a strategic area in the work programme of the OECD Nuclear Energy Agency (NEA) Radioactive Waste Management Committee (RWMC) and an area of traditional strength of this Committee.

So in May 2011, a group of scientists and experts from some member countries like the United States of America (U.S.), Germany, and The Netherlands proposed to establish a further working group of the Integration Group for the Safety Case (IGSC) of the NEA Radioactive Waste Management Committee (RWMC). This working group - named the Salt Club - would represent a similar working group as the Clay Club which was founded in the year 2000.

The proposal sent to the chairman of the IGSC in May 2011 has been entitled "Co-operative Project of IGSC on "Safe Disposal of Long-lived and Heat Generating Radioactive Waste in a Deep Geological Repository in Rock Salt".

At the 13th IGSC meeting in October 2011, the proposal to establish a "Co-operative Project of IGSC on Safe Disposal of Long-lived and Heat generating Radioactive waste in a Deep Geological Repository in Rock salt" was presented to the IGSC. The IGSC endorsed the foundation of the Salt Club and approved the proposed working approach, work topics, and duration of the start-up phase.

Similar to the Clay Club /NEA 12a/, the Salt Club /NEA 12b/ is intended to promote the exchange of information and shared approaches and methods to develop and document an understanding of salt formations as a host rock for a high-level waste repository.

The Salt Club should serve as the international focal point and catalyst for the following general objectives:

- The timely and cost-effective exchange of information on both favorable and challenging attributes of rock salt as a host rock formation for deep geological repositories (and underground research laboratories [URLs]) for long-lived and heat generating radioactive waste;

- The establishment and accomplishment of joint research activities on the characterization of rock salt formations, on the design, construction, operation and closure of repositories in rock salt, on thermal, hydraulic, mechanical, and chemical (THMC) processes crucial for their construction, operation, closure and safety, and on assessing the safety of repositories in rock salt;
- The establishment of a constructive international dialogue on rock salt science and engineering;
- Knowledge transfer, including to nations with small programs or programs in their initial state and adequate rock salt deposits for a repository;
- Fostering education and training as first steps in knowledge management.

3.5.2 Starting situation

A wealth of knowledge and experience has resulted from research and development (R&D) activities in fields like site investigations, in particular with regard to the application of geophysical techniques, geomechanics, geochemistry, modelling, and performance assessment for more than four decades, which included large-scale experiments in underground laboratories (URLs).

In the USA practical information was gained through licensing and operation of the Waste Isolation Pilot Plant (WIPP). In Germany, most useful information was obtained from the exploration of the Gorleben site, the operation and licensing of closure of the Morsleben repository, RD&D performed in the Asse mine which served as a 1st generation URL. Yet there is more work to be done to expand the potential use of salt as a repository host rock.

The Salt Club will make the current knowledge base on rock salt more readily available within the NEA-IGSC member nations and especially nations with adequate rock salt deposits for a repository.

3.5.3 Proposed activities mission and objectives of the Salt Club:

Most important items to be realized in order to underpin the use of rock salt as a repository host rock are:

- Perform fundamental joint research into areas where understanding is incomplete;
- Transfer methods and tools for the nation's salt disposal facilities and mining operations to analyse their operations to ensure safe, secure, long-term functionality of the underground structures;
- Promote the information exchange, approaches and methods and methodologies, technologies in order to understand the characteristics of rock salt and to use its advantages to host a repository;
- Afford technical experts access to and interchanges with the latest international developments in salt mechanics sciences;
- Discuss performance assessment, models, reliability and quality of data, evaluate national and international (i. e. European Commission) R&D activities;
- Exchange with other working groups (i. e. the Implementing Geological Disposal Technology Platform (IGD-TP)) on issues of common interest;
- Disseminate results at conferences, workshops, and on similar occasions, and for – transparency reasons - to the interested public;
- Address the fundamental issue of knowledge management that exists because current experts and researchers for salt applications are aging and retiring, but the knowledge they possess will be needed more than ever.
- Encourage research on regulatory aspects, public and political acceptance

3.5.4 Organizational structure and mode of operation and cooperation

To accomplish the above mentioned objectives, the Salt Club includes representatives from key organizations in the U.S., Germany, and The Netherlands directly involved in research on the safe disposal of radioactive waste in rock salt. The radioactive waste disposal programmes of these countries currently possess the state-of-the-art knowledge, models, expertise, equipment, instruments, and facilities for deep geological disposal of long-lived radioactive waste in rock salt. Scientists from Poland have al-

so expressed their intention to participate in view of the planned nuclear power plant deployment in their country.

Further participants may include waste management nations with adequate rock salt deposits for safe disposal of long-lived radioactive waste as well as any other national and international organization expressing interest in obtaining/ receiving the information. They will be invited to participate in the Salt Club as delegates, or to receive the information developed by the Salt Club.

The Salt Club hold regular annual meetings at which its work program and single projects will be established, updated, and reported about and organizational issues will be addressed.

The Salt Club is composed of senior technical experts with experience in assembling or reviewing the understanding of salt formations as host rocks for deep geologic disposal projects. Members are NEA member countries represented by responsible ministries who appoint delegates to the Salt Club. Delegates represent waste management agencies, regulatory authorities, academic institutions, and research and development institutions. Salt Club delegates have a level of seniority in their organizations such that they can mobilize resources as contributions to Salt Club initiatives.

The duration of the Salt Club Mandate is preliminary until the annual meeting of the IGSC in October 2015. Given the nature of the Salt Club, an extension of the mandate is envisaged which is to be determined at the discretion of the IGSC.

The German Federal Ministry of Economics and Technology (BMWi) is member of the Salt Club and appointed the following German institutions as delegates to the Salt Club (so far):

- Bundesamt für Strahlenschutz (BfS)
- Bundesanstalt für Geowissenschaften Und Rohstoffe (BGR)
- DBE Technology GmbH
- Gesellschaft für Anlagen- und Reaktorsicherheit (GRS) mbH, Braunschweig (currently the chair of Salt Club)
- Projektträger Karlsruhe Wassertechnologie und Entsorgung des BMWi

3.5.5 The starting work programme

The starting work programme agreed among the club members during the kick-off meeting held in Paris on 20 April 2012 comprises the following items:

1. A topical report on salt deposits throughout the world, to be made available by the U.S.
2. Natural analogues issue for rock salt
 - workshop to be held in week 38 (September 2012) in Braunschweig at the GRS offices;
 - publish a co-authored paper on natural and anthropogenic analogues;
3. Create a common FEP catalogue for a HLW repository in rock salt
 - considering NEA guidelines and clay FEP-catalogue of the NEA Clay Club
4. A Salt Knowledge Archive (scope, definition, collection of ideas, available information on KM-state-of-the-art (NEA))
5. A Safety Case Archive
6. Concept for publishing common or co-authored papers

3.6 Implementing Geological Disposal-Technology Platform (IGD-TP)

In the years 2006 – 2007 initiated by the European Commission (EC) a consortium of European radioactive waste management organizations carried out a feasibility study called Co-ordination Action on Research, Development and Demonstration Priorities and Strategies for Geological Disposal (CARD) on establishing a technology platform for final disposal in deep geological formations.

According to the results of the CARD-project, the waste management organizations share the opinion that it was time to take action to license the construction and operation of deep geological repositories for spent fuel, high-level waste, and other long-lived radioactive waste. They also agreed that a European Technology Platform would be the appropriate tool to facilitate the implementation process.

A Vision Document /IGD 09/ was prepared by an Interim Executive Group (IEG) with members from SKB (Sweden), Posiva (Finland), Andra (France) and the Federal Ministry of Economics and Technology (BMWV, Germany). The Vision Document is written for all stakeholders interested in radioactive waste management. A broad consultation process has been performed during summer 2009 and the comments received have been considered in the final version of this document.

The Vision was formulated as follows /IGD 09/:

"Our vision is that by 2025, the first geological disposal facilities for spent fuel, high-level waste, and other long-lived radioactive waste will be operating safely in Europe.

Our commitment is to:

- build confidence in the safety of geological disposal solutions among European citizens and decision-makers;
- encourage the establishment of waste management programmes that integrate geological disposal as the accepted option for the safe long-term management of long-lived and/or high-level waste;
- facilitate access to expertise and technology and maintain competences in the field of geological disposal for the benefit of Member States."

The Objectives of the technology platform are /IGD 09/:

- "to define, prioritize, initiate, and carry out European strategic initiatives that will facilitate the stepwise implementation of safe, deep geological disposal of spent fuel, high-level waste, and other long-lived radioactive waste by addressing the remaining scientific, technological and social challenges, and
- to support the waste management programmes in the member states."

The organization of the IGD-TP is shown in Fig. 3.1.

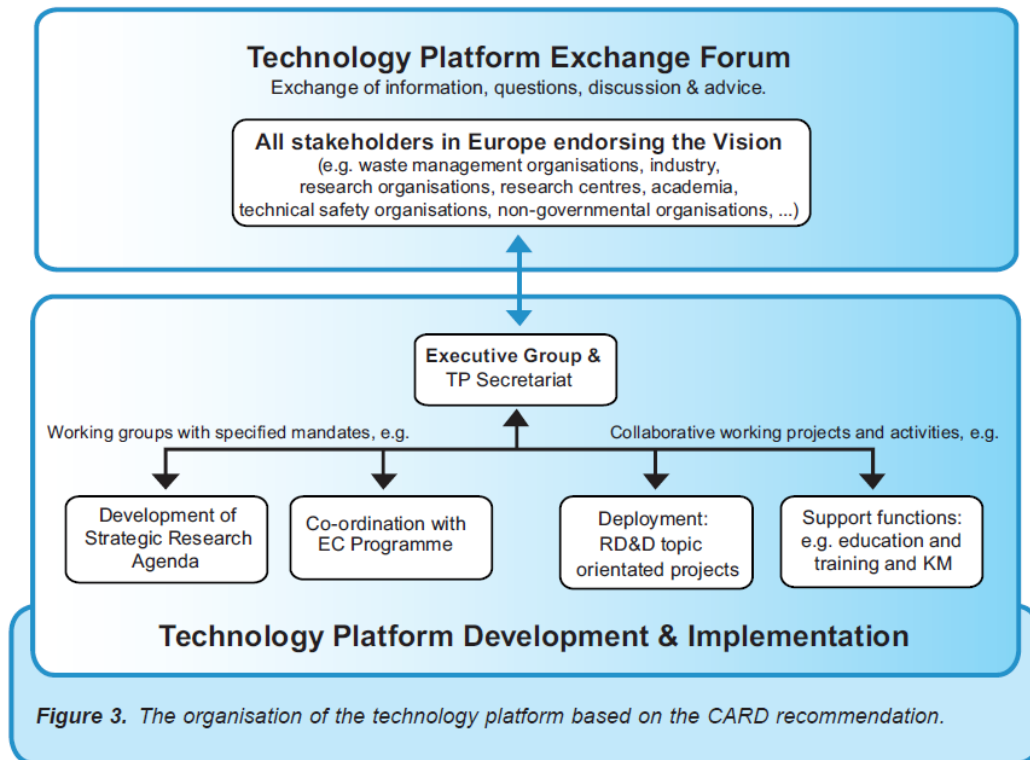


Fig. 3.1 The organization of the Technology Platform IGD-TP

One of the most important actions after launching the IGD-TP on 12 November 2009 in Brussels was to work out a Strategic Research Agenda (SRA) the emphasis of which being on RD&D activities that are critically important for the programmes closest to licensing but which, at the same time, produce results that are useful and of interest to other participating programmes as well.

The SRA was drafted by a SRA working group and intensively discussed before publication during a SRA seminar held in Brussels on 16 June 2010.

The following steps were taken by the SRA working group for completion of the first draft:

- Step 1: Compilation of RD&D issues
- Step 2: Classification of RD&D issues
- Step 3: Identification of common RD&D needs
- Step 4: Prioritization of Topics within each Key Topic
- Step 5: Information and consultation process (see above)

and resulted the following Key Topics

- Key Topic 1: Safety case
- Key Topic 2: Waste forms and their behavior
- Key Topic 3: Technical feasibility and long-term performance of repository
- Key Topic 4: Development strategy of the repository
- Key Topic 5: Safety of construction and operations
- Key Topic 6: Monitoring
- Key Topic 7: Governance and Stakeholder involvement
- Cross-cutting Activities

The Strategic Research Agenda (SRA) identified and prioritized the RD&D issues that could be pursued together in Europe to achieve the IGD-TP's vision. The SRA was published in July 2011.

From the salt option perspective the following topics were identified and proposed for inclusion into the SRA:

- Key Topic 1: Safety case
 - Topic: Sensitivity and uncertainty analyses
- Key Topic 3: Technical feasibility and long-term performance of repository
 - Topic: Full-scale demonstration of plugs
 - Topic: Description of seals and plugs systems and modelling of their long-term behaviour with assessment of the consequences on long-term safety
 - Topic: Lab and modelling work on salt backfill long-term behaviour

It is assumed that the SRA will evolve with increasing membership and participation. As the duration of repository projects are nowadays known to possibly last for several decades, changes are expected in dependence of scientific and societal developments.

After finalization of the first SRA issue, as a next step a Deployment Plan (DP) /IGD 11/ was developed outlining how the Key Topics and other Cross-cutting Activities are

foreseen to be organized, funded and carried out by the Technology Platform and its members. A draft of the IGD-TP's DP was published for public consultation in late 2011.

The goal of the deployment of the activities flowing from the SRA is to assist the IGD-TP Executive Group members and participants in achieving the vision and the desired results by joint RD&D activities during the next years.

According to the draft DP five different generic types of Joint Activities may be considered for the deployment of the SRA Topics /IGD 11/:

- Organizational Working Group (ORWG) coming together for the specific purpose of organizing a Topic.
- Technical/Scientific Working Group (TSWG) with the specific purpose of development of a scientific or technical Topic
- Information Exchange Platform (IEP) providing for organized forums of exchange between the IGD-TP members and the other participants.
- Technical Project (TEP) covering technical or scientific work on a specific SRA Topic
- Technological Transfer (TT) concerning actors (generally two) with some (generally one) possessing knowledge that the others (generally one) are ready to acquire.

In the DP each SRA topic is classified according to this scheme and together with the overall timeline in the SRA report this permitted development of a Master Deployment Plan for the period 2011 – 2016. The guidance of the Executive Group was also considered in the identification of Topics that should be pursued first. The first Master Deployment Plan was presented on 28 December 2011. It comprises a list of envisaged Joint Activities (Tab. 3.1) that are detailed in Project Outlines, currently still under discussion.

Tab. 3.1 Listing of Joint Activities /IGD 11/

	SRA Topics and their deployment activities
1	Waste forms and behaviour: TSWG launched in 2011
2	Full scale demonstration of Plugging & Sealing: TSWG launched in 2011
3	Waste forms and their behaviour: TSWG on C14
4	Monitoring the Environmental Reference State:
5	Safety of construction and operations:
6	Materials interactions: TSWG and TEP especially cement and clay based interactions
7	Monitoring programme: TSWG
8	Safety Case: TSWG on process model
9	Safety Case Peer review: ORWG
10	Long-term stability of bentonite in crystalline environments: TEP
11	Various Topics belonging to different categories. Topics concern the governance of the decision making and various Topics related to technical feasibility of repository components
12	ORWG on Adaptation and optimisation of the repository
13	IEP on Communicating result from RD&D
14	Competence Maintenance, Education and Training: ORWG CMET
15	Nuclear Knowledge Management: ORWG NKM
16	WMOs IEP

The Master Deployment Plan together with the Projects Outlines constitute a useful management tool for the IGD-TP. Updates of the Master Deployment Plan are to be done in the future as for the SRA and Project Outlines will be developed as required according to the schedule of the Master Deployment Plan.

The IGD-TP SRA and DP will constitute a strategic and an action plan for the IGD-TP participants and especially for the Executive Group members. At the same time, the Euratom Framework Programmes (FP) are European Union instruments, which support the RTD and Innovation in the European Member States.

Therefore, depending on the precise content and scope of future FPs, a significant part of future FP calls for proposals can be based on the importance and planning of the IGD-TP SRA and DP. As part of the overall promotions of strategic RD&D carried out collectively within IGD-TP, the IGD-TP's Executive Group shall be prepared, if requested, to assist the EC in identifying relevant topics for possible inclusion in future FP calls.

4 Selected topics

4.1 Microbial Processes Relevant for the Long-Term Performance of Radioactive Waste Repositories in Clays

The primary purpose of the present work was to qualitatively evaluate the relevance of microbial activity for the long-term performance of a deep geological repository (DGR) for high level waste (HLW) and spent nuclear fuel (SF) and to identify which safety-relevant processes and properties can be potentially influenced by this activity. This work should also provide a basis for the quantitative estimation of the maximum possible effects of microbial processes on the barrier system of a DGR as well as for the consideration of microbial impact on radionuclide redox chemistry and transport in DGR environments in future work. The present analysis identified eight clay properties essential for maintaining safety functions of containment and retardation /SKB 11/ of the disposal system – swelling pressure, specific surface area, cation exchange capacity, anion sorption capacity, porosity, permeability, fluid pressure, plasticity – which can potentially be influenced by microbial processes in clay buffer and claystone within a DGR for HLW/SF.

Radioactive waste canisters and over-packs made either of cast metal, carbon steel or stainless steel represent a further component of the engineered barrier system which can be strongly affected by microbial activity in clay buffer or in adjacent host rock. According to the current state of knowledge, iron(III)-reducing, sulphate-reducing, fermentative, methane-producing, and methane-oxidizing microbes can be considered to be present in any clay formation to be utilized either as a source of clay buffer material or as a host rock for a DGR for HLW/SF. The growing body of observations suggests also that each habitat includes a massive number of microbial niches with perhaps only a small proportion of the species being metabolically active at the habitat's conditions, the remainder becoming not extinct – which makes microbes discontinuously different from larger organisms /PAT 09/. Thus, e. g., hyperthermophilic microbial species, which are characterized by a preferential growth around 90 °C, are available in the currently rather cold environments, such as deep clay formations, and can become active as soon as temperatures in a DGR increase as a result of the placement of HLW/SF.

Moreover, it can further be concluded from the available experimental data that clays contain electron donors and electron acceptors in amounts sufficient for these mi-

crobes to remain active – even though perhaps at low metabolic rates – during very long periods of time. Additional sources of electron donors or electron acceptors will inevitably be added to the repository system as a result of DGR excavation, placement of radioactive waste as well as backfilling and sealing of the DGR. In this regard, it is important to bear in mind that the ability of microbes to use sophisticated systems to access distant electron donors and acceptors will ease a possible limitation of their local availability on activity of microbial population. A schematic summary of possible sources of electron donors and acceptors identified in the present analysis for a DGR in clay as well as of microbial metabolism products of major importance for its long-term performance is given in Fig. 4.1.

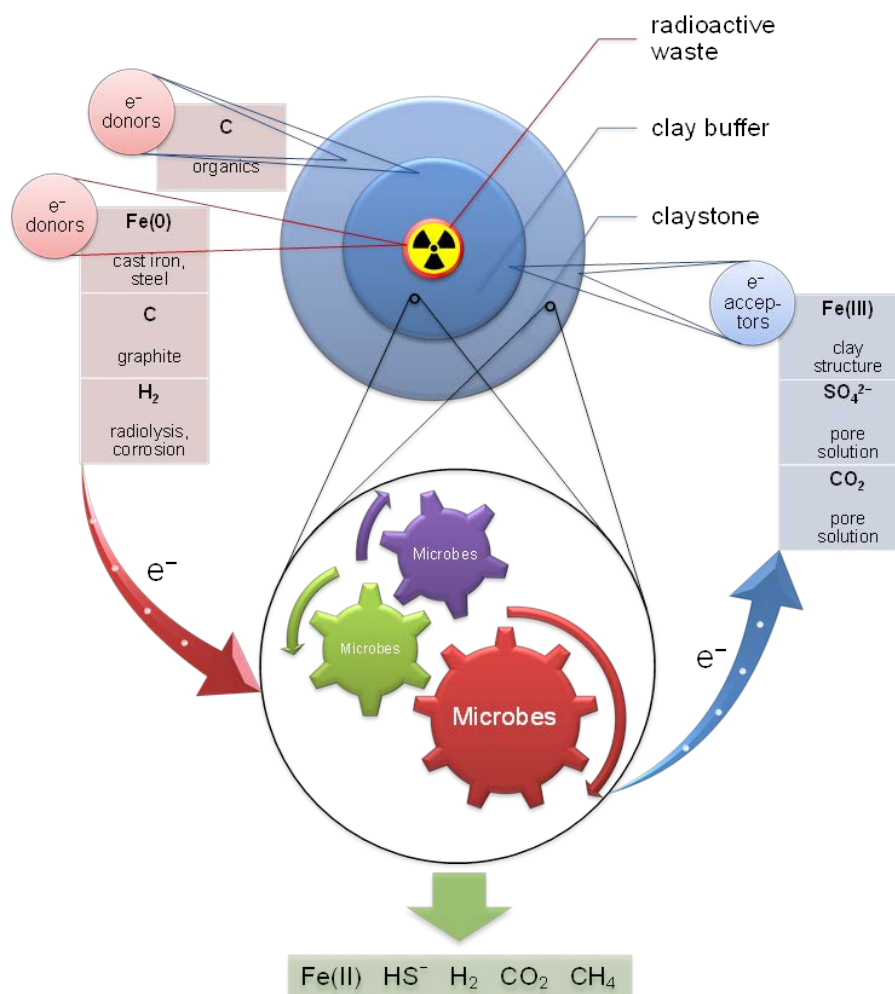


Fig. 4.1 Schematic summary of sources of electron donors and acceptors for microbial activity in a DGR in clay as well as of microbial metabolism products of major importance for its long-term performance

Structural Fe(III) of clay mineral layers represents the primary electron-accepting reactant in redox reactions driven by Fe(III)-reducing and methane-producing microbes as well as by sulphate-reducing microbes in the case of limited supply of sulphate. However, even in the case that the latter microbes predominantly use sulphate as the terminal electron acceptor, the product of their metabolism, hydrogen sulphide, reacts with structural Fe(III) in an abiotic redox reaction, which is facilitated by further, organic products of metabolism of sulphate-reducing bacteria. Accordingly, deterioration of clay properties accompanying destabilisation and transformation of clay structure as a result of microbial actions aimed at reducing Fe(III) to Fe(II) directly in the mineral structure or at dissolving Fe(III) and making it available for intracellular redox reactions can be considered as the primary microbial impact on clay.

Microbial reduction of structural Fe(III) has so far been demonstrated to produce up to ~1 – 2 mmol structural Fe(II) per g clay by a solid-state transformation pathway alone and to significantly deteriorate clay's swelling pressure, cation exchange capacity, and specific surface area while improving clay's anion sorption capacity. As a result of the production of ~1.2 mmol structural Fe(II) per g clay – either through direct reduction by microbes or through a reaction with the microbially produced hydrogen sulphide – the clay structure becomes destabilized and a release of Fe(II) accompanied by releases of other structural ions of clay begins. For example, Lower Miocene mudstones and dolomites from Madrid Basin in Spain provide a conclusive mineralogical record of microbial reduction of Fe(III) and release of Fe(II) from biotite and chlorite that were depleted of Fe by up to 40 weight % /SAN 09/. Microbial dissolution of biotite in these sediments was accompanied by microbial sulphide production and precipitation of iron sulphides, which either formed along the exfoliation planes of biotite grains (Fig. 4.2 (A)) or replaced biotite crystallites inheriting thereby structural habits of the latter.

Another clay-dissolution pathway in the presence of microbes proceeds by a direct chelation and solubilisation of structural Fe(III) by microbially produced, low-molecular-weight organic acids, siderophores, and possibly flavins. Microbial production of chelating compounds in the repository environment was recently judged particularly important in the safety analysis of radioactive waste disposal while being one of the least understood processes /PED 05/. Their synergistic effect on clay dissolution, which can be assumed to exist based on observations made for Fe(III) (hydr)oxides, is another critical, yet unresolved research issue (Tab. 4.1).

The clay dissolution proceeding by either reductive or non-reductive pathway results in a release of silica and, in the presence of soluble potassium, in the irreversible conversion of swelling smectites to non-swelling illites. The latter reaction is greatly accelerated due to microbial activity. Without microbial activity, this most important diagenetic clay reaction occurs in mudstones and shales over a temperature range of 50 – 180 °C and geological times of 0.5 – 300 million years /POL 93/. Due to microbial activity, however, this reaction strongly accelerates and results in the reduction of ~1.2 mmol Fe(III) per g smectite and the formation of illite in as little as 14 days at as low temperature and pressure as of 25 °C and 0.1 MPa (Fig. 4.2 (B)) /KIM 04/.

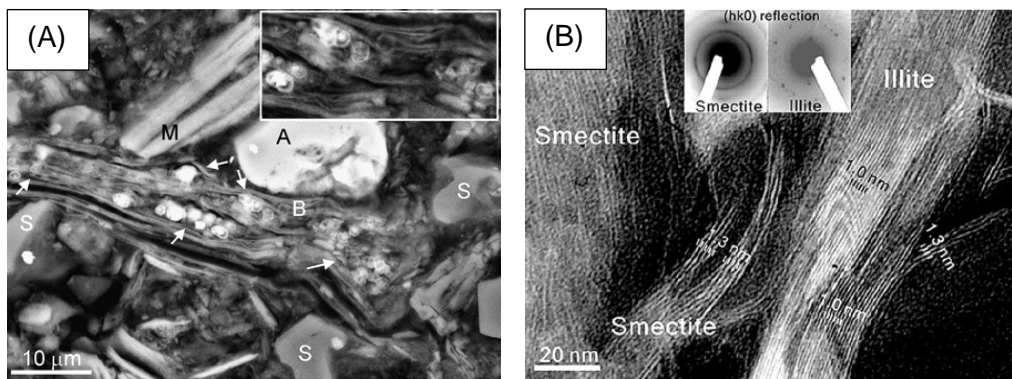


Fig. 4.2 (A) Scanning electron microscopy micrograph of bacteria-shaped, iron-rich sulphides (arrowed) arranged between the exfoliation planes of biotite (denoted by B) grains (see inset with a width of 20 μm for higher magnification) /SAN 09/. (B) Transmission electron microscopy micrograph of the microbially reduced smectite sample with a ~40-nm-thick packet of 1.0-nm illite layers embedded in the matrix of 1.3-nm smectite layers /KIM 04/.

Precipitation of the released silica and the neo-formed illite in pore space can result in a decrease of porosity and permeability of clay as well as in an increase of fluid pressure that can eventually lead to the temporal loss of clay plasticity and to discharge of the clay-confined fluid. As a further consequence of clay dissolution, clay's swelling pressure, cation exchange capacity, and specific surface area become irreversibly deteriorated. It is important to realize that clay half-lives in subsurface settings can vary between just under one hundred thousand years up to a few million years in the presence of millimolar concentrations of hydrogen sulphide, which have been observed in rock formations considered as potential DGR hosts at the condition of sufficient electron donor availability. These timescales are comparable with the above-mentioned timeframe of one million years relevant for safety analyses, for which an assessment of the safety of a potential DGR for HLW/SF after its closure should be carried out in ac-

cordance with regulatory requirements in many countries. Therefore, an estimation of timescales for microbially-driven reduction and dissolution of clay in deep subsurface remains an important subject for future studies (Tab. 4.1).

In a further microbial process, formation of biofilms, clay dissolution can be accelerated by at least one order of magnitude due to an increase of acidity within a biofilm or biofilm-confined pore spaces by up to four orders of magnitude. Another increase in the dissolution rate can be expected to result from a significant reduction of metabolic expense of secreting electron shuttles or Fe(III)-chelators in a biofilm, where they can be effectively reused. Since the extracellular polymer matrix and the boundary of biofilm allow microbes to control the level of metal ions in order to provide optimal metabolic conditions despite possible presence of toxic substances, biofilm formation can lead to accumulation of some metals at levels exceeding those in contacting aqueous solution by up to several orders of magnitude. This accumulation is, however, selective and unique for each specific subsurface environment, so that the possible net effect of biofilm formation on cation and anion sorption capacities of clay can be assumed to depend on the solute identity. Furthermore, the formation of biofilms can substantially influence mass transport and hydrodynamics in porous media by strongly reducing its porosity and permeability and making it even impermeable within short periods of time as observed in column experiments or during the defueling operations in the damaged Three Mile Island reactor. Still, the issue of biofilm formation in the DGR environment has not been given proper attention in the scientific literature, which leaves the questions on whether the biofilms can form in clay buffer, claystone or at their interfaces and on how large can be their effect on clay dissolution largely unanswered (Tab. 4.1).

The formation of biofilms also favours – but is not a prerequisite for – the occurrence of the process of microbially influenced corrosion, which is most closely identified with activity of sulphate-reducing bacteria. The ability of sulphate-reducing bacteria to accelerate corrosion of waste canister or over-pack materials has been so far a major concern of microbial research related to final disposal of radioactive waste in geological formations. As a result of activity of sulphate-reducing bacteria, rates of anaerobic corrosion of iron-based materials can increase by at least two orders of magnitude as compared to abiotic ones and reach as high values as of $700 \mu\text{m yr}^{-1}$, and uniform corrosion can change to pitting corrosion. It cannot currently be concluded from the available experimental data whether, and if so to what extent, the change to pitting corrosion is favoured by which one of the identified four mechanisms of microbially influenced corrosion. This exposes a clear research demand on this topic in order to be able to eval-

uate the possibility of occurrence of pitting corrosion in a DGR for HLW/SF and to quantify its maximum possible effect (Tab. 4.1).

Both an in situ experiment in the Opalinus Clay in the Mont Terri underground research laboratory and a mock-up experiment simulating the waste disposal architecture pursued in Belgium have demonstrated a potential high impact of sulphate-reducing bacteria on pore water chemistry and on performance of metals at repository conditions in disturbed clay. In the first case, a compelling evidence of the activity of sulphate-reducing bacteria in a disturbed deep clay formation has been obtained. In this experiment, synthetic pore water had been circulating in a borehole for five years /WER 11/. As a result of an unintentional placement of a degradable source of organic carbon (presumably, the highly soluble glycerol from gel-filling of reference electrodes used for a continuous monitoring of redox potential and pH of the borehole solution), a substantial activity of sulphate-reducing bacteria has developed in the borehole solution and adjacent clay within a few months after the start of the experiment. This activity led to a more than threefold decrease of sulphate concentration from the synthetic pore water value of 14.7 mmol l^{-1} to 4.3 mmol l^{-1} at the end of the experiment – despite a continuous in-diffusion of sulphate from the surrounding claystone – and an intermediate increase of sulphide concentration to 1.0 mmol l^{-1} , which did not exceed this value due to observed precipitation of ferrous sulphides /STR 11/ /WER 11/. This experiment has revealed the presence in clay of spore-forming sulphate-reducing bacteria and, quite unexpectedly for a rather cold ($\sim 30 \text{ }^\circ\text{C}$) clay environment, of hyperthermophilic sulphate-reducing bacteria, which thrived in the clay samples exposed to a temperature of $80 \text{ }^\circ\text{C}$ /STR 11/.

In the second, mock-up experiment, strong indications of microbially influenced corrosion have been observed on multiple locations of the lining and, most notably, of the heat-generating tube most distant from the hydration tubes despite the high density of $1.8 - 2.0 \text{ g cm}^{-3}$ and temperature above $100 \text{ }^\circ\text{C}$ (up to $137 \text{ }^\circ\text{C}$) for about four years as well as the incomplete water saturation of the backfill /KUR 04/. In one location at the interface between the lining and the backfill, a $\sim 450\text{-}\mu\text{m}$ -thick deposition layer composed of presumably a mixture of chromium oxides (Cr_2O_3) and chromium sulphides (Cr_2S_3) formed with severe, up to $150\text{-}\mu\text{m}$ -deep pits underneath (Fig. 4.3 (A) – (C)). A similar formation of chromium sulphide on stainless steel upon exposure to sulphate-reducing bacteria has been observed in other studies and suggested to occur as a result of a reaction of chromium oxide layer – passivating the steel surface against corrosion – with H_2S produced by sulphate-reducing bacteria /DUA 06/. In another location

at the interface between the tube and sand, thick granular deposition formed from nanoparticles consisting of iron and sulphur (Fig. 4.3 (D) – (F)). Since only metallic iron and ferrous ions were found to be present in the deposition /KUR 04/, these nanoparticles were most likely of ferrous sulphide, which is characteristic of microbially influenced corrosion induced by sulphate-reducing bacteria.

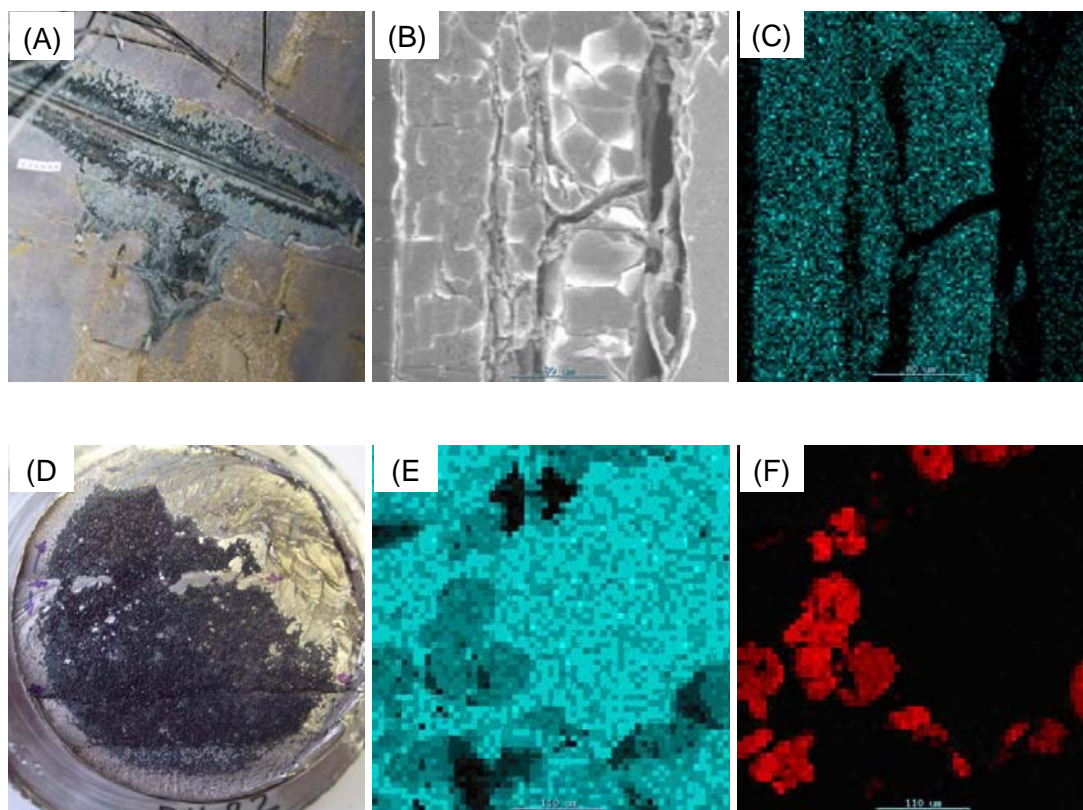


Fig. 4.3 Locations indicative of microbially influenced corrosion on the lining (A) and the heat-generating tube (D) after the five-year-long contact with back-fill consisting to 60 % of clay and with sand, respectively. Scanning electron microscopy micrograph (B) and energy-dispersive X-ray spectroscopy map of sulphur (C) across the interface between a stainless steel and the deposit from (A). Energy-dispersive X-ray spectroscopy maps of iron (E) and sulphur (F) in the deposit from (D) /KUR 04/.

The recent experimental studies revealed that an increase of clay density up to 2.0 g cm^{-3} by compaction can reduce corrosion rates due to activity of sulphate-reducing bacteria by an order of magnitude but not to eliminate that. Furthermore, no elimination of this activity can be expected as a result of temperatures of up to $100 \text{ }^\circ\text{C}$, as they are still conducive for hyperthermophilic sulphate-reducing bacteria present in clays. Owing to the ability of sulphate-reducing bacteria to reduce structural Fe(III) of

clays directly or through production of hydrogen sulphide, their activity can negatively influence eight safety-relevant properties of clay. This aspect of activity of sulphate-reducing bacteria was strongly underrepresented in previous experimental investigations in the field of geological disposal of radioactive waste and requires a proper consideration in the future research activity (Tab. 4.1).

It appears also that in no case should the potential impact of sulphate-reducing bacteria be underestimated based on a possible argument of comparably low biomass of the microbes in contact with metal surfaces or dissolved metals. The timeframe of their potential activity must be considered concomitantly, as in a space of several years a population of sulphate-reducing bacteria confined in a relatively small biofilm encountering sub-micrometre concentrations of dissolved metal in a deep subsurface environment is able to immobilize the metal in precipitates in amounts which would correspond to its economic deposit if extrapolated to geologic scales. Based on observations made for deep subsurface environments, the timeframe of microbial activity in clay formations to be chosen for radioactive waste disposal can be expected to exceed the above-mentioned timeframe of one million years relevant for safety analyses. Therefore, a quantification of the maximum extent of the identified potential effects of microbial activity in clays should give a proper account of long-term changes in the DGR environment which can be of relevance for a possible activation or facilitation of microbial processes unfavourable for the DGR performance (Tab. 4.1).

Production, conversion or consumption of gases in reactions involved into microbial reduction of Fe(III) or sulphate, organics fermentation, reduction of CO₂, and methane oxidation represent a further important issue for the consideration of the overall microbial impact on the long-term performance of radioactive waste repositories in clays. A build-up of gas overpressure around a DGR for HLW/SF because of a disparity between the gas diffusion and gas production rates can result in a fracturing of the clay rock preceded by loss of clay plasticity and accompanied by gas discharge from the DGR. This build-up can be even amplified in a DGR in clay populated with methanogenic microbes, as increased hydrostatic pressures can strongly favour growth and metabolic activity of methanogens. In this case, a DGR may represent a system characterized by a positive feedback with respect to the increase of hydrostatic pressure. Since an in situ experiment in the Opalinus Clay measured microbial methane concentrations comparable to those in hydrocarbon-contaminated subsurface settings where methanogenesis was a major microbial process, future research effort should be aimed at providing data necessary for a quantification of the potential impact of methanogens on

the DGR safety (Tab. 4.1). A further research topic demanding extensive investigation is related to the very recently revealed ability of microbes to induce significant H₂ formation from common minerals and rocks, which may potentially provide additional sources of gas as well as electron donors and acceptors in the repository environment. Thereby, a total microbial gas production utilizing electron donors indigenous to the clay within the containment-providing rock zone and to backfilling and sealing components of a DGR should be set in relation to the gas production as a result of the corrosion of waste canisters and other iron-based materials, which has been considered so far the major source of gas in a DGR.

Tab. 4.1 Research agenda for future work aimed at estimating effects of microbial activity on long-term performance of radioactive waste repositories in clays

Microbial process	Research issue
reduction of clay	reduction rate
dissolution of clay	dissolution rate production and synergistic effect of organic acids, siderophores, and flavins
biofilm formation	occurrence in a subsurface clay environment effect on microbial clay reduction and dissolution
sulphate reduction	pitting corrosion rates for iron-based materials in contact with clays rates of reduction of structural Fe(III) in clay by microbially-produced hydrogen sulphide
gas production	effect of increased (hydrostatic) pressure on activity of methanogens in clays H ₂ formation from minerals in the host rock and in backfilling and sealing components of a DGR
all processes	inventories of electron donors and acceptors in a DGR size of microbial population and its dependence on long-term changes in the DGR environment methodological basis for predicting spatial and time predominance of microbial processes in a DGR

While the occurrence of either of the discussed microbial process in the repository environment – even though perhaps at only low metabolic rate – appears to be backed by the available experimental data, the question of their interplay at repository conditions should be considered still open. Contrary to the earlier, simplistic conception of the dominance order of microbial processes, which was based solely on energetic considerations, the present view recognises that their occurrence critically depends on local

heterogeneity of microbial habitats with respect to, most importantly, the availability of electron donors and acceptors. Quantifying inventories of electron donors and electron acceptors both indigenous to a geological formation chosen to host a DGR and those to be introduced there during the excavation, operation, and closure of a DGR is indispensable for predicting which microbial processes may be active or predominate at which locations within the containment-providing rock zone and at which times after the DGR closure. Future studies should develop a methodological basis and identify parameters and data required for implementation of such an approach in safety analyses of deep geological repositories (Tab. 4.1).

4.2 Basic issues for radionuclide inventory of vitrified waste

The primary aim of the present work was to determine the inventories of the radionuclides and stable elements in vitrified waste produced at La Hague between June 14, 1989 and January 29, 2007 and delivered to Germany, which are of importance for long-term safety analyses of final repositories for radioactive wastes. For a subset of these radionuclides and stable elements, the inventories were determined – either by direct measurements or by involving established correlations – and reported by AREVA. This allowed verification of the validity of application of a model approach utilizing the data of burnup and activation calculations and auxiliary information⁷ on the reprocessing and vitrification process operated at La Hague.

Specifically, the model values obtained for burnups of 33 GWd/t_{HM} and 45 GWd/t_{HM} – assumed to be representative and limitative of spent nuclear fuel reprocessed at La Hague, respectively – were found to provide conservative estimates of the average and the maximum inventories of fission and activation products in vitrified waste delivered to Germany except for two radionuclides, ⁷⁹Se and ¹²⁶Sn, as discussed in more details below. This generally applies to the total radionuclide inventories in vitrified waste. When inventories in individual delivered CSD-V canisters are concerned, for one further radionuclide, ⁹⁹Tc, the maximum model value was still smaller than inventories reported for 38 out of the total of 3017 CSD-V canisters. This was attributed to the variation of content of spent nuclear fuel in CSD-V canisters, which was evidenced by year-

⁷ This kind of information is very valuable for carrying out such a verification considering that vitrified waste delivered to Germany from La Hague was produced by mixing during the reprocessing and vitrification process of reprocessing wastes produced from spent nuclear fuel characterized by different burnups and cooling times and originating from reactors of different types operated in different countries.

to-year comparison but otherwise not quantifiable, with contents in some of canisters apparently exceeding the average value of 1.814 t_{HM} per CSD-V canister used to calculate the maximum model inventories.

In the case of actinides, the present approach was found to show a poorer overall performance. An application of the uranium and plutonium separation factor of 0.9988 characteristic of the PUREX process implemented in reprocessing facilities at La Hague /MAD 95/, /DER 98/, /GIR 08/ to the model inventories obtained with burnup calculations provided conservative estimates of total inventories of uranium and plutonium isotopes in vitrified waste and of their average inventories in individual CSD-V canisters. For instance, the total deliveries of 20.3 and 19.6 kg of ^{235}U and ^{239}Pu to Germany were estimated to be 45.4 and 35.6 kg, respectively, by the model. Considering that both inventories – that of ^{235}U depleted during the irradiation in reactor and that of ^{239}Pu concurrently enriched – are overestimated, the disagreement between the model and measured values was attributed to a model underestimation of uranium and plutonium reclamation during reprocessing of spent nuclear fuel. The maximum inventories of uranium and plutonium isotopes in individual CSD-V canisters, however, were satisfactorily predicted only for ^{234}U , ^{236}U , ^{238}Pu , and ^{241}Pu .

Whereas a similar performance was observed for the transuranic isotope ^{237}Np , the present approach shows a strongly deteriorated performance for ^{241}Am , ^{243}Am , ^{244}Cm , and ^{245}Cm . Indeed, the use of spent nuclear fuel specifications UOX1 representative of the fuel reprocessed at La Hague (burnup of 33 GWd/ t_{HM} , ^{235}U enrichment of 3.5 %) resulted in a considerable underestimation of the total delivered inventories in vitrified waste. It is only with a burnup of 45 GWd/ t_{HM} , which is the maximum burnup of spent nuclear fuel eligible for reprocessing at La Hague, that the present model conservatively estimated the total delivered inventories of 2227, 953, 291, and 18 kg of these actinides, respectively, and their average inventories in individual CSD-V canisters. The maximum inventories in individual CSD-V canisters were in this case satisfactorily predicted for ^{243}Am , ^{244}Cm , and ^{245}Cm but not for ^{241}Am .

The strong non-linear dependence of build-up of ^{243}Am , ^{244}Cm , and ^{245}Cm in spent nuclear fuel on burnup was concluded to disqualify the use of an average, representative burnup for estimating the inventories of these actinides both in vitrified waste and spent nuclear fuel, because it inherently implies a linear dependence of actinide inventory on burnup. The fact that that the burnup of 33 GWd/ t_{HM} may indeed be equal to the average burnup of spent nuclear fuel reprocessed at La Hague or be even higher than that

does not contradict the fact that fuel assemblies irradiated to burnups higher than 33 GWd/t_{HM} were reprocessed at La Hague /BIG 98/.

The reason for the model underestimation of inventories of ²⁴¹Am, which show a nearly linear dependence on burnup, on the contrary, was suggested to be related to a contribution of an additional waste stream, which distinguishes this radionuclide from most of the other radionuclides during the reprocessing in La Hague and was not accounted for in the initial model. Namely, a time lag of at least three years between the separation of plutonium and its dispatching to plants manufacturing mixed oxide fuel may apply for half of the plutonium stored at La Hague by the end of 2007. During this time, fissile ²⁴¹Pu decays with the half-life of 14.35 years to gamma-emitting ²⁴¹Am, and a purification of plutonium oxide powder becomes necessary in order to decrease radiation hazard to the personnel of fuel fabricating plants and to decrease the content of neutron absorber ²⁴¹Am in fabricated fuel.

The re-dissolution and purification of aged PuO₂ after an interim storage for a few years was successfully carried out at La Hague since 1990, and a delayed input of ²⁴¹Am into the waste stream directed to vitrification was additionally accounted for in the present model. As a result, the modified model appeared to conservatively estimate the total and average inventories of ²⁴¹Am in vitrified waste based on the representative burnup of 33 GWd/t_{HM} and the reasonable assumption that PuO₂ purification takes place after a two-year delay. The maximum ²⁴¹Am inventory in individual CSD-V canisters was conservatively predicted for 3013 out of 3017 CSD-V canisters by the modified model based on the burnup of 45 GWd/t_{HM} and the assumption of a three-year delay of PuO₂ purification.

Concerning the above mentioned model underestimations for ⁷⁹Se and ¹²⁶Sn, an inspection of the method of determination of ⁷⁹Se and ¹²⁶Sn inventories by AREVA /ARE 06b/ revealed that AREVA used decay half-lives of 65,000 and 100,000 years for these two radionuclides, respectively, in order to calculate their inventories in CSD-V canisters from the measured neodymium contents. These decay half-lives became outdated between 1995 and 1996 /OBE 99/, /JOE 10/. The present model, on the contrary, used the respective values of 327,000 years /JOE 10/ and 198,000 years /BIE 09/ corresponding to the current state of knowledge. This explained the difference between the model estimations versus the inventories reported by AREVA.

A corresponding correction of the data reported by AREVA resulted in conservative model estimates of the total and average inventories of ^{79}Se in vitrified waste and the average and maximum inventories of ^{79}Se in individual delivered CSD-V canisters. Similarly, the maximum inventory of ^{126}Sn in individual CSD-V canisters was conservatively estimated by the model value based on the burnup of 45 GWd/t_{HM}, whereas the average inventory of ^{126}Sn in vitrified waste and in individual CSD-V canisters still remained underestimated – though statistically insignificant this time – by the model value based on the burnup of 33 GWd/t_{HM}.

The present model generally assumed a time lag of four years between the discharge of spent nuclear fuel and its reprocessing at La Hague – in accordance with the design specifications – and a further time lag of one year between the reprocessing and the vitrification of the resulting concentrated fission product solutions necessary to provide for proper glass resistance to thermal shocks and devitrification /LIB 98/. Comparisons between the model predictions and the inventories of ^{134}Cs and ^{154}Eu reported by AREVA suggested an additional cooling time of 2.2 – 3.1 years for vitrified waste delivered to Germany. Estimations of cooling time based on ^{134}Cs or ^{154}Eu inventories are routinely used for verification of the consistency of the cooling time declared by the power reactor operator /PHI 80/, /WIL 06/. However, because of non-linear dependencies of their inventories on burnup and some dependency on the enrichment of fresh nuclear fuel, which broadly varied over spent nuclear fuel reprocessed at La Hague, the accuracy of such estimations in the present case is limited.

Still, the suggestion that the factual cooling time can exceed the time period of five years is not unreasonable considering that up to about 21 % of the CSD-V canisters delivered by AREVA to Germany were at least partially produced from the backlog of ~1200 m³ of the concentrated fission product solutions accumulated at La Hague since the start of the reprocessing of spent nuclear fuel from light water reactors in the plant UP2 in 1976. The according contribution to an increase of the average cooling time characteristic of vitrified waste delivered to Germany – though not quantifiable based on the data available to the authors – can be reasonably assumed to be sizeable.

Differently from ^{134}Cs and ^{154}Eu , content of ^{137}Cs in spent nuclear fuel changes linearly with burnup /PHI 80/, /WIL 06/ and does not depend on the enrichment of fresh nuclear fuel /WIL 06/. From the ratio of 1.12 between the calculated and the measured ^{137}Cs contents, an average burnup of 29.4 GWd/t_{HM} can be estimated for spent nuclear fuel, which was reprocessed at La Hague to produce vitrified waste delivered to Germany.

This burnup is consistent with the average value of 27.6 GWd/t_{HM} reported for spent nuclear fuel reprocessed at La Hague from 1989 to 1996 /WIS 01/ and the average burnup of ~25 GWd/t_{HM} characteristic of ~4800 irradiated fuel assemblies reprocessed at La Hague from 1976 to 1998 /BIG 98/.

Having proved the validity of application of a model approach utilizing the data of burnup and activation calculations to prediction of inventories of actinides, fission and activation products in vitrified waste, the present work estimated the minimum, average and maximum inventories of the radionuclides, which are of importance for safety analyses of final repositories for radioactive waste but were not reported by AREVA for delivered CSD-V canisters. The average and maximum inventories in individual CSD-V canisters predicted in the present approach were compared to the inventories predicted by Nagra for canisters with vitrified waste delivered from La Hague to Switzerland /NAG 08/. This comparison revealed a number of differences between these inventories despite the fact that the canisters delivered to Switzerland were produced in essentially the same way and from the common reprocessing waste stock as CSD-V canisters delivered to Germany.

Therefore, a further work is required in order to identify the reason for the discrepancy in the present estimation versus the Nagra estimation. Such a work would also address the recommendation by the international peer review of the Safety Report of the Project Opalinus Clay /NAG 02/ to obtain estimates of the inventories of ¹⁴C, ³⁶Cl, and ¹²⁹I in the vitrified waste in agreement with those of other countries with similar waste forms /NEA 04b/. Since vitrified waste from reprocessing of spent nuclear fuel at La Hague was delivered to several countries – Belgium, France, Germany, Japan, Netherlands, and Switzerland – an international effort would be indispensable for fulfilling this recommendation.

Activities of actinides, fission and activation products can generally be accurately calculated by the present approach for the case of a pre-disposal storage of vitrified waste during a specified period of time. This does not apply, however, to those radionuclides, which can be produced in CSD-V canisters during the pre-disposal storage by the neutron capture reaction. Taking into account thermal neutron capture cross sections and contents of stable elements to be considered in this regard, ⁴¹Ca, ⁵⁹Ni, ⁶³Ni, ³⁶Cl, and ¹⁴C were identified as such radionuclides, inventories of which can increase with time from the inventories of stable isotopes ⁴⁰Ca, ⁵⁸Ni, ⁶²Ni, ³⁵Cl, and ¹⁴N as well as ¹⁷O. Therefore, it is recommended that this issue be considered in future research activity.

The present work suggests that performing burnup calculations with isotope inventories resulting from a two-year pre-irradiation storage of fresh nuclear fuel is necessary for obtaining reliable estimations of inventories of ^{226}Ra , ^{229}Th , and ^{232}U in vitrified waste. Furthermore, an estimation of maximum inventories of some isotopes relevant for long-term performance of radioactive waste repositories requires performing burnup calculations with minimum burnups characteristic of vitrified waste produced at La Hague. Additionally, an estimation of the average and maximum radionuclide inventories in vitrified waste requires burnup calculation data covering typical ranges of impurity contents in fresh nuclear fuel and cannot confidently be derived with datasets relying alone on conservative assumptions about impurity contents.

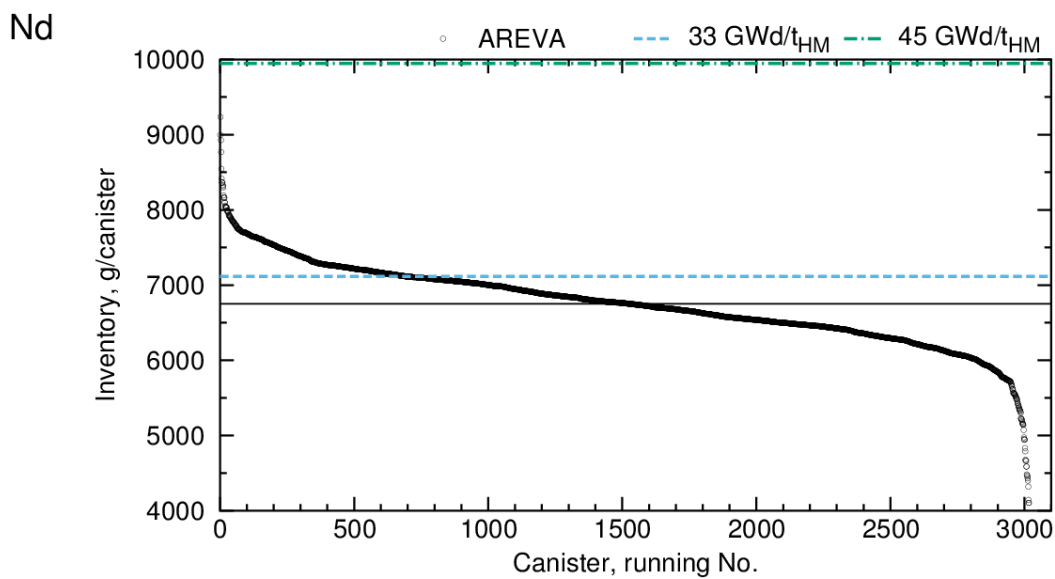


Fig. 4.4 Inventories of neodymium (at the time of vitrification) in CSD-V canisters delivered by AREVA to Germany

Inventories reported by AREVA are represented by 3017 empty circles, and the average reported inventory is shown as solid line. Model CSD-V inventories were estimated from burnup calculation data for burnups of 33 and 45 GWd/t_{HM} (UO₂ fuels with 3.5 and 3.8 % ^{235}U , respectively) and are shown as dashed and dot-dashed lines. Average time lag of five years between the discharge of spent fuel and the production of CSD-V canisters is assumed.

As a further research issue, the possibility of the use of the measured neodymium inventories in vitrified waste (Fig. 4.4) accompanied by radionuclide-specific correlation factors as an alternative prediction method should be proved. Indeed, AREVA used this method to determine the inventories of ^{79}Se , ^{93}Zr , ^{107}Pd , ^{126}Sn , and ^{135}Cs in vitrified waste produced at La Hague /ARE 06b/. Furthermore, the inventories of ^{243}Am and ^{245}Cm in vitrified waste were calculated from the measured neodymium and ^{244}Cm con-

tents /ARE 06b/. Moreover, the interstate agreements for delivery of vitrified waste in CSD-V canisters produced at La Hague operate with the total quantity of neodymium in spent nuclear fuel shipped by a state of origin for reprocessing to France as the measure for the total activity to be delivered back to the state of origin of spent nuclear fuel /ARE 08/. This fact indicates that estimation of radionuclide inventories in vitrified waste based on neodymium inventories can be considered a reasonable alternative and, possibly, a reference calculation method.

Inventories of oxides of stable elements in vitrified waste delivered by AREVA to Germany either exclusively originate from glass frit (as is the case for SiO_2 , B_2O_3 , Li_2O , ZnO , and CaO), come as glass frit constituents and process additives (Na_2O and Al_2O_3) or come as products of tributyl phosphate degradation during the reprocessing (P_2O_5) and products of corrosion of steel components of fuel assemblies, reactor equipment, and melting crucible (Fe_2O_3 , NiO , and Cr_2O_3). A further important stable constituent of vitrified waste, ZrO_2 , comes as a constituent of glass frit, a fission product, and a corrosion product.

The ranges of variation of reported contents of glass constituents in vitrified waste delivered to Germany exceed those given for the reference R7/T7 glass in the literature. Moreover the average inventories of Fe_2O_3 , NiO , and Cr_2O_3 reported by AREVA are about three to fivefold lower than the minimum literature values for the reference R7/T7 glass. The average content of calcinate in vitrified waste delivered from La Hague to Germany, on the contrary, significantly exceeds the average total content of oxides of the radioactive and stable isotopes originating from spent nuclear fuel reported for the reference R7/T7 glass. This difference may be explained by the presence of significant amounts of nitrates in vitrified waste.

With regard to the inventories of stable elements in vitrified waste, the present situation appears to be not quite satisfactorily. A reliable estimation of the inventory of, e. g., ZrO_2 – measured by AREVA in the reference R7/T7 glass /ARE 06a/ but not reported for vitrified waste delivered to Germany – or NO_3 – apparently not measured by AREVA but important for safety analyses of final repositories for radioactive wastes – is currently not possible and requires additional data from AREVA on, e. g., the mass of glass frit added to calcinate to produce CSD-V canisters. A future research project involving international cooperation could possibly improve this situation.

4.3 Repository sealing and closure

4.3.1 THERESA

From 29 September to 1 October 2009 an international conference on "Impact of Thermo-Hydro-Mechanical-Chemical (THMC) processes on the safety of underground radioactive waste repositories" was held in Luxembourg /TIM 09/. The conference and workshop was jointly organised by European Commission (EC), EIG EURIDICE (European Underground Research Infrastructure for Disposal of Nuclear Waste in Clay Environment) and KTH (Royal Institute of Technology) in the framework of the EC projects TIMODAZ (Thermal Impact on the Damaged Zone Around a Radioactive Waste Disposal in Clay Host Rocks) and THERESA (Coupled **Th**ermal-Hydrological-Mechanical-Chemical Processes for Application in **R**epository **S**afety **A**ssessment) /THE 09/. The conference focused on the appraisal of the understanding of processes and respective modelling capabilities regarding the assessment of the impact of combined effects such as excavation, buffer emplacement and thermal output on the host rock's integrity and on the short- and long-term performance of engineered barrier systems (EBS) in nuclear repositories.

In the foreground of the THERESA salt group discussions was the long-term evolution of the excavation disturbed zone (EDZ) in a salt repository. The discussion addressed in particular the current understanding of the near field processes affecting EDZ evolution on the long term, especially its re-compaction and the related significance for reliable long-term performance assessments.

Of special interest for the German project partners was the question of EDZ reduction with regard to the new approach of the safe containment of HLW within a Containment Providing Rock Zone (CPRZ) which together with the repository mine defines the repository system /AkEnd 2002/.

In the frame of the former European Commission Cluster Conference on the "Impact of the excavation disturbed or damaged zone (EDZ) on the performance of radioactive waste geological repositories" held in Luxembourg 2003 /DAV 05/, the EDZ was defined, and the relevant processes leading to dilatancy and re-compaction were described. First models to describe dilatancy were available and implemented. Re-compaction, however, could not be modelled reliably at that time.

During the conference and workshop in the fall of 2009 it was found that in the meantime, considerable progress has been made regarding the development and implementation of models describing dilatancy and re-compaction. First models describing healing by re-crystallization have been implemented. Still, open issues remain regarding the reliable prediction of EDZ evolution and long-term re-compaction or healing, respectively.

THERESA showed that the currently implemented models still need further validation, especially to show they are suited for calculating in-situ configurations. In order to decide which models with which parameters describe the reality adequately, more experimental data, both existing and specially obtained for this objective, both from lab tests and in-situ experiments, will have to be considered.

A prerequisite for the adequate prediction of damage and healing of rock salt is the application of the dilatancy concept, where the stress dependent dilatancy boundary yields the criterion whether dilatation or compaction is dominating. The processes, which are active in the dilatant stress domain and which produce damage, are described by constitutive models which are generally based on micro-mechanical deformation processes. They are generally controlled by dislocation mechanisms. Whether the decrease of the porosity and the permeability is dominated by poro-elastic compaction in dependence on the minimum or the mean stress and by time dependent processes is still under debate.

The results of the salt group discussions have been summarized as follows:

- The thermo-hydro-mechanical (THM) near field processes and their coupled impact on EDZ generation is adequately understood and also adequately represented in the THM-models currently being implemented in advanced computer codes such as Code_Bright, FLAC, JIFE.
- The existing experimental data base as well as the experimental possibilities within the THERESA project on EDZ reduction is scarce and thus insufficient for the necessary model confirmation along with the required proof of the functioning of EBS in interaction with the EDZ on the long term.
- Additional laboratory research is thus still needed
 - to achieve an adequate understanding of EDZ reduction and representation in THM-models,

- to provide a sound basis for the reliable engineering of EBS in interaction with EDZ under consideration of the requirements of the system of Structural Eurocodes.
- Performance assessment calculations conducted within the THERESA project on basis of currently used models revealed hints for an adequate EDZ reduction after a time period of no more than about 3000 to 4000 years. This period will be shorter if technical improvements are carried out, e. g. refacing of contours by excavation of the EDZ. Therefore, a long-term significance of EDZ will fade away. This preliminary result, however, suffers of the uncertainties still existing with proper understanding of the long-term reduction (re-compaction) of EDZ.

The principal challenges remaining with regard to filling the gaps of understanding the coupled processes of damage and re-compaction (or self-sealing, respectively) in rock salt are:

- Further long-term compaction tests at moderate stresses with the consecutive measurement of permeability and porosity. The testing duration has to be much longer than several months, otherwise the empirical equations for the extrapolation of the compaction behaviour cannot be checked adequately.
- Development, validation (including validation of their suitability for in-situ application), and calibration of generally agreed constitutive models for the re-compaction of dilated rock salt.
- Model implementation in numerical codes, enabling reliable extrapolations to long-term in-situ conditions.
- Understanding of physical processes which control the efficiency of healing in dilated rock salt with respect to humidity effects.
- The impact of a pore-pressure (gas and salt solutions, respectively), i. e. chemical and hydraulic interaction.

The delineated research is considered necessary also to fulfil the requirements of the safety case of a HLW repository. In this context, the proof of function (e. g. tightness) of EBS in interaction with EDZ is required to be state-of-the-art. Concerning conventional geotechnical barriers, state-of-the-art technology is defined for instance by the system of Structural Eurocodes (<http://eurocodes.jrc.ec.europa.eu>) and the related national standards. If these regulations are applied the efficiency of a conventional geotechnical

barrier is shown with an adequate degree of reliability. The degree is quantitatively defined on a risk based approach, which is fixed by regulatory specifications. In this regard, the system of Structural Eurocodes forms a sound basis for licensing a geotechnical barrier of a final repository.

It has to be stated, however, that proper function of the EBS seals (shaft and drift seals) depends significantly on a reliable prediction of the EDZ's state. With the above issues resolved, reliable predictions of the interaction of the EBS with the surrounding host rock or the EDZ will be possible and the standards and regulatory specifications representing the state-of-the-art will be fulfilled.

4.3.2 Workshop Sealing Systems in a Repository for HLW

In August 2010, the GRS- Repository Safety Research Division and the Project Management Agency "Projektträger Karlsruhe – Wassertechnologie und Entsorgung (PTKA-WTE) of the German Ministry for Economics and Technology" organised a Workshop on Sealing Systems in a Repository for Heat Generating High-Level Radioactive Waste /GRS 10/.

A bilateral expert meeting held in April 2010 resulted the need to pursue the discussion on the role of engineered barrier systems (EBS) under consideration of the new approach of the safe containment of the radioactive waste in a Containment Providing Rock Zone (CPRZ) /AKE 02/.

The objectives of the workshop were to analyse

- the state-of-the-art regarding the proof of function of EBS and
- to identify the related need for R&D.

35 experts from 18 different German institutions experienced since many years in R&D on Radioactive Waste Disposal participated in the workshop with presentations and discussions on state-of-the-art and open questions regarding

- types of engineered barrier systems
- engineering proof of engineered barrier systems
- suitability of native sealing materials

- suitability of non-native sealing materials
- impact of the contact zone between EBS and the host rock
- behaviour of EDZ around EBS.

Because of the broad spectrum represented by the participating institutions it was expected that the workshop results described in the following would represent the present state of knowledge adequately.

4.3.2.1 Workshop Results

The EBS consisting of different components is to compensate for the unavoidable violation of the geological barrier which is due to the necessary mining activities.

One of the major results of the workshop was the conclusion that the development of closure and sealing concepts for the different repository voids (e. g., disposal cells, drifts, and shafts) needs identification and consideration of the specific safety requirements that account for the specific situation and which are to be taken into consideration during respective R&D works. The requirements result mainly from safety analytical model calculations for different evolutions of the repository system.

Independent from the results of the individual analyses the following requirements are of general importance for the EBS with regard to the sealing effectiveness against fluids (liquids and gases) in the post-closure phase:

- immediate effectiveness against any intrusion of solutions
- continuous effectiveness in the post-closure phase for probable repository evolutions in the long term.

The following items are important with regard to the verification procedure:

- the required hydraulic resistance of the EBS, consisting of sealing material, contact zone, EDZ and intact host rock;

In this regard the long-term stability of sealing materials against prevailing solutions and the possibly occurring alteration of the materials with time as well as the resulting impact on the hydraulic properties are to be investigated.

The permanent existence of a contact pressure at the EBS-host rock interface is considered important when using swelling sealing materials.

Consideration of the EDZ questions still existing with respect to the interrelationship between the mechanical behaviour (dilatancy and re-compaction) and the permeability (permeability/dilatancy-relation). These questions are to be answered urgently, especially with regard to EDZ reduction.

- the evolution of the compaction of crushed salt used as native backfill and sealing material in the dry and the moist state as well as the achievable final state;

This issue requires the analysis of the relevant processes and the formulation and the improvement of material models as well as their validation on basis of back-calculations of reliable laboratory experiments. The investigation of the long-term stability of self-sealing backfill (SSV) /HER 12/ as additional backfill material in case of a brine intrusion is to be pursued as well.

- the required functional period, which is to be determined by performance assessment calculations for all repository concepts;
- the transition from a systematic-deterministic to a reliability-oriented semi-probabilistic design and verification procedure;
- the applicability of a probabilistic verification procedure as part of the EBS integrity proof is to be developed further.

The workshop participants agreed that a technical in-situ demonstration on a 1:1-scale would be necessary before any EBS realisation. This necessity arises also from the new safety requirements published by BMU (German Federal Ministry of the Environment, Nature Conservation and Reactor Safety) in September 2010 /BMU 10/. In this context, the following items are to be considered:

- proof of the robustness of repository components; manufacturing, construction, and function are generally to be tested in advance (or be proven adequately);
- checking the realization of EBS-requirements;

- identification, characterization, and modelling of the safety relevant processes (confidence building, model qualification);
- comprehensive identification and analysis of safety relevant scenarios;
- identification, appraisal and handling of uncertainties.

4.3.3 Self-healing backfill

In Germany disused potash mines have been used for the disposal of low level radioactive waste. Potash mines are still used as repositories for chemical wastes. In repositories technical barriers must be built in order to prevent brine intrusion, mobilization and transport of radionuclides and toxic substances.

During the last ten years scientists and technicians of the GRS department for Final Repository Safety Research have developed and patented a self-sealing material (SVV) for technical barriers in salt and potash mines /EUR 04/. Extensive laboratory and in-situ research has proven that this material is suited to stop brine intrusions and form reliable long-term stable seals which develop their sealing properties at the first contact with brines and maintain their chemical hydraulic and mechanical properties over geological time frames /SAN 02/, /HER 05/, /HER 07/, /HER 10/, /HER 12/. This paper gives an overview over the SVV properties derived from laboratory and large scale in-situ experiments.

4.3.3.1 Materials

SVV is a fine-grained dry material consisting of either pure water free $MgSO_4$ or of a mixture of water free $MgSO_4$ with halite and sylvite. SVV is self-sealing. It develops its sealing capacity upon contact with brine. Salt solutions with different chemical composition in contact with $MgSO_4$ can trigger the formation of a brine-tight seal. The origin of the salt solution may be a natural brine inflow or a manmade technical solution. For the construction of technical barriers the fine-grained dry SVV material must be emplaced between bulkheads and flooded. Thus an immediate sealing effect is obtained. If drifts must be protected against possible brine inflows in an unpredictable future it is sufficient to emplace loose dry SVV material in the drift and wait for the arrival of the brine. In both cases SVV will develop its sealing properties upon contact with the brine.

Independently from their origin and chemical composition all brines are capable to trigger the sealing reaction in the SVV. For practical reasons, for the construction of SVV dams, brine compositions should be in chemical equilibrium with the mineralogy of the surrounding salt formation. For sealing constructions in rock salt, a NaCl-rich halite saturated solution is recommended. In the surroundings of the potash beds carnallite (a potash ore salt containing mainly carnallite, kieserite, halite and anhydrite) or HARTSALZ (hard salt, a potash bed containing sylvite, halite, kieserite and other sulfate minerals), brines with high Mg and K contents, IP21 or IP19 solutions are adequate. In the extremely soluble potash salt tachyhydrite (a potash formation containing tachyhydrite, carnallite, and halite) CaCl₂- and MgCl₂-rich brine is recommendable.

4.3.3.2 SVV-brine reaction

The self-sealing of SVV upon contact with brine is due to a chemical reaction where water from the brine is incorporated in the crystal lattice of hydrated salt minerals. This is a dynamic process by which anhydrous MgSO₄ is transformed in MgSO₄ hydrates and brine water is consumed. The brine gets oversaturated and precipitates the oversaturated minerals. The newly formed minerals, the hydrates and the precipitates have a higher volume than the original pore space of the dry SVV. This volume increase reduces the open pore space and decreases the permeability. The reaction is finished when the water from the intruded brine is totally consumed. At this stage, a dry impermeable seal is formed. When this reaction takes place in a restricted volume (for example in the space between two bulkheads filled with SVV), the volume increase leads to a pressure build up which acts upon the excavation disturbed zone (EDZ) thus reducing further the permeability of the system dam-EDZ-salt.

4.3.3.3 SVV and natural analogs

Natural self-sealing reactions are well-known in salt formations. Examples are secondary kainite seams at the top of German salt structures or above primary potash beds /ZIN 65/, Fig. 4.5. The secondary kainitic potash rocks are the results of solution metamorphism where solutions from the overburden interact with primary potash beds like carnallite (potash rock consisting mainly of carnallite, kieserite, halite and anhydrite) or hard salt (potash rock consisting mainly of sylvite, kieserite halite and anhydrite).

The motor of the transformation of HARTSALZ hard salt and / or carnallite into kainitic potash salt is an under-saturation of the solution in MgSO₄. During the dissolution of

the primary potash rocks, the saturation of sylvite (KCl) is reached at an early stage. At this stage the solution is still under-saturated in kieserite ($\text{MgSO}_4 \cdot \text{H}_2\text{O}$). This means that kieserite from the potash rocks will continue to be dissolved. Each mole of newly dissolved kieserite brings one mole of water into the solution. At the same time one mole of KCl and one mole of MgSO_4 in the solution are combined and precipitate as kainite ($\text{KCl} \cdot \text{MgSO}_4 \cdot 3\text{H}_2\text{O}$) depleting the solution of 3 moles of water. This means that more water is removed from the solution than is added. The consequence is the formation of a new potash rock kainite that uses up the intruded solution. As the molar volume of the newly formed kainite is larger than the combined molar volumes of sylvite and kieserite which are removed from the system pathways are obstructed and no more solution can enter the system. A self-sealing process has sealed effectively previously existing solution pathways.

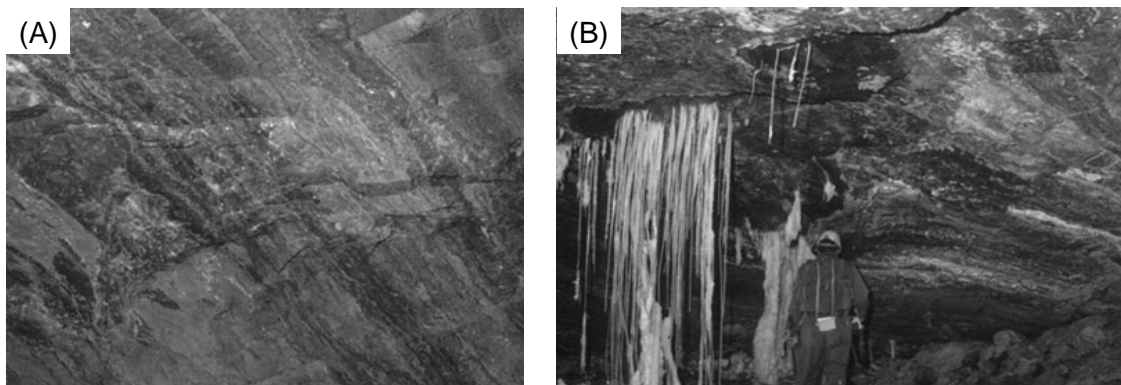


Fig. 4.5 (A) Dry kainite layers in the mine Brefeld, Germany indicate a natural sealing of brine pathways (Foto /BRO 01/); (B) due to mining activities reactivated brine pathways in layers of kainite, bloedite and epsomite

4.3.3.4 Laboratory experiments and results

First results of laboratory experiments have been reported by /HER 07/. Some of the figures below are reproduced here in order to give a comprehensive overview over the entire work with SVV. In most experiments pure anhydrous MgSO_4 and three different brines were used. Tab. 4.2 shows the chemical compositions of these brines.

Tab. 4.2 Composition of the solutions in SVV experiments

Brine	Density [g/ml]	Na	K	Ca	Mg	Cl	SO ₄
		[mmol/kg H ₂ O]					
NaCl	1.200	6104	-/-	-/-	-/-	6106	-/-
IP21	1.304	250	156	1	4109	7955	316
Tachyhydrite	1.455	53	32	4551	2107	12730	-/-

Fig. 4.6 shows a schematic diagram of the setup for the measurements performed with SVV and brine. Dry SVV was emplaced in pressure cells and flooded with brine. The volume and mass of the initially dry SVV was registered as well as the volume and mass of the brine pumped into the cells. The increasing brine pressure needed to maintain a constant brine flow into the cells was registered as well as the buildup of a crystallization pressure within the cells. At the start of brine injection the brine entering the large open pore space between the grains of anhydrous MgSO₄ encounters no resistance.

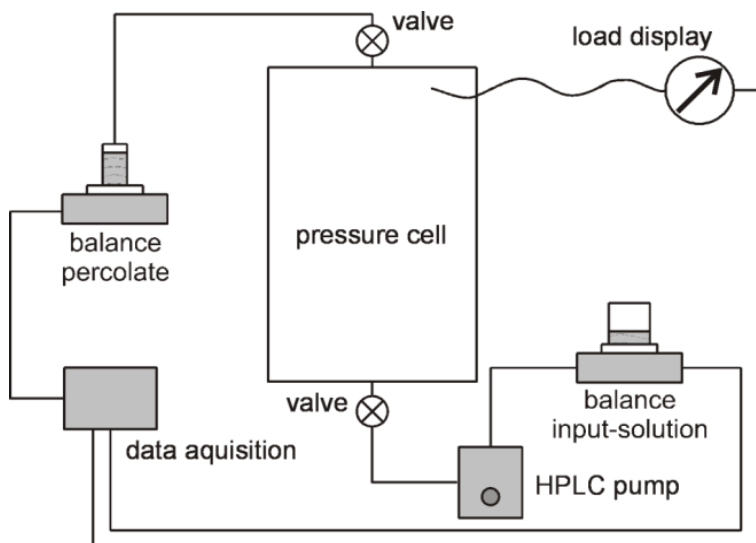


Fig. 4.6 Schematic diagram of the equipment for crystallization pressure measurements (from /HER 07/)

As the hydration reaction starts immediately after the first contact of brine with SVV, the volume of the system increases rapidly and the free pore space accessible to the brine is gradually reduced. Thus it is necessary to increase the brine pressure in order to maintain a constant brine flow rate. In laboratory experiments, brine pressures of up to 9 MPa were used. In the in-situ experiments however lower brine pressures of up to

3.0 MPa were not exceeded in not to fracto avoid fracturing the surrounding rocks. Fig. 4.7 shows schematically the relationship of brine pressure, brine mass and crystallization pressure in a constant volume. Fig. 4.8 shows photographs of the experiments in pressure cells of different sizes and in large pressure tubes.

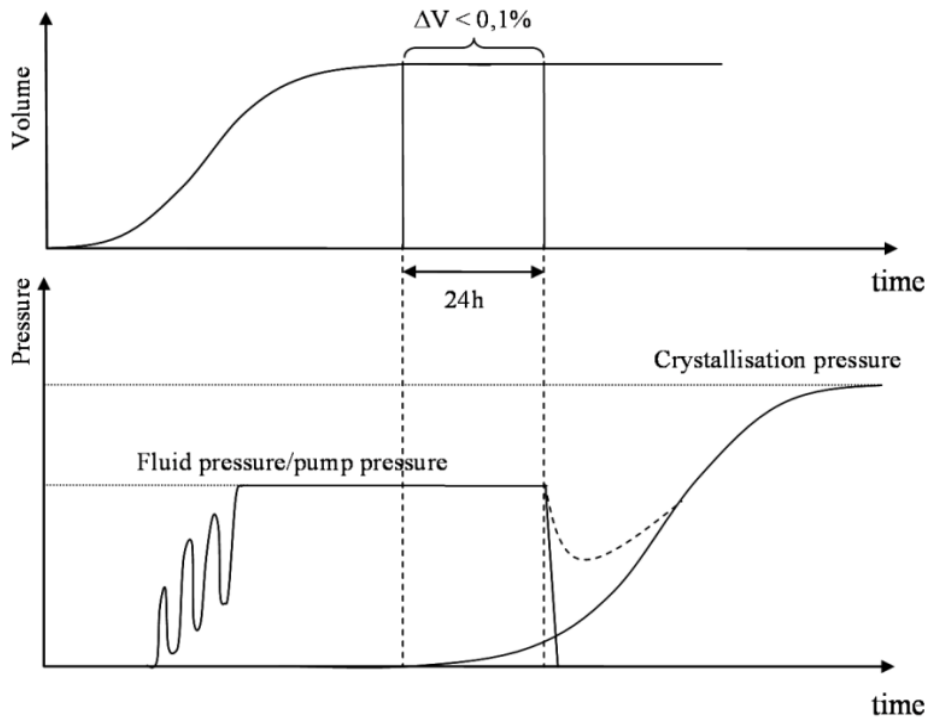


Fig. 4.7 Schematic diagram of the development of fluid pressure, crystallization pressure and volume changes during the flooding of SVV with brines (from /HER 07/)

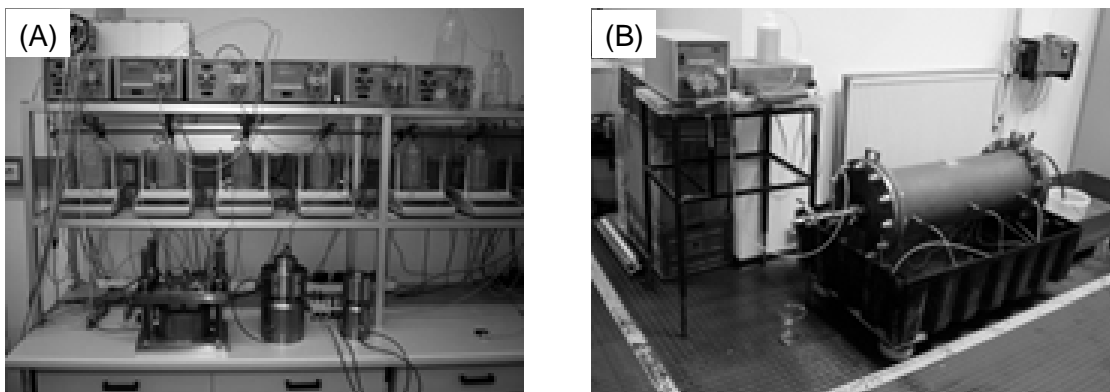


Fig. 4.8 Laboratory experiments with SVV at different scales: (A) in pressure cells of different sizes and geometries, (B) in large pressure tubes (from /HER 07/)

The results of the laboratory tests can be summarized as follows:

- Initial porosity of dry SVV 30 – 40 vol.-%,
- Residual porosity of SVV after reaction with brine 2 – 5 vol.-%,
- Crystallization pressures (Tab. 4.3) dependent on the mineralogical composition of the dry SVV, the chemical composition of the brine and the solid-solution ratio (which can be influenced by the allowed brine pressure),
- Mineralogical composition of resulting SVV seal depends on initial mineralogical composition of dry SVV and of chemical composition of brine,
- Permeability of reacted SVV is generally low, between 10^{-18} – 10^{-21} m² (Fig. 4.9),
- Porosity-permeability relationship of reacted SVV is comparable to that of crushed dry and wet rock salt (Fig. 4.10),
- Geotechnical properties of resulting SVV seal after reaction with brine show a large scattering but in general they are comparable to the properties of rock salt (Fig. 4.11).

Tab. 4.3 Crystallization pressures from measurements in pressure cells of different sizes with pure MgSO₄ and three brines at different solid-fluid ratios

Brine type	Solid-solution ratio		Crystallization pressure [MPa]	
	Range	Mean	Range	Mean
NaCl	1.7 – 2.0	1.9	1.4 – 8.7	3.5
IP21	1.5 – 1.9	1.7	1.7 – 6.9	4.4
Tachyhydrite	1.3 – 1.5	1.4	2.8 – 8.9	5.6

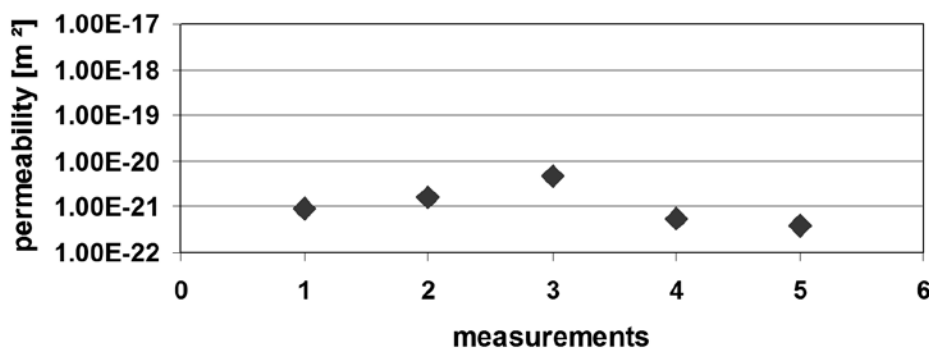


Fig. 4.9 Example of permeability measurements on samples from an experiment in a pressure tube of 3 m length and 20 cm in diameter with pure MgSO₄ flooded at 8 MPa with tachyhydrite brine (figure from /HER 07/)

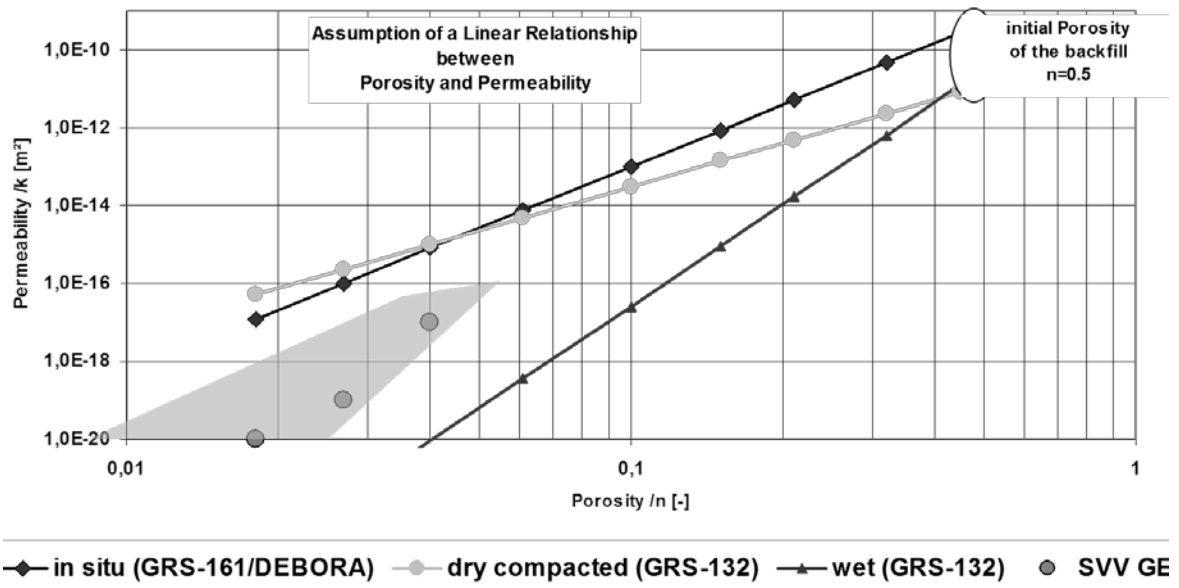


Fig. 4.10 Porosity-permeability relationship of SVV samples with IP21 brine compared to data for dry and wet crushed rock salt (from /HER 07/)

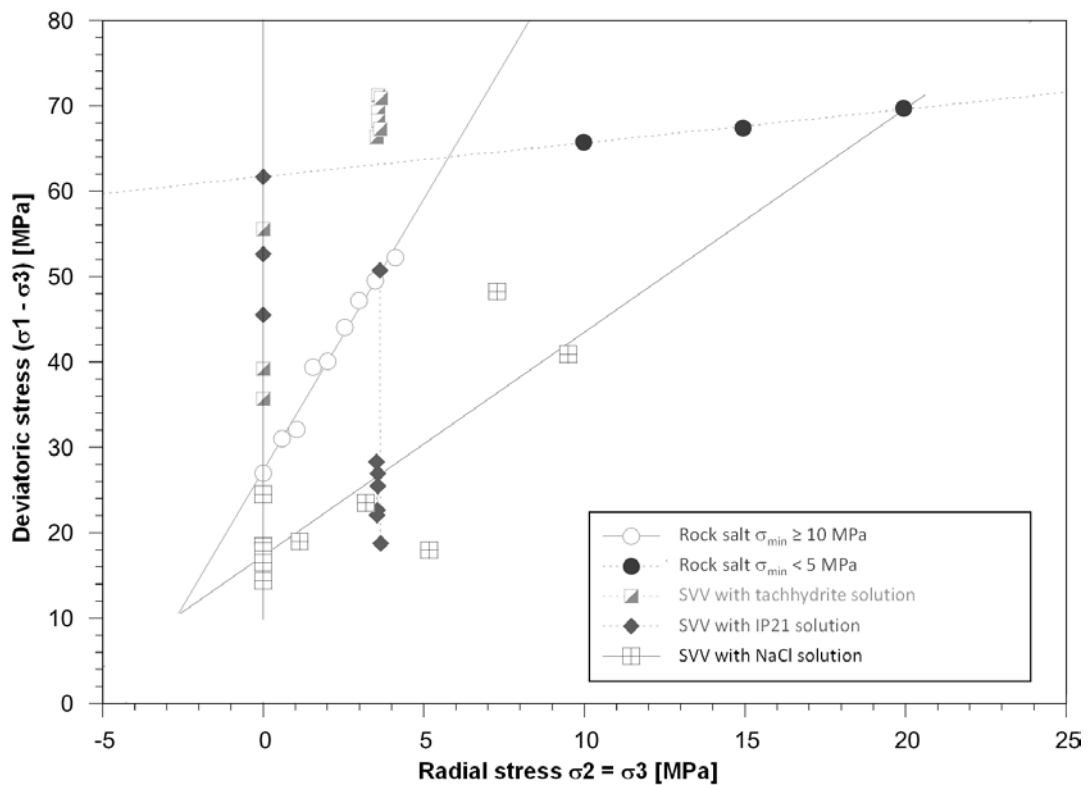


Fig. 4.11 Geotechnical data of SVV compared to data of rock salt, uniaxial measurements (no confining pressure) and triaxial measurements (confining pressure between 1 and 10 MPa)

4.3.3.5 Technical requirements for the construction of seals with SVV

A technical barrier with an SVV-seal consists of:

- the excavated rock section which is to be sealed including its excavation disturbed zone,
- the SVV sealing element,
- two bulkheads at both ends of the sealing element which confine the volume in which SVV can expand during the reaction with brine,
- and the brine needed for the reaction.

The material of the bulkheads and the chemistry of the brine should be adapted to the boundary conditions of the rock sections which must be sealed. Suitable bulkhead materials are CaO based salt concrete (in sections with pure rock salt) or MgO based SOREL concretes (in potash rock sections). Bulkheads may also consist of reacted SVV. SVV-bulkheads can be used in all types of salt formations. Permeability's of the salt concrete and the SOREL concretes are generally $< 10^{-19}$ m² and thus low enough for the required bulkhead constructions.

Suitable brines for the different rock sections are NaCl-rich brine (in a rock salt environment), Mg-rich IP19 or IP21 brine (in potash rocks containing carnallite and sylvite) and CaCl₂-rich brine saturated in tachyhydrite (in potash rocks with tachyhydrite and carnallite).

The technical requirements for the construction itself are relatively low. No special preparation of the excavation is required. A rough surface does not impede a good contact between the SVV seal and the surrounding rocks. Salt dust on the rock surface is no problem either.

The removal of the excavation disturbed zone prior to the emplacement of the dry SVV material is desirable but no precondition, because the crystallization pressure leads rapidly to a closure of this permeable zone. This has been shown in the large scale in-situ experiments with SVV seals in rock salt as well as in potash rock formations. The emplacement of the dry SVV can be made very easily by blowing the fine grained material into the allocated place. No compaction of the emplaced dry SVV is required.

The brine injection can be made with normal water pumps. Brine emplacement should be performed as fast and as uniform as possible in order to introduce the maximum possible amount of brine uniformly into the SVV material. Lessons learned during the from in-situ tests performed in the mines of the ASSE and TEUTSCHENTHAL show, that additional brine injections after the first flooding can be help-full to obtain sooner a higher crystallization pressure and thus a lower permeability of the system excavation disturbed zone – SVV seal (Fig. 4.10). Thus technical constructions using SVV can be built relatively easy, fast and at low costs.

4.3.3.6 In-situ-experiments and results

Fig. 4.12 and Fig. 4.13 show principle schemes of two SVV seals in two large boreholes in potash rocks.

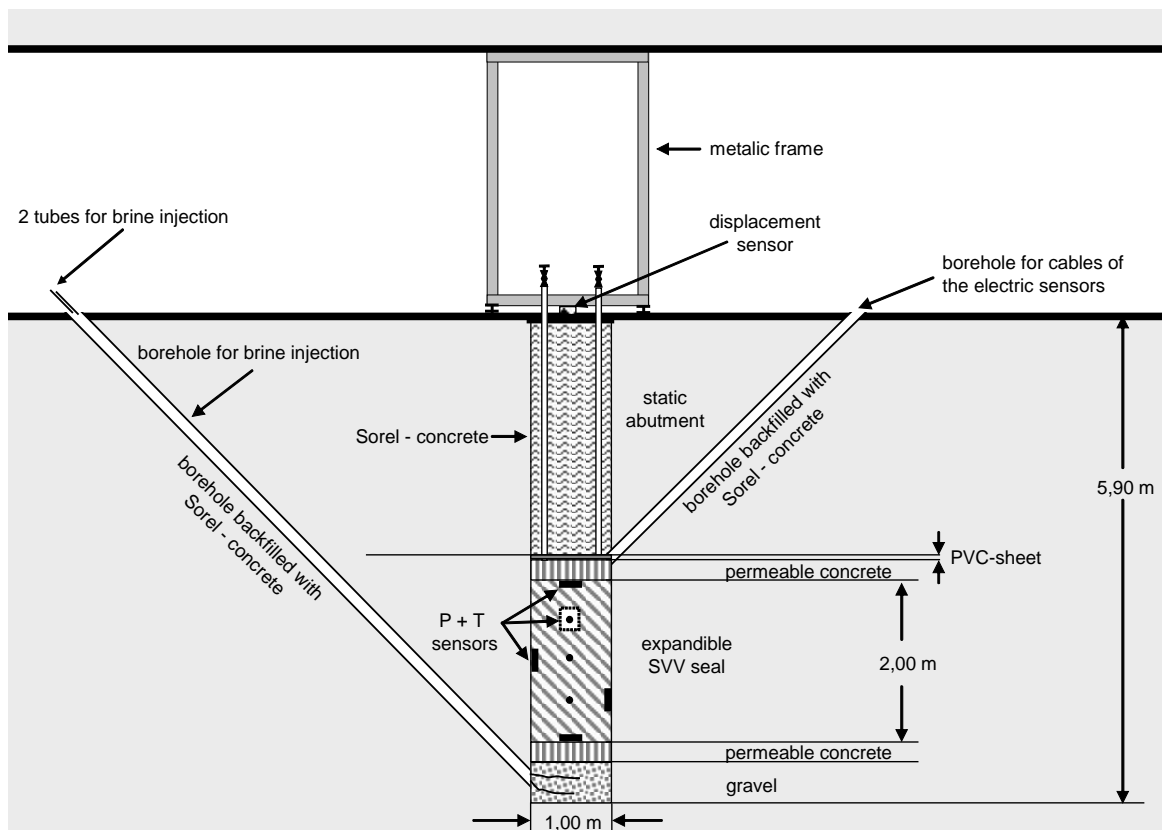


Fig. 4.12 Concept and instrumentation of a SVV seal of pure anhydrous $MgSO_4$ flooded with tachyhydrite brine in a vertical borehole (about 6 m deep, 1 m in diameter) in the potash formation carnallite in the Asse mine

In one experiment a vertical borehole and the other a horizontal borehole were sealed. In both boreholes the SVV element was kept in place by a bulkhead of SOREL concrete. In the carnallite potash rock of the Asse mine the borehole was vertical, 6 m deep and 1 m in diameter. The SVV element was 2 m long. In the mine Teutschenthal the experiment was emplaced in potash rock containing tachyhydrite and carnallite. The borehole was 7.2 m long, 1.2 m in diameter and the SVV element was 2.7 m long.

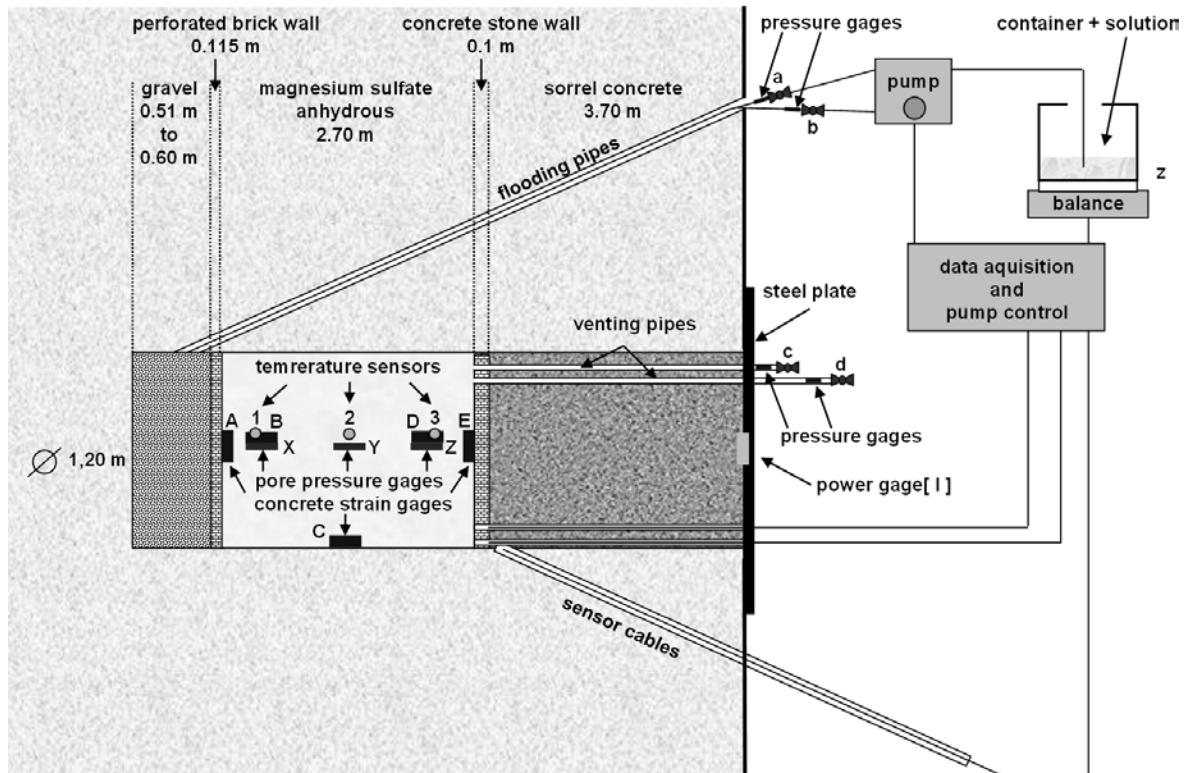


Fig. 4.13 Concept and instrumentation of a SVV seal of pure anhydrous MgSO_4 flooded with tachyhydrite brine in a horizontal borehole (1.2 m in diameter, 7.2 m length) in the potash formation tachyhydrite in the mine Teutschenthal

The borehole in the Asse mine was situated in the vicinity of old mine workings. Rock permeability tests of the carnallite rock were made in a 10 cm diameter borehole prior to the drilling of the large borehole. The short term permeability measurements rendered the erroneous impression that the rock section was impermeable and thus suitable for the planned SVV-test. The large borehole was drilled and the seal was constructed and instrumented. Fig. 4.12 shows the concept of the seal. In the lower part of the borehole 2 m were filled with SVV. Above this SVV element a bulkhead of SOREL concrete was built.

The SVV element was flooded with brine slightly oversaturated in halite and almost saturated in antarcticite, bischofite and carnallite, called tachyhydrite brine (Table 1). The history of the flooding of the SVV element and the subsequent injection tests is shown in Fig. 4.14. The flooding of the SVV element was started from the bottom of the borehole. With brine pump (BESTA-HD 2-300) an injection rate of 5 liter per minute was kept constant until the injection pressure reached 3.5 MPa. This brine pressure was maintained over 8 hours. Then the system started to leak. Brine started to seep out of cracks into mine workings 20 m below the borehole. The brine migrated along had moved on cracks of the excavation disturbed zone. The pathways in the EDZ had been activated and further injected brine was lost. The brine injection had to be stopped.

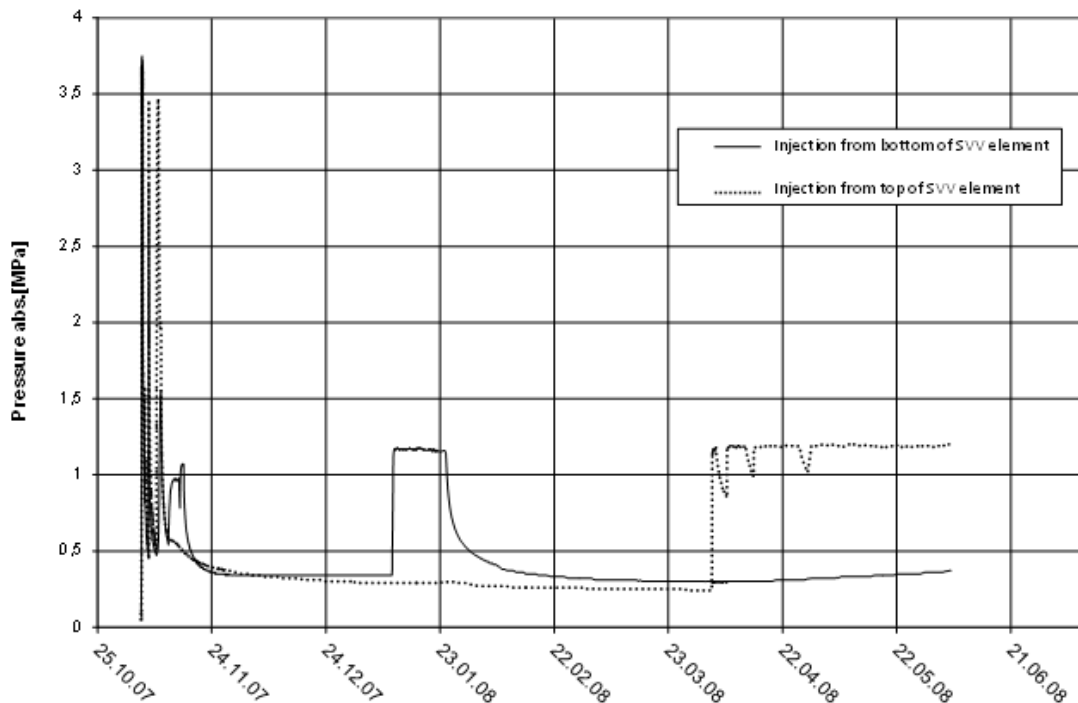


Fig. 4.14 Development of brine pressures during the flooding of the SVV element in a vertical borehole in the Asse mine in October / November 2007

Subsequent injection tests; one in January 2008 with brine injection from the bottom and a second one started in April with brine injection from the top of the SVV element

A few days later a second attempt was made to flood the SVV element with an injection pressure of 3.5 MPa. This time the brine was injected not from the bottom of the SVV element but from the upper part. Again the injection had to be stopped shortly after the injection pressure had reached 3.5 MPa. Again the brine dropped from the ceiling of the mine workings below.

After about one week later a new injection was performed with a brine pressure of only 1 MPa. At this pressure no brine could be injected anymore and no brine was lost in the EDZ. This brine pressure was maintained for about three days, and then the injection was stopped. We wanted to allow the SVV to react and form the expected seal.

The total amount of brine injected from both ends was registered. It was higher than the calculated volume of the open pore space in the anhydrous MgSO_4 . But because part of the brine had left the borehole through the EDZ it was not clear how much brine was still present in the SVV element. We assume that less brine than the amount needed for complete hydration of the anhydrous MgSO_4 had been retained in the SVV element. Nevertheless, the reaction was triggered.

About 7 weeks later a new injection test was made, this time with a brine pressure of 1.2 MPa (Fig. 4.14). This brine pressure was maintained for about 2 weeks. Only negligible amounts of brine could be injected. This was a clear indication indicating that the brine was not lost in the cracks of the EDZ.

A further injection test was made about 10 weeks later. Again the injection pressure was kept constant at 1.2 MPa. This time the brine was injected from the upper side of the SVV element. The brine pressure was kept constant for almost three month, when until the experiment had to be interrupted. The administration of the Asse mine had given order to stop all activities which were not directly related to the closure measures of the mine.

During the three weeks of the last injection test with a brine pressure of 1.2 MPa only negligible amounts of brine had been injected. The former pathways were not accessible for the brine (at least not at the applied pressure and for the length of observation time).

The development of the total pressure in the SVV element was measured at 5 different positions (Fig. 4.15). Total pressure includes brine pressure and crystallization pressure. At the start of the reaction the total pressure consists mainly of the applied fluid pressure. As the hydration goes on the brine is consumed, the brine pressure decreases and crystallization pressure goes up. At the end of the reaction the brine is consumed and the total pressure consists exclusively of crystallization pressure (Fig. 4.7).

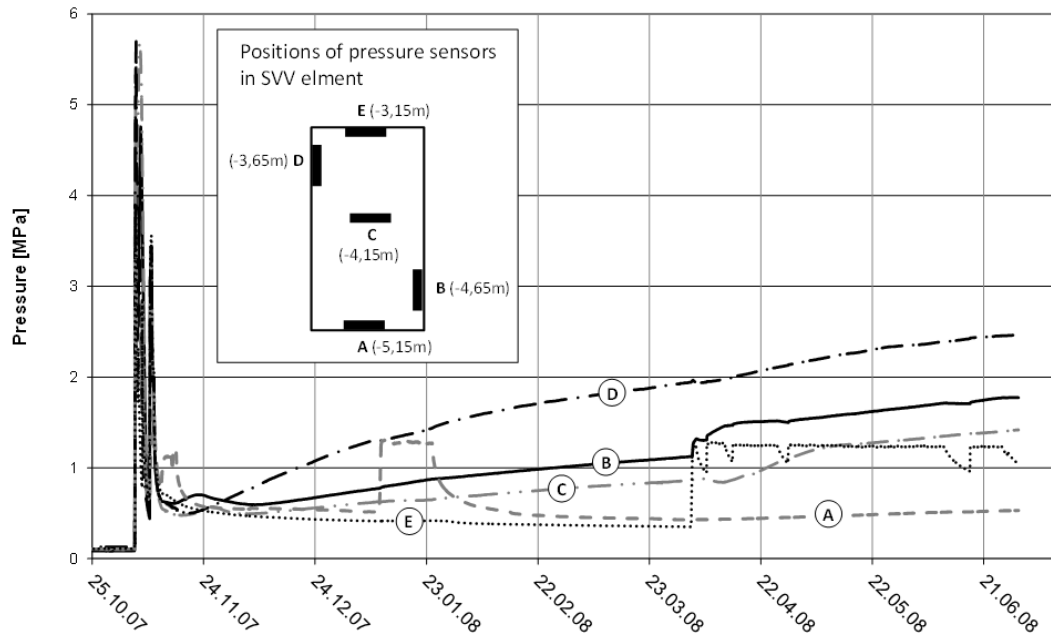


Fig. 4.15 Development of total pressure (brine pressure and crystallization pressure) at different locations in the SVV element in a vertical borehole in the Asse mine

Fig. 4.15 shows that the pressure development in the SVV element was not uniform. With one exception all sensors registered rising pressures indicating a continuous enhancement of the sealing quality of the SVV element. By comparing the injection events at different times (Fig. 4.14) with the response (or lack of response) by the pressure sensors (Fig. 4.15) it can be shown between which pressure sensors brine pathways still existed and where they were interrupted by volume increase. At the end of the experiment the highest pressure was 2.5 MPa and the lowest 0.5 MPa, both with rising tendency. The continuous pressure increase was due in part to the still ongoing hydration process and to some extent to the convergence of the carnallite rock. Both effects lead to a continuous improvement of the sealing property of the SVV element.

As an outstanding result it can be noted, that brine pathways which had been opened at the start of the experiment at 3 MPa brine pressure were not accessible anymore after only 6 weeks at the lower brine pressure of 1 MPa. This result could be confirmed by two subsequent injection tests with slightly higher brine pressures of 1.2 MPa. We can assume with a high degree of confidence that pressures in the SVV will continue to rise and eventually will exceed 3.5 MPa. At this point the EDZ fractures cannot be accessed anymore by brines with pressures below or equal to 3.5 MPa, at least not in the rock interval sealed by the SVV element.

A similar experiment in an even larger, but this time in a horizontal borehole (1.2 m in diameter and 7 m length) was started in September 2009 in the extremely soluble tachyhydrite potash rocks in the Teutschenthal mine (Fig. 4.13). In this test too, a few hours after the start of the flooding of SVV element brine injection had to be stopped at a brine pressure of 3.5 MPa because the system started to leak. Brine appeared in cracks of the excavation disturbed zone and poured leaked into the drift at the front end of the borehole. In this case, too a smaller than optimum amount of brine had been injected into the SVV element.

Therefore about three weeks later a new attempt was made to inject more brine (Fig. 4.16). This time a lower brine pressure of only 1.8 MPa was applied over several hours and a small amount of brine could be injected.

In January 2010 brine was injected a third time. This time no substantial brine volume could be injected more. The flow rate of the injected brine was very low but constant which allowed the calculation of the total intrinsic permeability of the system SVV-EDZ-potash rock system. The permeability turned out to be in the order of 10^{-19} m^2 . Only two of the pressure sensors even registered the brine pressure applied during this injection test. The pathways through the SVV element had already been closed partially.

A further injection test with a brine pressure of 2.3 MPa was made performed four months later in August 2010. The brine pressure was kept at 2.3 MPa only for a short time until a very low but constant flow of brine flux was obtained which allowed the calculation of the permeability. The derived permeability was only slightly lower than in January.

A last injection tests was performed in March 2011 with a slightly higher injection pressure of 2.8 MPa. Again the brine pressure was maintained only for a short time, long enough to measure the flow rate and to calculate the permeability. With a value of $8 \cdot 10^{-20} \text{ m}^2$ the permeability was almost two orders of magnitude lower than in January 2010. After the test the brine pressure was released in order not to weaken the still developing sealing system. A new injection test is planned in February 2012. It is foreseen to rise increase the injection pressure up to 3.5 MPa and to keep it the system at this pressure for several weeks.

The development of the crystallization pressures in the different parts of the SVV element is shown in Fig. 4.16. As observed earlier in the Asse SVV test in this test again

the crystallization pressures developed not uniformly. The highest value was around 3 MPa and the lowest at 1 MPa. The pressure sensor with the high value was not affected by the several injection tests, because in this part of the SVV element the crystallization pressure was higher than the applied brine pressures in the tests. All the other sensors with lower crystallization pressures than the brine injection pressure recognized the higher pressure applied to the system by the new injection. In these parts the newly injected brine reacted with still available anhydrous $MgSO_4$ and led further volume increase by simultaneously consuming the brine. Therefore the brine pressure decreases after each injection test but leveled out at a higher level than in the test before. The pressures will go up further by the combined effect of a still ongoing reaction and the convergence of the potash rock. Thus the already very low permeability of the system SVV-EDZ-potash rock system will further be reduced.

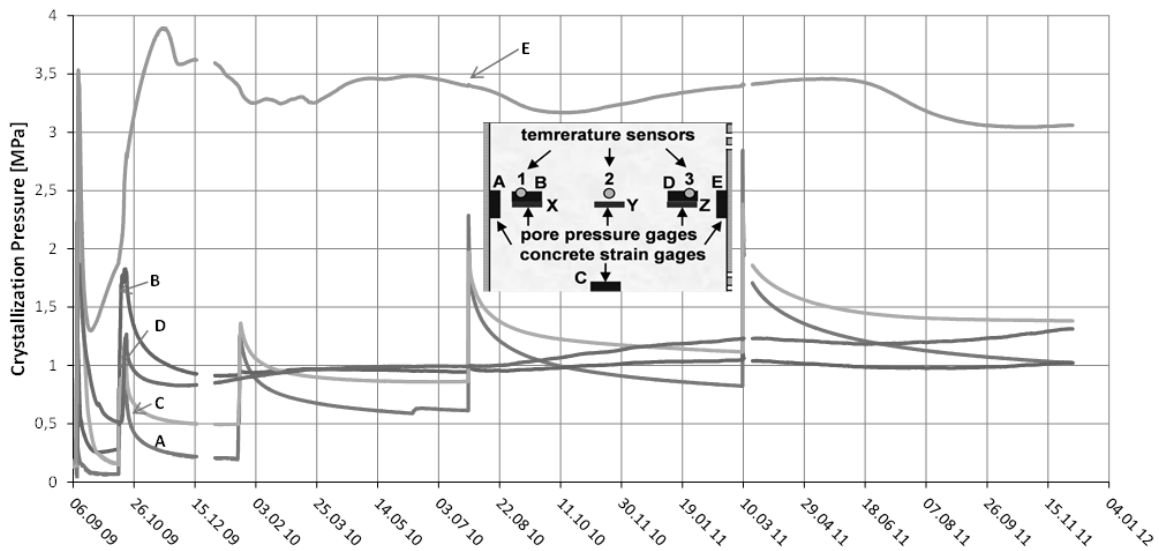


Fig. 4.16 Development of crystallization pressures in the SVV element in a horizontal borehole in tachyhydrite potash rocks in the mine Teutschenthal after flooding with tachyhydrite brine and after the three subsequent injection tests

The relatively high temperatures at the beginning of the exothermic reaction of brine with anhydrous $MgSO_4$ (Fig. 4.17) cannot be avoided. But this fact poses no real problems. In the contrary the high temperatures in an early stage of the consolidation process of SVV lead to an improvement of the sealing capacity. At the observed temperature between 70 and 80 °C the solubility of $MgSO_4$ is higher than at 25 °C (the temperature of the surrounding salt formation). By the subsequent fast cooling the system reaches a high degree of oversaturation which is equilibrated at 25 °C by the precipita-

tion of high amounts of $MgSO_4$ hydrates. Thus the high values of temperature enhance the system rather than damaging it. No formation of temperature induced local cracks has been observed. In the contrary obviously existing former cracks in the excavation damaged zone have been obviously closed due to the reaction. Freyer et al. /FRE 06/ investigated the thermal stability of the mineral association carnallite-tachyhydrite. They have shown that these minerals are stable up to 140 °C in the absence of a gas phase. Therefore it seems not very likely that carnallite and tachyhydrite will be damaged to a large extend by the short temperature peak observed in our experiments.

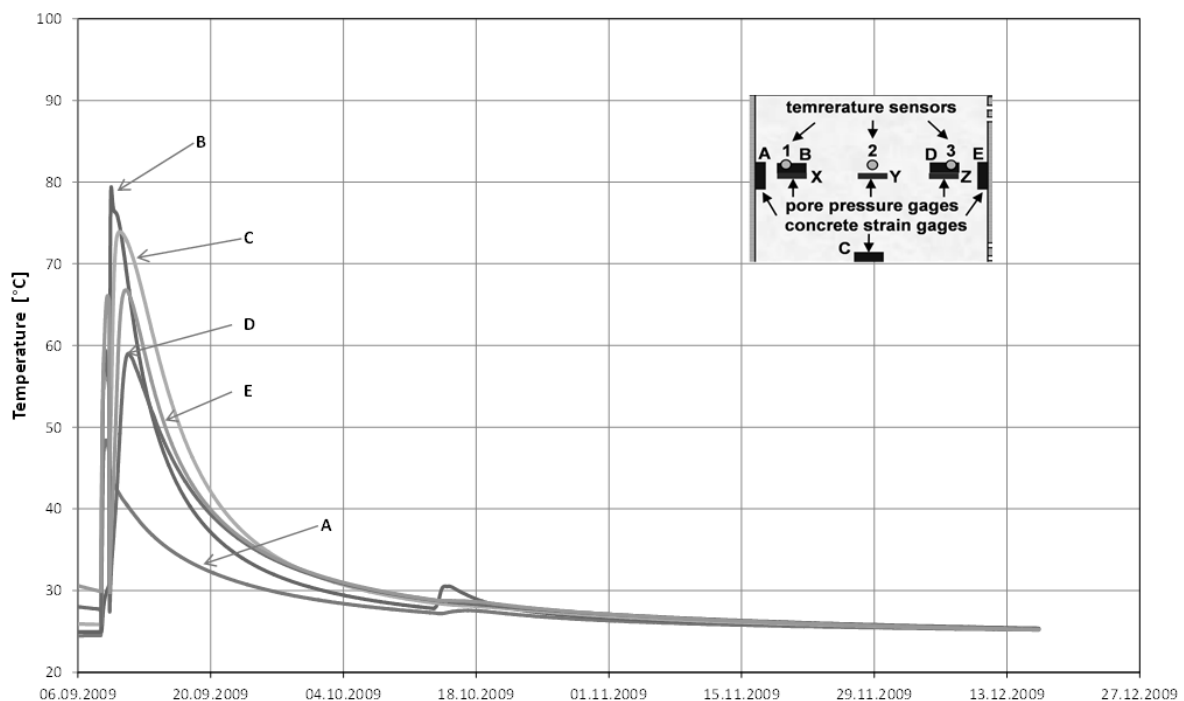


Fig. 4.17 Development of temperatures in the SVV element in a horizontal borehole in tachyhydrite potash rocks in the mine Teutschenthal after flooding with tachyhydrite brine and after subsequent injection tests

4.3.3.7 Long term behavior of SVV seals

The sealing potential of SVV is based mainly on the hydration process of the anhydrous $MgSO_4$. This process sets in spontaneously with the first contact of brine with the SVV material and is finished relatively fast when all the available brine is consumed or when all the available $MgSO_4$ is completely hydrated. As described in chapter 2 the large volume increase is due to the formation of different $MgSO_4$ hydrates and to the minerals precipitated from the over-saturated brine. The total volume of the system an-

hydrous MgSO_4 plus brine is smaller than the resulting volume at the end of the reaction. In technical barriers the volume in which SVV can expand is confined by bulk-heads. That means that only a limited volume of brine can be injected in the SVV element and can react with anhydrous MgSO_4 . This amount is controlled by the volume of open pore space between the grains of anhydrous MgSO_4 . Different brines with different chemical composition contain different amounts of water. The theoretical volume expansion depends on the brine composition. The volume changes during the reaction can be quantified by geochemical model calculations. In a confined space the volume increase leads to the built up of a crystallization pressure. The resulting volume and the crystallization pressure however are not stable. They are subject to changes over time. The first mineral assemblage is meta-stable but it develops towards long-term stable minerals. Higher MgSO_4 hydrates will lose their water and will be transformed successively in lower hydrates in the order: epsomite, hexahydrate, pentahydrate, starkeyite, and finally the long-term stable kieserite. This transformation leads to a volume reduction and to a decrease of crystallization pressure. It is essential to know how a SVV seal develops in the long run and how the sealing properties evolve, i. e. if the seal maintains its sealing properties over geological time frames or not. The answer is yes, the seal maintains its sealing properties at all times and yes, a final stable equilibrium will be reached in all cases indifferent of the brine composition.

This statement however must be underpinned by facts. We therefore analyzed the evolution of the mineral assemblages formed by the reactions of anhydrous MgSO_4 with the three brine types used in the experiments.

After the water consumption in the reaction with NaCl solution the mineral assemblage consists roughly of about 40 % bloedite ($\text{Na}_2\text{Mg}(\text{SO}_4)_2 \cdot 4\text{H}_2\text{O}$), 28 % hexahydrate ($\text{MgSO}_4 \cdot 6\text{H}_2\text{O}$), 14 % Epsomite ($\text{MgSO}_4 \cdot 7\text{H}_2\text{O}$), 10 % halite (NaCl) and 8 % bischofite ($\text{MgCl}_2 \cdot 6\text{H}_2\text{O}$). These are approximated numbers from X-ray measurements and may differ from real contents. Nevertheless, they give a good orientation.

X-ray analyses showed that six month later epsomite had disappeared. It had been transformed in lower hydrates (hexahydrate, pentahydrate ($\text{MgSO}_4 \cdot 5\text{H}_2\text{O}$), and starkeyite ($\text{MgSO}_4 \cdot 4\text{H}_2\text{O}$). Also part of the hexahydrate had been transformed in pentahydrate and starkeyite. From originally 28 % hexahydrate after 6 month only 9 % were still present. After six month about 22 % pentahydrate and 10 % of starkeyite were present in the new mineral assemblage. The transformation of higher into lower hydrates will continue until the long-term stable monohydrate (kieserite $\text{MgSO}_4 \cdot 1\text{H}_2\text{O}$) is formed.

The dehydration leads to the liberation of water into the system. This water however is immediately taken up by anhydrous MgSO_4 which had not been hydrated in the first place because of a deficit of water in the system. We mentioned that the brine volume that reacts at the start is limited by the initial pore space. This brine volume is not sufficient for the total hydration of all the anhydrous MgSO_4 in the SVV element. That means that part of the MgSO_4 will still be present and can react with new arriving water. That means that the dehydration does not damage the seal but will lead to further hydration. In this ongoing process the total volume of the system never becomes smaller than the volume of the initial anhydrous MgSO_4 plus brine /HER 07/. Thus the sealing properties of the system will be maintained during the whole process of dehydration. Geochemical modelling with the thermodynamical database of /HAR 84/ confirmed the experimental results and the evolution towards a long term stable paragenesis.

The final long-term stable paragenesis of SVV with NaCl solution will consist of kieserite, halite and small amounts of bloedite. If IP21 solution is involved the long term stable paragenesis will be: kieserite bischofite, carnallite, halite and some anhydrite. In the case of tachyhydrite solution the long term stable mineral assemblage will be: kieserite, bischofite, anhydrite, some carnallite and halite. For more details see /HER 11/.

4.3.3.8 Summary and Conclusion

A self-sealing material (SVV) for technical barriers in salt and potash mines was developed by GRS. SVV consists basically of anhydrous MgSO_4 . In contact with brine SVV becomes hydrated and increases its volume. The open pore space and the permeability are drastically reduced. In technical barriers, SVV can be confined between static abutments and flooded with brine. Due to the volume increase a crystallization pressure builds up which renders the material impermeable to further brine inflow. The crystallization pressure leads to the closure of the excavation damaged zone. The initially metastable mineralogical composition of the hydrated SVV will be transformed into thermodynamically long-term stable assemblages. The mechanical properties of SVV are comparable to those of rock salt. In-situ experiments in salt and potash formations have demonstrated that SVV is well suited for the construction of brine tight seals which resist to high brine pressures, even in mechanically disturbed rocks.

The results of laboratory and in-situ tests with SVV have demonstrated that this material is suitable for the construction of brine-tight seals in rock salt and potash formations.

The properties of SVV after reaction with brine are comparable to those of rock salt and potash rocks. After reaction with brine an SVV sealing element has a very low permeability low permeability, $<10^{-20} \text{ m}^2$. In-situ tests in large vertical and horizontal boreholes show that SVV seals can be constructed and are efficient. An up-scaling of the small scale laboratory test results to full scale technical constructions is feasible. The special value of the in-situ tests lie in the fact, that it could be shown, that highly permeable rock sections with EDZ fractures can be effectively sealed with little effort and small costs. The technically very demanding task of sealing very soluble and mechanically disturbed potash formations has been accomplished. It has been demonstrated that the initially metastable mineralogical composition of the SVV element after hydration will be transformed into thermodynamically long-term stable assemblages. Furthermore it can be assumed that SVV seals will improve in time due to convergence of the salt formation.

4.4 New aspects of bentonite re-saturation – Task Force on EBS

4.4.1 Bentonite-sand mixtures

Since the vapour flow model had been applied exclusively to re-saturation of pure bentonite the question arose whether the model could also reproduce re-saturation of bentonite-sand mixtures. From a theoretical point of view this appeared to be feasible since bentonite itself consists not only of clay but also of 20 % to 40 % of other minerals that can be considered as inert with respect to the re-saturation process. To test if the range of applications for the vapour flow model could be extended to bentonite-sand mixtures Benchmark 2.1 (BM 2.1) of the Task Force on EBS (TF EBS) was modelled with the experimental code VIPER (**V**apour transport **I**n **P**artially saturated bentonite as **E**ngineered barrier for **R**epositories). This benchmark was concerned with the “Isothermal Test” (ITT) performed in the Canadian Underground Research Laboratory by AECL /GUO 06/.

For the ITT a 50:50 mixture of Saskatchewan bentonite and sand was emplaced and compacted to a dry density of 1730 kg/m^3 in a vertical cylindrical borehole in the Canadian underground rock laboratory (URL) /GUO06/. The resulting bentonite-sand body was confined by a massive concrete plug on top as indicated in Fig. 4.18 (A). The compacted buffer material had a height of 2 m, a radius of 0.62 m, and an initial water content of ~17.5 % by weight. After emplacement and instrumentation, the ITT was left

undisturbed and monitored for six and half years during which pore water was taken up from the adjoining granite host rock. The transient data acquired by the installed instrumentation was supplemented by an extensive post-test investigation of the buffer material. A thorough sampling to determine water content and density of the bentonite-sand buffer was conducted by /DIX00/.

The bentonite-sand cylinder was divided into horizontal layers numbered from A to H with increasing depth. The numerical model was restricted to re-saturation within mid-plane (layer E). To cope with the radial symmetry of the set-up the solution algorithm used in VIPER was expanded accordingly.

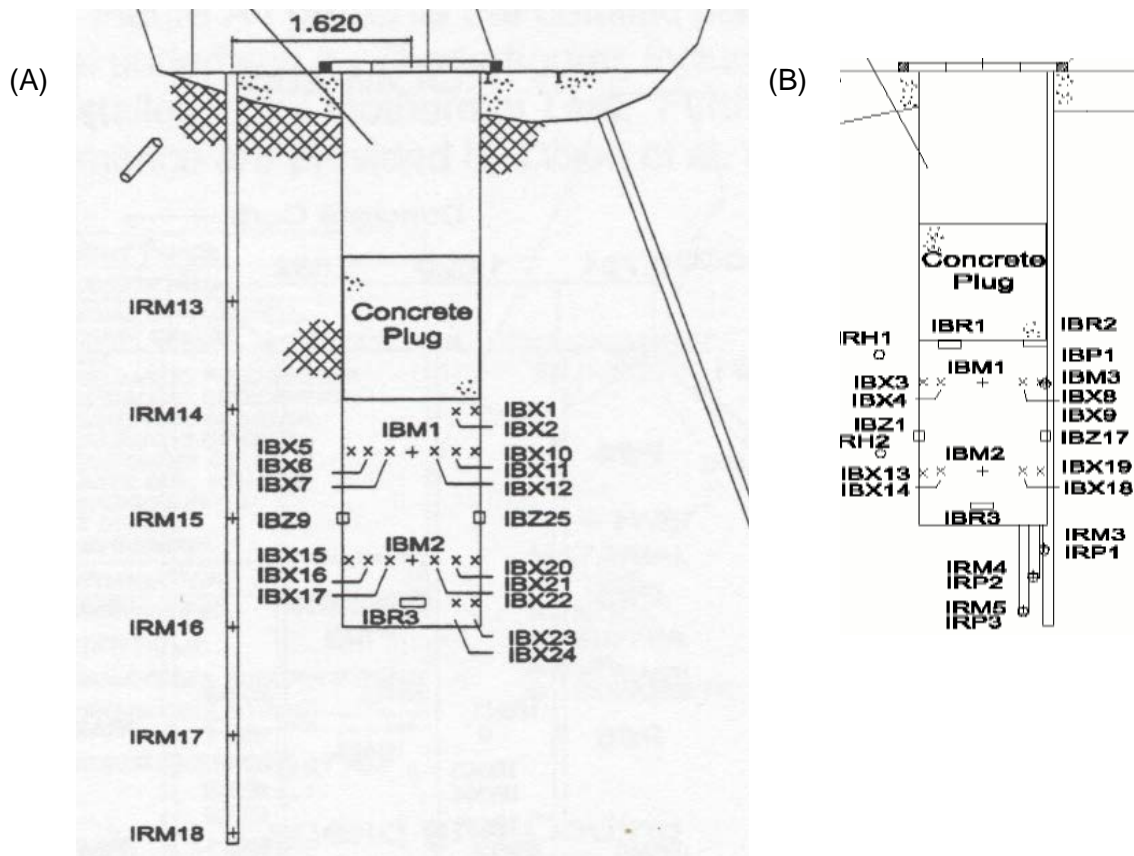


Fig. 4.18 Set-up of ITT and location of the psychrometric sensors IBX<number>; (A) from /GUO06/, (B) from /ÅKE08/

Work on this test case turned out to be more difficult than expected. Vapour flow alone did not explain the measured temporal evolution of the water content. Adapting the vapor flow model to the special properties of a bentonite-sand mixture did not improve the numerical results significantly. In order to eliminate formal errors in the model the equations used in VIPER as well as their implementation were checked extensively but no severe errors were found. Since the water content in the clay in BM 2.1 was initially al-

ready very high it was then suspected that re-saturation had (in compliance with the conceptual model) reached a stage where it was not dominated by vapor transport anymore. Therefore a balance equation for water based on two-phase flow theory was derived and tentatively incorporated into the code VIPER. This improved the modelling results somewhat but not satisfyingly. Moreover, it turned out then that the two-phase flow approach could not be reconciled with the vapor diffusion concept. Finally, it was not possible to identify a distinct set of parameters for the model.

Breakthrough was inspired by the work of the ‘chemical group’ of the Task Force which was related to diffusion of cations in the interlamellar space of the clay particles and as a result the assumption of the immobile interlayer water in the vapor diffusion model was dropped. Instead a diffusive migration of interlayer water according to self-diffusivity was assumed. The related diffusion coefficient depends on the water content and increases with the amount of hydrate layers at the interlayer cations. The balance equation used up to that time was extended accordingly to a double-continuum model and implemented in code VIPER. This lead to a decisive improvement of the modelling results for Benchmark THM 2.1 without introducing new parameters that needed calibration. Fig. 4.19 shows the transient development of water content at three different locations in the middle plane of the buffer as well as the water content distribution as extensively measured in a post-test investigation campaign. A detailed description of the model and the experiment can be found in /KRÖ 11/.

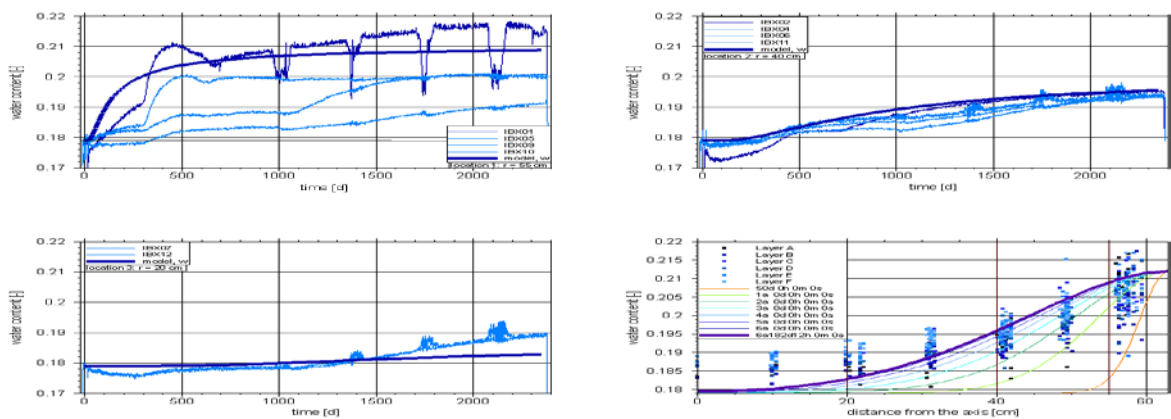


Fig. 4.19 Results from in-situ measurements and from model calculations for the ITT including interlayer diffusion; from /KRÖ 11/

4.4.2 Non-isothermal in-situ test

For the ITT-model an isothermal version of the second balance equation for the inter-lamellar water was sufficient. Of course, the equations were parallel extended to the non-isothermal case. Many new and rather complex terms came into existence from this exercise and were implemented in the code. The option of non-isothermal water uptake against a temperature gradient was then tested with a numerical model for BM 2.2, the Canister Retrieval Test (CRT) performed by SKB at the Hard Rock Laboratory at Äspö /KRI 07/.

For the CRT a vertical deposition hole was bored with a depth of 8.55 meters and a diameter of 1.76 meters. At the perimeter of the hole 16 filter mats with a width of 10 cm were installed with uniform spacing, 0.15 m from the bottom of the hole up to 6.25 m height. Ring-shaped as well as cylindrical bentonite blocks were placed in the hole to encase a heater with the dimensions of a KBS-3 canister. As buffer material MX-80 was chosen. The outside diameter of the canister was 1,050 mm. An inner gap of 1 cm remained between heater and the bentonite rings. The volume between the bentonite blocks and the borehole wall was filled with bentonite pellets. The complete test set-up is shown in Fig. 4.20.

At the beginning of the test water was pumped into the pellet-filled gap. There were indications that the water had not only been filled voids between the pellets but also the inner gap between heater and the bentonite rings. After direct filling-up water was supplied artificially via the filter mats to ensure saturation conditions at the outside of the compacted bentonite.

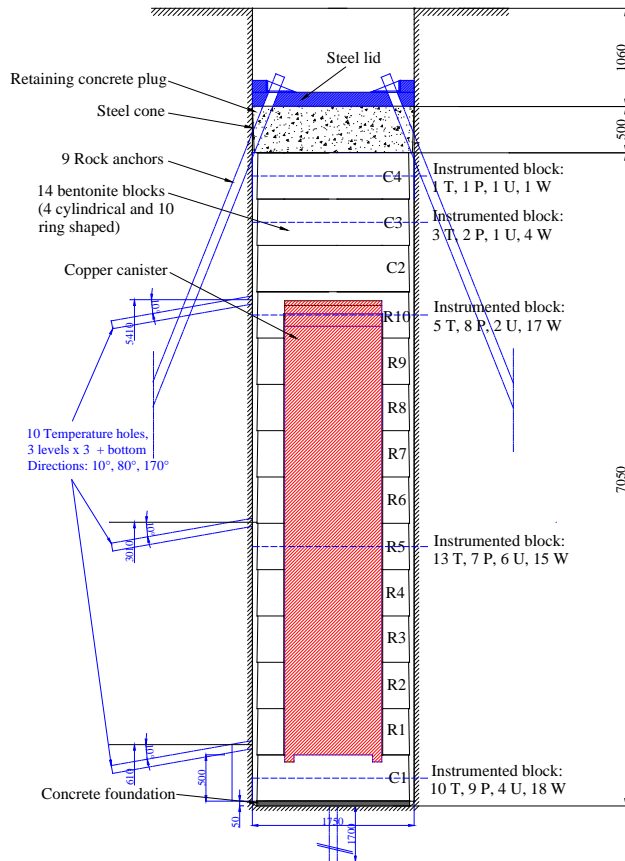


Fig. 4.20 Sketch of the Canister Retrieval Test; from /KRI07/

The modelling exercise concentrated on the water uptake in the horizontal mid height of the experiment (see Fig. 4.21 (A)). A disc of the buffer was modeled assuming rotational symmetry. It encompasses

- (A) the inner gap (0.01 m width)
- (B) the ring shaped bentonite block (0.285 m width)
- (C) the outer gap filled with bentonite pellets (0.055 m width)

as indicated in Fig. 4.21 b).

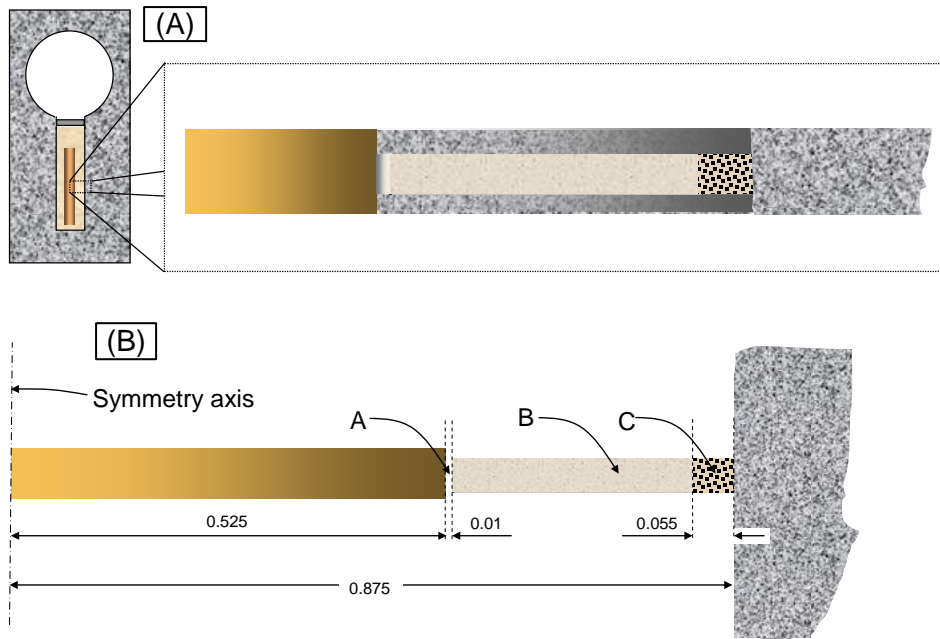


Fig. 4.21 Location of the model domain (A) and dimensions (B) ; from /KRI07/

Earlier model calculations with VIPER for the CRT without interlayer water diffusion reproduced the measurements well but only for an initial period of time /NOS 08/. The increasing differences between measurements and model results beginning after 60 and 110 days, respectively, had already indicated a missing process. Introducing interlayer water diffusion improved the results considerably.

According to the theoretical framework behind VIPER condensation can only occur in a state after the end of swelling. This state is locally reached in the model for the CRT, indeed. Thus the code had to be supplemented in this respect.

With the help of this last code modification the hydraulic data from CRT could satisfactorily be reproduced. Fig. 4.22 shows a comparison of measurements (symbols) and model results (lines) in terms of relative humidity as well as of suction based on sensor data at different radial distances.

It has to be mentioned here that despite the comparatively simple model concept a feature as complex as a counter-flow system of vapour and interlayer water was actually observed in the model. The gradient of the water content which is assumed to be the driving force for the interlayer water diffusion relates in a complex manner to the vapour density distribution. This complexity is illustrated by Fig. 4.22 showing plots of the key

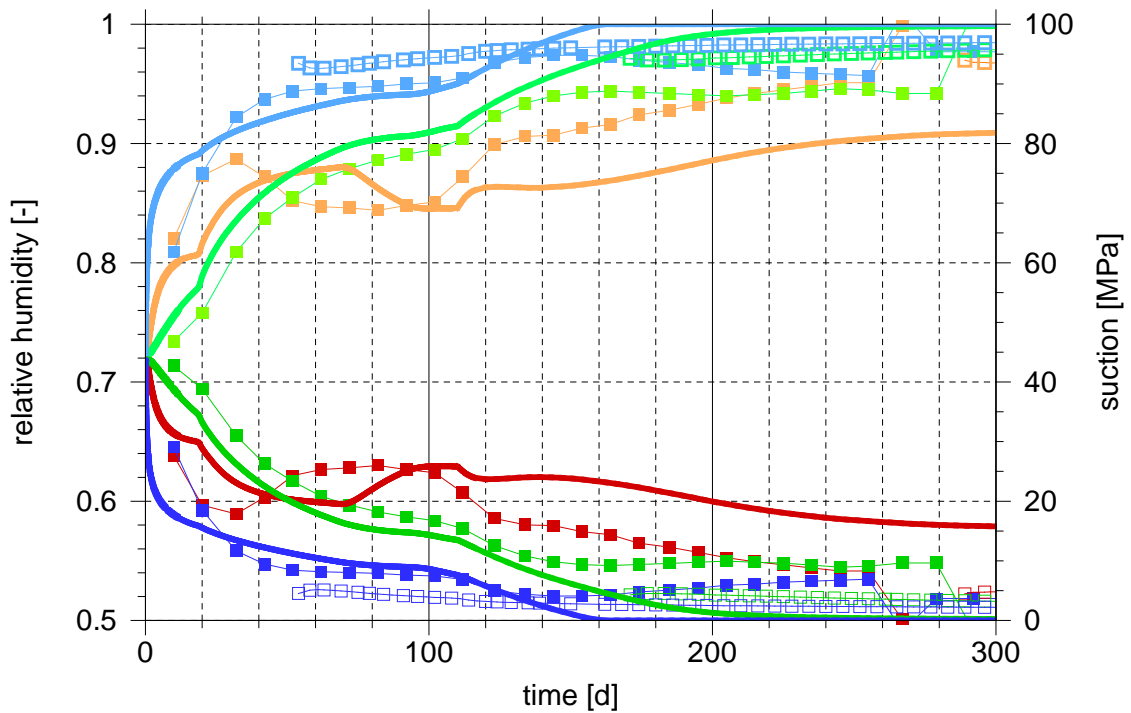
quantities as spatial distributions at four points in time ($t = 0$, $t = 10$ d, $t = 110$ d, $t = 650$ d).

The development of the water content in Fig. 4.23 shows that the initially highly saturated zone at the heater dries. The water content next to the heater drops even below the initial value of the non-wetted part of the bentonite rings. Concurrently, the vapor density rises here leading to vapor diffusion away from the heater. The effect of condensation can be seen in Fig. 4.23 as an increase of the water content above the value represented by the dashed line. This line depicts the state of maximum content of interlayer water without any water in the pore space. Note: This is the first application of VIPER using the option of condensation.

At the cool side of the buffer more and more water is taken up. The related increase of water content reaches the heated zone eventually but not the boundary at the heater. At the same time the vapor density does not only rise at the heater but also remains to be elevated. A vapor flux away from the heater is thus maintained without changing the water content accordingly.

After starting the experiment the initially high water content at the boundaries begins to level out at both sides of the buffer (heated and cool side). While the water content drops down at the heater a high water content spreads out from the cool side due to the continuous water supply until a dynamic equilibrium is reached. Apparently, a counter-flow system is then established in which

- interlayer water migrates in the direction of the gradient of the water content i. e. towards the heater,
- interlayer water dehydrates at the heater providing a source for vapor in the pore space, and
- vapor is then transported in the direction of the gradient of the vapor density i. e. away from the heater.



- rel. humidity: rh-sensor at 585 mm
- rel. humidity: rh-sensor at 685 mm
- rel. humidity: rh-sensor at 785 mm
- rel. humidity: s-sensor at 585 mm
- rel. humidity: s-sensor at 685 mm
- rel. humidity: s-sensor at 785 mm
- rel. humidity: model at 585 mm
- rel. humidity: model at 685 mm
- rel. humidity: model at 785 mm
- suction: rh-sensor at 585 mm
- suction: rh-sensor at 685 mm
- suction: rh-sensor at 785 mm
- suction: s-sensor at 585 mm
- suction: s-sensor at 685 mm
- suction: s-sensor at 785 mm
- suction: model at 585 mm
- suction: model at 685 mm
- suction: model at 785 mm

Fig. 4.22 Measured and calculated relative humidity/suction for the CRT;
from /KRÖ 11/

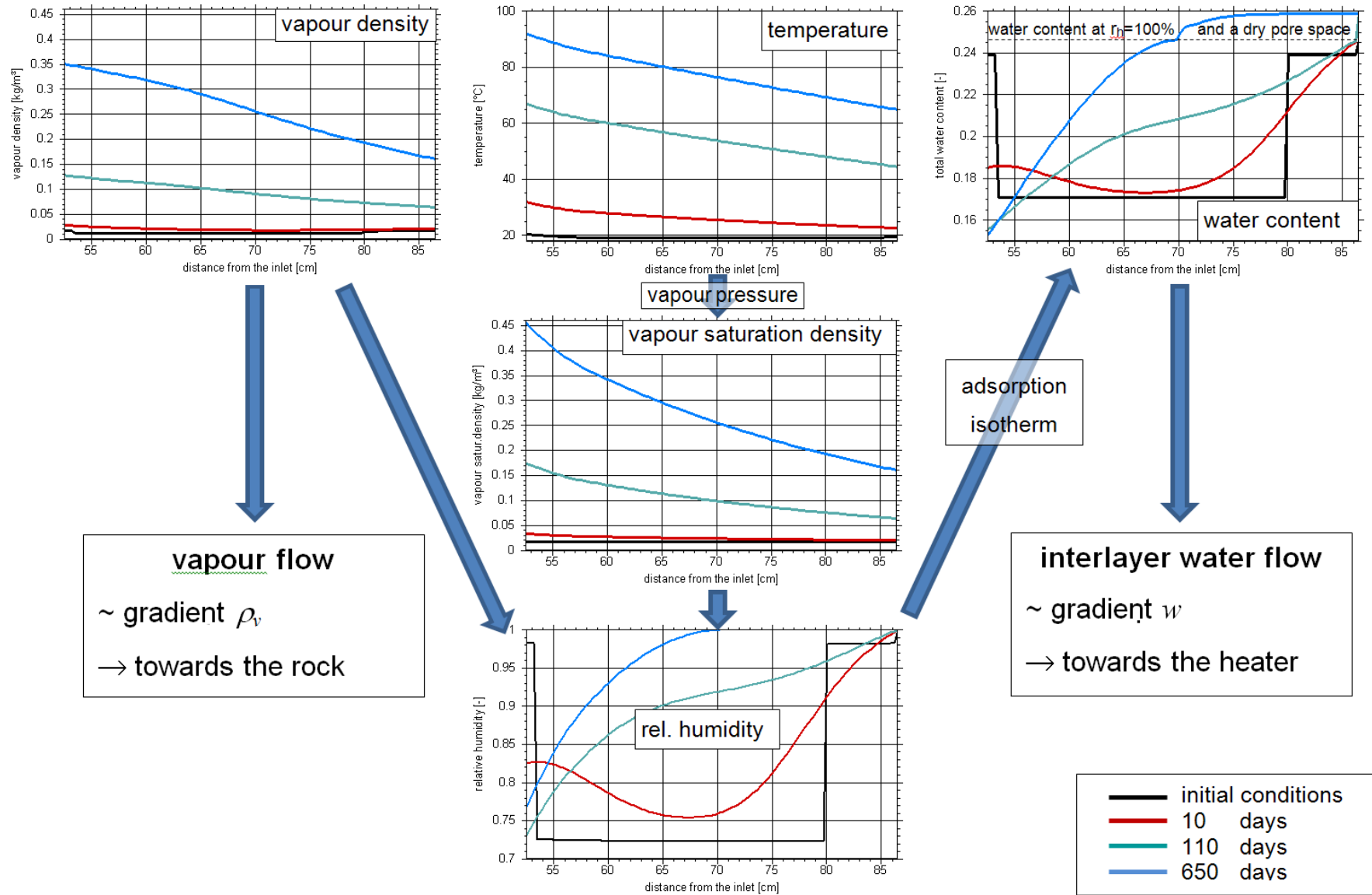


Fig. 4.23 Physical interaction in the CRT-model; from /KRÖ 11/

4.4.3 Status report

Checking the balance equations during modelling of BM 2.1 it became obvious that a comprehensive compilation of the theoretical background for the code was missing. A status report (/KRÖ 11/) was therefore written parallel to the modelling exercise. It represents the present development status including the latest modifications to cope with BM 2.1 and 2.2 and puts emphasis on

1. the theory about re-saturation of precompacted bentonite barriers via water vapour,
2. the microstructural and conceptual model,
3. the bentonite properties relevant to the model,
4. the derivation of the related balance equations,
5. the numerical method for approximating these balance equations, and
6. the models and model results for qualifying VIPER for non-isothermal bentonite re-saturation under conditions that are expected in a real repository.

4.4.4 Steady-state conditions

Discussions in the TF EBS had shown that there is no conclusive experimental evidence about the steady-state conditions after a non-isothermal re-saturation. Characteristic for the present state of knowledge are the two laboratory experiments performed by CEA /GAT 05/ and CIEMAT /VIL 05/ that formed the basis for the first two test cases in the TF EBS. The two tests of CEA indicate a evenly distributed water content distribution at a level related to a fully vapour saturated pore atmosphere. However, both tests were terminated before reaching such a state. Contrary to these results the test of CIEMAT showed after about a year of running the experiment no changes in the relative humidity which was considerably lower at the heated side than at the cool side of the sample. Similarly ambivalent are the results of the mock-up test in the Febex-project (e. g. /SAN 06/). It is thus unclear whether the re-saturation models are able to describe the steady-state conditions correctly. To answer this question with a view to hydraulic conditions a laboratory experiment was devised.

Goals and concept of the experiment were presented and lively discussed at a workshop of the TF EBS. Several constructive suggestions for improvement were re-

inspected by the staff at the GRS-laboratory and accordingly incorporated into the concept.

The design of the experiment had been chosen to achieve the highest possible similarity to the tests performed in the framework of the EBS-project /KRÖ 04/ to provide a consistent extension of the existing test data. The procedure for measuring the transient moisture field in the specimen as successfully applied in the EBS-project was used again. Due to the superimposed temperature gradient a different kind of measuring cell was required, though because it was imperative to cut and preserve the specimen very fast in order to avoid evaporation of water from the heated slices. Therefore a set of 10 plastic rings replaced the steel cylinder as shown in Fig. 4.24. The cylindrical bentonite samples had a diameter of 5 cm and a length of 9.5 cm.

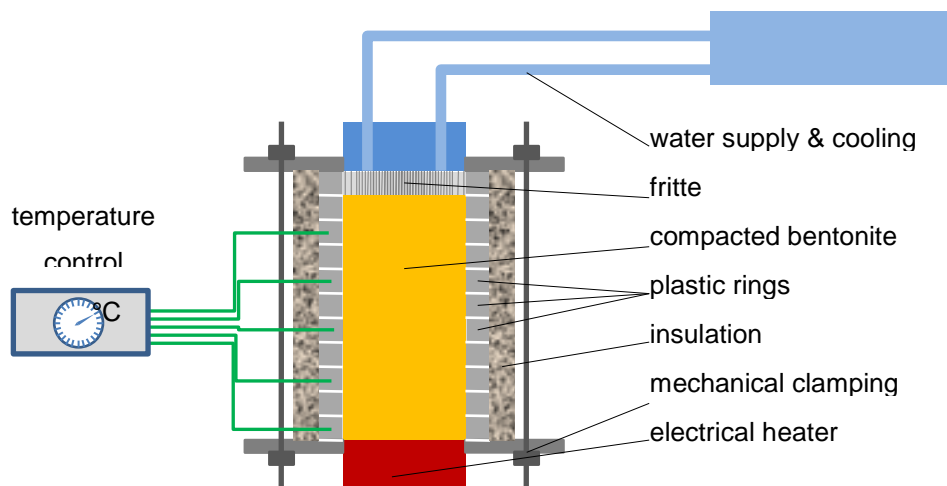


Fig. 4.24 Principle of the test set-up

Pre-tests were performed to optimise the experimental set-up with a view to approximate a linear temperature gradient over the length of the specimen as closely as possible. They also showed that the initially envisaged cutting technique with wires did not work out well so that a putty knife had to be used instead.

The actual tests began in June 2010. Two of the four cells for parallel measuring were assigned to very long test periods. One of them is running from the beginning on and still in operation. Accompanying model predictions indicated a required running time of about 2 years until steady-state is reached. According to the present model concepts this is equivalent with a full saturation of the specimen. However, the results obtained so far suggest that significantly more time will be required.

Water content distributions have been measured so far for time intervals up to 32 weeks. Another test which was foreseen to last 104 weeks had to be terminated prematurely after 72 weeks because of irregularities in the data for the water uptake rate. While the distribution seems to fit into the present trend this remains to be confirmed by measurements for longer periods of time. A graphical compilation of the measured water content distributions is given in Fig. 4.25. For most of these distributions a second test has been performed which reproduced the previously derived data rather good.

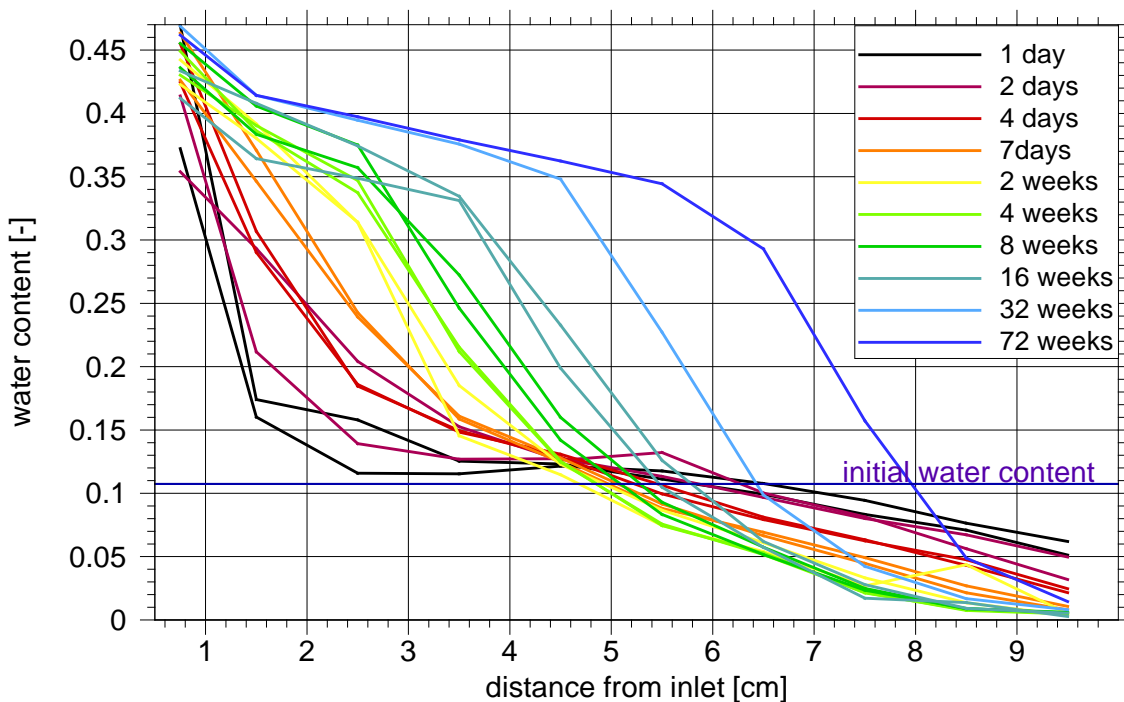


Fig. 4.25 Evolution of the water content distribution in the tested bentonite specimen

In the beginning the bentonite dries at the heated side⁸ as expected. For early times the distributions show at the water inlet⁹ characteristics that suggest a diffusion-like migration as the water transport process. This sort of observation is consistent with an isothermal re-saturation. However, after about 2 weeks a steep, ramp-like distribution has formed which keeps the slope during the remaining observation period. When this

⁸ temperature: approx. 90 °C; x=10 cm

⁹ temperature: approx. 25 °C; x=0.5 cm

ramp reached the heated and dried out side after 16 weeks the water content rose here even at the heater again.

Fig. 4.25 provides also means for quickly estimating the minimum test duration required to reach steady-state. The water content of 0.25 represents approximately the arithmetic mean between the initial water content and the water content at full saturation. This value is related to a position within the test cell that moves over time towards the heated end of the specimen. For the sake of simplicity it is assumed here that steady-state conditions are reached when the value of 0.25 hits the heated side.

The data points derived from the measurements so far are depicted in Fig. 4.26. Included as a polygon in black is a projection that indicates a minimum time to reach steady-state of about 3 years. However, if the trend becomes convergent towards steady-state a significantly longer period of time could be required.

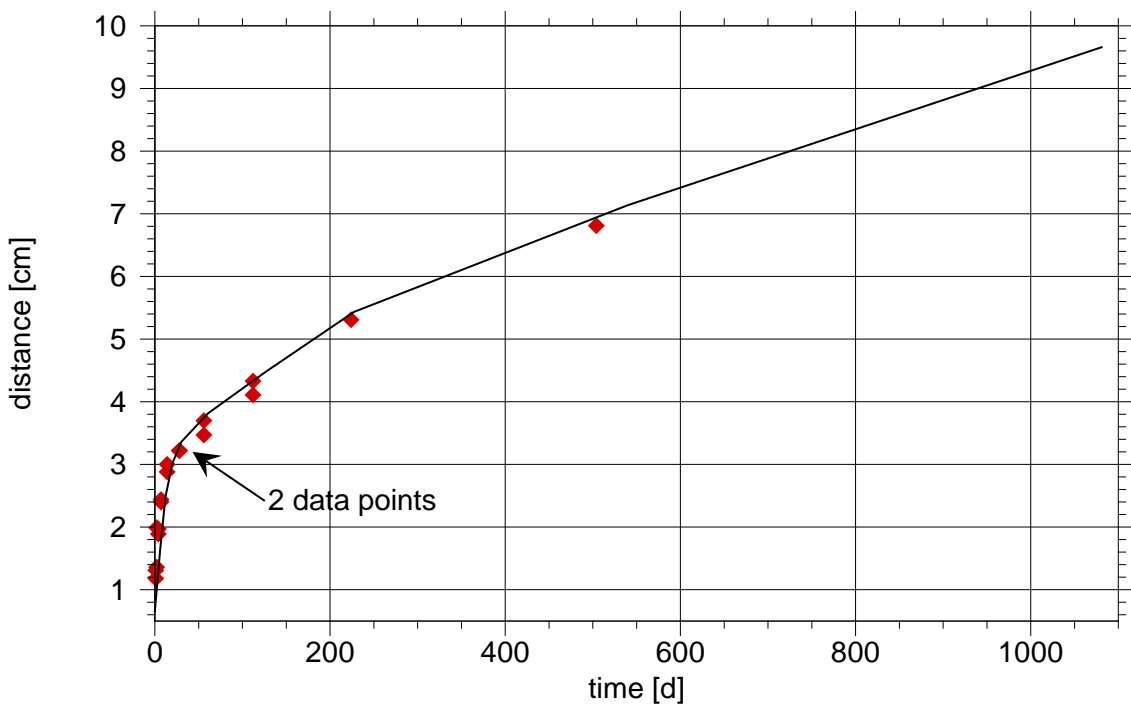


Fig. 4.26 Position of the value of 0.25 in the water content distributions over time

Fig. 4.27 depicts the accumulated amount of inflowing water. The curve shows initially a curvature that is typical for a diffusion-like water uptake. After 20 to 30 days, however, the curve is almost linear and stays that way up to now. Since the water content evolution in Fig. 4.25 as well as the inflow rate indicated by Fig. 4.27 do not show signs

of reaching steady-state continuation of the experiment especially of the already long running tests is strongly recommended.

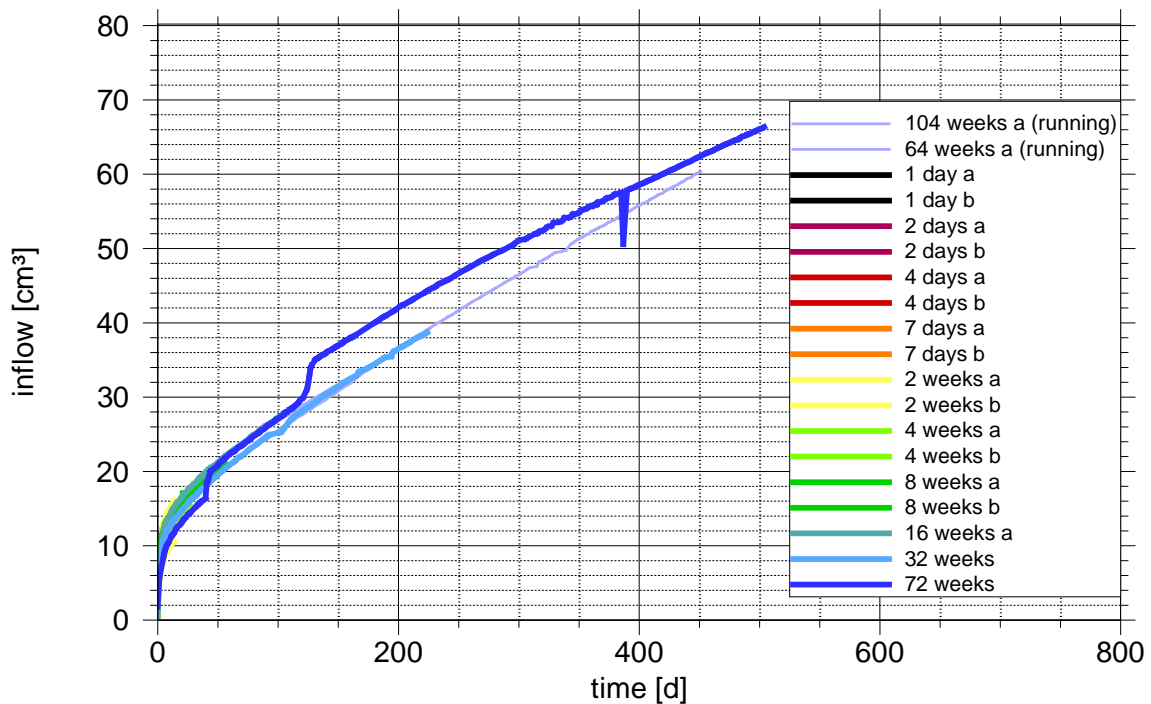


Fig. 4.27 Accumulated water inflow

4.5 Workshop “Grundsatzfragen Hydrogeologie”

During the last decades the hydrogeology of the overburden in Northern Germany has been investigated by different national organizations with respect to the question of radiological disposal in deep geological formations, particularly in salt domes. In the frame of a surface and underground geoscientific exploration programme of the Physikalisch-Technische Bundesanstalt (PTB) and the Federal Institute for Radiation Protection (BfS), respectively, in the years 1979 to 1999 comprehensive investigations have been performed at the Gorleben site. The evaluation and interpretation of the investigation results was performed by the Bundesanstalt für Geowissenschaften und Rohstoffe (BGR). A final documentation with the results of the exploration programme and a comprehensive publication lists can be found in /KOE 07/, /KLI 07/ and /BOR 08/.

The hydrogeological conditions in the sedimentary formations in Northern Germany have been intensively discussed in the past and were partially interpreted in a different way. Hence, GRS and Projektträger Forschungszentrum Karlsruhe, Wassertechnologie

und Entsorgung (PTKA-WTE) performed a workshop with the topic „Fundamental question hydrogeology – reduction of inconsistencies in the interpretation of results“. The workshop took place on 5./6. November 2009 at GRS in Braunschweig /FLU 10/. National experts, who were involved in different aspects of the hydrogeology in Northern Germany in research projects as well as in concrete site investigations, have been invited for a scientific discourse. It was the objective to compile existing knowledge, identify inconsistencies in interpretations and define and possibly answer open questions. 24 Persons from ten institutions participated in the workshop. The state of research was presented in ten papers.

In the frame of the workshop results of different studies on geology, hydrogeology, flow and transport modelling, and on the impact of climate changes in Northern Germany have been presented and discussed by the participants. Concerning the hydrogeology of Gorleben site comprehensive investigations were performed until the moratorium in year 2000. However, model calculations performed in the same time frame could not consider all of the investigation results, because these calculations were often performed simultaneously to the exploration works. Therefore, with all results available now, open questions and inconsistencies could be clarified. This is the basis for a state-of-the-art description of the flow and transport processes in the overburden. All data received from the exploration programme are comprehensively documented in the reports of BGR, e. g. /KLI 07/, /KOE 07/. The updated hydrogeological model for Gorleben site will be available soon.

BGR as well as BfS do not see substantial research needs on the overburden with respect to the long-term safety assessment for a potential repository at Gorleben site. The following questions have been raised at the workshop:

- Location and dimension of hydraulic windows
For groundwater flow modelling the position and dimension of hydraulic windows are of crucial importance.
With regard to Gorleben site the geological model is currently being updated. This model will be the basis for a site-specific flow calculation.
- Heat transport
Consideration of the heat transport in hydraulic models describing the transport of mineralized water above salt structures can provide important information on transport and subsidence rates. As a prerequisite for such modelling exercises further R&D work is necessary.

- Hydrogeological modelling

For a realistic assessment of the future evolution the understanding of processes and conditions occurring in the past are very important. The evaluation of the paleohydrogeology and therewith the selection of realistic initial and boundary conditions for hydrogeological modelling is difficult, because of the questions concerning geology and geometry of the hydrogeological model, mentioned above. Up to now there is no comprehensive three-dimensional hydrogeological models for the whole area available, which include the exploration results from the area north of the river Elbe. With future three-dimensional model calculations including these results the existing models should be verified. Inverse model calculations could help to check the geological structural model, particularly with regard to the location and distribution of aquitards in the overburden of the salt dome. One important question is, which changes of models used so far are necessary to achieve consistence of the salt- and freshwater-distributions and –movement for the recent hydrogeological state. Further it has to be checked, which additional assumptions and simplifications are acceptable and which have to be re-considered and modified.

- Paleohydrogeology, genesis of groundwater

The last issue is also correlated to the genesis of groundwater. In general the paleohydrogeological situation and the genesis of groundwater for the Gorleben site are known. However, especially for the interpretation of measured values for ^{14}C open questions exist. These questions can be answered by additional model calculations.

Generally, open questions concerning the interpretation of hydrogeological isotope data can be answered by detailed isotope-geochemical model calculations for the groundwater taking into account land use as well as climate conditions and their short-term changes.

- Climate, formation of erosion channels and treatment in performance assessment

The formation of glacial channels in Northern Germany would substantially influence the hydrogeology of an overburden, since such channels might form down to depths of about 500 m thereby eroding sediments of the overburden and the host formation itself. Due to current knowledge the formation of channels is independent from the formation of the overburden and from the existence of channels formed in the past at the site under consideration. The formation of such glacial channels might occur not only at Gorleben site but also at other potential repository sites in Northern Germany. For the assessment of the future evolution of a site a statement about possible future climate changes with realistic time frames and sequences of

different states are of special interest. The relevance of channel formations for the long-term safety need to be assessed. In this respect it is of great importance to investigate the consequences and the depth of the channels in the host formation.

- **Cryogenic fissures**

The formation and the consequences of cryogenic fissures in the salt formation require further fundamental research work. Investigations on formation and extension of such cryogenic fissures have just started.

- **Uplift rate, subsidence rate, balance of salt release**

It needs to be analyzed, whether the balance of salt release from the salt formation calculated with hydraulic models can substantially contribute to the estimation of future subsidence rates.

4.6 Impact of climatic conditions on geosphere modelling

For the long-term safety assessment of repositories for radioactive waste generally very long timescales have to be considered. As stated in the German safety requirements governing the final disposal of heat-generating radioactive waste an assessment period of one million years has to be addressed /BMU 10/. During this time frame significant changes of the climate will occur also impacting the environment including hydrogeology, geomorphology, hydrology, flora and fauna as well as human habits. In the following subsections it is shown by application of transport models, how climatic changes might impact flow and transport of radionuclides released from a repository. In section 0 the potential impact on biosphere processes is investigated.

4.6.1 Objectives and approach

The prediction of changes in long-term climate proves to be difficult. On the one hand climate is a result of numerous single natural and anthropogenic aspects. On the other hand their long-term changes are not completely known, and particularly their interactions are complex and not fully understood until now /NOS 08b/. Due to the high complexity of the system, the prediction of long-term climate changes over about 1 Mio. years is a big challenge and bears many uncertainties.

Nevertheless there are many scientists worldwide, who work on this topic. The reason therefore is often the assurance of food and water supply, as well as the estimation of

necessity and requirement of safety precautions, e. g. coast protection. However, also the long-term safety analyses of repositories need predictions of long-term climate change, to consider possible impacts on processes occurring in the repository system and therewith on the potential radiation exposure. Impact of climate changes need to be addressed in the safety case and are considered with respect to biosphere-, geosphere and also near-field processes. In some countries climate changes are integrated into biosphere models of different type and complexity. The kind of biosphere model depends on the countries, which attach different importance to the biosphere modelling, because of varying types of host rocks, repository design but also different consequences of climate change, like glaciation or not.

Within the long-term safety analyses of Sweden and Finland the acquisition and modelling of possible future biospheres is given a high priority. Therefore, and with regard to the near geographical position to Germany, their investigations of possible climate changes will be used as a basis for the geosphere calculations performed here. The results from the Swedish and Finnish study are used to develop a temporal sequence of conceivable climate changes for the next 1 Million years in Northern Germany, since the emphasis in this study is put on climate transitions. In a previous work /FLU 09/ flow and transport calculations have been carried considering different constant climate states. Flow calculations were performed until stationary flow fields were reached and with these constant flow fields radionuclide transport calculations were performed over time frames of 1 Mio. years. In the new study presented here, changes of flow fields caused by climate changes are transiently modelled. It is one objective to compare transient results with those received for constant conditions

4.6.2 Assessment of long-term climate changes in Sweden and Finland

Studies of the past climate in northern Europe show an oscillation of warm and cold periods. Since approximately 1 Million years the cold periods continued mostly about 100,000 to 150,000 years. The cooling is characterized by an increasing ice sheet and widespread permafrost. The depth of permafrost depends on the duration of the low temperature. In addition there is an influence of the inland ice sheet, which causes a melting of permafrost with regard to ice load. After the retreatment of ice, the permafrost will increase again. The warm periods of the past are connected with the maximal insolation of the northern hemisphere and lasted approximately 10,000 until 15,000

years. They caused a melting of ice and permafrost. Their maximum is mentioned as climate optimum.

Additional studies of the future climate in northern Europe show, that the rotation of warm and cold periods will very likely during the next 1 Million years. Orbital changes and the resulting insolation, which affect the climate to a great extent, can be predicted over the next Million years with comparably high accuracy, e. g. /NOS 08b/. And because of the similarity of today's planetary conditions with that during the Holstein MIS11-period, this future period can be compared with that past climate period between 360,000 and 420,000 years before present.

However, the prediction of duration and amount of precipitation and temperature during single periods and therefore the existence and extent of permafrost, inland ice and dry seasons is very difficult. Not to mention the forecast of man-made effects to the climate.

Therefore the climate studies can give a general survey of single climate duration and characteristics. In addition it's possible to deduce the range of discrete climate states and to get an idea about the climate transitions.

4.6.2.1 Investigations of SKB (Sweden) and POSIVA Oy (Finland)

In Sweden four main climate change scenarios were investigated:

- A reference case, which is similar to the Weichselian ice age,
- a scenario of a warm period with different intensities,
- a scenario of increasing ice sheet development, and
- a scenario of increasing permafrost development.

These scenarios are not representing the most likely appearance and sequence of the different climates. They are rather mentioned to receive the maximal range of climate states and possible transition between them. This approach has the advantage, that the most important climate impacts on the repository system and the radionuclide transport will be included. The following discrete climate states will be under examination: the temperate, periglacial and glacial climate as well as the flooding of the area.

The reference case is very similar to the Weichselian ice age, see Fig. 4.28. As an assumption, only the natural cause of climate change, the orbital configuration, is considered. The first glacier advance take place about 60,000 years and continue about 10,000 years. The thickness of the ice-sheet is about 2,000 meter. Previously temperate and periglacial periods rotate. At the beginning the temperate climate predominate, later on the periglacial climate. The maximum duration of each climate is about 10,000 years.

The second glacier advance takes place in about 90,000 years and continue about 20,000 years. The thickness of the ice-sheet is about 3,000 meter. Afterwards a marine transgression happened and persisted about 10,000 years. The sea level rise is not mainly a consequence of thermal expansion or increasing water availability due to the melting glacier. The flooding is mainly a result of the isostatic subsidence of the earth crust.

Between the glacial stages the climate moved to periglacial conditions interrupted by short periods of temperate climate, about 2,000 years at maximum. The periglacial climate is characterized by the growth of permafrost, which reached its maximum depth of 250 m after about 50,000 years. The freezing of permafrost in the periglacial and its thawing in the temperate climate periods occur even if the periods are only a few thousand years long. Often the increase of permafrost is a fast process of a few thousand years. But in some cases it takes a long time, for example between 23,000 and 30,000 years, see Fig. 4.28.

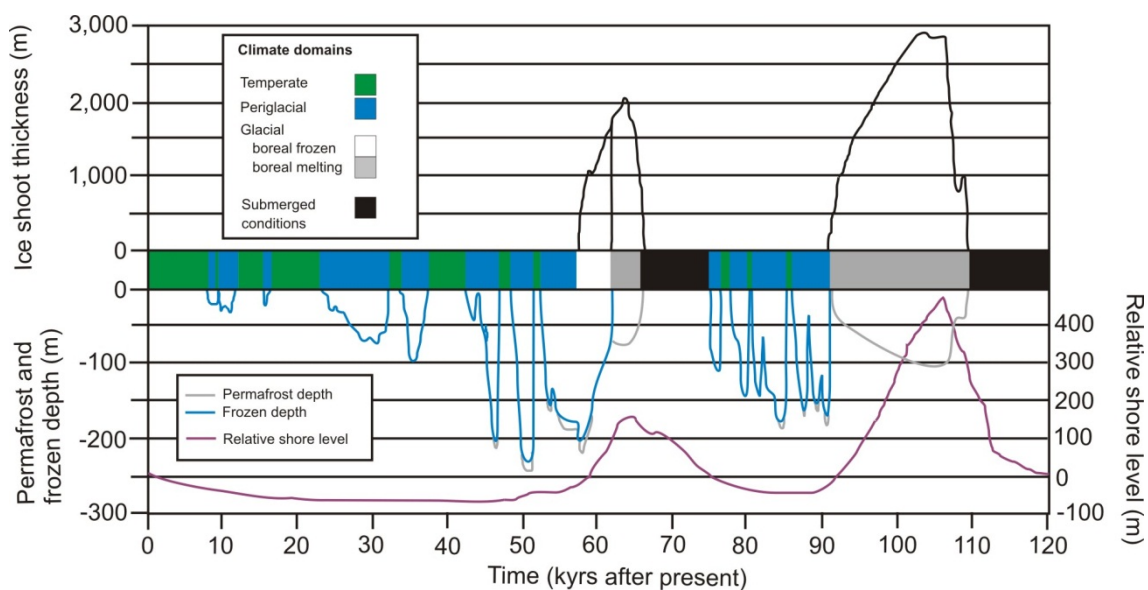


Fig. 4.28 Climate during the reference glacial cycle in Forsmark (Sweden) /SKB 10/

The Scenario of global warming is a modification of the reference case and assumes an increasing anthropogenic generated CO₂ concentration. Therefore the global warming will continue within the next 60,000 years and leads to a temperate climate. Afterwards the glacial cycle of the Weichselian reference case occur again. That means that there will be a change of temperate and periglacial climate and the next glaciation will occur after about 110,000 years. A similar sequence of climate states is predicted in the BIOCLIM project /BIO 04/ and mentioned in /NOS 08b/.

According to different greenhouse gas concentrations mentioned in BIOCLIM, a second scenario of global warming is considered, which leads to a very long time of temperate climate about 110,000 years, see Fig. 4.29. Afterwards temperate and periglacial conditions rotate and lead over to the next glacial cycle, which is mentioned in the reference case.

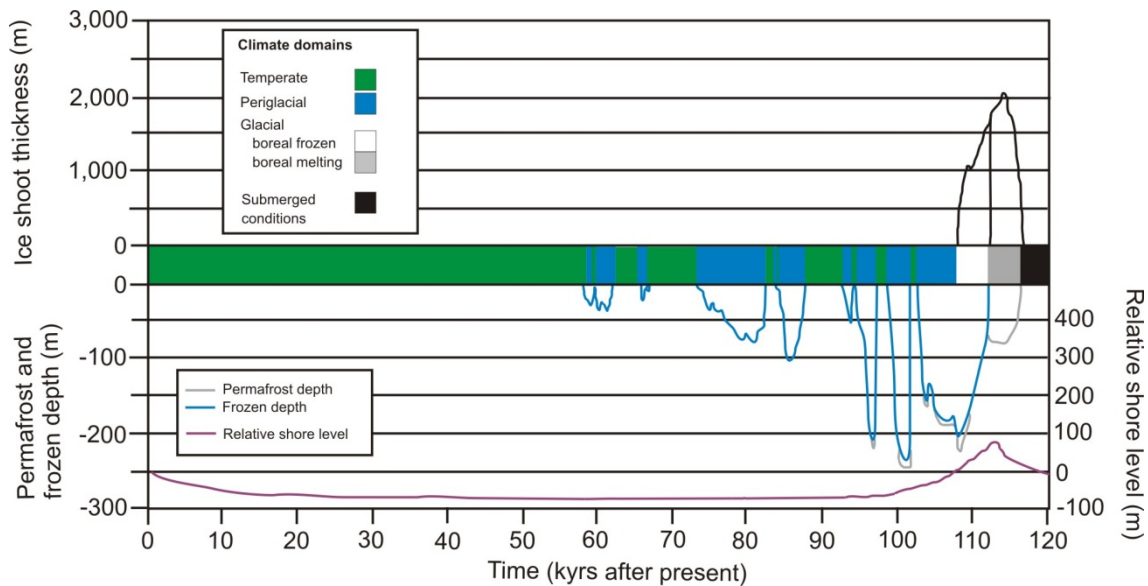


Fig. 4.29 Climate during the moderate global warming scenario in Forsmark (Sweden) /SKB 10/

Scenarios of intensified growth of ice sheets and permafrost were also considered. They pay special interest to the reaction of technical barriers, especially the bentonite buffer, in case of additional weight caused by ice load, as well as the impact of a frozen bentonite buffer.

Within the scenario of intensified ice sheets growth it is assumed, that there will be a glaciation about 50,000 years after present. Until then temperate and periglacial conditions change.

The scenario of intensified permafrost growth assumes that there will be periglacial conditions between 8,000 and 110,000 years. Only at the beginning it is interrupted by about three temperate periods of a few thousand years length.

The research in Finland mainly concern five different climate changes for the investigation area Olkiluoto, see scenarios A – E in Fig. 4.30. They continue interglacial and glacial conditions as well as permafrost. Often changing periods of glacial and permafrost conditions or temperate and permafrost conditions are combined and separated shown.

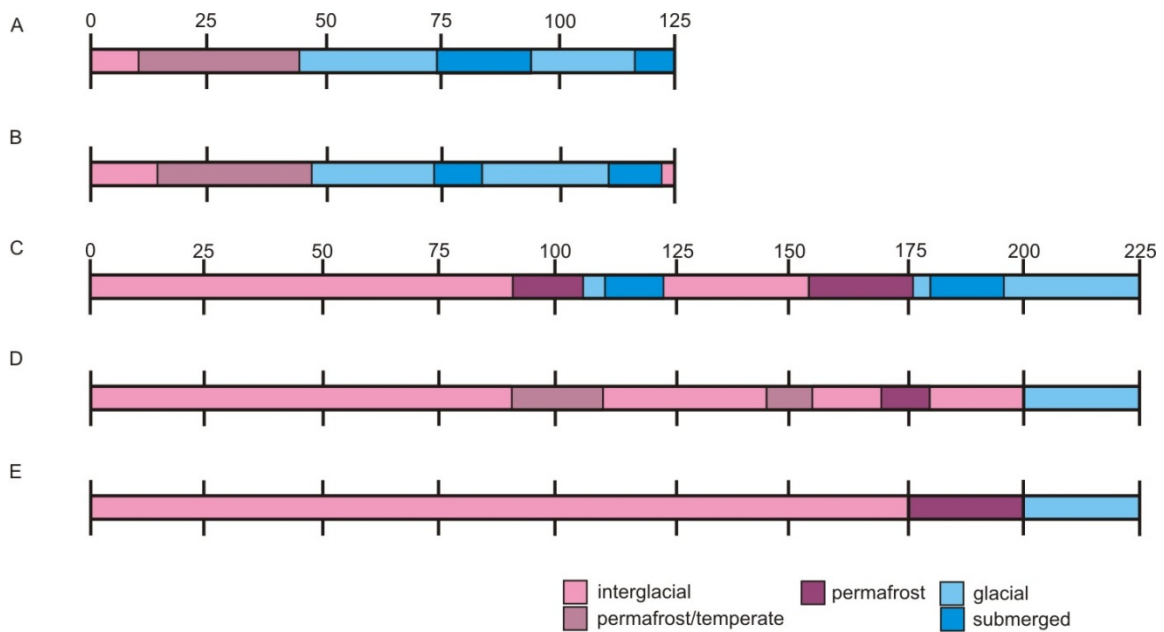


Fig. 4.30 Climate of Olkiluoto up to 125,000 years after present for scenario A and B and up to 225,000 years after present for scenarios C, D, E /CED 04/

Scenario A based on results from model calculations, which were done from King-Clayton for the Swedish investigation area Äspö. They contain the Milankovitch cycle as most important input data. Due to the colder climate around the Finish investigation area Olkiluoto, the time sequences of climate were modified. The scenario starts with an interglacial. After 10,000 years after present there is a change between temperate conditions and permafrost, which continue about 40,000 years. Afterwards the climate gets colder and reached glacial climate for the next 30,000 years. The following warmer period cause a flooding of the investigation area, which persist about 20,000 years. A second glaciation reached the area about 90,000 years after present and remains about 25,000 years. Afterwards the area is flooded again.

Scenario B is similar to the Swedish reference case and described in the passage of the Swedish investigations, see above.

The Scenarios C, D and E based on scenarios considered in the BIOCLIM project. They assume different atmospheric CO₂ concentrations for the next 5,000 years, see Fig. 4.31. As a function of the CO₂-concentration there are different surface temperatures, which are depicted in Fig. 4.32.

Scenario C is calculated with a continuously, relative low CO₂ concentration of about 300 ppmv, which is considered as the naturally occurring CO₂ concentration.

Scenarios D and E assume a higher atmospheric CO₂-concentration because of an additional anthropogenic CO₂ input. That causes a linear increase of the concentration until the peak after about 500 years. The maximal CO₂ concentration is 1,700 ppmv for scenario E and 1,200 ppmv for scenario D. Afterwards the concentration is decreasing, but remains within a higher level as the beginning concentrations. This is about 500 ppmv for scenario D and about 700 ppmv for scenario E.

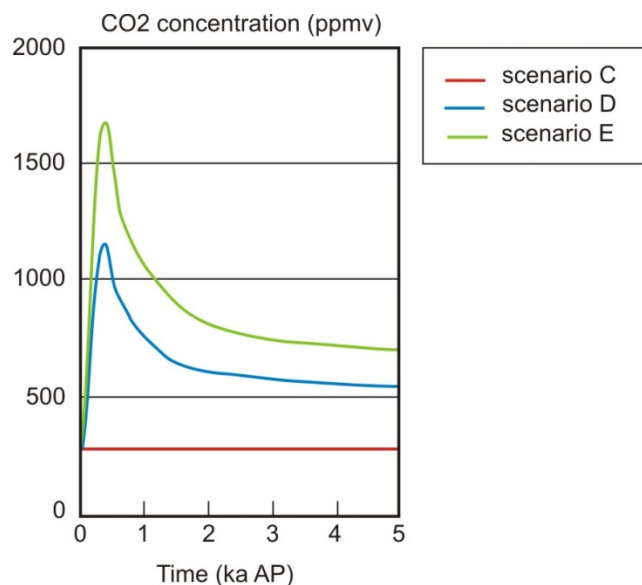


Fig. 4.31 Atmospheric CO₂ concentration assumed in scenarios C, D and E /CED 04/

The higher CO₂ concentrations of scenario D and E compared to scenario C cause a different surface temperature. However, the principle trend of the temperature is similar between the scenarios, with exception of the peak at the beginning. That means, that the temperature decrease until about 100,000 years, then it increases until about

115,000 years, before it decreases again. The graphs for scenario D and E are almost identical but shifted about 0.5 – 1°C.

The temperature in scenario C is more different. It shows major differences in the fluctuation of the temperature, which especially occur after 100,000 years. Also the warming about 100,000 and 115,000 years is more pronounced as in the scenarios D and E. With regard to the different temperatures it is assumed, that the existing ice sheets will be completely melt in the northern hemisphere: for scenario D within the next 200,000 years, for scenario E within the next 150,000 years. Afterwards the ice sheet will increase again. But the next period of wide-ranging ice cover is not expected before 170,000 years after present.

About 100,000 years and 175,000 years there is a cooling in scenario C, which is characterized by a sequence of permafrost, a short glacial climate state as well as a following flooding. During the first cooling the sequence continues about 30,000 years. At this time the permafrost remains about 15,000 years, the glacial climate a few thousand years and the time of flooding about 10,000 years. The second cooling remains about 40,000 years. It contains permafrost of about 20,000 years, which is displaced by a glacial climate of a few thousand years and a flooding of about 15,000 years.

During the cooling in scenario D about 100,000, 150,000 und 175,000 years, permafrost developed about 10,000 until 20,000 years after present.

Scenario E assumes a very long interglacial of about 175,000 years. Afterwards permafrost developed and persists about 25,000 years. The next glacial climate is not assumed before 200,000 years.

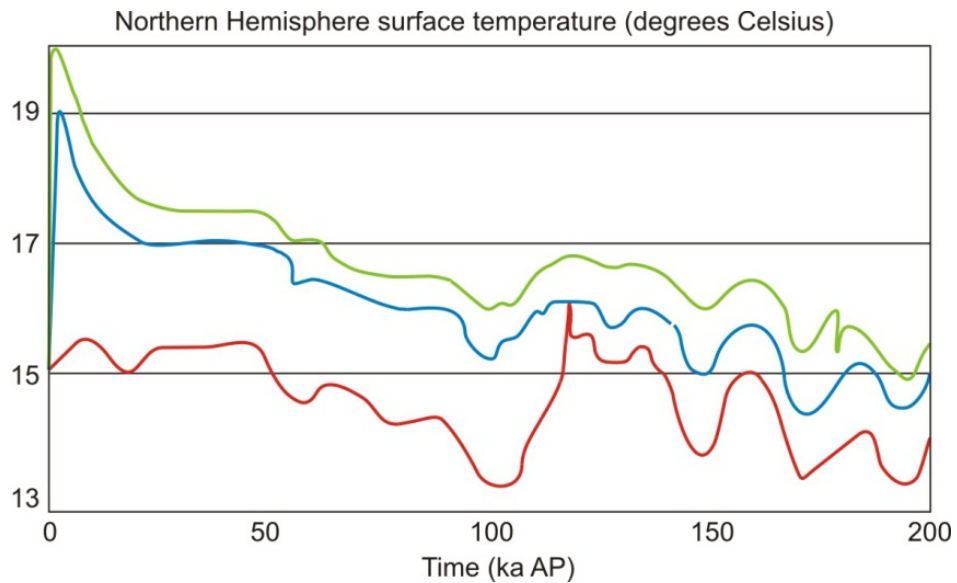


Fig. 4.32 Graph of the surface temperature with regard to the CO₂ concentration /CED 04/

4.6.2.2 Summary and results

The results of the Swedish and Finish investigations are compiled in Fig. 4.33. It shows the climate change between temperate/interglacial, periglacial and glacial conditions as well as the time of flooding during a timescale of at least 120,000 for the investigation area Äspö/Sweden (above) and Olkiluoto/Finland (below).

Important issues to mention are:

- The Swedish results assume an earliest ice-cover of the investigation area Äspö about 50,000 years a.p. („extended ice sheet duration scenario“). For the reference case it is assumed after about 60,000 years, in the “warm scenarios” earliest after about 110,000 years.

Due to the geographical location of the Finish investigation area Olkiluoto, it is assumed, that it would be a few thousand years earlier covered with inland ice.

- Periglacial conditions are earliest established in both countries after about 8,000 years in the „cold scenarios” („extended ice sheet”, „severe permafrost”), after about 25,000 years in the reference case and after about 60,000 years in the „warm scenarios” („global warming”, „extended global warming”, „Szenario C, D, E”).

The „cold scenarios“ and the „reference case“ are characterized by often occurring periglacial periods of longer duration compared to the „warm scenarios“.

- The persistence of marine flooding is assumed to be 10,000 years in the different scenarios for Sweden and 20,000 years in the reference case of Finland.

During the „cold scenarios“ (extended ice sheet, severe permafrost) the temperate and periglacial climate is changing for the next 120,000 years. The temperate climate persists about 2,000 until 10,000 years, the periglacial about 5,000 until 70,000 years. Within the extended ice sheet scenario, 60,000 years of periglacial is replaced by glacial conditions and afterwards there will be a marine transgression of about 10,000 years. Therefore in 80 percent of the considered time cold climates occur like periglacial or glacial conditions. The results were confirmed by the “widespread glaciation scenario” calculated with Earth System Models of Intermediate Complexity (EMIC) and documented in /NOS 08b/, which shows a first glaciation about 178,000 years a.p. and therefore only about 10,000 years earlier.

During the reference case (scenario A, B) temperate, periglacial and glacial conditions rotate. The appearance of the temperate and periglacial climate is about a few thousand until 23,000 years, of the glacial climate about 7,000 until 22,000 years. After the coverage with inland ice there is a marine transgression of about 10,000 years duration. Therefore periglacial and glacial conditions occur more than half of the considered time. Climate predictions based on statistical regularities derived from past climates as well as calculations based on an average CO₂ concentration of 230 ppm show similar results /NOS 08b/.

During the „warm scenarios“ (global warming, extended global warming, Szenario C, D and E) there will be mostly a temperate climate (60 % until 90 %). Periglacial conditions occur at the earliest after 60,000 years and persist only a few thousand years. From 75,000 years the periglacial periods will be longer but 25,000 years at maximum. Glacial conditions begin at the earliest after about 110,000 years. The „extended global warming scenario” is similar to the „super interglacial condition scenario” calculated with EMIC documented in /NOS 08b/.

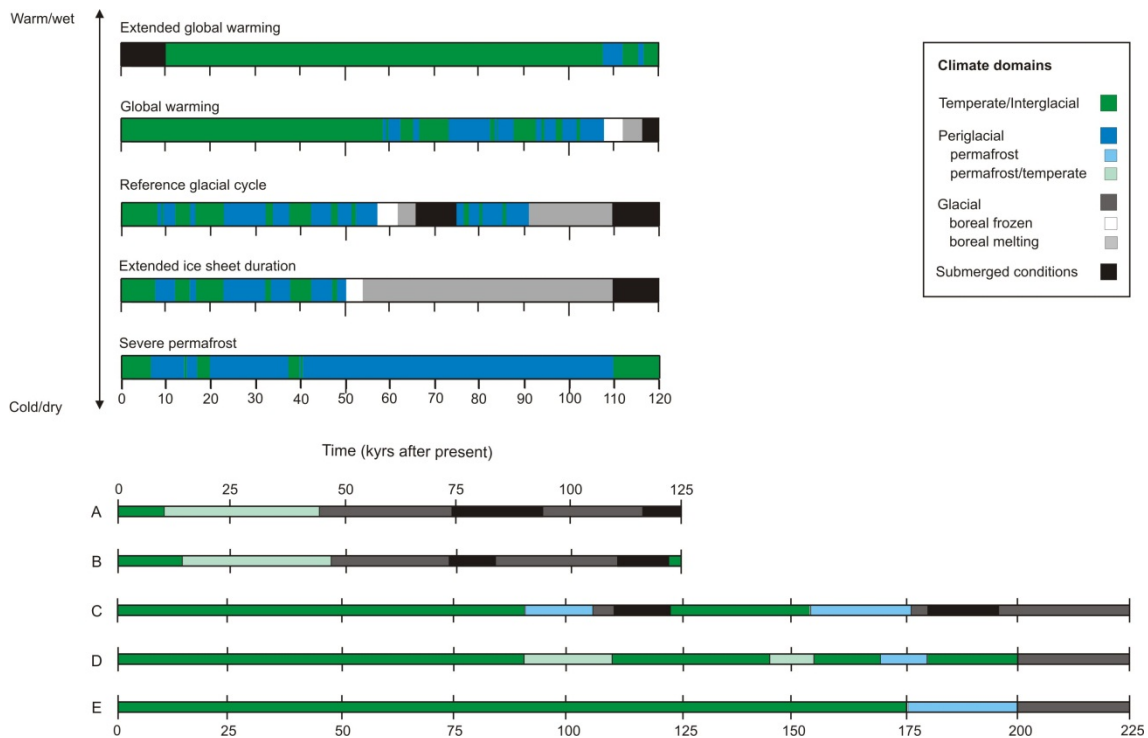


Fig. 4.33 Summary of future climate cases analyzed in the safety assessments SR-Site (top) and for Olkiluoto (bottom) /SKB 10/, /CED 04/

4.6.3 Derivation of possible climate changes in Northern Germany

The Swedish and Finnish investigations described in 4.6.2.1 show the spectrum of possible climates and transitions, which could be also supposable for Northern Germany. German investigation of paleodata, orbital configurations as well as model calculations with different greenhouse gas concentrations (e. g. /NOS 08b/, /BIO 04/, /ARC 05/) confirms the results. However the geographical position and especially the further distance to the area of glacier formation have to be considered. They lead to modifications within the time scales of different climate states as well as the duration time of marine transgression and inland ice coverage. Hence for Northern Germany there will be the following suggestions:

1. The periodical marine transgression of the Scandinavia investigation areas after ice coverage is not assumed. The reason therefore is that the isostatic subsidence of the lithosphere, which mainly causes the flooding in Scandinavia, has to be neglected in Germany. Therefore the flooded period will be replaced by another period of periglacial conditions.

2. The development of ice cover is unlikely at least for the next glacials. Instead a dilatation similar to the Weichselian ice sheet would be expected. Therefore the coverage time will be replaced by a longer time of periglacial conditions. But it will be distinguished between a near-glacier and far-glacier position, which differ in the melt-water amount.

Additional suggestions are:

3. Cold periods are characterized by a periglacial climate, which leads to the development of permafrost.
4. Warm periods are characterized by a sea level rise and therefore marine transgression, which could lead to a flooding of the investigation area.
5. The transitions between warm (temperate, Mediterranean) and cold climates (periglacial) are characterized by boreal conditions.
6. Cooling takes longer (few millennia) as the warming (few centuries until millennia).
7. The duration of a glacial cycle (interglacial maximum until glacial minimum) is estimated to be 120,000 years. It will be explained with the fact that these time period was typically for the cycle within the last 700,000 years.

The derivation of possible climate changes in Northern Germany is documented in terms of two climate cycles: The first cycle assumes a moderate development of atmospheric CO₂-concentrations, which leads to temperate climate conditions during the next 50,000 years. The temperate climate is characterized by a rotation of terrestrial, coastal and aquatic conditions. It starts with a terrestrial site over 5,000 years. Due to sea level rise, it is assumed that the area will be near the coast for the next 5,000 years. Afterwards it will be flooded for 5,000 years with a water column of 50 m, and after this time it will be a coastal site for the same time duration. Then it will be a terrestrial site again for 30,000 years. After these 50,000 years the concentration of anthropogenic greenhouse gases will decrease and the climate will mainly depend on orbital configuration again. Therefore the change between temperate and periglacial conditions starts again and persists about 70,000 years. The appearance and duration of periglacial conditions influence the development of permafrost concerning thickness, broadening and continuity. During the time of periglacial conditions a permafrost thickness of 150 m at maximum is expected. With regard to /KLI 07/ a thickness of 50 m (half of the first aquifer), 100 m (complete first aquifer) and 150 m (complete first aquifer and aquitard) will be set in the model

(Fig. 4.36). With the exception of river Elbe, which remains as unfrozen part of the underground, so called talik, a continuously permafrost developed.

The following cycles will base on the Weichselian ice age. Within the cycle temperate and periglacial climate conditions are rotated. The periglacial climate prevail and last 70,000 years. During this time permafrost of different thickness will develop, with 150 m at maximum. The development of permafrost is shown in Fig. 4.34 /KLI 07/.

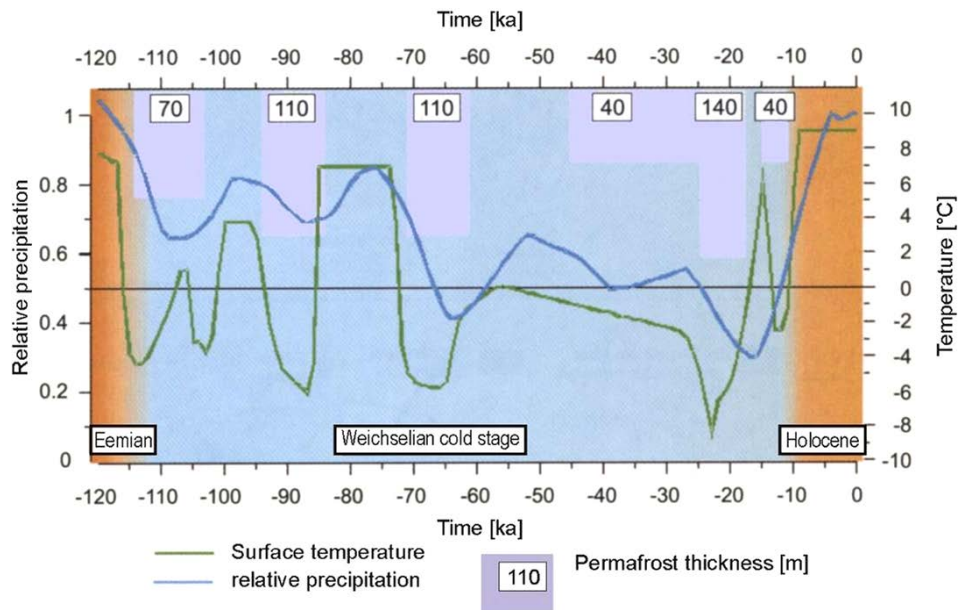


Fig. 4.34 Calculated permafrost thickness during Weichselian in Northern Germany /KLI 07/

Tab. 4.4 Climate during the first 120,000 years a.p. with regard of a moderate CO₂-concentration during the first 50,000 years

0 – 5,000 years	temperate, terrestrial
5,000 – 10,000 years	temperate, coastal: sea water rise
10,000 – 15,000 years	temperate, aquatic: marine transgression (50 m WS)
15,000 – 20,000 years	temperate, coastal: lowering of sea level
20,000 – 50,000 years	temperate, terrestrial
50,000 – 55,000 years	periglacial, near-glacier conditions: permafrost 50 m
55,000 – 70,000 years	periglacial, near-glacier conditions: permafrost 100m
70,000 – 75,000 years	periglacial, far-glacier conditions: permafrost 50 m
75,000 – 85,000 years	periglacial, far-glacier conditions: no permafrost
85,000 – 90,000 years	periglacial, near-glacier conditions: permafrost 100m
90,000 – 110,000 years	periglacial, near-glacier conditions: permafrost 150 m
110,000 – 115,000 years	periglacial, near-glacier conditions: permafrost 100 m
115,000 – 120,000 years	temperate, terrestrial

Tab. 4.5 Climate after the first 120,000 years a.p. with regard to the Weichselian ice age concerning /KLI 07/

0 – 10,000 years	temperate, terrestrial
10,000 – 20,000 years	periglacial, far-glacier conditions : permafrost 50 m
20,000 – 30,000 years	temperate, terrestrial
30,000 – 40,000 years	periglacial, near-glacier conditions: permafrost 100 m
40,000 – 58,000 years	temperate, terrestrial
58,000 – 65,000 years	periglacial, near-glacier conditions: permafrost 100 m
65,000 – 82,000 years	temperate, terrestrial
82,000 – 100,000 years	periglacial, far-glacier conditions : permafrost 50 m
100,000 – 110,000 years	periglacial, near-glacier conditions: permafrost 150 m
110,000 – 115,000 years	periglacial, near-glacier conditions: permafrost 50 m
115,000 – 120,000 years	temperate, terrestrial

4.6.3.1 Model structure

The Gorleben salt structure and its overburden serve as a reference site for this study. A comprehensive dataset is available on the geology and hydrogeology of the overburden /KLI 07/, /KOE 07/. The Gorleben-Rambow salt structure has a length of ca. 30 km

and a varying width between 1.5 km and 4 km. It strikes SW-NE and is crossed at the surface by the river Elbe and its tributaries Lößnitz and Seege /KLI 07/.

The Tertiary and Quaternary sedimentary overburden of the salt dome and its neighboring rim synclines form a system of aquifers and aquitards (Fig. 4.35) of up to 430 m thickness /KLI 02/. The basis of the regional flow system is represented by the Tertiary Rupel Clay. The Tertiary Lower Brown Coal Sands and Eochatt silts and the Quaternary Elsterian channel sands form the lower aquifer /LUD 02/. The intercalated aquitard is a set of the Tertiary Hamburg Clay and the Quaternary Lauenburg Clay Complex, which is superposed by mostly Weichselian and Saalian sediments representing the upper aquifer /KLI 02/. Main structural elements of the system are the salt dome itself with the adjacent northwestern and southeastern rim synclines, a contact of the salt dome to the lower aquifer in the glacial meltwater channel, the so-called Gorleben channel, formed by glacial erosion during the Elsterian cold stage, and hydraulic connectivities between the two aquifers, so-called hydraulic windows, likewise formed by glacial erosion /KLI 07/.

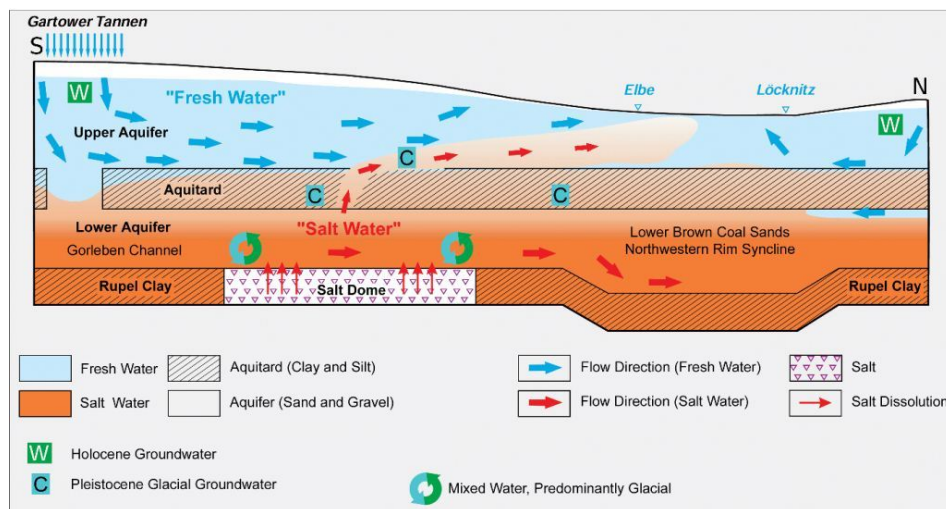


Fig. 4.35 Schematic cross section of the hydrogeological system at the reference site Gorleben (modified from /KLI 02/)

The hydraulic system can be roughly divided into a lower aquifer, an intercalated aquitard and an upper aquifer. Due to the contact of the Zechstein salt to the Quaternary aquifer in the Gorleben Channel, salt can be dissolved by the groundwater. The groundwater shows a stratification into an upper fresh water body and a lower salt water body /LUD 02/. The distinct relief of the basis of the fresh water body is caused by the relief of the aquitard as well as by the regional groundwater flow. Groundwater re-

charge takes place in the area of the Gartower Tannen in the south and in the lowlands north of the river Elbe. The highest fresh water thicknesses occur in those areas of the rim synclines where the salt water descends due to its higher density as well as where the aquitard is missing. The lowest thicknesses are found in the entire area of river beds and lowlands north of the river Elbe and above the Gorleben salt dome. The salt water/fresh water interface rises from the Gorleben Channel to the north and reaches the water table close to the river Elbe /KLI 07/, /LUD 02/.

An important parameter for the estimation of radionuclide transport by groundwater is the groundwater flow velocity. It depends on the

1. amount of groundwater and therefore the distance to the glacier and the development of surface temperature,
2. depths of permafrost and therefore reduction of the aquifers cross section,
3. aquifer characteristic (permeability, cross section, constrained or not),
4. number and extension of taliki, which cause an upstream of groundwater and therefore a reduced flow velocity in the deep aquifer layer.

Therefore different model assumptions will help to observe the effects to radionuclide transport. First of all several periods of increasing and decreasing permafrost are considered. They are interrupted by no permafrost periods. The permafrost development is realized in two different ways: a fast development/reduction and a smooth transition between the different permafrost thicknesses, see Fig. 4.36. Both are derived from information of permafrost development in Fig. 4.34. During the fast development/decreasing the maximum permafrost thickness exists longer than in the other case. Therefore it is expected, that the influence on groundwater flow is much higher as in the case of smooth permafrost transition.

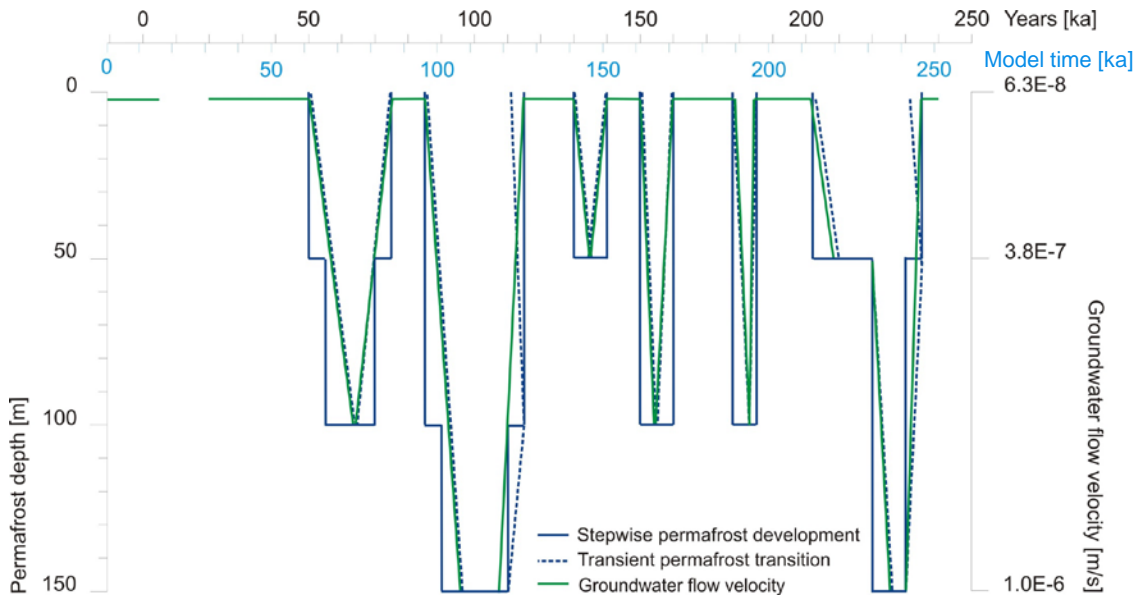


Fig. 4.36 In the model assumed development of permafrost and groundwater flow velocity in two different climate cycles

Furthermore the groundwater input rate of meltwater through the boundary is an important parameter considered in the model. It is adapted as a varying groundwater flow velocity, depending on the distance of the investigation area to the glacier and the development of surface temperature and therefore melting of the glacier. The annual access of meltwater during summer is neglected. The maximal groundwater flow velocity $1.0E-6$ m/s is adapted from BGR /FLU 09/. It is reached in case of a meltwater maximum amount from the nearby glacier of $3,153.6$ m³/a and a frozen first groundwater aquifer until 150 m depth. Without permafrost and a glacier, which is far away from the model area, the meltwater amount is set to 200 m³/a /FLU 09/ with a groundwater flow velocity of $6.3E-8$ m/s. The values for 50 and 100 m permafrost depths are interpolated. The data used in the model are summarized in Tab. 4.6.

Tab. 4.6 Model-Parameter

Permafrost depth	GW flow velocity.	GW input	Reference
m	m/s	m ³ /a	
0	$6.3E-08$	200	/FLU 09/
50	$3.75E-07$	interpolated	
100	$6.88E-07$	interpolated	
150	$1.0E-06$	3153.6	/FLU 09/

4.6.3.2 Parameterization

Flow and transport were simulated using the codes d^3f /FEI 99/ for groundwater flow and r^3t /FEI 04/ for radionuclide transport, which were developed under the auspices of GRS and are able to deal with very large model areas and long periods in time. Main characteristic of d^3f is the possibility to calculate the transient, density-driven transport of salt. Transport simulations with r^3t are based on flow fields calculated by d^3f . The most important feature of r^3t is its ability to simulate pollutant transport considering radioactive decay, sorption and geochemical reactions.

A two-dimensional conceptual model was set up based on a schematic cross section (Fig. 4.35) and geological and hydrogeological information given by numerous publications (e. g. /KLI 07/, /KLI 02/, /LUD 02/). The model has a length of 16.4 km and a depth of 400 m (Fig. 4.37, note that all figures of the model show a vertical exaggeration of 10). It consists of three hydrogeological units, representing the upper aquifer, an intercalated aquitard and a lower aquifer. The aquifers have a thickness of 100 m, while the northwestern rim syncline is realized with an additional thickness of the lower aquifer of 150 m. The aquitard has a thickness of 50 m and is locally interrupted by two hydraulic windows, i. e. local absence of the aquitard. One hydraulic window is close to the southern boundary of the model and a second hydraulic window at the northern boundary of the northwestern rim syncline. Both are 50 m wide. The contact between the lower aquifer and the cap rock of the salt dome in the Gorleben Channel is included in the model set-up and marked in red in Fig. 4.37.

The hydrogeological parameters were assigned to the three different units according to different publications about the Gorleben aquifer system (cited in /FLU 09/). The porosity φ of the aquifers is 0.2, the aquitard has a porosity of 0.05. A uniform longitudinal dispersion length α_L of 10 m, a transversal dispersion length α_T of 1 m and a molecular diffusion coefficient D_m of $1 \cdot 10^{-9} \text{ m}^2 \text{ s}^{-1}$ are set for the entire model domain. The only parameter, which is varied during the simulations, is the permeability k . For the present state, the aquifers have a permeability of $1 \cdot 10^{-12} \text{ m}^2$ and the aquitard has a permeability of $1 \cdot 10^{-16} \text{ m}^2$. For the permafrost conditions, the permeability is varied according to Fig. 4.36 (see text below).

The salt concentration is given in form of a relative concentration /FEI 99/:

$$c_{rel} = \frac{c_{abs}}{c_{abs,max}} \quad \text{with} \quad c_{abs} = \frac{m_{tracer}}{m_{tracer} + m_{H_2O}} \quad (4.1)$$

and

c_{rel} = relative salt concentration = relative salt mass fraction [-]

c_{abs} = absolute salt mass fraction [-]

$c_{abs,max}$ = maximum absolute salt mass fraction [-]

m_{tracer} = mass of salt [kg]

m_{H_2O} = mass of water [kg].

The expected salt concentrations range between fresh water (minimum absolute salt mass fraction = 0.0) to saturated brines (maximum absolute salt mass fraction = 0.265, equivalent to 360.54 g L⁻¹).

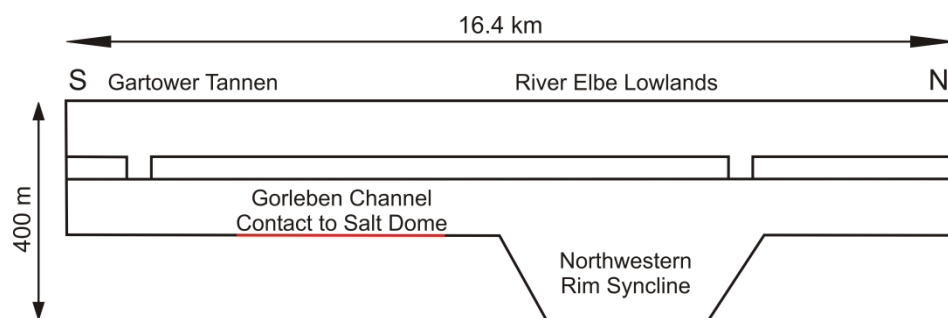


Fig. 4.37 Geometry of the groundwater flow and transport model, vertical exaggeration: factor 10

In order to model potential future climate transitions, the present state of the hydrogeological system needed to be simulated first. It is assumed that the present state of the system could evolve since the end of the last glacial maximum of the Weichsel Cold Stage, which marks the beginning of the Holocene. Therefore, the model run starts at 11,500 a before present. The initial salt concentration is set according to /KLI 07/ and /KOE 00/. For the upper 70 m of the model, fresh water conditions ($c_{rel} = 0.0$) are defined. In the lower 30 m of the upper aquifer the salt concentration rises linearly from $c_{rel} = 0.0$ to $c_{rel} = 1.0$. The aquitard and the lower aquifer show salt water conditions with $c_{rel} = 1.0$. The temperature rises linearly from 8° C at the surface to 20° C at the bottom

of the model according to the groundwater temperature /KAP 61/ and the geothermal gradient /LEG 04/ in Northern Germany. Heat transport is not calculated in the simulations.

Boundary conditions are set according to /KLI 07/, /KLI 02/ and /LUD 02/. In the Gorleben Channel, where the lower aquifer has contact to the salt dome, salt can be dissolved. Therefore, the salt concentration at this location is set to $c_{rel} = 1.0$ at a length of 4 km (red line in Fig. 4.37). At the southern and the northern part of the model surface, groundwater recharge of 160 mm a^{-1} is defined in form of an inflow of freshwater with a velocity of $5.1 \cdot 10^{-9} \text{ m s}^{-1}$ and a salt concentration of $c_{rel} = 0.0$. In the center of the surface, a hydrostatic pressure is given. Here, fresh water may infiltrate ($c_{rel} = 0.0$) or groundwater of different salinity may be discharged (in- and outflow boundary condition). At the northern boundary, an inflow of groundwater into the lower aquifer is defined with a velocity of $6.3 \cdot 10^{-8} \text{ m s}^{-1}$ and a salt concentration of $c_{rel} = 0.0$. After 11,500 a model time, the present state of the hydrogeological system is met. For future temperate, terrestrial climate, the boundary conditions remain unchanged.

Assuming a sea water inundation, the lateral inflow of groundwater into the lower aquifer ceases. At the model surface a time-dependent pressure boundary condition is defined representing 5,000 a of a transgression, 5,000 a of a sea-level high-stand at 50 m, and another 5,000 a of a regression for another 5,000 a. This corresponds to the time frame between 16,500 a and 31,500 a of the first cycle as defined in Tab. 4.4 in section 4.6.3 and adapted to the model time in Fig. 4.36. The salt concentration at the surface is set to a sea water concentration of $c_{rel} = 0.13$ according to /ING 98/.

Permafrost conditions are simulated by a drastic reduction of the permeability to $k = 1 \cdot 10^{-20} \text{ m}^2$. Permafrost growth and decay is either simulated using a stepwise function of the permafrost thickness or by a transient function according to Fig. 4.36. With a thickness between 0 m and 150 m, the permafrost only affects the upper aquifer and the aquitard. Two zones in these hydrogeological units remain unfrozen (taliki) during the entire model time due to the assumed thermal influence of the rivers Elbe and Seege at the model surface, i. e. the original permeability is maintained. A large unfrozen zone with a width of 5 km is located in the area of the Elbe lowlands above the north-western rim syncline. At the lateral boundaries of this zone, transition zones with a width of 500 m are defined in which the permeability decreases linearly to the reduced value of $k = 1 \cdot 10^{-20} \text{ m}^2$. Another small unfrozen zone is located at the southern boundary of the model with lateral transition zones with a width of 50 m. At the model surface,

a hydrostatic pressure and an in- and outflow boundary condition for the salt concentration are defined. The southern boundary of the lower aquifer is modeled with the same boundary condition for hydrostatic pressure as the surface and with the same implicit boundary condition for the salt concentration during the times of future permafrost occurrence. At the northern boundary of the lower aquifer, a maximum inflow of glacial meltwater with $c_{rel} = 0.0$ is assumed with a velocity of $1.0 \cdot 10^{-6} \text{ m s}^{-1}$ /KOE 00/ during times of maximum permafrost thickness of 150 m. For the times of a permafrost thickness of 100 m or 50 m the inflow of freshwater into the lower aquifer is interpolated and shows velocities of $6.88 \cdot 10^{-7} \text{ m s}^{-1}$ and $3.75 \cdot 10^{-7} \text{ m s}^{-1}$. Employing a transient function for the permafrost thickness, the inflow velocity of glacial meltwater is defined by a transient function as well.

In former model simulations, three different potential future climate states were investigated in detail: The constant climate, the sea water inundation and the permafrost conditions /FLU 09/. After modelling the present state of the hydrogeological system as described above, the model was run assuming constant hydrogeological parameters and constant boundary conditions for each climate state until reaching the steady-state. The steady-state flow fields and salt concentrations, as well as radionuclide distributions for the sea water inundation and the permafrost conditions can be compared to the results for the flow and transport simulations conducted in this study.

For all transport simulations (this study and /FLU 09/) the radionuclides Cs-135, C-14, I-129 and Zr-93 were selected as well as the radionuclides of the uranium-238 decay series U-238, U-234, Th-230 and Ra-226. The radionuclides are released into the model domain at a point source in the center of the contact to the salt dome in form of a delta pulse of 1 mol during one year starting at the present state (11,500 a model time) in all simulations. In the case of the uranium decay series only an inflow of 1 mol of the parent nuclide U-238 was assumed. The occurrence of the daughter nuclides results from a build-up by radioactive decay only. In all simulations the radionuclides have the initial concentration of 0 mol m^{-3} in the model domain. This holds for both the dissolved as well as for the sorbed radionuclides.

Half-lives /MAG 06/ and sorption coefficients (K_d -values) derived from sorption experiments using Gorleben sediment and groundwater samples /SUT 98/ are compiled in Tab. 4.7. Constant sorption coefficients were assigned for each hydrogeological unit. Transport simulations were conducted on transient flow fields in this study, thus the analysis of the salt concentration distribution during the flow simulation is a crucial as-

pect for the assignment of K_d -values (e. g. Fig. 4.38). The limit between fresh water and saline water is at a salt concentration of $c_{rel} = 0.0375$ (in this case equal to the total dissolved solids (TDS) of $TDS = 10 \text{ g L}^{-1}$ according to /SUT 98/). During the entire model run, the lower aquifer and most of the aquitard show saline conditions, and the K_d -value is assigned accordingly. For the upper aquifer, this task is a bit more complex. Until reaching the present climate state, the salt concentration in the upper aquifer is mostly higher than 10 g L^{-1} , while during the sea water inundation between 16,500 a and 31,500 a after present, the salt concentration is higher than 10 g L^{-1} . The K_d -value for saline conditions was assigned to the upper aquifer until the end of the sea water inundation. The timeframe from 31,500 a to 251,500 a represents the time of permafrost growth and decay or present climate conditions. During this time frame, the upper aquifer mostly shows lower salt concentrations and thus can be regarded as a freshwater aquifer with according sorption coefficients (Fig. 4.38).

Tab. 4.7 Half-lives (HL) /MAG 06/ and K_d values /SUT 98/ of the considered radionuclides

Limit between fresh water ("Fresh") and saline water ("Saline") at $TDS = 10 \text{ g L}^{-1}$

Radio-nuclide	HL [a]	K_d , sand (aquifer) [ml g ⁻¹]		K_d , silt, clay (aquitard) [ml g ⁻¹]	
		Fresh	Saline	Fresh	Saline
Cs-135	$2.00 \cdot 10^6$	70	2	400	70
C-14	$5.73 \cdot 10^3$	0.2	0.2	2	2
I-129	$1.57 \cdot 10^7$	2	0.1	2	2
Zr-93	$1.50 \cdot 10^6$	40	40	100	40
U-238	$4.47 \cdot 10^9$	2	0.6	80	20
U-234	$2.46 \cdot 10^5$				
Th-230	$7.54 \cdot 10^4$	200	200	2000	200
Ra-226	$1.60 \cdot 10^3$	40	2	300	40

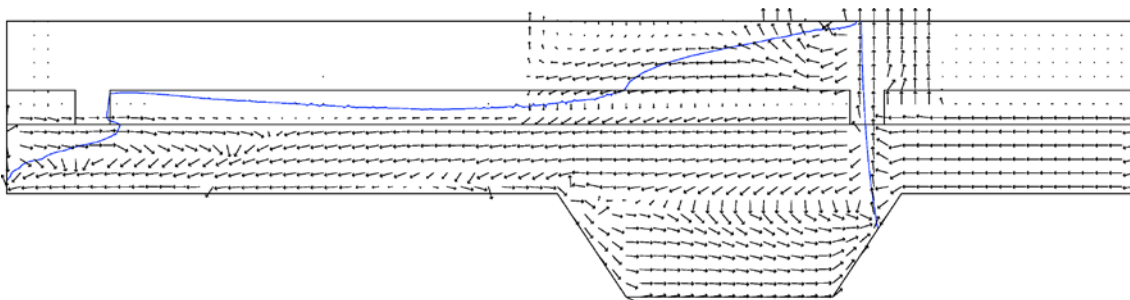


Fig. 4.38 Flow field and isoline for $c_{rel} = 0.0375$ ($TDS = 10 \text{ g L}^{-1}$) during a period with 100 m permafrost (190,000 a model time)

The transport simulations were run on transient flow fields that resulted from a highly complex sequence of possible future climate states and transitions. The most important difference of these transport simulations and those conducted by /FLU 09/ is that simulations by /FLU 09/ were run on constant flow fields, that were computed assuming constant boundary conditions. Therefore the salt concentration distribution and the flow field differ for the different approaches of the studies. For the present climate state and the sea water inundation, saline conditions prevail in the entire model domain and K_d -values were set in agreement with the model simulations conducted in this study. During permafrost conditions, not only the upper aquifer but also the aquitard shows freshwater conditions. The flow fields and the salt concentration distributions resulting from the former simulations are depicted and described in detail in /FLU 09/. A matrix for the assignment of the sorption coefficients for the different hydrogeological units and for the different climate states as provided by /FLU 09/ and as assumed in this work is given in Tab. 4.8.

Tab. 4.8 Matrix for the assignment of the K_d -values for the transport calculations in the two studies, derived from the flow fields and salt concentrations of the flow calculations (Fig. 4.38)

Limit between fresh water ("Fresh") and saline water ("Saline") at TDS = 10 g L⁻¹

Climate state		Upper aquifer	Aquitard	Lower aquifer
Present Climate	this study	saline	saline	saline
	/FLU 09/	saline	saline	saline
Sea Water Inundation	this study	saline	saline	saline
	/FLU 09/	saline	saline	saline
Permafrost	this study	fresh	saline	saline
	/FLU 09/	fresh	fresh	saline

The boundary conditions for the transport calculations were defined according to the boundary conditions for the flow simulations. For the present climate state a Dirichlet condition for the inflow into the lower aquifer with 0.0 mol m⁻³ is assigned. An in- and outflow boundary condition is stated for the model surface. This depends on the flow direction, which is given by the flow field. The concentration in the case of an inflow is assumed to be 0.0 mol m⁻³. In case of an outflow, the radionuclide concentration is set to the concentration in the outflowing groundwater. The same boundary conditions are applied to the future temperate, terrestrial conditions. The boundary conditions for the surface are also adopted for the sea water inundation but in this case the northern

boundary of the lower aquifer is assumed to be impermeable, as no inflow from the north exists. For the permafrost states, the inflow and outflow boundary conditions at the model surface are maintained. Here again an inflow of fresh water into the lower aquifer can be observed, which is realized by a Dirichlet condition with 0 mol m^{-3} . At the southern boundary of the lower aquifer a hydrostatic pressure is defined for the flow simulations, thus an inflow and outflow boundary condition is applied to this boundary as described above. The same set of boundary conditions was employed by /FLU 09/ to the former simulations assuming constant conditions. Unlike the new simulations, former simulations were run for a model time of one million years.

4.6.3.3 Results

A detailed description of the results of the former model simulations (including background to the model set-up and input data and assumptions) is given in /FLU 09/. The results of the flow and transport simulations conducted in this study are compared to results from those former model calculations assuming constant boundary conditions of one climate state. The results for the present state are identical for both realizations and are the basis for further simulations. The present state is met after 11,500 a model time. Most important characteristics of the present flow field as specified by /KLI 07/ could very well be described by the simulation (Fig. 4.39), e. g. the presence of two areas of groundwater outflow at the model surface, southward groundwater flow in the upper part of the lower aquifer between the contact to the salt dome and the northern boundary of the model, and northward groundwater flow in the lower part of the lower aquifer between the contact to the salt dome and the rim syncline. At the contact to the salt dome, salt is dissolved and transported to the rim syncline according to the flow direction. There, the saline groundwater descends due to its higher density. The model shows a density stratification of the groundwater with increasing salinity with depth, while the fresh water – salt water interface shows a distinct morphology.

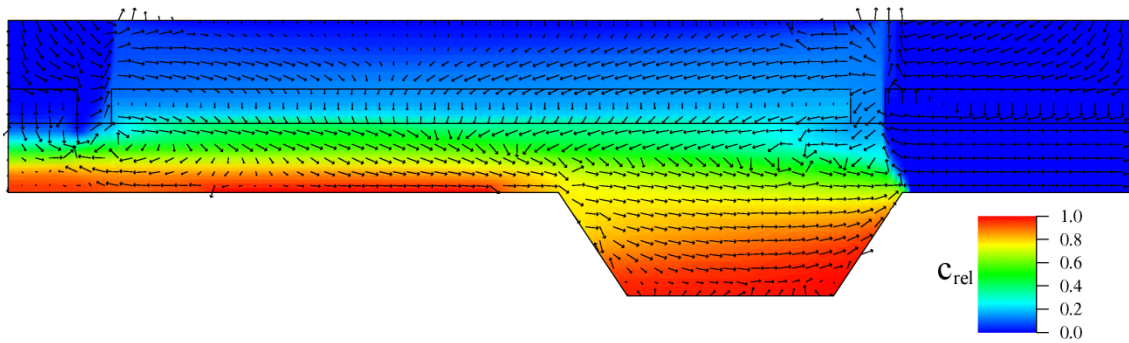


Fig. 4.39 Relative salt concentrations and velocity field for the present state (11,500 a model time)

Based on this flow field and salt concentration distribution, a sea water inundation of the area was simulated. For former calculations, it was assumed that the inundation starts at 11,500 a model time and persists until the systems reached a steady-state. During a sea water inundation advective groundwater flow ceases and convection drives the transport of salt. The entire upper aquifer already shows a salt concentration equal to that of the sea water of $c_{rel} = 0.13$ after approx. 1,000 a. After 50,000 a density stratification of the groundwater occurs with increasing density with depth and an abrupt increase of the salt concentration within the aquitard from $c_{rel} = 0.17$ to $c_{rel} = 0.39$.

Until the end of the calculations, salinity increases, in particular in the lower aquifer, resulting from the dissolution of salt and diffusive transport. After 600,000 a of sea water inundation, almost steady-state salt concentrations are reached. These range from $c_{rel} = 0.13$ at the surface to $c_{rel} = 0.85$ at the basis of the northwestern rim syncline with maximum concentrations of $c_{rel} = 1.0$ at the salt dome contact (Fig. 4.40). An abrupt increase of the concentration within the aquitard is observed here again, now with higher values between $c_{rel} = 0.29$ and $c_{rel} = 0.74$.

Evaluating the results of the former model simulations, it could be stated that an inundation time of only a few thousands of years has a clear influence on the salt concentrations in the upper aquifer and in the aquitard which approach the concentration of the sea water. During this period, the salt concentrations of the lower aquifer are hardly affected by the changed boundary conditions. For a more realistic simulation of a possible future sea water inundation of the area, a time of only 15,000 a was considered for the sea water inundation in this study with 5,000 a transgression, 5,000 a sea level high stand and 5,000 a regression. The inundation is assumed to start at 5,000 a after present.

At 31,500 a model time, the horizontal density stratification is already clearly visible (Fig. 4.41), but with lower salt concentrations than for the former simulations. In the upper part of the lower aquifer the salt concentration ranges from $c_{rel} = 0.3$ to $c_{rel} = 0.7$, while in the northwestern rim syncline it rises up to $c_{rel} = 0.85$. The flow velocity is drastically reduced compared to the present state (Fig. 4.39) but still higher than in the quasi steady-state of the former simulations after 600,000 a model time (Fig. 4.40). The convection cell in the lower aquifer is still distinct and the flow directions are maintained in most of the model domain. The flow direction is alternating on a small scale as a consequence of the equilibration of the fingering structures, which developed in the early stage of the sea water inundation.

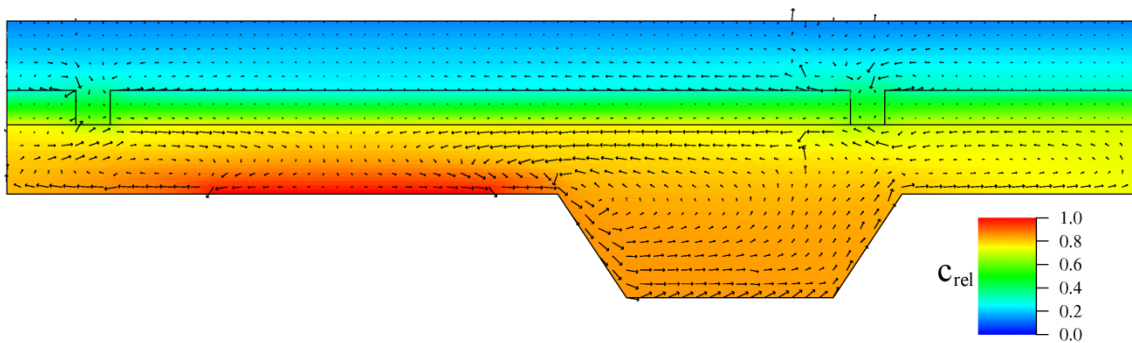


Fig. 4.40 Relative salt concentrations and velocity field after a sea water inundation for steady-state conditions at 600,000 a model time /FLU 09/

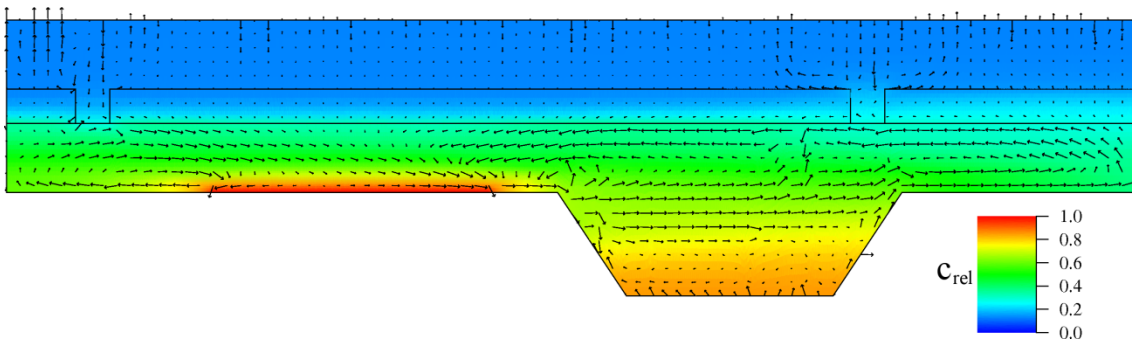


Fig. 4.41 Relative salt concentrations and velocity field after a sea water inundation of 15,000 a (31,500 a model time)

Permafrost conditions were modeled by /FLU 09/ for the same time frame as the sea water inundation (600,000 a model time, Fig. 4.42). The salt concentrations are in a quasi steady-state by then. After 10,000 years already, the model shows a quasi steady-state flow field. Highest flow velocities occur in the northern part of the lower aquifer, where the high inflow of glacial meltwater occurs. Part of this inflow is drained to the surface at the northern hydraulic window and the talik below the river Elbe. The

southbound groundwater flow is partly reversed in the area of the contact area to the salt dome. Despite the high inflow from the north, this back flow results from the dissolution of salt and the higher density of the groundwater, thus the convection cell between the contact to the salt dome and the rim syncline is maintained. South of the salt dome, the flow is solely directed southward but with a clearly reduced flow velocity. The inflow of glacial meltwater into the lower aquifer results in a significant reduction of the salt concentration in the northwestern rim syncline to $c_{rel} = 0.1$ to $c_{rel} = 0.3$.

The salt concentration also decreases in all other areas of the model domain. In the permafrost regions, diffusion processes prevail so that steady-state salt concentrations are only reached very slowly in dependence on the initial conditions. The higher the initial concentration, the later the steady-state salt concentration is reached. At the present state, fresh water conditions dominated in the north and south of the upper aquifer with higher salt concentrations up to $c_{rel} = 0.07$ in the center. Steady-state salt concentrations are reached in the northern talik after about 90,000 a. Due to the low permeability in the permafrost regions, steady-state conditions are not reached in these areas until the end of the simulation.

Main features of the simulations for the permafrost climate state by /FLU 09/ are the high velocities in the lower aquifer, the slow transport by diffusion in the frozen zones of the upper aquifer and the strongly reduced salt concentrations in the entire model domain, in particular in the northwestern rim syncline.

The potential future sequence of permafrost growth and decay is a composite of climate states with and without permafrost with a thickness between 0 m and 150 m, which is either modeled as a set of discrete climate states or as a transient evolution. Regarding the discrete climate states, two different model assumptions were realized. During the times with a permafrost thickness of 50 m, the lateral inflow from the north is either given as a boundary condition for the lower aquifer only or defined for the lower aquifer and the lower part of the upper aquifer. Results for all three realizations showed little differences in the salt concentration distribution and flow field. Only the results for the flow simulation with a stepwise definition of the permafrost thickness and of the meltwater inflow, assuming an inflow into the lower aquifer only, are described here. Additionally, this simulation was selected as a basis for the transport simulations.

At the end of the simulation at 251,500 a (Fig. 4.43), the salt concentration distribution in the model area is similar to the concentration at the end of the permafrost simulation

by /FLU 09/. Higher salt concentrations remain in the northwestern rim syncline with values between $c_{rel} = 0.3$ to $c_{rel} = 0.4$ and south of the contact to the salt dome. The permafrost regions in the upper aquifer show a salt concentration mainly below to $c_{rel} = 0.01$, while in the area of the northern talik it is slightly higher with values up to $c_{rel} = 0.05$. The flow field is similar to the flow field of the present state (Fig. 4.39) concerning the flow direction and flow velocity due to the fact that present boundary conditions were applied for the last 10,000 a model time.

During the sequence of different permafrost climate states in alternation with the terrestrial climate, which each only last several thousand years, the hydrogeological system responds quickly to the changing boundary conditions.

After the sea water inundation at 31,500 a until the first permafrost occurrence in the upper aquifer the salt concentration decreases continuously. Assuming permafrost conditions with a thickness of 50 m (Fig. 4.44), a large part of the meltwater inflow can be drained through the northern hydraulic window and through the aquitard. Additionally, surface water infiltrates through the taliki and sinks down into the lower aquifer, especially through the southern hydraulic window. Other than in the simulations by /FLU 09/ the groundwater flow direction south of the contact to the salt dome is not solely directed to the south. Flow directions in the center and northern part of the lower aquifer are mainly in good agreement with those during the constant permafrost conditions (Fig. 4.42). The salt concentration distribution is similar to that at the end of the model simulation (Fig. 4.43).

For a permafrost thicknesses of 100 m, a lower inflow of glacial meltwater is assumed than for the simulations by /FLU 09/. The maximum inflow, which was defined for the former model runs is now correlated to a permafrost thickness of 150 m, resulting in a smaller inflow for the permafrost thickness of 100 m. Nevertheless, the flow field is very similar to the flow field given by /FLU 09/. The upper aquifer is frozen in the entire depth except in the taliki preventing advective groundwater flow. The salt concentration distribution also is very similar, but slightly higher for the new simulations, especially in the northwestern rim syncline. Here, a larger volume of glacial meltwater was able to lower the salt concentration during a longer model time in the former simulations. The same holds for the salt concentration in the lower aquifer between the contact to the salt dome and the southern model boundary.

As expected, the results for a permafrost thickness of 150 m do not differ much from those for a permafrost thickness of 150 m (Fig. 4.45). The aquitard shows a small permeability during the terrestrial, temperate climate, thus freezing and thawing of the aquitard has almost no influence on the flow field. The higher inflow into the lower aquifer leads to reduced salt concentrations in the northwestern rim syncline, but not in the southern part of the lower aquifer.

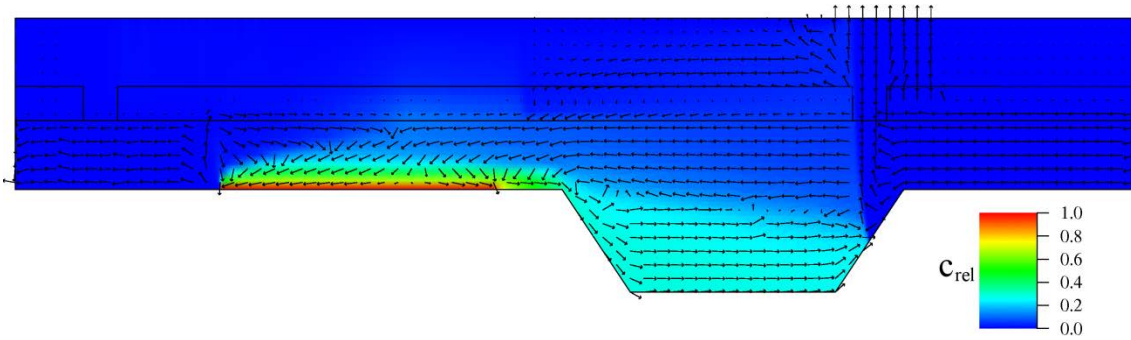


Fig. 4.42 Relative salt concentrations and velocity field after permafrost conditions for steady-state conditions at 600,000 a model time /FLU 09/

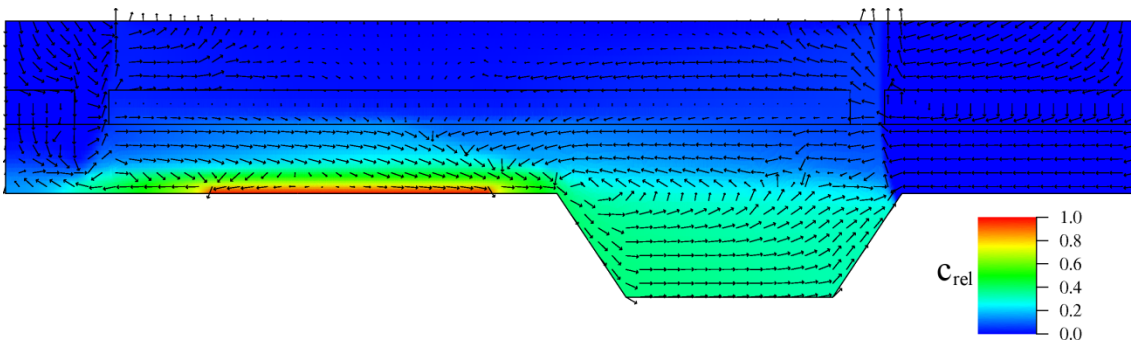


Fig. 4.43 Relative salt concentrations and velocity field at the end of the second cycle at 251,500 a model time

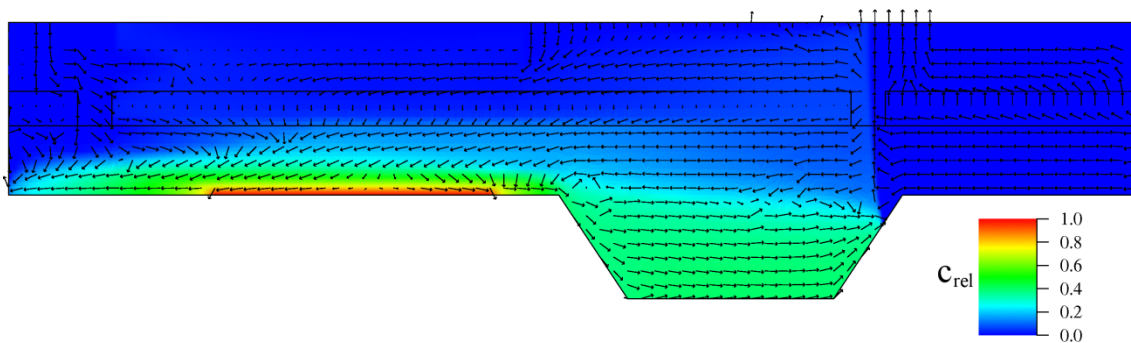


Fig. 4.44 Relative salt concentrations and velocity field in the middle of a period with 50 m permafrost thickness at 146,500 a model time

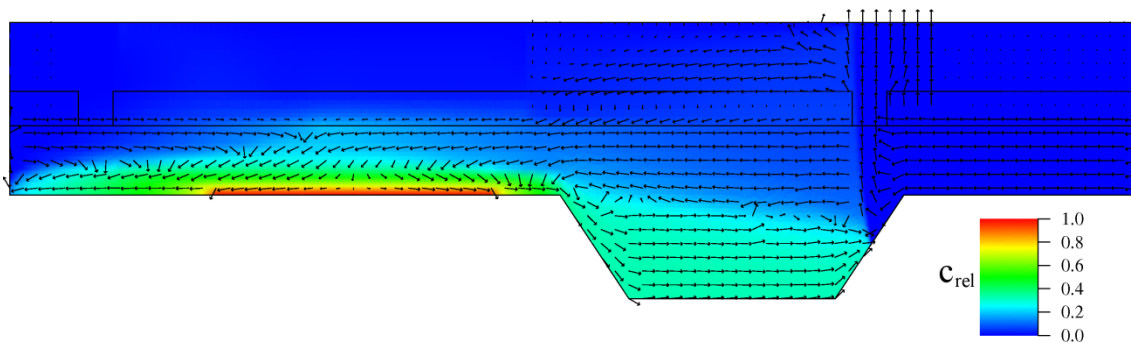


Fig. 4.45 Relative salt concentrations and velocity field at the end of a period with 150 m permafrost thickness at 240,500 a model time

Apart from modelling the permafrost and the sea water inundation climate states /FLU 09/ conducted simulations for a possible future constant climate state. Therefore all boundary conditions as defined for the present state were maintained and the model was run until reaching the steady-state after ca. 300,000 a. The results of the flow simulations conducted in this study are in good agreement with the results of the constant climate state as modeled by /FLU 09/. Therefore the consideration of different climate states within a realistic sequence of glacial cycles in flow simulations is not necessarily important for future climatic evolutions as presented here. Nevertheless, this may be of greater importance for other climate states and transitions.

Based on the flow field for the present state and on the steady-state flow field for the permafrost climate state /FLU 09/ ran transport simulations for a model time of 10^6 a. In order to compare the model results of this study to those results by /FLU 09/, the concentration distributions of the different radionuclides are compared at the same model time of 251,500 a.

According to the flow direction of the present state (Fig. 4.39), Cs-135 and the other considered radionuclides are transported within the lower aquifer to the north and into the northwestern rim syncline (Fig. 4.47). A second transport path is directed through the aquitard into the upper aquifer, where Cs-135 reaches the surface after ca. 156,000 a. The aquitard shows a relatively high sorption coefficient, thus the transport through the aquitard is strongly retarded. Cs-135 does not reach the northern hydraulic window after 251,500 a model time (Fig. 4.46).

C-14 has the shortest half-life of the considered radionuclides and a very low sorption coefficient. Thus it has the lowest concentration in the model area after 251,500 a model time (Fig. 4.47). One transport pathway to the surface is through the aquifer above the contact to the salt dome. In contrast to Cs-135, C-14 is also transported through the northern hydraulic window into the upper aquifer and from there, according to the flow field, to the south. At 251,500 a model time, the centre of the model domain C-14 can be observed in the entire centre of the model domain.

The sorption of I-129 is even weaker in the aquifers than the sorption of C-14, whereas the half-life is significantly higher. After 1,000 a model time, I-129 has reached the model surface. The two major transport pathways are the same as for C-14, namely through the aquitard and through the northern hydraulic window. After 251,500 a model

time, the distribution of I-129 is similar to the distribution of C-14, while its concentration is considerably higher (Fig. 4.48).

U-238 has the longest half-life of the considered radionuclides. With a low sorption in the lower aquifer, the transport to the north is facilitated. From the northern hydraulic window, it is transported to the south in the upper aquifer. Here, the transport through the aquitard to the surface is of less importance due to the high sorption capacity of the aquitard. Highest U-238 concentrations at the model surface at 251,500 a model time can be observed above the northern hydraulic window (Fig. 4.49). The daughter nuclides of U-238 only occur in the model domain due to radioactive decay (not depicted). Therefore the daughter nuclides show a similar distribution to that of U-238 but with lower concentrations. Th-230 notably accumulates at the interface of the lower aquifer and the aquitard and shows higher concentrations than in the neighbouring sediments. Compared to Th-230 the sorption of Ra-226 is weaker, leading to a facilitated transport and elevated Ra-226 concentrations in the upper aquifer.

Zr-93 shows a very strong sorption capacity, thus it only reaches the interface between the aquitard and the upper aquifer after 251,000 a model time (not depicted). Also the lateral transport is strongly retarded. Zr-93 does not even reach the north-western rim syncline within the simulation time.

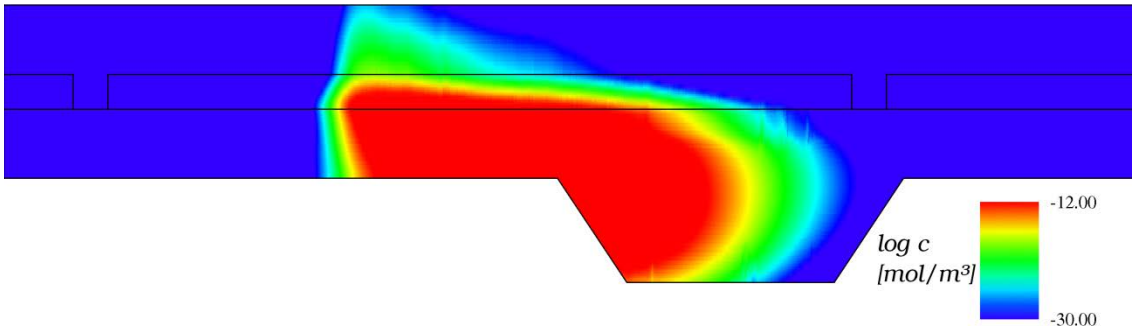


Fig. 4.46 Logarithmic plot of the Cs-135 concentration distribution at 251,500 a model time /FLU 09/, based on the present state flow field

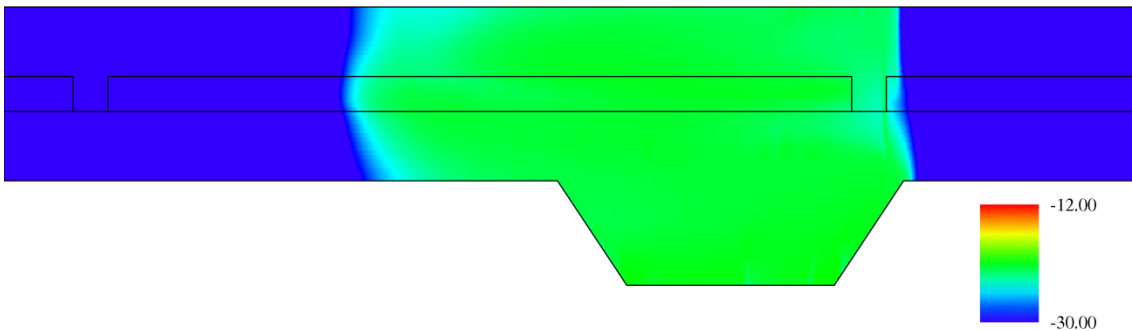


Fig. 4.47 Logarithmic plot of the C-14 concentration distribution at 251,500 a model time /FLU 09/, based on the present state flow field

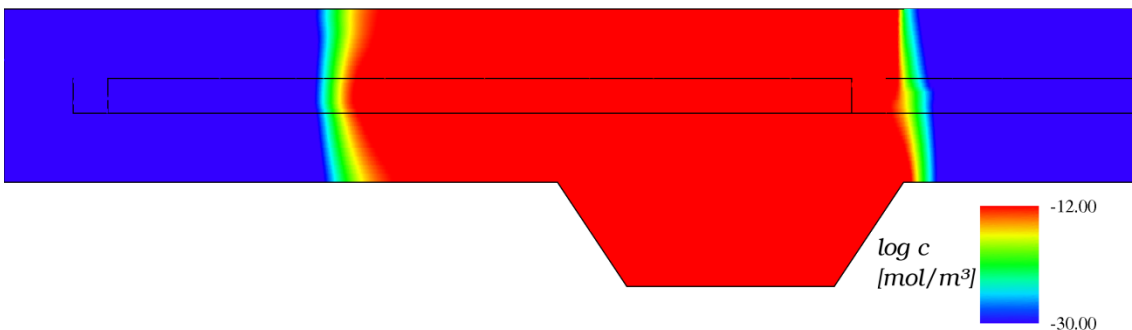


Fig. 4.48 Logarithmic plot of the I-129 concentration distribution at 251,500 a model time /FLU 09/, based on the present state flow field

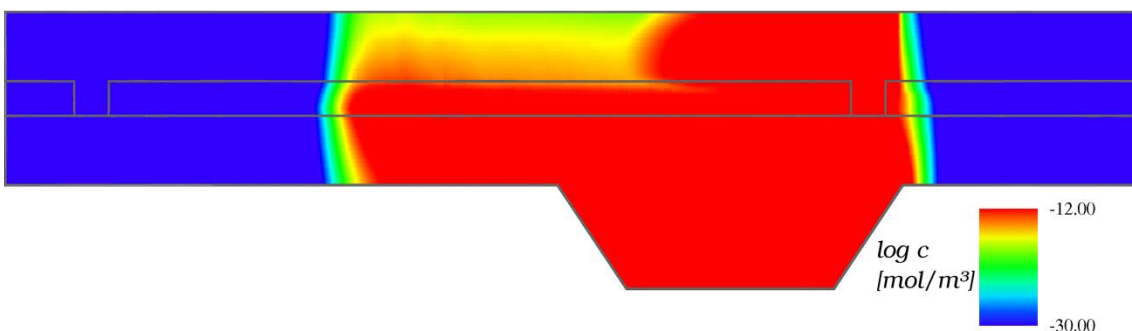


Fig. 4.49 Logarithmic plot of the U-238 concentration distribution at 251,500 a model time /FLU 09/, based on the present state flow field

For the permafrost climate state, the upper aquifer is defined as a fresh water unit, which leads to an elevated sorption of the radionuclides on the sediments. The aquitard also showed freshwater conditions in the simulations by /FLU 09/, while in this study the flow simulations resulted in salt water conditions in the aquitard (chapter 4.6.3.2). Therefore, radionuclide transport through the aquitard is expected to be facilitated in the present simulations compared to those by /FLU 09/.

From the contact to the salt dome the groundwater flow in the lower aquifer is directed to the south and shows a high flow velocity. Accordingly, radionuclides are generally transported to the south and out of the model domain within in the lower aquifer. Frozen zones in the upper aquifer show a low permeability and are more or less impermeable to advective transport, thus diffusion is the driving force of the radionuclide transport in these areas. The southern hydraulic window and the southern talik serves as the main transport pathway to the model surface.

The strongly sorbing Cs-135 completely remains within the model domain during the 251,500 a model time (Fig. 4.50). As expected it is transported within the lower aquifer to the south, but does not reach the southern model boundary. Cs-135 can be observed within the aquitard above the area of distribution in the lower aquifer, but the low permeability of the permafrost areas and the higher sorption coefficient in the upper aquifer, caused by the fresh water conditions, prevent Cs-135 from migrating into the upper aquifer.

C-14 with its low sorption coefficient in all three hydrogeologic units shows a broader concentration distribution (Fig. 4.51), even in the permafrost areas in the upper aquifer. Predominant pathways to the surface are the southern hydraulic window and talik and the permafrost areas directly above the source location. The highest amount of C-14 is transported to the southern boundary of the lower aquifer according to the dominant transport pathway of Cs-135. After 251,500 a model time, a strongly reduced concentration of C-14 remains in the model domain, with is a result of the lower sorption coefficient as well as the short half-live of C-14.

I-129 shows the broadest concentration distribution after 251,500 a model time. In the southern part of the model domain, the distribution is similar to that of C-14, because of their similar sorption coefficients, but I-129 has a higher concentration, which results from the longer half-live. As the only one of the considered radionuclides, I-129 is transported to the north against the groundwater flow direction. In the area of the

northern hydraulic window, where a certain amount of groundwater is discharged to the surface, I-129 reaches the surface and is transported within the upper aquifer to the south.

U-238 shows a similar distribution after 251,500 a model time (Fig. 4.53), but in contrast to Cs-135 it reaches the model surface and the southern model boundary and is therefore transported out of the model domain. The most important pathway to the surface is the southern hydraulic window and the southern talik. A certain amount of U-238 is transported by diffusion against the flow direction to the north, but to a minor degree than I-129, and it does not reach the north-western rim syncline after 251,500 a.

A similar distribution is observed for the considered daughter nuclides of U-238, again with lower concentrations. Th-230 is strongly sorbed in the aquitard, hence its highest concentration is found at the interface of the lower aquifer and the aquitard. Because Ra-226 originates from radioactive decay of the sorbed and the dissolved fraction of Th-230, it shows a slightly higher concentration than Th-230 mainly in the lower aquifer.

As a consequence of its high sorption coefficients Zr-93 stays within the vicinity of the contact to the salt dome, where the source is located. After 251,500 a it reaches the aquitard and approaches the interface to the upper aquifer. The lateral transport within the lower aquifer to the south is restricted to a range of 800 m only.

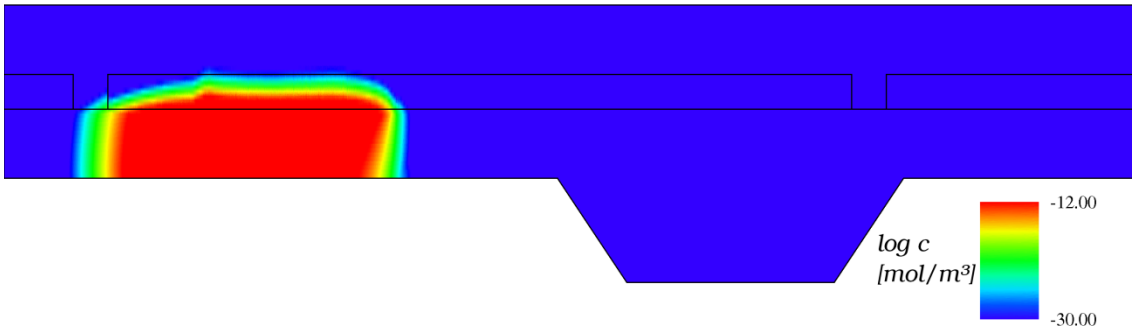


Fig. 4.50 Logarithmic plot of the Cs-135 concentration distribution at 251,500 a model time /FLU 09/, based on the steady-state permafrost flow field

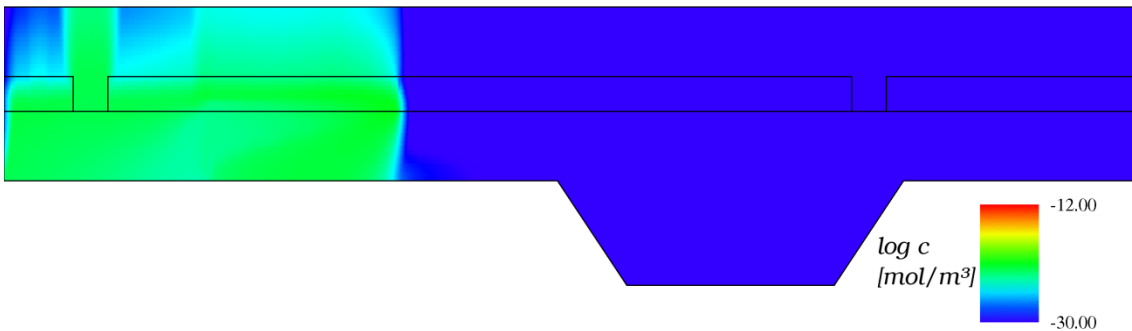


Fig. 4.51 Logarithmic plot of the C-14 concentration distribution at 251,500 a model time /FLU 09/, based on the steady-state permafrost flow field

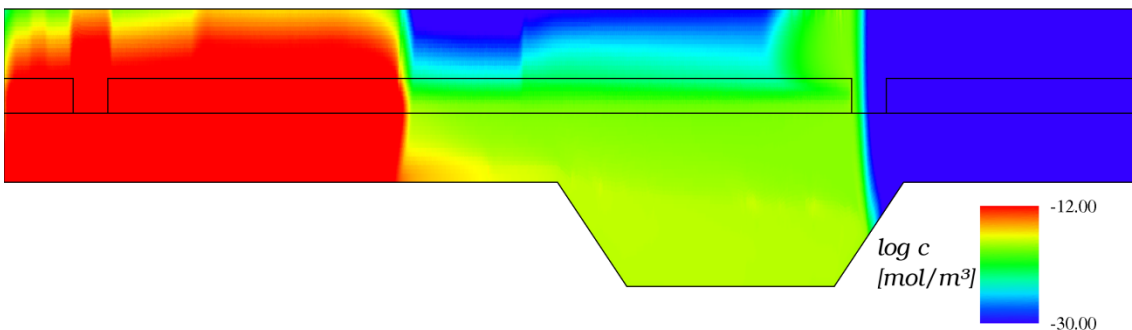


Fig. 4.52 Logarithmic plot of the I-129 concentration distribution at 251,500 a model time /FLU 09/, based on the steady-state permafrost flow field

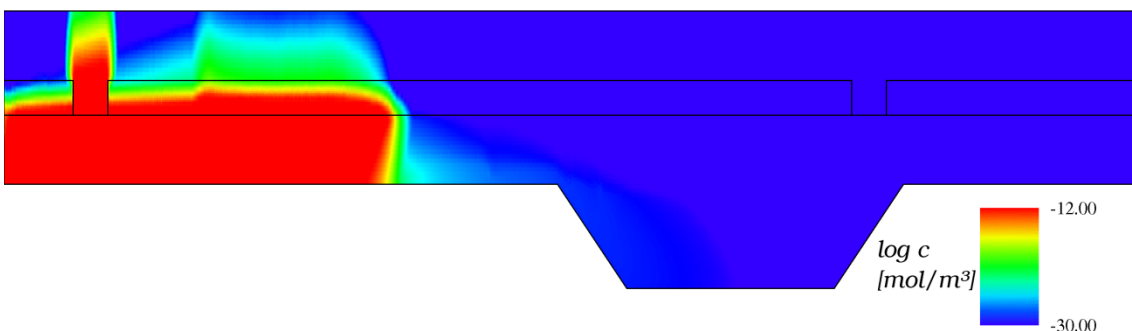


Fig. 4.53 Logarithmic plot of the U-238 concentration distribution at 251,500 a model time /FLU 09/, based on the steady-state permafrost flow field

Regarding a more realistic sequence of climate states and transitions with a sea water inundation and a sequence of permafrost growth and decay, the preferred pathway for radionuclide transport is a set of the pathways resulting from each single climate state. For the present state the main pathway led through the aquitard and through the lower aquifer to the northern hydraulic window. For the permafrost conditions it led to the southern boundary of the lower aquifer. For the sea water inundation, the radial transport from the source resulted in a transport pathway vertically through the aquitard. In this transient case, most of the radionuclides are transported via all three major transport pathways. The flow direction and velocity as well as the transport of salt are transient and a result of the changing boundary conditions. As stated above, the flow field responds to climate changes fairly quickly. Resulting transport patterns and radionuclide distributions are therefore a result of the complex flow field and the applied boundary conditions.

During the sea water inundation, the transport of the radionuclides is dominated by low advective flow and radial diffusive transport. During the glacial cycles, the flow direction in the lower aquitard reverses frequently. The resulting distribution of Cs-135 (see Fig. 4.54) is similar to the distribution after a long-lasting sea water inundation /FLU 09/. Cs-135 is transported more or less radially from the source (note again that the figures are all vertically exaggerated by a factor of 10). The main transport pathways are through the aquitard above the contact to the salt dome and through the southern hydraulic window. During the times of present conditions, the upper aquifer is shows its original permeability, allowing for groundwater flow and radionuclide transport. During periods with permafrost in the upper aquifer, Cs-135 remains in these areas and starts migrating again after permafrost decay.

Transport patterns of C-14 are more complex (Fig. 4.55). The first breakthrough to the upper aquifer occurs above the contact to the salt dome. Shortly after the sea water inundation has ended, C-14 reaches the northern hydraulic window and the model surface. At the end of the first permafrost period at ca. 85,000 a, C-14 is observed to reach the surface above the southern hydraulic window, too. At ca. 100,000 a, the C-14 concentration in the center of the upper aquifer is remarkably reduced by radioactive decay, while it still increases in the area of the northern and southern hydraulic window. Especially in the area of the northern hydraulic window, the effect of the changing boundary conditions is visible. During permafrost conditions, the high inflow of glacial meltwater lowers the C-14 concentration within the hydraulic window, but leaving a higher concentration in the upper aquifer north of the hydraulic window. During temper-

ate, terrestrial conditions, this effect is evened out due to the decreasing inflow into the northern aquifer and the recurring groundwater recharge. The periodically reversing flow direction in the lower aquifer effects the transport in the lower aquifer in a similar way.

As discussed above, the sorption coefficient of I-129 is similar to that of C-14 and therefore the transport pathways and distribution of both radionuclides are similar. Due to the longer half-life of I-129, it shows a higher concentration in the model area at the end of the simulation (Fig. 4.56).

The existence of the three transport pathways in this simulation is clearly visible for the transport of U-238 (Fig. 4.57). While in the former simulations the transport was either bound to the north (and through the aquitard) or to the south, the concentration distribution in the upper aquifer is now a result of all formerly identified transport pathways. The influence of the alternating boundary conditions, as described for C-14, is also being observed for U-238 and all the considered daughter nuclides. After 251,500 a highest concentrations of Th-230 are found in the aquitard. An elevated concentration of Ra-226 remains in the lower aquifer.

Considering the high sorption coefficients of Zr-93 it could be proved that the impact of changing climatic conditions and applying a more realistic set of climate transitions on the transport of Zr-93 is almost insignificant. At the end of the simulation, it has reached the upper aquifer and has a maximum lateral distribution within the lower aquifer of ca. 1,000 m.

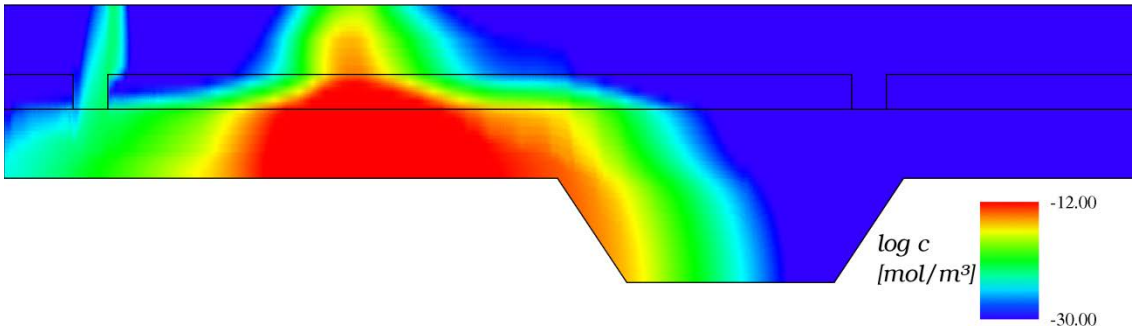


Fig. 4.54 Logarithmic plot of the Cs-135 concentration distribution at the end of the second cycle at 251,500 a model time

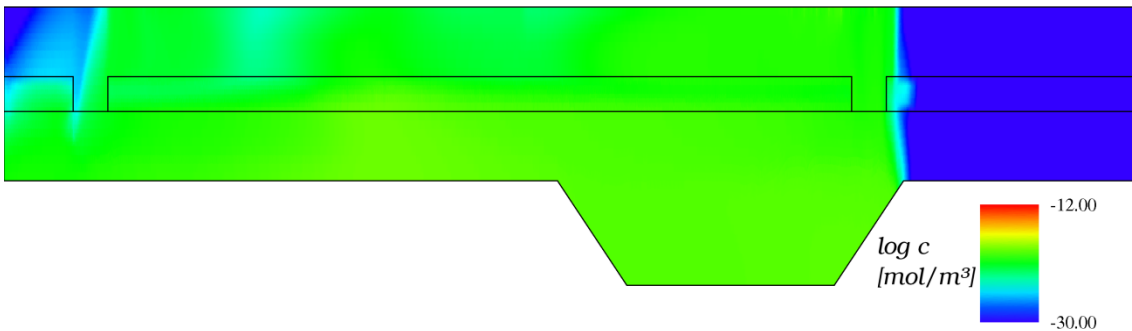


Fig. 4.55 Logarithmic plot of the C-14 concentration distribution at the end of the second cycle at 251,500 a model time

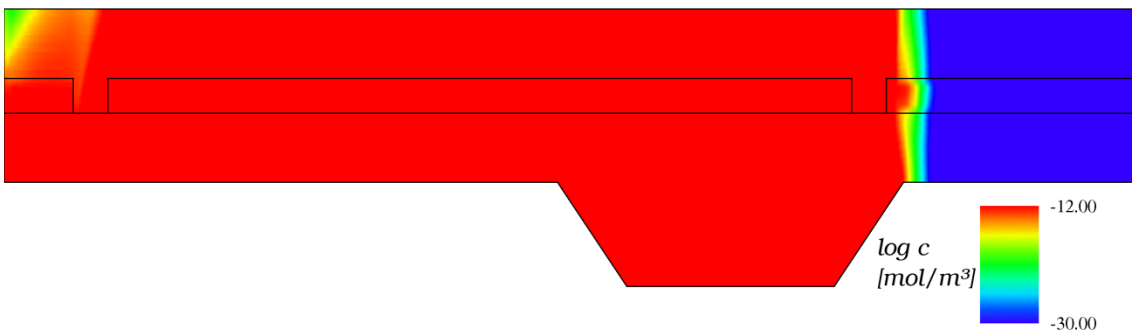


Fig. 4.56 Logarithmic plot of the I-129 concentration distribution at the end of the second cycle at 251,500 a model time

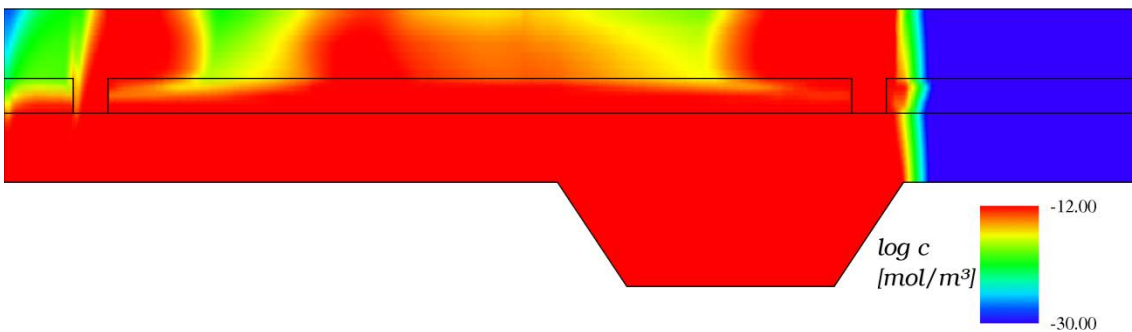


Fig. 4.57 Logarithmic plot of the U-238 concentration distribution at the end of the second cycle at 251,500 a model time

4.6.4 Summary

In this study the impact of transient flow conditions caused by long-term climate changes on radionuclide transport in the far field of a repository is addressed for the first time. Temporal changes of glacials and periglacials derived from investigations in Sweden and Finland serve as a basis for the future climate cycles considered here. The major results are as follows. The results of the flow simulations show that the flow field and the salt water distribution at the endpoint in time of 251,500 years are in good agreement with those calculated for a constant climate by /FLU 09/. This shows that the system responds quickly to changing boundary conditions of the altered climate states of a glacial cycle. Further sea water inundation has only low influence on groundwater flow and transport of salt.

However, regarding the radionuclide transport calculations significant differences between transient and constant flow modelling are recognized. It becomes obvious that transport patterns are a set of the three different flow features of the different unique climate states, e. g. a high flow velocity from North to South in the lower and a partly low permeable upper aquifer during strong permafrost compared to a flow from South to North in the lower and quite high flow in the permeable upper aquifer at present climate. The strongest impact is seen for weakly sorbing radionuclides (such as C-14 and I-129), and the lowest impact for strongly sorbing radionuclides, like Zr-93. This is in agreement with observations for constant climates, as stated in /FLU 09/. In general the calculation shows that the impact of climate transitions on flow and radionuclide transport in the overburden of a repository host rock is strong and need to be addressed by transient model calculations in long-term safety assessment.

4.7 Impact of climate conditions on biosphere modelling

One important aspect of climate changes for the long-term safety assessment of radioactive waste repositories is its impact on the surface environment and therewith on the exposure pathways for humans in the future, which are dependent on the environmental characteristics mentioned. This topic needs to be addressed in a safety case for radioactive waste repositories and has been dealt with in international projects like BIOMASS /IAE 03b/, BIOMOSA /OLY 05/ and particularly in BIOCLIM /BIO 04/. The topic of BIOMASS describes the development of reference biosphere systems according to a fixed methodology. The methodology begins with defining the assessment context and the identification and justification of the biosphere systems. Those biosphere systems are then described in further detail and potentially exposed groups are considered. Finally the model is developed, calculations are done and further iterations can be used to refine the model. The international project BIOMOSA considered the application of the BIOMASS methodology at specific sites, as compared to a generic methodology application. In the BIOCLIM project the investigation of long-term climate changes and their impact on biosphere modelling was addressed.

The work presented here is a continuation of the study described in /NOS 08/, where six different climate states have been considered. The most relevant results are described in the following; a more detailed description can be found in /SEM 12/. In a first step a critical justification of the climate states covering the potential future climate evolution in Northern Germany is performed. As a result three additional climate states are selected to comprehensively cover colder and warmer climates with different amounts of precipitation, which might develop in the far future. For each climate state a representative analogue station, where the respective climate occurs today (in the following called reference station), is selected. The different climate states and the corresponding climate stations are shown in Fig. 4.58 and Tab. 4.9.

In order to quantify the impacts generic biosphere models for each climate station are developed and biosphere dose conversion factors (BDCFs) are calculated. The approach considers a normalised radionuclide concentration in a surface-near aquifer, from where the radionuclides enter the biosphere. There are two scenarios assumed in the model used in this work: ground water raises to the soils used for agriculture (RGW scenario) or the soils are contaminated by irrigation with ground water (well scenario).

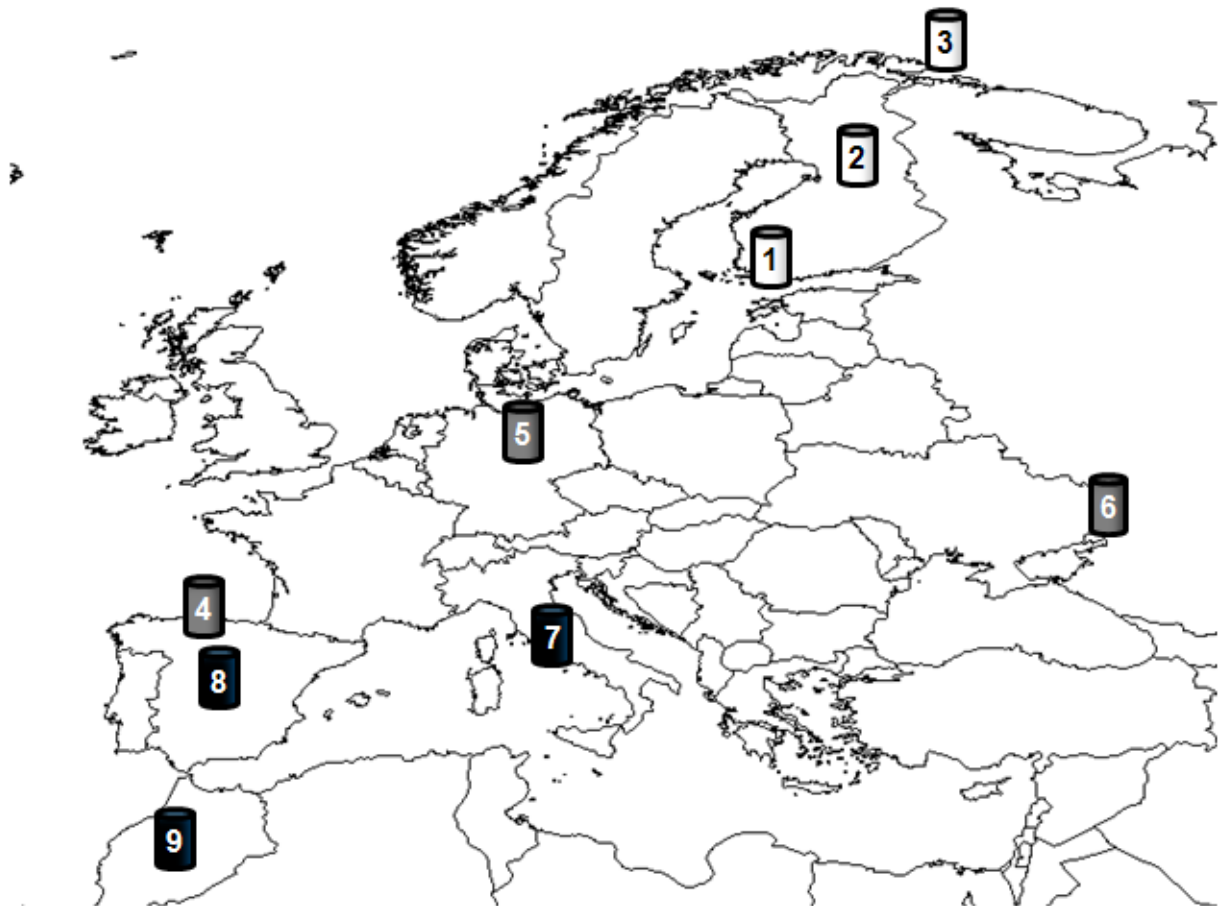


Fig. 4.58 Selection of discrete reference climate regions

Grey depicts temperate, black subtropical and white boreal climate conditions.

Tab. 4.9 Köppen/Geiger climate classification and climate data for the reference climate regions

Reference climate region	Number in Map	Köppen/Geiger classification	Annual average temperature [°C]	Annual precipitation [mm]
Turku	1	Dfb boreal	4.8	576
Sodankyla	2	Dfc boreal	-0.4	508
Vardo	3	ET boreal	1.6	544
Santander	4	Cfb temperate	13.9	1198
Magdeburg	5	Cfb temperate	9.2	513
Rostov	6	Dfa temperate	8.4	483
Rome	7	Csa subtropical	15.6	874
Valladolid	8	Csb subtropical	12.1	364
Marrakesh	9	BS subtropical	19.9	241

The contribution of different food types to the ingestion BDCF are shown in Fig. 4.59 for the Rome and the Magdeburg reference climate region. These climate regions have been selected since those two reference climate regions are used for modelling the impact of climate transitions. The most marked difference is the increased contribution of the drinking water to the ingestion BDCF at the Magdeburg compared to the Rome reference climate region. This is an effect of the higher radionuclide concentration in plant and animal food at the Rome reference climate region, resulting from the higher activity concentration in soil due to higher irrigation rates. In addition to this different consumption habits influence the results.

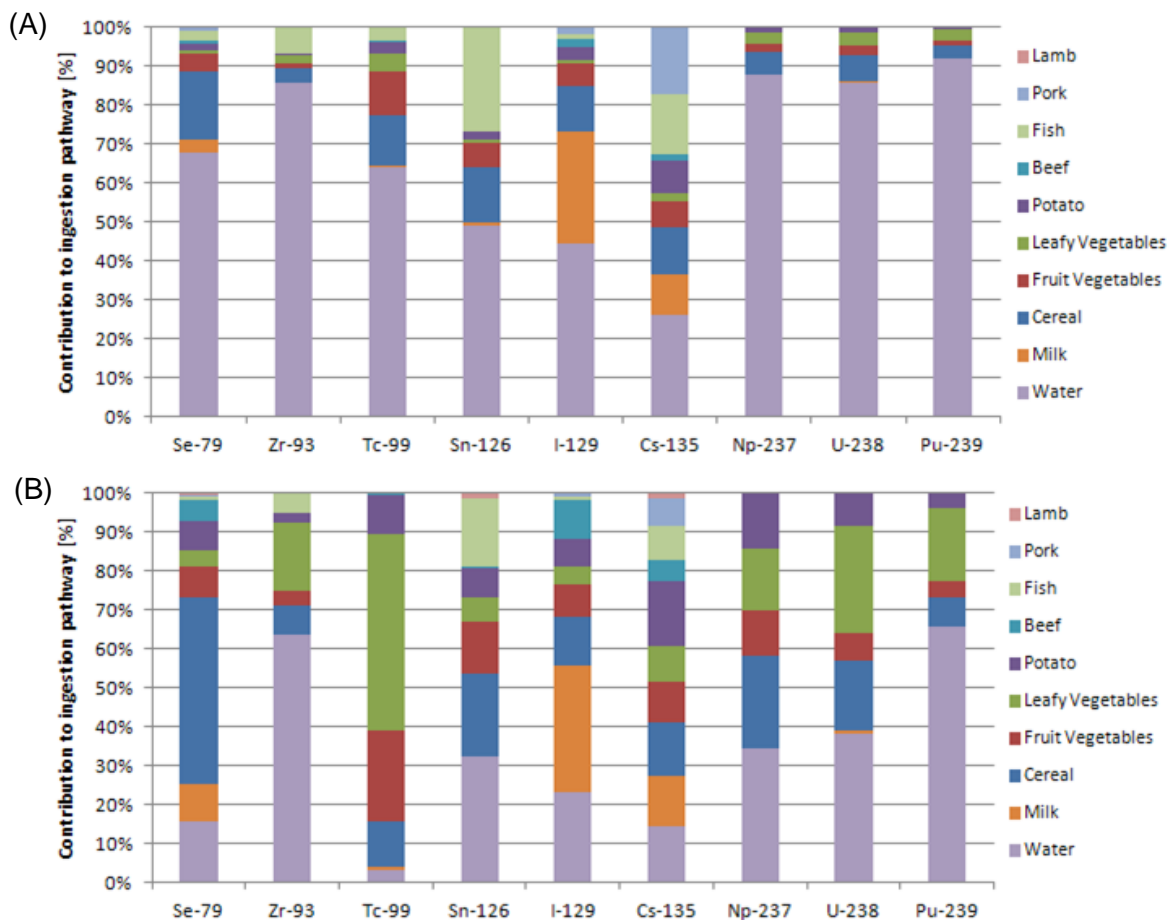


Fig. 4.59 Comparison of the contribution of food types on the ingestion BDCF of selected radionuclides for (A) the Magdeburg and (B) Rome reference climate region and sand soil

In Tab. 4.10 the total BDCF for the nine reference climate regions are shown for the “Well” scenario for sand soil. The parameters used for the model, including the transfer factors soil to plant, are the same as in /NOS 08/ for the sandy soil. For organic soil the transfer factors soil to plant and migration factors calculated from distribution coeffi-

cients from /IAE 10/ were used. The lowest BDCF for sandy soil can always be found in the Vardo reference climate region. Since no agriculture is done in this permafrost reference region, the soil is not irrigated with contaminated groundwater, i.e. exposure only happens by consumption of contaminated drinking water and fish. The highest BDCF for 12 of 17 radionuclides can be found in the Valladolid reference climate region. This region has the highest irrigation amounts compared to the other reference climate region. At the Marrakesh reference climate region the annual precipitation is lower than at Valladolid, but since agriculture is done during the cooler and more humid autumn, winter and spring months the irrigation amounts are lower than in Valladolid. The high BDCF for Cs-135 at the Turku reference climate region can be explained by the assumed high transfer factor for caesium in boreal climates /NOS08/. Since Sn-126 and Zr-93 are highly accumulated in fish compared to crops in sand soil, both radionuclides also have their maximum BDCF at Turku, since a large amount of fish is consumed at this reference climate region. Maximum BDCFs for Cl-36 and Se-79 are found for the Marrakesh reference climate region, due to high irrigation rates and consumption habits favouring food types with high chlorine and selenium accumulation (e.g. cereals).

The ratios between maximum and minimum values of a radionuclide specific BDCF for the nine reference climate regions and sand soil ranges from 1.9 for Th-230 and Pu-239, to 81.4 for Nb-94 (Tab. 4.10). Since the amount of consumed drinking water does not change between the different climate regions, low ratios are found for radionuclides where drinking water is the main contributor to the ingestion pathway to the total BDCF (see Fig. 4.59). The BDCF for Nb-94 is determined predominantly by the external exposure and the external exposure is determined by the radionuclide accumulation in soil. Due to this, the BDCF for Nb-94 is correlated to different average irrigation amounts at the reference climate regions and the migration of Nb-94 in soil showing highest values for climate states with highest irrigation rates.

The same calculations have been performed for organic soil. In general similar tendencies are observed. However, since the activity concentrations in organic soil and in plants grown in organic soil are usually higher than in sand soil, the contributions of ingestion of food, external exposure and inhalation are higher than to the contribution of ingested drinking water compared to contributions in sand soil scenarios. Due to this, variations in consumption habits of food have a higher impact on the variations of the BDCF, resulting in more extreme variations of the BDCF at the different reference climate regions. This is exemplarily illustrated by the maximum to minimum ratio for Nb-94, which is again the highest but with a much higher value of 2490 for the organic soil.

Tab. 4.10 BDCF for reference regions for the “Well” scenario and organic soil. The BDCF are in Sv/a per 1 Bq/l in near surface ground water

Climate	BS	Csa	Csb	Cfb	Cfb	Dfa	Dfb	Dfc	ET	Min	Max	Ratio Max/Min
Reference region	Marrakesh	Rome	Valladolid	Santander	Magdeburg	Rostov	Turku	Sodankyla	Vardo			
Cl-36	4.4E-05	6.3E-06	7.0E-06	1.5E-06	2.2E-06	5.8E-06	1.8E-06	1.5E-06	8.1E-07	8.1E-07	4.4E-05	53.6
Ni-59	2.4E-07	2.7E-07	3.2E-07	9.1E-08	1.1E-07	2.4E-07	7.8E-08	6.4E-08	4.8E-08	4.8E-08	3.2E-07	6.8
Se-79	1.9E-05	1.3E-05	1.5E-05	2.8E-06	3.1E-06	1.8E-05	3.6E-06	3.4E-06	2.2E-06	2.2E-06	1.9E-05	8.6
Zr-93	1.2E-06	1.3E-06	1.3E-06	9.4E-07	9.3E-07	1.1E-06	1.7E-06	1.7E-06	8.0E-07	8.0E-07	1.7E-06	2.2
Nb-94	7.4E-05	8.5E-05	1.0E-04	1.4E-05	2.6E-05	7.8E-05	1.0E-05	5.1E-06	1.2E-06	1.2E-06	1.0E-04	81.4
Tc-99	1.6E-05	1.4E-05	1.6E-05	7.0E-07	7.2E-07	6.9E-06	8.7E-07	8.4E-07	4.7E-07	4.7E-07	1.6E-05	34.9
Pd-107	1.0E-07	1.1E-07	1.4E-07	5.1E-08	5.9E-08	1.0E-07	4.4E-08	3.7E-08	2.7E-08	2.7E-08	1.4E-07	5.1
Sn-126	2.3E-04	2.5E-04	2.9E-04	1.1E-04	1.3E-04	2.3E-04	4.7E-04	4.5E-04	5.2E-05	5.2E-05	4.7E-04	8.9
I-129	3.4E-04	3.4E-04	3.7E-04	1.4E-04	1.8E-04	3.1E-04	1.8E-04	1.5E-04	8.9E-05	8.9E-05	3.7E-04	4.1
Cs-135	1.0E-05	9.8E-06	1.1E-05	4.3E-06	5.5E-06	8.9E-06	6.1E-05	3.2E-05	1.7E-06	1.7E-06	6.1E-05	36.6
Ra-226	4.3E-04	4.8E-04	5.3E-04	2.7E-04	2.8E-04	3.9E-04	2.6E-04	2.4E-04	2.1E-04	2.1E-04	5.3E-04	2.5
Th-230	3.8E-04	4.0E-04	4.3E-04	2.6E-04	2.6E-04	3.4E-04	2.5E-04	2.4E-04	2.3E-04	2.3E-04	4.3E-04	1.9
Pa-231	1.2E-03	1.2E-03	1.3E-03	5.9E-04	6.0E-04	9.9E-04	5.6E-04	5.4E-04	5.2E-04	5.2E-04	1.3E-03	2.4
Np-237	2.1E-04	2.6E-04	2.9E-04	9.3E-05	9.5E-05	2.0E-04	8.9E-05	8.5E-05	8.0E-05	8.0E-05	2.9E-04	3.6
U-238	7.2E-05	9.5E-05	1.1E-04	4.1E-05	4.1E-05	6.9E-05	3.9E-05	3.7E-05	3.5E-05	3.5E-05	1.1E-04	3.0
Pu-239	3.2E-04	3.2E-04	3.4E-04	2.0E-04	2.0E-04	2.7E-04	2.0E-04	1.9E-04	1.8E-04	1.8E-04	3.4E-04	1.9
Am-243	2.8E-04	2.8E-04	3.0E-04	1.6E-04	1.7E-04	2.4E-04	1.7E-04	1.6E-04	1.5E-04	1.5E-04	3.0E-04	2.1

Parameters for reference biosphere models are subject to uncertainty. In order to estimate the impact of the uncertainties on the BDCFs and to identify the most relevant parameters in the second step a probabilistic uncertainty and sensitivity analysis is performed. This probabilistic analysis is restricted to Se-79, Tc-99, Cs-135, I-129, Np-237, U-238, Pu-239 and to the temperate and the Mediterranean climate states.

In order to evaluate the sensitivity of the respective parameters Spearman correlation coefficients have been calculated. The results are presented in the form of tornado charts. A value of 1 would signify a perfect monotone relation. Negative values signify a negative correlation between the parameter and the BDCF, positive values a positive correlation. Only the ten parameters with the highest absolute correlations are shown. Most parameters show a positive correlation with the BDCF. Only the migration factors in arable and pasture soil show a negative correlation, since higher migration factors result in lower radionuclide concentration in soil and thus lower BDCF.

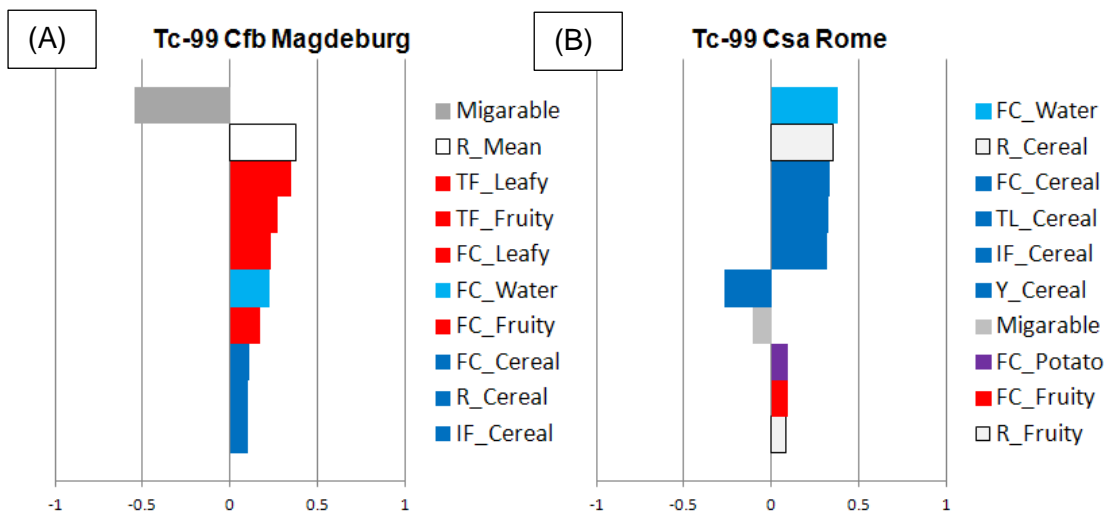


Fig. 4.60 Tornado chart for the sensitivity analysis of Tc-99 for sand soil and the (A) Magdeburg and (B) Rome reference climate region

Exemplarily the results for the sensitivity analysis for Tc-99 are shown. They indicate that the BDCF is mainly affected by parameters influencing the radionuclide activity concentration in certain food types, like leafy vegetables, fruit vegetables and cereals (Fig. 4.60). This agrees with major contributions of those food types to the ingestion pathway calculated by the deterministic model and shown in Fig. 4.59. For the two reference climate regions, the contributions of various food types are quite different, re-

sulting in quite different tornado charts. The BDCF of the deterministic model for those two reference climate regions vary by a factor of 20.

In general, the results of the sensitivity analysis agree well with the observations from the deterministic calculations, i. e. the most important exposition pathways and the respective model parameters observed in the deterministic calculations showed up as the most sensitive ones in the sensitivity analysis. A further result from uncertainty analyses is that the spread of the probabilistic BDCF distributions is in most cases larger than the differences between the deterministic BDCF of the temperate and Mediterranean reference climate regions. These results suggest that the uncertainty of the parameters may have a larger impact on calculated BDCF than parameter changes between reference climate regions.

A further important question is, whether the calculation of discrete climate states is sufficient to judge the impact of climate changes on potential radiation exposures of individuals. It is conceivable that effects or processes occurring during climate changes lead to an increased accumulation and/or release of radionuclides in the biosphere resulting in higher doses compared to that calculated for discrete climate states. In order to shed light on this question key processes are identified, which might lead to such an increased accumulation and/or release of radionuclides. After identification of such processes first modelling approaches are developed to implement the respective processes and to simulate selected examples of transient biosphere systems driven by climate changes. The most relevant processes are expected during the transition to warmer climates, particularly for redox sensitive radionuclides, which may change their chemical speciation under drier, more oxidised conditions and thereby become more available to plants. Two scenarios, drying of a lake and drying of a fen have been chosen to investigate such transition states.

In order to quantify the effects for the transition, which are a sequence of quite complex processes, we tried to keep the models as simple as possible. As the duration of the described transition processes is difficult to judge, three different time frames for the transition period are assumed in the calculations: 1, 10, and 100 years, respectively.

Fig. 4.61 shows the conceptual model presenting transition processes for redox sensitive radionuclides. Initially a lake/fen is considered, which is already dried out. The sediment of the former lake/fen has an activity concentration caused by contaminated ground water.

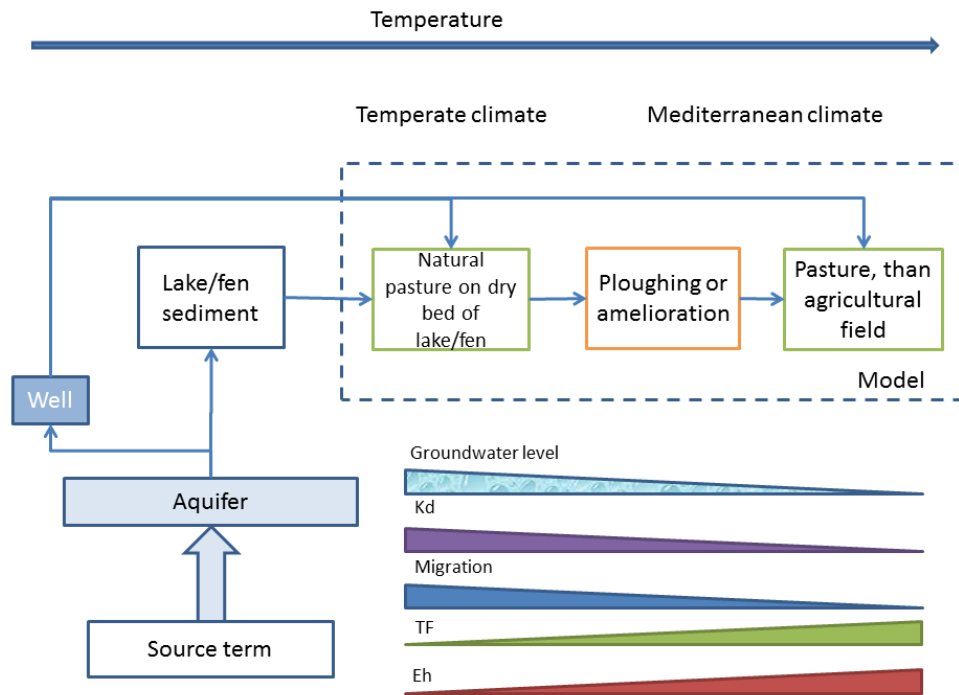


Fig. 4.61 Conceptual model for estimating the radiation exposure to man in case of agricultural use of dry lake sediment

Three stages are considered. In the first stage the radionuclide concentration of the lake sediment is in balance with the concentration in ground water, which is the only source of radionuclides and determined by the K_d -value of each radionuclide. This stage has not been modelled, instead an initial radionuclide concentration of 1000 Bq/kg in soil was assumed, which can be correlated to typical K_d -values of 1000 ml/g for many elements under reducing conditions.

In the second stage – after a period of drying out – the lake bed can be used as pasture, if the soil is still humid enough for the growth of grass and solid enough for domestic animals. Radionuclides are in reduced, immobile state corresponding to a low uptake from the soil solution into the plant (grass).

In the third stage the lake continues to dry; the moisture content falls below the wilting point. Under dry and therewith aerated conditions radionuclides become oxidised and most of them therewith more mobile. This is further facilitated by enrichment of soil with oxygen by ploughing.

From stage 2 to stage 3 the transfer factor soil-to-plant increases by one to two orders of magnitude. At the same time, the radionuclide migration in soil decreases, because

of longer half-life time of radionuclides in soil. Migration in arid, unsaturated soils is general significantly slower than in floodplain, lowland or in swamp. The parameters for diffusion and convective transfer are 4 – 5 times lower. For example, for Cs-135 the half-life time in arid soil is 55 – 143 years, for swamp meadow 15 – 21 years /SAN 96/.

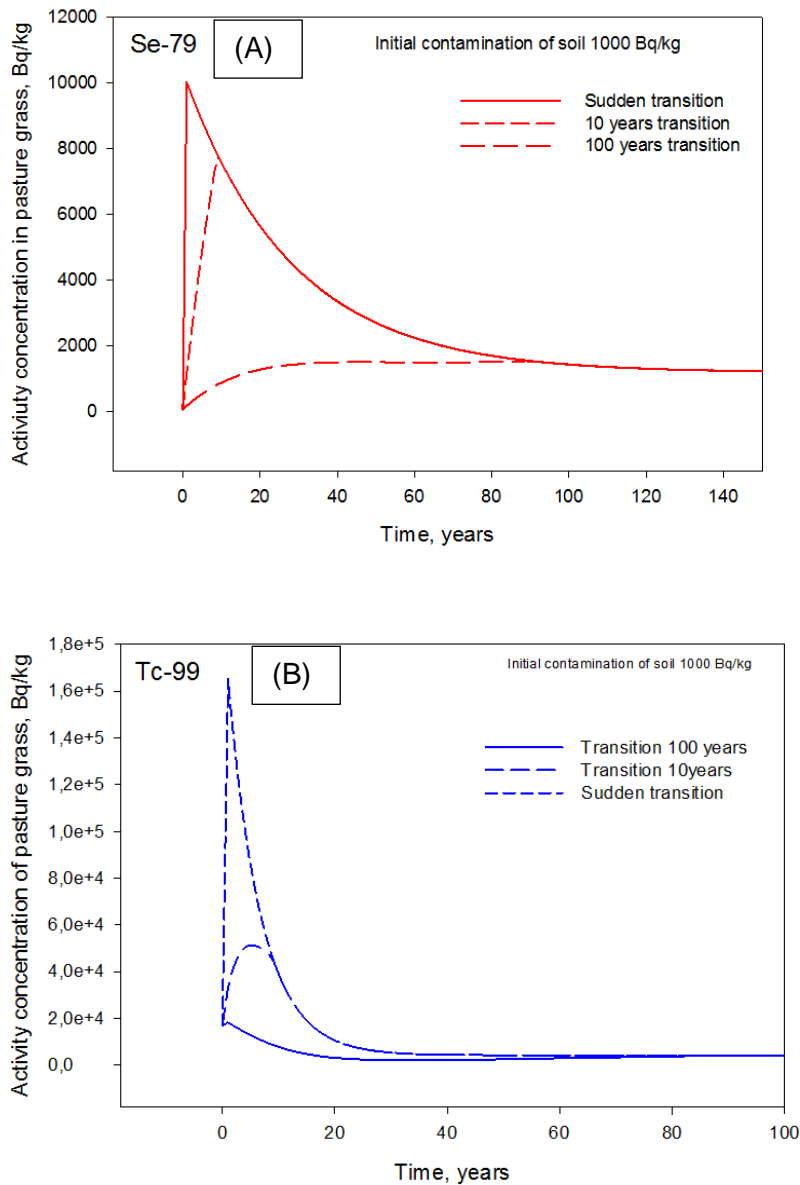


Fig. 4.62 influence of transition time on the behaviour of activity concentration of Se-79 (A) and Tc-99 (B) in pasture grass under full irrigation condition

The model calculations show that the contamination of plants could significantly increase due to an increasing mobility of redox-sensitive radionuclides. This effect was observed by simulating changes in activity concentrations in grass grown on the bed of a dried-out lake and a dried-out fen, respectively. Three processes play a crucial role in

the contamination of pasture grass in these scenarios: the increase of transfer of radionuclides from soil to grass caused by a change of the radionuclide redox state, the initial contamination of soil due to rising GW and the additional contamination of soil due to irrigation. During the transition, the contamination of grass with such nuclides as Tc-99 and Se-79 can increase by a factor of 1000 as shown in Fig. 4.62. However, the transition time frame is of high importance and longer time frames tend to will reduce the peak maxima. A transition of 100 years does not show any concentration increase (peak) compared to the final discrete climate state.

For these calculations high pre-contamination of the soil and a sudden transition between the redox states are assumed. With lower pre-contamination of the soil, the effects of the change in speciation on the exposure decrease since other, soil independent pathways like foliar uptake of radionuclides from irrigation water or use as drinking water increase in relative importance.

The crucial question is how these increased concentrations in plants impact the total BDCF. Depending on the radionuclide, different exposure pathways dominate the total exposure. For most of radionuclides the dominant pathway is ingestion of drinking water, fruits or vegetables. These pathways are independent of the contamination of pasture grass which explains that the BDCF for the transition and Mediterranean state do not differ for U-238 and Np-237. An effect on the total BDCF could only be observed for the redox sensitive radionuclides Se-79 and Tc-99, where the exposition pathways related to the contamination of soils are highly contribute to the BDCF.

In the case of Se-79, the contaminated pasture grass causes an increase in BDCF due to the relatively high importance of beef and milk for the exposure to this radionuclide. For Tc-99 the high peak of activity concentration in grass for this scenario (Fig. 4.62) results only in a moderate increase of exposure during the transition compared to the Mediterranean BDCF, since the exposure pathways involving grass only play a negligible role in the total exposure (Fig. 4.59).

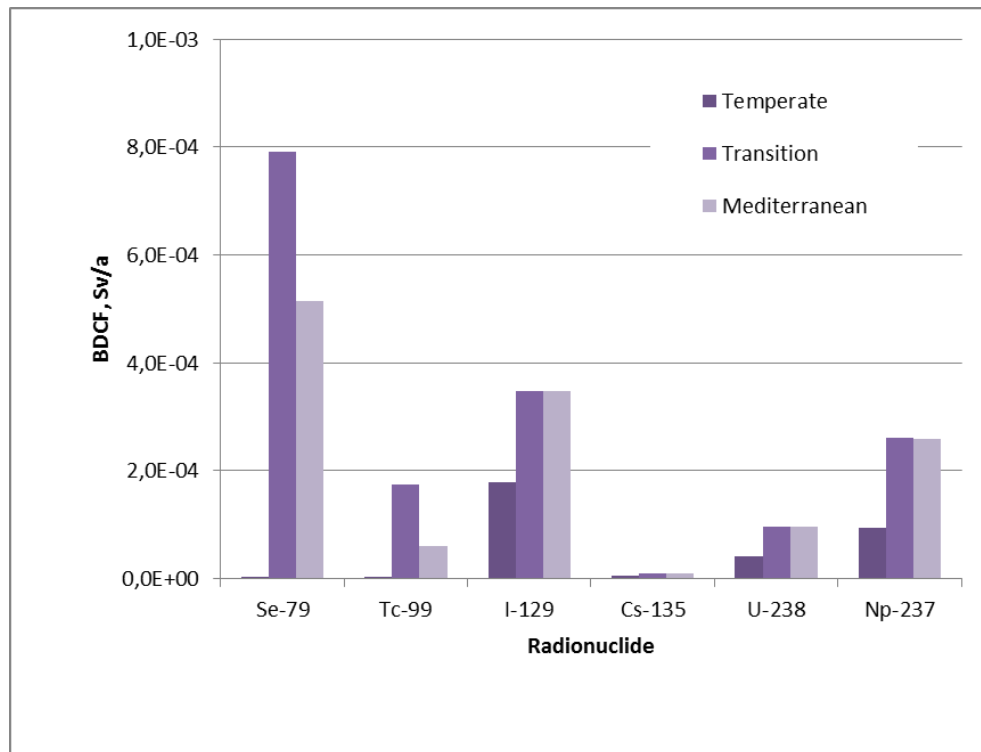


Fig. 4.63 BDCF calculated for the time before (Temperate), during (Transition), and after transition (Mediterranean)

The investigations presented here tried to estimate the impact of future climates and climate transition on processes in the biosphere and resulting potential radiation exposure to mankind by the use of generic, stylised models. The bandwidths covered by calculations for the nine discrete climate states are in a similar range as the bandwidths derived from parameter uncertainties. However, the uncertainty analysis can be regarded as a first estimation. More emphasis to derive probability density functions (pdfs) for the parameters and an approach for the treatment of correlations between the parameters is needed. The models also allowed calculating transition states for climate changes, which are of complex nature. The results indicate that climate transitions could cause radiation exposures increased compared to discrete climate states but not more than a factor of ten. Relatively high accumulations of redox-sensitive radionuclides in plants are smoothed, because other exposition pathways not related to radionuclide mobilisation in soils contribute to the overall BDCFs.

4.8 Natural Analogue study Ruprechtov site

Ruprechtov in Czech Republic (near city of Karlovy Vary) represents a Natural Analogue investigation site since mid-1990's. In the southern part of the investigation area an open pit kaolin excavation work started in the middle of the last decade (app. 2006). Since the so-called clay/lignite layers, containing the uranium enrichment investigated at the site even earlier, appear directly above the exploitable kaolin strata, the excavation work allowed to address specific questions and to perform few additional investigations (with regard to previous investigations) at the site. The objective of these additional investigations carried out at Ruprechtov site during reporting period was twofold,

- to survey the hydrogeological-geochemical parameters in/around boreholes near the mining area, which might become influenced by groundwater drawdown as a result of pumping in the area, in turn provoking a change in redox conditions and therewith affecting the mobility of uranium in the system.
- to check the conceptual model, namely the general bedding conditions (tertiary layers, tertiary basis, groundwater bearing layers, extension of fractures providing hydraulic contact to the underlying pre-tertiary rocks, spatial and structural distribution of uranium enrichments and further clarification of U bearing minerals.

Detailed results can be found in /NOS 12/. Important aspects from the study are summarized in the following.

4.8.1 Impact of mining-related disturbances on the uranium enrichment

During two drilling campaigns altogether four new research boreholes were drilled and cased (NAR1, NAR2, NAR3 and NAR4) with a total length of app. 90 m. The location of the research boreholes at Ruprechtov site is presented in Fig. 4.64. Main aim of the new research boreholes in the Ruprechtov site was to monitor possible changes in hydrogeological and geochemical conditions in the vicinity of the open pit kaolin mining. Therefore, part of the boreholes were placed at locations without any influence of open pit mining to be expected, the other part close to or even within the progressive mining area. The latter have been supposed to become directly affected with regard to water level and possible oxidation effects in groundwater.

In addition, the drill cores obtained were used to get complementary information about petrographic and geochemical characteristics of the tertiary sediment complex as well as for further laboratory experiments.

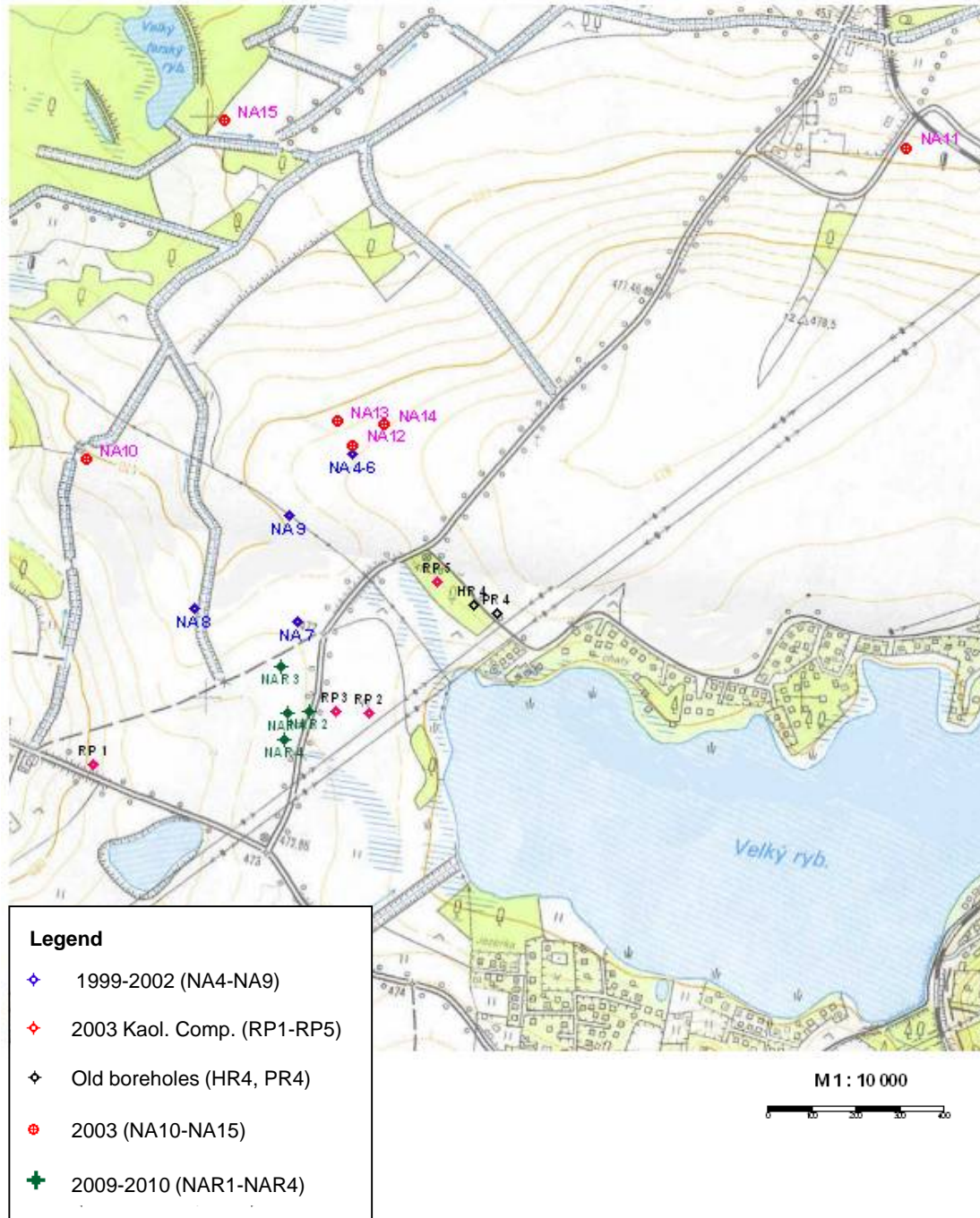


Fig. 4.64 Location of all investigation boreholes at Ruprechtov site

The new boreholes (of current project phase) are marked in green color

One important aspect was the observation of water heads to identify potential disturbances of groundwater conditions in the clay lignite layers by kaolin mining. Both, new

and existing monitoring wells allowed a continuous monitoring of the groundwater levels in the vicinity of the quarry and also to monitor the impact of mining on the groundwater regime. In 2011, the mining area boundaries reached the positions of the wells NAR3 and NA7. The excavation of surrounding rocks slowly developed until well NAR3 had to be cut. In the area of interest, two basic groundwater systems exist, a shallow circulation in the sediments of Tertiary age and a deeper circulation in the fracture system of the underlying crystalline rocks, in general hydraulically isolated from each other, see e. g. /NOS 06/, /NOS 09/. Monitoring wells for both groundwater horizons are available. Until 2005 – before the start of mining operations – circulations in the crystalline as well as Tertiary rocks were similar, without significant difference in the dynamic behavior of groundwater levels in boreholes of both horizons. After the start of open pit works (app. 2006) it became clearly visible, that the wells located near the mine area show a different behavior. Fig. 4.65 shows that the groundwater levels in wells NA7B, RP2, RP3, RP4, NAR1, NAR2, NAR3 change in a different way compared to the wells NA4, NA5, RP5, NA12, although some wells have very short periods of observation. The first group of wells, located in the excavation area, exhibits a faster response to rainfall. The movement of groundwater levels in these wells is faster with larger fluctuations, but the long-term trend is similar to the wells outside of the excavation area. The difference between the maximum and minimum measured value of the groundwater level is for a borehole, not affected by the mining – e. g. RP5, only 0.3 m, for a typical borehole in the mining area, e. g. NA7B it is 1.7 m. Further, for wells NAR3 and NA7B the groundwater level was decreased by about 2 m due to the strong pumping in the mining area. These changes show the circulation imbalance due to the mining. In conclusion, influenced wells are NAR3, NAR4, RP2, RP3, RP4, NA8, which are located directly in the quarry and east from the excavation area. These fluctuations in the piezometric levels may lead to variability in the local groundwater flow directions. However, the recorded groundwater levels indicate that the decrease of the water level is not pronounced enough to reach the uranium layers, and with it to allow oxygen to easily penetrate into the uranium-rich layers.

Nevertheless, groundwater analyses in the new boreholes and for selected older wells (as references) have been performed. The results from a comparison of uranium concentrations in the groundwater of the monitoring wells prior to the mining (1999 – 2005) and after start of mining (2009 – 2012) are illustrated in Fig. 4.66. The graph shows that during the monitoring period no increase of uranium in groundwater due to oxidation caused by kaolin mining can be observed.

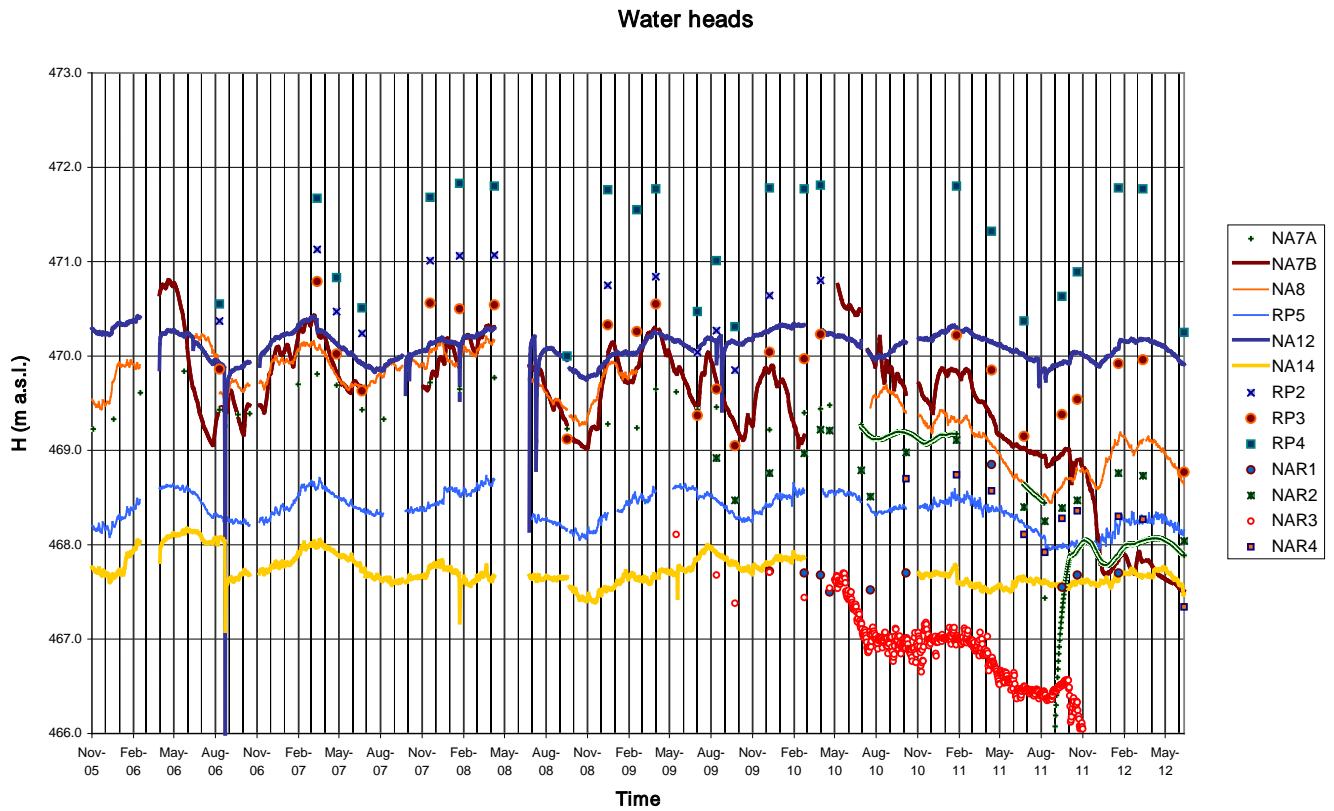


Fig. 4.65 Evolution of groundwater levels in the boreholes between the years 2005 and 2012

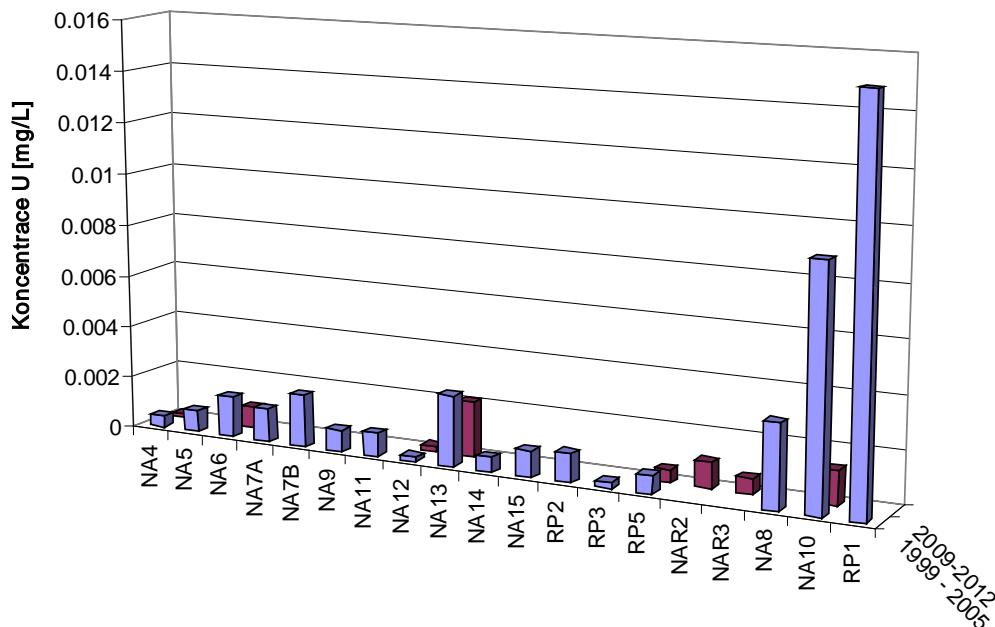


Fig. 4.66 Comparison of uranium concentrations (in mg/L) in groundwater in monitoring wells before mining (1999 – 2005) and after mining (2009 – 2012) at Ruprechtov locality

This is further supported by the redox conditions analyzed in the new boreholes nearby the excavation area. The geochemical conditions at the site are characterized by low mineralized waters with ionic strengths in the range of 0.003 mol/l to 0.02 mol/l. Nearly all waters in the clay/lignite horizon, also those from the new boreholes, are of Ca-HCO₃-type with total DIC concentrations up to 450 mg/l. The pH-values vary in a range of 6.2 to 8, the Eh-values from 435 mV to -280 mV. More oxidizing conditions with lower pH-values are found in the near-surface granite waters of the infiltration area. Selected groundwater data for boreholes considered here are compiled in Tab. 4.11. The new boreholes show slightly lower pH values compared to the other clay/lignite wells, which might indicate some mixture with infiltrating waters. However, the in situ Eh-values are quite low, indicating a strong redox buffering of the system. Displaying the data in the Eh/pH diagram (using Geochemists workbench /BET 06/, and the uranium update of NEA thermodynamic database /GUI 03/) shows that under these conditions uranium is still expected to occur in the reduced U(IV) redox state, see Fig. 4.67, left.

Tab. 4.11 Specific groundwater data for selected boreholes

Well	Horizon	pH	Eh	U	Fe ²⁺	S ²⁻	δ ³⁴ S	SO ₄ ²⁻
	[m]		[mV]	[µg/l]	[mg/l]	[mg/l]	[‰]	[mg/l]
NA4	34.5 - 36.5	7.0	n.a.	0.15	1.8	0.1	24.63	19.8
NA6	33.4 - 37.4	7.8	-280	0.8	0.7	0.11	23.5	49.5
NA12	36.5 - 39.3	6.7	-160	0.2	2	n.a.	20.11	22.9
NA13	42.2 - 48	7.65	-252	2.1	0.7	0.065	n.a.	22.9
NAR2	24.8 - 28.8	6.53	-135	1.0	1.7	0.02	14.27	25
NAR3	20 - 24	6.35	-175	0.6	2.9	0.01	13.01	14.4

In order to check for the redox determining components the measured Eh-values are compared to calculations for specific redox-pairs. This was already done for the existing wells /NOS 10/, but here also the new boreholes are included. Due to the occurrence of significant amounts of sulphide minerals and dissolved sulphide and the redox pairs SO₄²⁻/HS⁻, and the heterogeneous redox pairs SO₄²⁻/pyrite have been included. Many natural systems are dominated by redox pairs of iron. Therefore we also calculated the couple Fe²⁺/Fe(OH)₃ considering a relatively fresh amorphous precipitate according to data from (Langmuir 1997). The results are shown in Fig. 4.67, right.

A reasonably good agreement is found for all boreholes, including the new ones, between the redox potential measured by the Pt-electrode and the SO₄²⁻/HS⁻ and SO₄²⁻/pyrite couple, respectively, whereas the redox pair Fe²⁺/Fe(OH)₃ shows low agreement

in particular for nearly all boreholes. As discussed before there is strong evidence that microbial sulphate reduction and oxidation of organic matter occurs in the clay lignite horizon. In particular the $\delta^{34}\text{S}$ values in the boreholes from the clay/lignite horizon are strongly increased with respect to the values in the infiltration waters. Furthermore, the existence of sulphate reducing bacteria has been shown and pyrite minerals in framboidal shape, typically formed by microbial processes, are frequently found in the clay/lignite layers. The observed sulphide values in the clay/lignite waters are significant but not too high, ranging from 0.05 to 0.12 mg/l. Microbial catalysis efficiently accelerates the sulphate reduction and operational redox potentials resulting from this kinetic process may closely approximate equilibrium values. This might explain the agreement of measured and calculated values for the $\text{SO}_4^{2-}/\text{HS}^-$ couple.

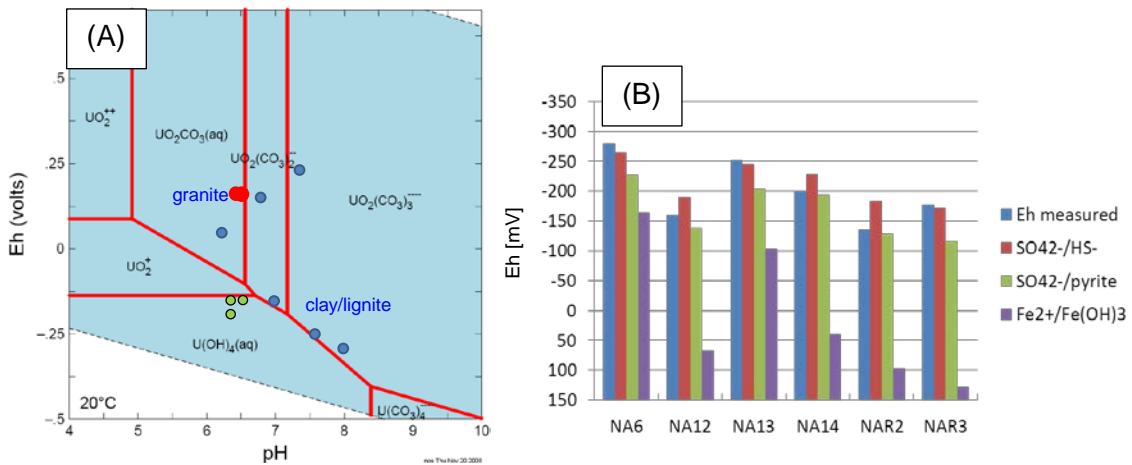


Fig. 4.67 (A) Eh/pH diagram with the new boreholes NAR2, NAR3 and NAR4 (green dots). (B) Measured Eh-values compared to potential redox pairs

Further the uranium determining mineral phases have been analyzed again including the data from the new boreholes. An appropriate method to understand which uranium phases control the uranium solubility in the natural system is the calculation of saturation indices. The calculation results are shown in Fig. 4.68. The groundwaters from the clay/lignite horizon are strongly oversaturated with respect to the crystalline uraninite and coffinite indicated by saturation indices (SI) in the range between 5 and 7. The mixed valence uranium oxides $\text{UO}_{2.25}$ and $\text{UO}_{2.33}$ are also oversaturated (SI between 2.5 and 4). The mixed valence oxide $\text{UO}_{2.66}$ is always undersaturated with SI values below -0.8 with exception for NAR2. No saturation of U(VI) minerals was indicated. Assuming an uncertainty range of ± 0.6 (shaded area in Fig. 4.68) for the saturation index, resulting from uncertainties in the thermodynamic data, the results indicate that

the uranium concentration in groundwater is controlled by amorphous UO_2 and/or ningyoite.

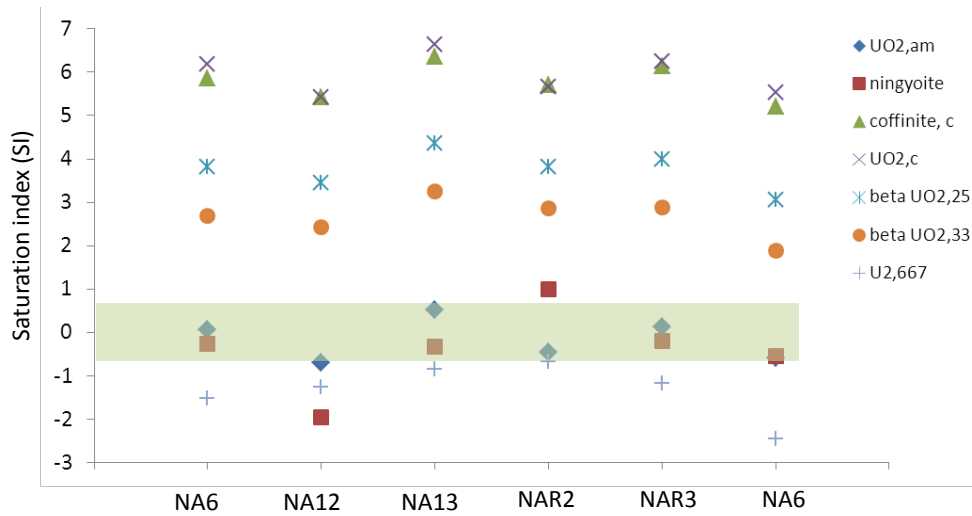


Fig. 4.68 Saturation indices of various U(IV) minerals calculated for groundwater from old and new boreholes

In conclusion all analyses show that regarding the uranium enrichment and mobility of uranium no impact caused by the excavation work occurred in the new boreholes. Even for boreholes in the direct vicinity of the excavation, where an impact on the water heads could be observed, the geochemical conditions in the clay/lignite layers are well buffered and stay in a reducing state, where the mobility of uranium is limited. The results from the new boreholes very well support the assumptions for the geochemical conditions stated in previous reports, e. g. /NOS 09/, NOS 10/.

In order to identify impact of oxidation on the clay/lignite layers with high uranium content, another strategy was applied. Material from the excavated area, where the clay/lignite layer has been exposed to the surface at least for several months, was taken by manual, horizontal sampling from the surface down into a depth of app. 50 to 70 cm (cf. Fig. 4.69, left). In 2009 and 2010 in total three drill cores were obtained.

One drill core, OC-A of approx. 55 cm length, was divided into 16 pieces as shown in Fig. 4.69 (top left) and analyzed for its uranium content. Each second section was also analyzed for U-series disequilibria by University Helsinki with the method described in /NOS 08c/.

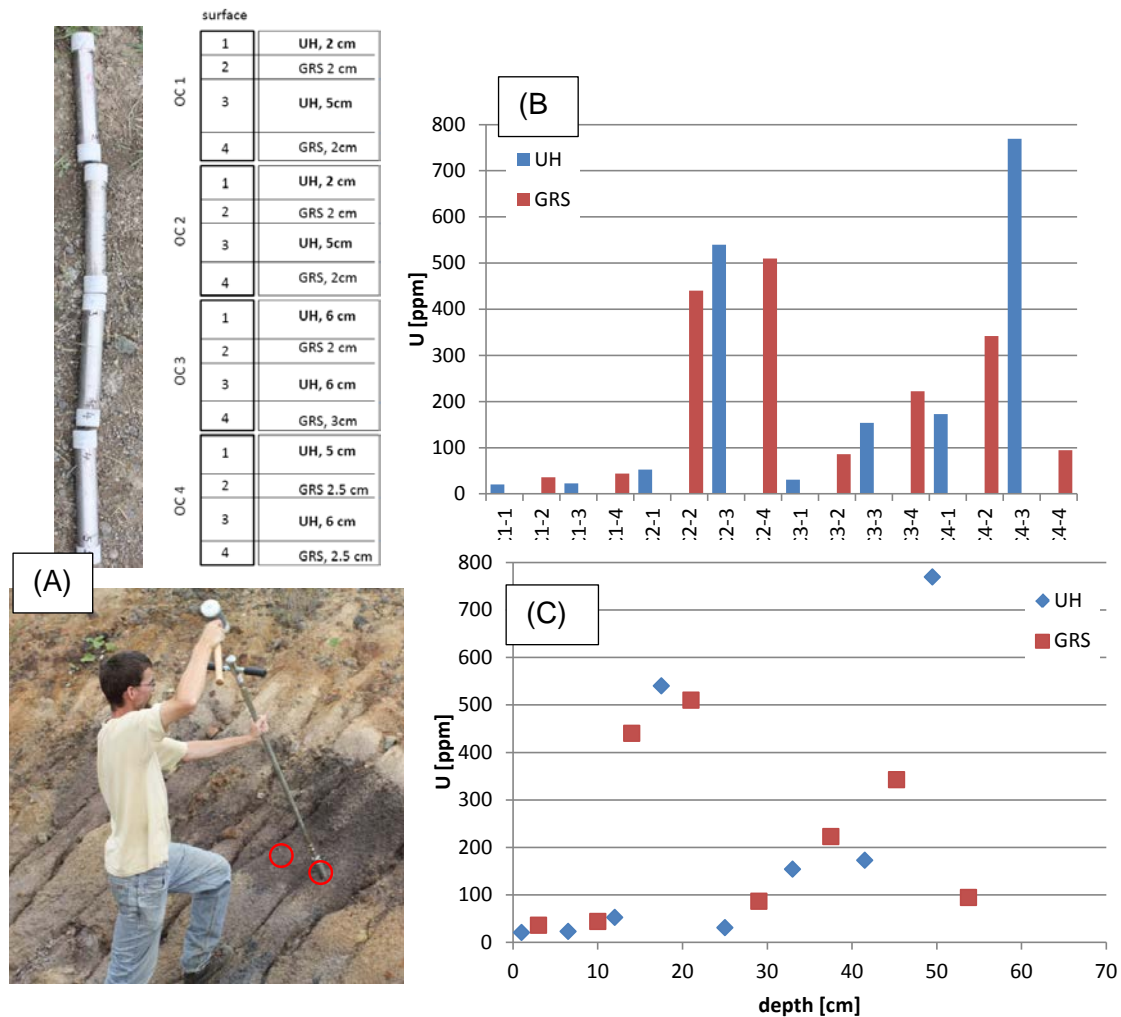


Fig. 4.69 Manual drilling of material from a clay/lignite layer exposed to the surface (A). Uranium content analyzed by ICP-MS (B) and α -spectrometry (C) in the sub-samples of the open pit from core OC-A

As shown in Fig. 4.69 the uranium content varies between 20 and 770 ppm. The highest uranium contents occur in the depth from 15 to 25 cm with more than 500 ppm and from 45 to 55 cm with a maximum value of 769 ppm. The U content is also increased in the depth between 30 and 45 cm with values up to 200 ppm. The figures also demonstrate a nice agreement, between measurements by ICP-MS and by alpha spectroscopy.

The corresponding uranium disequilibrium series results for the bulk samples are shown in Fig. 4.70. All data plot into the area of old uranium accumulation, to some extent similar to the data from the clay/lignite layers of the deeper boreholes. One difference is that particularly the bulk outcrop samples taken near from the surface show

very low $^{234}\text{U}/^{238}\text{U}$ ratios in the range of 0.5, which are much lower than the lowest $^{234}\text{U}/^{238}\text{U}$ ratios observed in the deep borehole samples of about 0.8. This is a strong indication that some uranium leaching has already occurred in the samples. It is expected that preferably the more accessible U fractions are going to be leached. For U(IV)/U(VI) separation and sequential extraction it is known from previous work, e. g. /NOS 08c/, that the oxidized and more accessible fractions have ratios above unity (between 1.2 and 3), whereas the less accessible U(IV) fractions have ratios significantly below unity. A leaching of the more accessible U fractions would therefore decrease the $^{234}\text{U}/^{238}\text{U}$ ratio down to values of 0.5, which are typical for the U(IV) fractions found in the clay/lignite layer. Chemical leaching should also increase the $^{230}\text{Th}/^{238}\text{U}$ values, since Th is expected to be immobile.

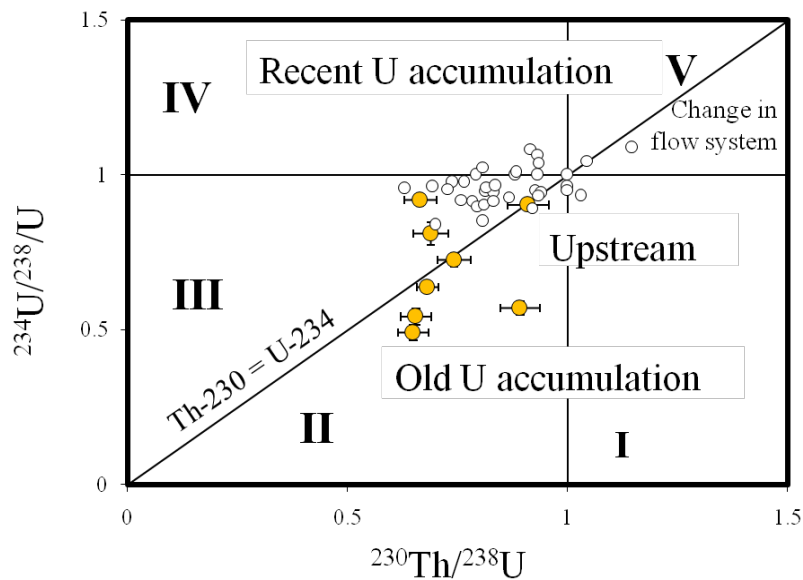


Fig. 4.70 Activity ratios $^{234}\text{U}/^{238}\text{U}$ against $^{230}\text{Th}/^{238}\text{U}$ measured for individual samples

Yellow circles represent results for samples from open pit and white circles represent results from different boreholes

This is further confirmed by the analyses of $^{234}\text{U}/^{238}\text{U}$ activity ratios in leachates from sequential extraction (according to the method described in /HAV 06/) performed at samples from the open pit core OC-C. This core was taken as a parallel borehole, 10 cm beneath core OC-A and shows similar distribution of the uranium concentration with depth. The analyses of three different samples are shown in Fig. 4.71. Sample P2_16 originates from 45 cm depth and shows similar activity ratios as observed in previous undisturbed samples from clay/lignite horizon, with Ar values in the range of 1.5 to 2 for the three first extraction steps (assumed to be U(VI)) and values about 0.5

to 0.8 for steps 4 and 5 (assumed to be U(IV)). The two samples P2_5 and P2_11 from <20 cm distance to the surface show similar values for step 4 and 5 but values significantly below 1 for leachates from the first three steps. This is expected, if the more mobile uranium, preferably U(VI) with AR above unity is leached from the system.

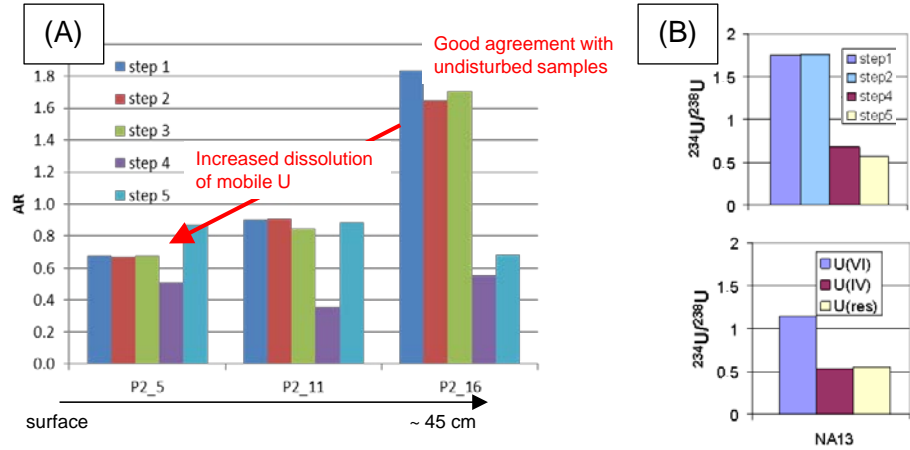


Fig. 4.71 $^{234}\text{U}/^{238}\text{U}$ activity ratios in leachates from sequential extraction in different sections of the outcrop core (A) and in leachates as well as in U(IV)/U(VI) separation fractions of an undisturbed clay/lignite sample from borehole NA13 (B)

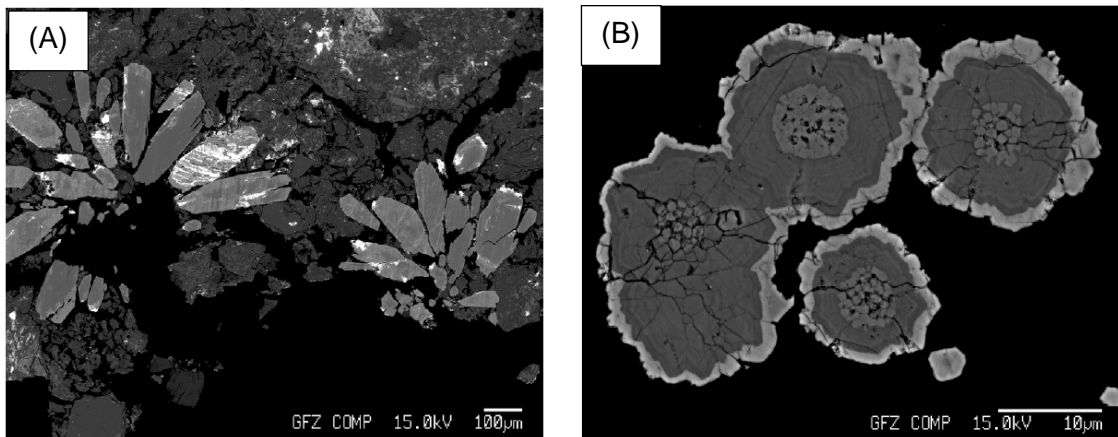


Fig. 4.72 (A) Grains of anhydrite (medium bright) intensively transformed into gypsum (dark), OC2-2; (B) systematically organised grains of pyrite with grey rim enriched by As (up to 5 wt.%), OC3-4

All the results from isotope analyses are well in agreement with results from mineralogical analyses. XRD analyses as well as selected mineral images taken by a JEOL thermal field-emission type electron-probe X-ray microanalyzer JXA-8500F (HYPERPROBE) at the Deutsches GeoForschungsZentrum GFZ, Potsdam show that in surface near samples (down to a depth of app. 20 cm) no pyrite can be found. In-

stead, only gypsum occurs in quite distinct concentrations. On the other hand pyrite is the dominating sulphate mineral in deeper depth. Typical mineral images are shown in Fig. 4.72 for segment OC2-2, ~15 cm and OC3-4, ~38 cm depth. This further supports the assumption that the first 20 cm of the open pit clay/lignite layer are significantly altered causing alteration. The alteration front has not reached the layers in 45 cm depth. These investigations are also important to demonstrate the strength of the uranium isotope disequilibrium series analyses to identify different uranium phases and geochemical alteration reactions in a natural system.

4.8.2 Verification of the conceptual model

4.8.2.1 Background

For many years, the investigations at Ruprechtov site have been dependent on a number of wells, drilled down to a depth of some tens of meters, enabling (among others):

- the recovery of core samples and with it, sediments from the site to become analyzed by manifold methods
- the carrying out of well logs and well tests to obtain information on stratigraphy, rock parameters as well as hydraulic conditions in the underground
- the recovery of groundwater samples for geochemical and isotopic lab analyses

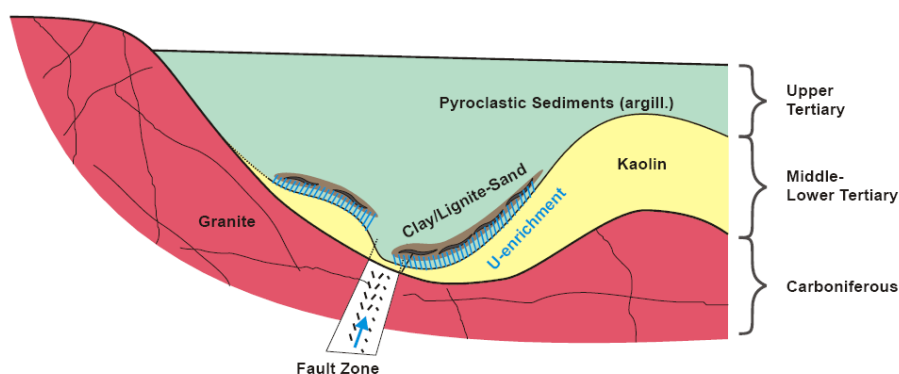


Fig. 4.73 Schematic geological cross section of Ruprechtov investigation area with main geological units

Based on the results of all well-based investigations, model assumptions could already be developed conclusively describing from where the uranium – accumulated in the

clay/lignite-sand layer – originates, in what way it could be transported to its current deposit and why it has been accumulated there. In Fig. 4.73 the fundamentals of the model assumptions are compiled:

- underlying (and nearby outcropping) granite representing the uranium source
- transport of mobilized uranium via fractures and fault zones in fresh, but also kaolinized granite
- accumulation of uranium within depressions of the hanging tertiary sediments which in turn are caused by a strong morphology of the former granitic earth's surface at this place. The accumulation of uranium additionally is also depending on a distinct geochemical milieu influenced by lignitic sediments swept along the depressions

4.8.2.2 Occasion of open-pit mining

Since all model assumptions have been based mainly on individual boreholes giving more or less just information on that very point (plus some additional information from existing maps), the beginning of open-pit works at Ruprechtov site for kaolin (mid of last decade) has been associated (among others) with the possible chance of an in situ-review of the geological and stratigraphic conditions of the site. The original state of the site as well the current one is shown in Fig. 4.74 and Fig. 4.75, respectively.

The opportunity mentioned above, of course, has been heavily influenced by the extent of mine works and its accessibility. Both unfortunately have not quite reached the desired level, but nevertheless, the main features of the model assumptions could be identified and documented.



Fig. 4.74 Aerial view of Ruprechtov site during first years of NA investigations

The photograph is from S to N with the Ore Mountains in the background. The investigation area extends from bottom left and left of Velký rybník pond (middle right)



Fig. 4.75 Space view of Ruprechtov site after beginning of kaolin open pit mining

The mining area can be identified by white-color left of Velký rybník pond

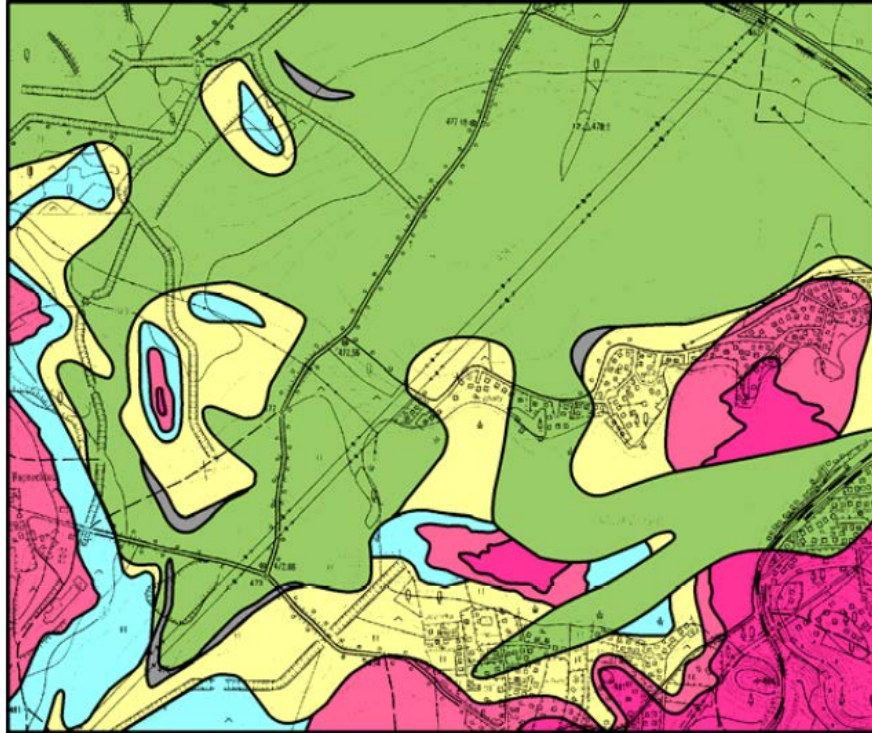


Fig. 4.76 Detailed geological map of Ruprechtov site based on geological mapping 1:10 000. In the lower right Velký rybník pond is located

The open pit mining today mainly covers the middle left section of the figure where a single updoming of granite (red), surrounded by kaolin (light blue) and kaolinized granite (yellow) is mapped within the overall tertiary sediments (green); outcropping lignite is mapped in grey color

The strong morphology of the former granitic earth's surface (at this very place) is reflected by the 'spots' of granite surrounded by tertiary pyroclastic sediments (Fig. 4.76).

4.8.2.3 Exemplary geological features of open pit's exposures

Due to progressive mine works, most exposures of geological features were only temporarily available, if at all. Furthermore, the special conditions of kaolin mining with partly steep and deep slopes, muddy and slippery ground, active mining with operating machines often caused a general inaccessibility so that most exposures only could be documented by photographs. Below, some of the features detected during field visits are shown. Results analyzed on individual samples obtained are given in separate chapters.

The open pit mining at Ruprechtov site as performed by Kaolin-company allowed for studying the bedding conditions of the sediments as constructed and postulated from the former drillings and derived model assumptions. In general, the strong morphology of sedimentary strata close to underlain kaolin could clearly be proved (Fig. 4.77 ff).



Fig. 4.77 Central outcrop of kaolin open pit at Ruprechtov site showing inclined sediments of do-called hanging strata including coal lens on top of kaolin (right edge of the photograph)



Fig. 4.78 Marginal outcrop of kaolin open pit at Ruprechtov site close to NAR3 bore-hole

An inclined lignite seam (“Sample 1” with background radiation) is underlain (to the right) by clayey-sandy sediment with higher gamma-radiation, indicating the transition to top of kaolin

Gamma measurements along all outcrops also proved the effectiveness of coal layers with regard to uranium enrichment (Fig. 4.78, Fig. 4.79). But as also known from former drillings, coal seams and coal lenses must not be accompanied by higher U concentrations.



Fig. 4.79 Coal seam in the upper level of open pit's outcrop at Ruprechtov site; results of gamma measurements as well as position of sampling is indicated



Fig. 4.80 Isolated coal lens as well as coal seam with different gamma radiation

Fig. 4.80 with its rather steep orientated coal seam also demonstrates that – in addition to given structures by the morphology of former granitic surface and resulting sediment-filled depressions during tertiary – also tectonic movements must have happened. The existence of such movements has already been expected before, since Ruprechtov area is part of the *Ohře* Graben which originates from tectonic activity in the area as well as the widespread volcanism. The latter is demonstrated impressively by the large Doupovské hory stratovolcano, close-by, whose exhalations gave rise to the thick pyroclastic sediments covering the older rocks in the *Ohře* Graben widely.



Fig. 4.81 Outcrop in kaolin part of the Ruprechtov open pit

Clear structures in kaolin itself (e. g. Fig. 4.81) emphasize that these strata do not represent homogeneous mineral agglomerate which might isolate the underlain granite hydraulically from overburden sediments. Rather it can be seen that also hydraulic active pathways are present which have already been postulated earlier.

4.8.2.4 Conclusion

All geological exposures detected, analyzed and documented within the open pit kaolin mining activities at Ruprechtov site are in full compliance with the model assumptions derived from previous borehole investigations. So far, no facts could be ascertained that would contradict these assumptions.

4.8.2.5 Winning of air-influenced soil water

Although the locations of the wells drilled during the last campaign of Ruprechtov field work (especially NAR1, NAR3 and NAR4) have been chosen in order to find significant uranium mineralization at shallow depths and simultaneously to have the environment most probably influenced by mining, this requirements were not satisfied. The mining in the open pit progressed slowly during the project and therefore redox conditions were not affected by dropping of groundwater level. Even in case of NAR3 where surface has been lowered some 15 m groundwater drawdown has been not enough for such effects (Fig. 4.82).



Fig. 4.82 NAR3 drill hole after progress of mining activities in this area

Therefore, a new attempt to investigate groundwater influenced by atmosphere has been started by help of so-called suction cups. Porous filter cartridges have been digged in and sealed at several positions along the open pit which showed higher gamma counts as well as (nearby) lignite seams or lenses (SC1 – SC5, Fig. 4.83 and Fig. 4.84). Finally, 5 suction-cups were placed during the sampling campaign (8/2011).



Fig. 4.83 Position of installed suction cups along the eastern margin of Ruprechtov open pit – in the background the ore mountains

Firstly, the installation of suction-cups needed a shallow borehole performed with hand boring bar. Furthermore, the soil from digging has been merged with water to create a dense suspension. The suction-cup was immersed into this suspension and evacuated. The suspension reached the large pores of plastic frit and polyamide membrane filter, which is hidden inside. Part of the suspension was poured back into the shallow borehole and suction-cup was installed. This Installation procedure has led to a homogeneous connection among plastic frit, polyamide membrane filter and rock surroundings, which is necessary for the soil water inflow into the suction-cup. The remaining borehole was then backfilled. The tubes were connected to the hard plastic bottle (1 L) and the whole system was evacuated to -0.8 bar. The first samples taken after installation were discarded and original soil water was collected during next sampling. In October 2011, suction-cups 3, 4 and 5 unfortunately had to be removed due to progressing mining activities in the area.



Fig. 4.84 Position of installed suction cup 2 the cartridge is dug in at app. 100 cm depth

The sampling bottle remains above ground and is connected by the colorless tube. The blue tube allows for controlling the pressure status in the system

The samples of soil water were measured in the field for electrochemical parameters (pH, conductivity, dissolved oxygen, Eh) and then acidified in order to dissolve the precipitated iron on the walls of the collecting bottle. Subsequently, the samples were analyzed for uranium content by GRS and ÚJV Řež, a. s. The results in general show a very low pH of soil waters that allows release of relatively large amounts of iron which subsequently precipitate in the collecting bottles. This low pH is probably due to oxidation of pyrite. Waters are also rich in dissolved solids, because of the high water conductivity. High concentrations of uranium have been analyzed; the highest value was app. 15 mg/l (see Tab. 4.12). It is also interesting to note that uranium concentrations varied significantly during repeated sampling. It appears, that in the surface zone with uranium, which is uncovered by mining for a longer period of time, uranium enrichment occurs in the soil waters.

The cartridges (at depths of app. 50 to 100 cm) are connected to sampling bottles on surface by tubes, the soil-water is extracted by vacuum applied to the bottles. So far, the data gained emphasize good in situ-fitting of the cartridges. Unfortunately, positions SC3 to SC5 are no longer in operation due to mine expansion in that particular area.

Tab. 4.12 Summary of results from soil waters measurement

Cup No	Depth [cm]	Surface γ -activity [cps]	Sampling date	pH-value	Conductivity [mS/cm]	U-content [mg/L]
SC1	50	3,500	17.01.12	2.85	1.391	0.0028
SC2	100	800	17.01.12	2.64	2.66	0.7954
SC3	50	2,800	21.10.11	2.33	17.12	14.9831
SC4	70	2,800	21.10.11	2.52	5.73	2.3983
SC5	90	2,800	21.10.11	2.58	5.03	0.3215
SC1	50	3,500	13.06.12	2.58	1.87	0.2410
SC2	115	800	13.06.12	2.72	1.76	0.0727

4.9 Initiation of the Project VIRTUS (Virtual Underground Research Laboratory in Salt)

According to international consensus all countries using nuclear power consider the emplacement of high-level radioactive waste (HLW) in deep geologic formations as the best solution of the long-term final disposal /NEA 08b/. Potential host rocks primarily considered in Germany are rock salt and clay formations.

To acquire necessary experiences regarding construction of an underground repository and the long-term behavior of the host rock under the impact of HLW, e. g. heat and radiation, Underground Research Laboratories (URL) are operated in some countries. After closure of the Asse URL in 1995, however, an URL in Germany is no longer available.

Anyhow, to furnish research and waste management organizations with an adequate instrument for the analysis of the processes taking place in a repository system and for the development of repository concepts and designs the idea of a virtual URL/repository was born in 2006. The main objective is to provide a pre- and post-processing software platform for the various process-level codes currently in use that allows a comprehensible 3D-visualization and interpretation of the results of numerical simulations of safety relevant processes expected to occur in repositories in geologic salt formations. The software platform VIRTUS is assumed to help researchers as well as the interested public to better understand and appraise the complex coupled processes in a repository.

After intensive discussions it was finally decided to perform a preliminary study to assess the chances for a successful realisation of the project objectives in early 2010. In agreement with the German project funding agency the Projektträger Karlsruhe (PTKA) – acting on behalf of the Ministry for Economics and Technology (BMWV) – the GRS-division of repository safety research contracted the Fraunhofer Institut für Fabrikbetrieb und -automatisierung (IFF) as a competent software developer. GRS and IFF – in cooperation with the candidate future project partners Bundesanstalt für Geowissenschaften und Rohstoffe (BGR) and DBE Technology GmbH (DBE TEC) defined the project requirements as follows:

Visualisation of the URL and the geological environment

- Import and storage of the 3D geological structures and of URL or repository excavations
- Interactive visualisation of URL/repository including
 - virtual flight, free navigation, view from different perspectives
 - blend-in, blend-out of objects, transparencies
 - definition of sections

Editing of structures

- Adding/removal/displacement of objects like geotechnical barriers, waste containers...
- creation of disposal cells (boreholes, drifts, chambers)

Simulation of reference-experiments

- selection of sections from the 3D-geological model (cuboid-selection)
- construction of URL-experiment or repository systems
- selection of PLC (Code_Bright, Jife, FLAC, Rockflow)
- generation of input data files

Visualisation of PLC-modelling results

- Import of simulation results from PLC and post-processing

- Display of results (temperature, stress, displacements, migration of pollutants...)
- blend-in of experiment documents

Further aspects

- development of user interfaces
- integration of access authorization for user, administrator, visitor, ...

4.9.1 Preliminary assessment of the chances for a successful realisation of the project objectives

The first item that was investigated was the import of geological data from the openGEO software developed by BICAD and used by BGR. BGR provided a set of test data representing a generic salt dome (Fig. 4.85) with integrated mine layout (Fig. 4.86) which was imported by VIRTUS without any problem. Using respective navigation modes it is possible to look at the geological model from arbitrarily selected positions.



Fig. 4.85 Presentation of a salt dome imported from the openGEO software

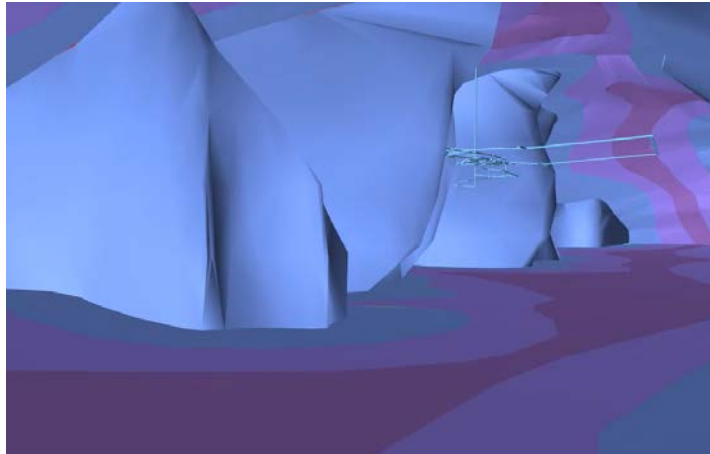
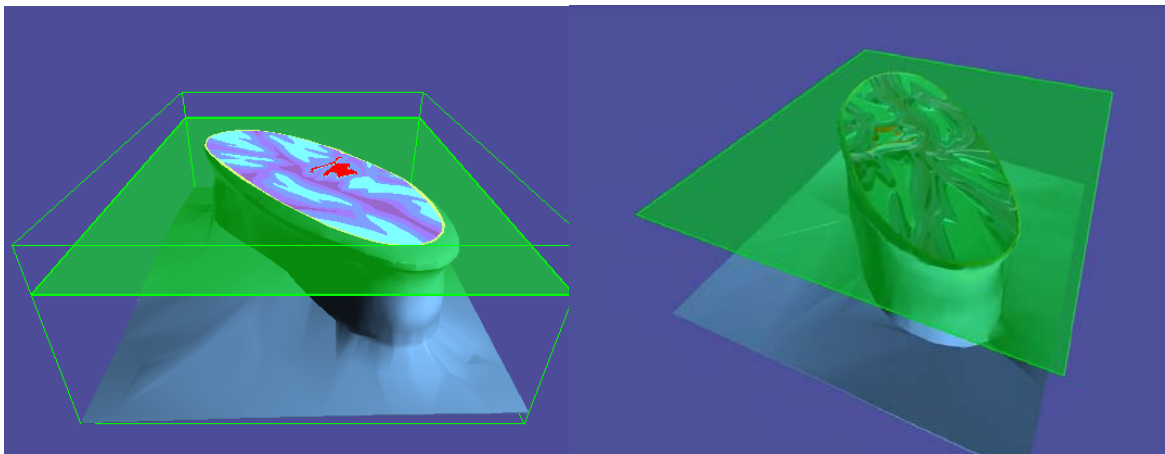


Fig. 4.86 View into the geological structures of a salt dome. Different geological strata are displayed in different colours. The mine layout can be seen in the background

The second item investigated was the definition of sections through the geological model (Fig. 4.87). By using the developed menu "Geology" it has been made possible to manipulate the position and orientation of sections in the 3D space. Each section is automatically closed (capping) so that the geological structures can be seen by the user. The automatic closing can be deactivated so that the user can look into the 3D-structure.



(A) losed surface

(B) transparent surface

Fig. 4.87 Section through a geological model imported from openGEO

The third item which was investigated was the visualisation of PLC-modelling results provided by GRS on basis of a numerical simulation of the direct disposal of spent fuel in a backfilled disposal drift in a salt repository. The simulation was done with the process-level code Code_Bright /OLI 96/.

The data set provided by GRS comprised a list of nodes and elements of the Code_Bright-generated finite element model as well as the evolution of temperature for each node for nine discrete points of time between year 1 and 100.

A graphic user interface was developed that enables easy import and manipulation of modelling results by the user. The import of test data from the Code_Bright PLC was successfully tested. It might happen that the simulation results are covered by geologis structures if a geological model has been loaded. In such a case it is possible to click on a FlyTo-Button initiating the camera to fly to the simulation relevant model area.

All simulation parameters are displayed in separate list so that the user can easily decide which parameter should be visualized. In addition to this, a "Colour Ramp" enables the user to select the colour the parameter results should be displayed with.

The finite element grids can be displayed in three different ways: As a scatter plot with the nodes, as a grid structure (edges of the finite elements), or as a surface model (surfaces of the elements).

Fig. 4.88 shows the simulation results of the afore-mentioned temperature calculation in form of differently coloured cloud of points.

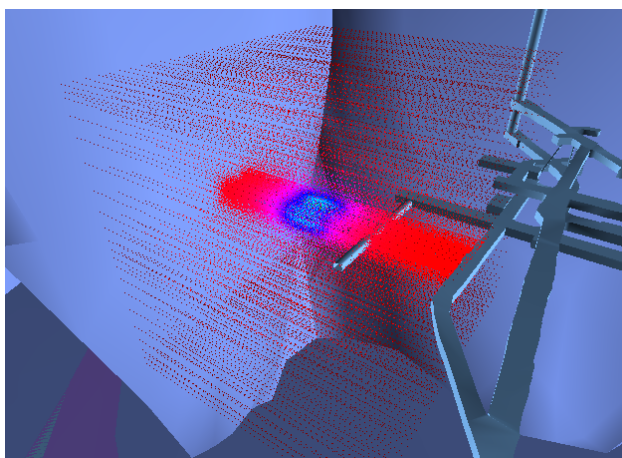
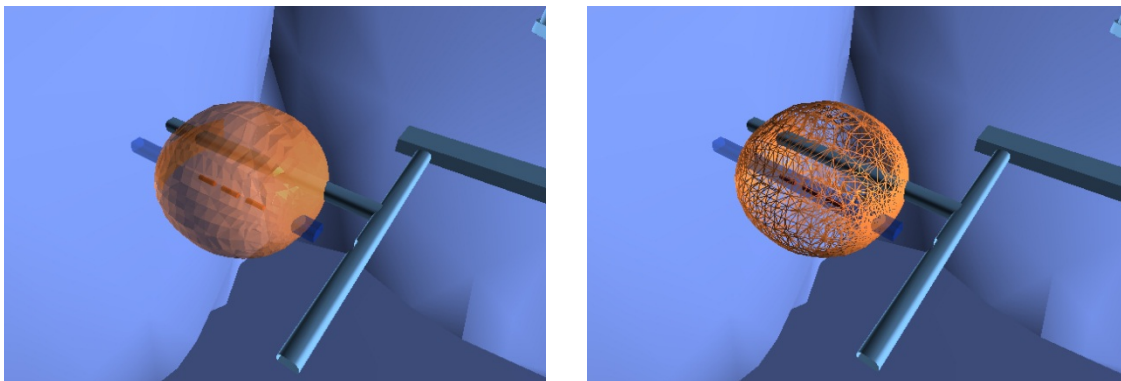


Fig. 4.88 Visualisation of the temperature distribution in and around two disposal drifts containing waste containers with disposed spent fuel

Further possibilities are to display the temperature distribution as closed or semi-closed iso-surfaces (Fig. 4.89).



(A) closed iso-surface

(B) transparent iso-surface

Fig. 4.89 Temperature distribution visualised in form of iso-surfaces

Another 3D-impression can be obtained by displaying the parameter data in two orthogonal arranged cuts which can be moved by the user through the area of interest (Fig. 4.90).

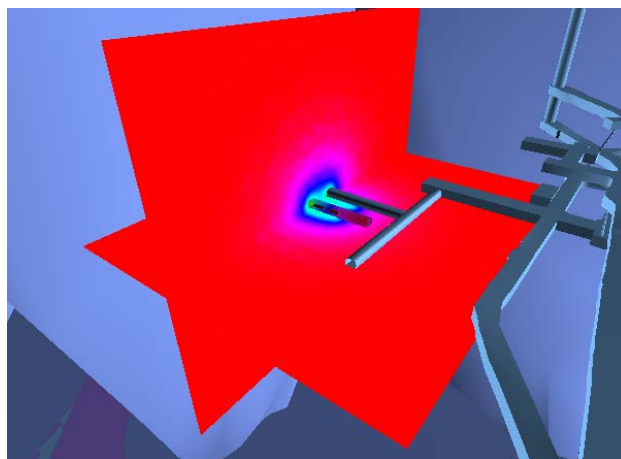


Fig. 4.90 Temperature distribution displayed in two orthogonal arranged cuts

4.9.2 Summary and appraisal of the preliminary study

In this preliminary study undertaken to assess the realisation possibilities of a virtual underground laboratory of a nuclear repository several requirements defined by GRS in co-operation with candidate future project partners were investigated. Among others, the import of geological data from the openGEO software as well as of mine layout da-

ta from CAD-software was successfully tested. Additionally, relevant possibilities for visualising the geological structures and the results of numerical simulations were investigated. The data used in this study were generated with process-level computer codes on basis of a comparably simple temperature calculation. In summary it was found and confirmed that the objectives of the envisaged VIRTUS software platform can be realised satisfactorily within a project duration of 3 years /BLÜ 10/.

5 Summary

Work performed within this project contributed to different aspects of the safety case, namely the assessment basis, methods and strategies to develop a safety case, long-term safety assessment and additional lines of evidence to be used in a safety case. Current national and international developments have been followed and discussed, R&D projects with relevance for post-closure safety of radioactive waste repositories have been analyzed and evaluated to improve process understanding and, where possible, new conceptual models and/or parameter sets to be considered in performance assessment have been proposed.

Developments in other countries and at the international level in general have been followed by participation in international committees and working groups, like RWMC, IGSC, Clay Club and Salt Club. The major results, publications, strategies and working aspects discussed or achieved in these groups during the last years are highlighted in this report. In this respect the state-of-the-art reports on methods in safety assessment (MeSA project), Indicators in the safety Case, and the guideline document for the development and application of thermodynamic sorption models for safety assessment purposes should be mentioned. Further in 2012 the IGSC endorsed the foundation of the Salt Club and approved the proposed working approach, work topics, and duration of the start-up phase. Similar to the Clay Club, the Salt Club is intended to promote the exchange of information and shared approaches and methods to develop and document an understanding of salt formations as host rock for a high-level waste repository.

One important new international contribution, which was strongly supported by this project, concerns long-term safety assessment. IGSC organised a project examining and documenting Methods for Safety Assessment for long-term safety of geological repositories for disposal of radioactive waste (MeSA, 2008 – 2011). The goals of the MeSA project were to review and summarise developments regarding safety assessment methods since 1991, when the last review report was produced by the Performance Assessment Advisory Group (PAAG). The report produced by MeSA presents a concise, clear, and up-to-date summary of performance assessment methods, underlines the degree of international consensus on performance assessment activities and methods, and provides an overview of the most important aspects and uses of performance assessment to a non-specialised audience. It emphasised also very detailed the essential role of safety assessment within in the safety case. The extensive review work lead to

several recommendations for future work regarding safety assessment and the safety case. This includes an update of the NEA brochure on the safety case concept, an update and enhancement of the NEA database of Features, Events and Processes (FEPs), a common project to exchange information and best practice on scenario development, and the development of a state-of-the-art report on safety indicators in safety assessment, based on further evaluation of responses to a questionnaire survey conducted during the MeSA project.

The latter recommendation was already realized during the last two years under aegis of GRS. The MeSA project has shown that the last several years have seen a number of important developments regarding the use of indicators in safety cases for geological disposal. On the basis of a survey performed with IGSC member organisations and of national and international projects dealing with the development and application of indicators an NEA status report on the use of indicators was produced. One important observation is that complementary indicators are now accepted by the majority of implementers and regulators as an important component of a safety case. The report also clearly shows the manifold use of indicators in a safety case, like supporting the safety case structure and applying multiple lines of reasoning, increasing the transparency of safety case arguments, assessment of repository safety and presenting impacts in the content of the natural environment, assessment of repository safety in different timeframes, addressing uncertainty in dose and risk calculations, assessment of subsystem performance, assessment of safety functions, scenario identification, and helping with communication, especially to non-technical audiences. The report gives some guidance on the use of indicators, which might be especially helpful for countries in an early stage of the repository programme.

In a second study on that topic a set of six indicators, previously recommended especially with regard to the safety function containment, have been applied in performance assessment calculations for repositories for HLW in a clay and in a rock salt formation. The detailed evaluation of the indicators allowed judging their applicability. The study very well showed the different results for some of the indicators with respect to clay and salt formations. Particularly indicators, which refer to actinides, deliver very different values, since due to strong sorption on bentonite and the clay host rock actinides are not released from the containment providing rock zone within one million years. For a repository in rock salt these radionuclides are important, since no sorption is considered during transport through the repository. In conclusion, the indicators *contribution to power density in porewater at the CRZ boundary*, and *contribution to radiotoxicity in*

groundwater are recommended for further use. For the indicator *proportion of the cumulative released quantity of substance over the safety case period*, it is strongly recommended to consider it nuclide-specific and not – as proposed – related to the total amount of all radionuclides. Further a cumulative representation of this indicator would be interesting. The indicators *concentration of released uranium and thorium in the porewater at the CRZ boundary* and *radionuclide concentration in the usable water near the surface* are not recommended.

A review and evaluation of literature was performed to qualitatively evaluate the relevance of microbial activity for the long-term performance of a deep geological repository in clay for high level waste and spent nuclear fuel and to identify which safety-relevant processes and properties can be potentially influenced by this activity. The analysis identified eight clay properties essential for maintaining safety functions of containment and retardation of the disposal system – swelling pressure, specific surface area, cation exchange capacity, anion sorption capacity, porosity, permeability, fluid pressure, plasticity – which can potentially be influenced by microbial processes in clay buffer and claystone. Important processes influenced by microbial activity are reduction of clay, dissolution of clay, biofilm formation, sulphate reduction, and gas production. This work provides a basis for the quantitative estimation of the maximum possible effects of microbial processes on the barrier system of a DGR in clay formations to be addressed in a future work.

Another topic dealt with inventories of radionuclides and stable elements in vitrified waste (CSD-V canisters) produced at La Hague and delivered to Germany, which are of high importance as input parameters for long-term safety analyses. For a subset of these radionuclides and stable elements, a dataset was available, since the inventories were determined – either by direct measurements or by involving established correlations – and reported by AREVA. This allowed verification of the validity of a model approach utilizing the data of burnup and activation calculations and auxiliary information on the reprocessing and vitrification process operated at La Hague. Having proved the validity of this approach the present work successfully estimated the minimum, average and maximum inventories of the radionuclides, which are of importance for safety analyses but were not reported by AREVA. A comparison with inventories predicted by Nagra for vitrified waste delivered from La Hague to Switzerland showed some differences, which are recommended to be addressed in a future bilateral or international framework.

Concerning bentonite re-saturation the range of applications for the vapour flow model VIPER was extended to bentonite-sand mixtures and systems under non-isothermal conditions. Both applications have been tested according to benchmark experiments within the EBS task force. The model application to the bentonite-sand mixture led to a significant improvement of the model, implementing a diffusive migration of interlayer water according to self-diffusivity. The related diffusion coefficient depends on the water content and increases with the amount of hydrate layers at the interlayer cations. The balance equation used in code VIPER was extended accordingly to a double-continuum model. Concerning the non-isothermal saturation of bentonite the model is able to describe the complex interactions during this overall process. In addition a laboratory experiment was started to characterize the final saturation state, because discussions in the EBS Task Force had shown that there is no conclusive experimental evidence about the steady-state conditions after a non-isothermal re-saturation. The experiment is running for more than two years, but the evaluation so far indicates a minimum time to reach steady-state of about 3 years. Therefore it is continued.

In this study the impact of climate changes on geosphere as well as on biosphere processes was investigated. In a previous work the impact of different discrete climate states was examined. The investigations presented here emphasized on climate transitions. With respect to the geosphere the impact of transient flow conditions caused by long-term climate changes on radionuclide transport in the far field of a repository is addressed for the first time. Temporal changes of glacials and periglacials derived from investigations in Sweden and Finland served as a basis for the future climate sequences considered here. The results of the flow simulations showed that the flow field and the salt water distribution at the calculation endpoint of 251,500 years are in good agreement with those calculated for a constant climate. This demonstrates that the system responds quickly to changing boundary conditions of the altered climate states of a glacial cycle. Regarding the radionuclide transport calculations significant differences between transient and constant flow modelling are observed, because the transport patterns are a set of the different flow features characteristic for the different unique climate states. The strongest impact was observed for weakly sorbing radionuclides (such as C-14 and I-129), and the lowest impact for strongly sorbing radionuclides, like Zr-93. This is in agreement with results for constant climates. In general the calculation showed that the impact of climate transitions on flow and radionuclide transport in the overburden of a repository host rock could be strong and need to be addressed by transient model calculations in long-term safety assessment.

The impact of future climate changes on biosphere modelling was investigated using generic, stylised models. Nine discrete climate states have been selected to cover the variety of potential different future climates occurring during the next million years in Northern Germany. The bandwidths covered by calculations for the nine discrete climate states are in a similar range as the bandwidths derived from uncertainty analyses based on parameter uncertainties. However, the uncertainty analysis should be regarded as a first estimation. More emphasis to derive probability density functions for the parameters and especially an approach for the treatment of correlations between the parameters is needed. The models also allowed calculating transition states for climate changes, which are of complex nature and particularly of interest for redox-sensitive radionuclides. The results indicate that processes occurring during climate transitions could cause radiation exposures, which are increased in comparison to discrete climate states. However, relatively high accumulations of redox-sensitive radionuclides in plants are significantly smoothed, because other exposition pathways not related to radionuclide mobilisation in soils contribute to the overall biosphere dose conversion factors.

Ruprechtov in Czech Republic (near city of Karlovy Vary) represents a Natural Analogue investigation site since mid-1990's. In the southern part of the investigation area an open pit kaolin excavation work started in year 2006. Since the so-called clay/lignite layers, containing the uranium enrichment investigated at the site even earlier, appear directly above the exploitable kaolin strata, the excavation work allowed to address specific questions and to perform few additional investigations (with regard to previous investigations) at the site. The first important result from the new project is that all geological exposures detected, analyzed and documented within the open pit kaolin mining activities at Ruprechtov site are in full compliance with the model assumptions derived from previous borehole investigations. So far, no facts could be ascertained that would contradict these assumptions. Further the impact of the kaolin mining on the uranium-enriched clay/lignite layers was investigated. In boreholes located in or in direct vicinity of the mining area, a clear effect of the mining activities on the water levels of the wells could be observed. However, groundwater analyses, including in-situ Eh/pH, element concentrations and isotopic signatures show that the system is geochemically well buffered and no oxidation effect could be identified. In order to identify the impact of oxidation on the clay/lignite layers with high uranium content, material from a location, where the excavation work had exposed the clay/lignite layer to the surface, was investigated. Mineralogical and element analyses, uranium disequilibrium series and sequential extraction measurements combined with $^{234}\text{U}/^{238}\text{U}$ activity ratio analyses clear-

ly confirmed the existence of an alteration front of about 20 cm into the surface of the uranium bearing clay/lignite layer. The installation of suction cups showed that the alteration can lead to quite high uranium concentrations in the surface water. These investigations also demonstrate the strength of the uranium isotope disequilibrium series analyses, which was significantly further developed by University Helsinki within the investigations at Ruprechtov site, to identify different uranium phases and geochemical alteration reactions in a natural system.

In a preliminary study undertaken here to assess the realisation possibilities of a virtual underground laboratory of a nuclear repository several requirements defined by GRS in co-operation with candidate future project partners were investigated. Among others, the import of geological data from the openGEO software as well as of mine layout data from CAD-software was successfully tested. Additionally, relevant possibilities for visualising the geological structures and the results of numerical simulations were investigated. The data used in this study were generated with process-level computer codes on basis of a comparably simple temperature calculation. In summary it was found and confirmed that the objectives of the envisaged VIRTUS software platform can be realised satisfactorily within a project duration of 3 years.

References

- /ÅKE08/ Åkesson, M.: EBS Task Force: Comments on Benchmark 2.1. Presentation on the 7th meeting of the SKB "Task Force EBS", Äspö, May 26-27, 2008.
- /AKE 02/ Auswahlverfahren für Endlagerstandorte. Empfehlung des AkEnd - Arbeitskreis Auswahlverfahren Endlagerstandorte, Dezember 2002.
- /AND 05/ Andra: Evolution phénoménologique du stockage géologique – Dossier argile 2005. Rapport Andra n° C RP ADS 04-0025 (English version available on Andra web site).
- /ARC 05/ Archer, D.; Ganopolski, A.: A movable trigger: Fossil fuel CO₂ and the onset of the next glaciation. *Geochem. Geophys. Geosys.* 6, Q05003, doi:10.1029/2004GC000891, 2005.
- /ARE 06a/ AREVA: Determination of guaranteed parameters of vitrified residues and their un-certainties. HAG QPR 132 Rev. 00, AREVA, 2006.
- /ARE 06b/ AREVA: Determination of additional parameters of vitrified residues and their uncer-tainties. HAG QPR 133 Rev. 00, AREVA, 2006.
- /ARE 08/ AREVA: Traitement des combustibles usés provenant de l'étranger dans les installa-tions AREVA NC de La Hague. Rapport 2008, AREVA, 2008.
- /AVV 12/ Allgemeine Verwaltungsvorschrift zu §47 Strahlenschutzverordnung: Ermittlung der Strahlenexposition durch die Ableitung radioaktiver Stoffe aus Anlagen oder Einrichtungen (28. August 2012). Erschienen im Bundesanzeiger, BAnz AT 05.09.2012 (2012).
- /BAL 07/ Baltés, B.; Röhlig, K.J.; Kindt, A.:Sicherheitsanforderungen an die Endlagerung hochradioaktiver Abfälle in tiefen geologischen Formationen – Entwurf der GRS. Gesellschaft für Anlagen- und Reaktorsicherheit (GRS) mbH, GRS-A-3358, Köln, 2007.

- /BAU 00/ Baudoin, P.; Gay, D.; Certes, C.; Serres, C.; Alonso, J.; Lührmann, L.; Martens, K.H.; Dodd, D.; Marivoet, J.; Vieno, T.: Spent fuel disposal Performance Assessment - SPA project. Final Report. EUR 19132 EN, Luxembourg 2000.
- /BEC 03/ Becker, D.-A.; Buhmann, D.; Storck, R.; Alonso, J.; Cormenzana, J.-L.; Hugi, M.; van Gemert, F.; O'Sullivan, P.; Laciok, A.; Marivoet, J.; Sillen, X.; Nordman, H.; Vieno, T.; Niemeyer, M., 2003: Testing of Safety and Performance Indicators (SPIN), EUR 19965 EN, European Commission, Brussels, <http://bookshop.europa.eu/>.
- /BEC 09/ Becker, D.-A.; Cormenzana, J.L.; Delos, A.; Duro, L.; Grupa, J.; Hart, J.; Landa, J.; Marivoet, J.; Orzechowski, J.; Schröder, T.-J.; Vokal, A.; Weber, J.R.; Weetjens, E.; Wolf, J.: Safety indicators and performance indicators. – PAMINA, Deliverable (D-N°:3.4.2); Braunschweig 2009.
- /BER04/ Berner, Ulrich; Streif, Hansjörg: Klimafakten-Der Rückblick: Ein Schlüssel für die Zukunft, 2004, ISBN 3-510-95913-2.
- /BET 06/ Bethke, C.M.: The Geochemist's Workbench Release 6.0, Hydrogeology Program, University of Illinois, 2006.
- /BIE 09/ Biennu, P.; Ferreux, L.; Androletti, G.; Arnal, N.; Lépy, M.-C.; Bé, M.-M.: Determination of ¹²⁶Sn half-life from ICP-MS and gamma spectrometry measurements. *Radiochimica Acta* 97, 687–694, 2009.
- /BIG 98/ Bignan, G.; Ruther, W.; Ottmar, H.; Schubert, A.; Zimmermann, C.: Plutonium isotopic determination by gamma spectrometry: recommendation for the ²⁴²Pu content evaluation using a new algorithm. *ESARDA Bulletin* 28, 1–6, 1998.
- /BIO 04/ BIOCLIM: Modelling sequential BIOSphere systems under CLIMate change for radioactive waste disposal, EC-Contract FIKW-CT-2000-00024, 2004
- /BLÜ 10/ Blümel, E.: Vorphase Virtuelles Untertagelabor im Steinsalz (VIRTUS plus) – Projektbericht, Fraunhofer Institut für Fabrikbetrieb und -automatisierung (IFF) Magdeburg, GRS-Auftrag UA 2950 (2010).

- /BMU 10/ BMU: Sicherheitsanforderungen an die Endlagerung wärmeentwickelnder radioaktiver Abfälle, Stand 30. September 2010,
http://www.bmu.de/atomenergie_ver_und_entsorgung/downloads/doc/42047.php
- /BOD 08/ Bodenez, P.; Röhlig, K.-J.; Besnus, F.; Vigfusson, J.; Smith, R.; Nys, V.; Bruno, G.; Metcalf, P.; Ruiz-Lopez, C.; Ruokola, E.; Jensen, M. (2008): European Pilot Study on the Regulatory Review of the Safety Case for Geological Disposal of Radioactive Waste. Symposium "Safety cases for the deep disposal of radioactive waste: Where do we stand?", 23-25 January 2007, Paris, France. OECD, Paris 2008, NEA No. 06319, ISBN 978-92-64-99050-0.
- /BOR 08/ Bornemann, O.; Behlau, J.; Fischbeck, R.; Hammer, J.; Jaritz, W.; Keller, S.; Mingerzahn, G.; Schramm, M.: Standortbeschreibung Gorleben, Teil 3: Ergebnisse der über- und untertägigen Erkundung des Salinars, Geol. Jb., C 73, 211 (2008).
- /BRO 01/ Brockt, G.; Fritz, K.-J.; Stedingk, K.; Witzke, T.: Die ehemalige Kaligrube Brefeld bei Staßfurt – Streiflichter aus einer faszinierenden Welt. Mineralien-Welt 12(2), 15-27, 2001.
- /BUE 85/ Bütow, E.; Brühl, G.; Gülker, M.; Heredia, L.; Lütke-meier-Hosseini-pour, S.; Naff, R.; Struck, S.: PSE-Abschlussbericht, Fachband 18 - Modellrechnungen zur Ausbreitung von Radionukliden im Deckgebirge. Projektleitung HMI; Berlin, 1985.
- /BUH 08a/ Buhmann, D.; Mönig, J.; Wolf, J.; Heusermann, S.; Keller, S.; Weber, J. R.; Bollingerfehr, W.; Filbert, W.; Kreienmeyer, M.; Krone, J.; Tholen, M.: Überprüfung und Bewertung des Instrumentariums für eine sicherheitliche Bewertung von Endlagern für HAW – ISIBEL. FKZ 02 E 10055 (BMW i), Gemeinsamer Bericht von DBE TECHNOLOGY GmbH, BGR und GRS. DBE TECHNOLOGY GmbH Peine, 2008.

- /BUH 08b/ Buhmann, D.; Mönig, J.; Wolf, J.: Untersuchungen zur Ermittlung und Bewertung von Freisetzungsszenarien. FKZ 02 E 10055 (BMWi), Gesellschaft für Anlagen- und Reaktorsicherheit (GRS) mbH, GRS-233, Braunschweig, 2008.
- /CAD 88/ Cadelli, N.; Cottone, G.; Orlowski, S.; Bertozzi, G.; Girardi, F.; Saltelli, A.: PAGIS: Performance Assessment of Geological Isolation Systems for Radioactive Waste – Summary Report. EUR Report 11775 EN, Luxemburg, 1988.
- /CED 04/ Cedercreutz, Jannika, POSIVA 2004-2006, Future Climate Scenarios for Olkiluoto with Emphasis on Permafrost, Dezember 2004, Helsinki University of Technology Rock Engineering – Geology, ISBN 951-652-132-0, ISSN 1239-3096.
- /DAV 05/ Davies, C.; Bernier, F.: Impact of the excavation disturbed or damaged zone (EDZ) on the performance of radioactive waste geological repositories.- Proc. of a European Commission Cluster conference and workshop, Luxembourg, 3 to 5 November 2003. EUR 21028 EN, 2005.
- /DER 98/ Deroubaix, D.: The French view for spent fuel treatment: reprocessing, conditioning and recycling. In: Status and trends in spent fuel reprocessing, IAEA-TECDOC-1103, International Atomic Energy Agency, 19–31, 1998.
- /DIX 00/ Dixon, D.A.; Chandler, N.A.: Physical properties of materials recovered from the Isothermal Buffer-Rock-Concrete Plug Interaction Test conducted at the URL. Ontario Power Generation, Nuclear Waste Management Division Report No. 06819-REP-01200-10003-R00, 2000.
- /DUA 06/ Duan, J.; Hou, B.; Yu, Z.: Characteristics of sulfide corrosion products on 316L stainless steel surfaces in the presence of sulfate-reducing bacteria. Materials Science and Engineering C 26, 624–629, 2006.
- /EUR 97/ European Commission: Evaluation of Elements Responsible for the effective Engaged dose rates associated with the final Storage of radioactive waste: EVEREST project. Volume 1: Common aspects of the study. Final report. EC, EUR 17449/1 EN, Luxemburg, 1997.

- /EUR 04/ European Patent Nr. 1 184 092 (00 120 249.8-2307). Verfahren zum Verhindern des Eindringens einer Salzlösung in einen Hohlraum einer Salzlagstätte. 2004.
- /EUR 09/ European Commission: PAMINA 2006-2009: European Project PAMINA (Performance Assessment Methodologies in Application to Guide the Development of the Safety Case). <http://www.ip-pamina.eu/>.
- /EUR 10/ European Commission and OECD/NEA: The Joint EC/NEA Engineered Barrier System Project: Synthesis Report (EBSSYN). Final Report. EUR 24232 EN, Luxembourg, 2010.
- /FEI 99/ Fein, E., and Schneider, A., d³f – Ein Programmpaket zur Modellierung von Dichteströmungen, Final Report, FKZ 02 E 349-96 (BMBF), GRS-139, Gesellschaft für Anlagen- und Reaktorsicherheit (GRS) mbH, Braunschweig (1999) 245 p.
- /FEI 04/ Fein, E.: Software Package r³t. Model for Transport and Retention in Porous Media, Final Report. FKZ 02 E 91482 (BMW), GRS-192, Gesellschaft für Anlagen- und Reaktorsicherheit (GRS) mbH, Braunschweig (2004) 319 p.
- /FIR 99/ Firestone. R.B.: Table of Isotopes - Volume I + II. Eighth edition. John Wiley and Sons. Inc.. New York. 1999.
- /FLU 09/ Flüge, J.: Radionuclide Transport in the Overburden of a Salt Dome – The Impact of Extreme Climate States, Verlag Dr.Hut, München (2009) 209 p.
- /FRE 06/ Freyer, D.; Voigt, V.; Böttge, V.: Zur thermischen Stabilität von Tachhydrit und Carnallit Kaili und Steinsalz, Heft1/2006, 28 – 37, 2006.
- /GAT 05/ Gatabin, C.; Billaud, P.: Bentonite THM mock-up experiments – Sensors data report. Technical data report NT DPC/SCCME 05-300-A, CEA, 2005.
- /GIR 08/ Giroux, M.; Grygiel, J.-M.; Boullis, B.; Masson, M.; Storrer, F.: The back-end of the fuel cycle in France: status and prospects. In: Spent fuel reprocessing options, IAEA-TECDOC-1587, International Atomic Energy Agency, 79–100, 2008.

- /GRS 10/ GRS: Verschlussysteme in Endlagern für wärmeentwickelnde Abfälle in Salzformationen, Workshop der GRS in Zusammenarbeit mit dem Projektträger Karlsruhe PTKA-WTE, Braunschweig, 24. – 25. August 2010, FKZ 02 E 10548 (BMWi), GRS-267.
- /GUI 02/ Guillaumont R, Fanghänel Th, Fuger J, Grenthe I, Neck V, Palmer DA, Rand MH, OECD: NEA-TDB, Chemical Thermodynamics, Vol. 5. Update on the chemical thermodynamics of uranium, neptunium, plutonium, americium and technetium. Elsevier, 2003.
- /GUO06/ Guo, R.; Dixon, D.: The Isothermal Test: Description and Material Parameters for Use by the Engineered Barriers Systems Task Force. Technical Memorandum, 06819(UF)-03700.3 SKB-T05, Ontario Power Generation, 2006.
- /HAR 84/ Harvie, D. E.; Moller, N.; Weare, J. H.: The prediction of mineral solubilities in natural waters: the Na-K-Mg-Ca-H-Cl-SO₄—OH-HCO₃-CO₃—H₂O system to high ionic strength at 25°C, *Geochimica et Cosmochimica Acta*, v. 48, 723-751, 1984.
- /HER 05/ Herbert, H.-J.; Kull, H.; Müller-Lyda, I.. Weiterentwicklung eines Selbst Verteilenden Versatzes (SVV) als Komponente im Barriersystem Salinar. Final report. FKZ 02 C 0830 (BMBF), GRS-220, ISBN 3-931995-90-9, 53 p., 2005.
- /HER 07/ Herbert, H.-J.: Self Sealing Backfill (SVV) – A salt based material for constructing seals in salt mines. Proceedings of the 6th Conference on the Mechanical Behaviour of Salt, 22-25, Hannover, Mai 2007.
- /HER 11/ Herbert, H.-J.; Hertes, U.; Meyer, L.; Hellwald, K.; Dittrich, J.: Qualifizierung von Strömungsbarriere in Salzformationen. Final report FKZ 02 C 1335 (BMBF), GRS-263, ISBN 978-3-939355-40-3, 201 p., 2011.
- /HER 12/ Herbert, H.-J.; Meyer, L.; Hertes, U.: SVV a self-sealing material for technical barriers in salt mines – experimental results.- In: Ed. Bérest et al., Proc. Mechanical Behavior of salt VII, p.255-262, Taylor & Francis Group, London. ISBN 978-0-415-62122-9., 2012.

- /IAE 95/ IAEA: The Principles of Radioactive Waste Management, Safety Fundamentals, Safety Series No. 111-F. IAEA, Vienna, Austria, 1995.
- /IAE 97/ IAEA: Joint Convention on the Safety of Spent Fuel Management and on the Safety of Radioactive Waste Management. IAEA, Vienna, Austria, 1997.
- /IAE 99/ IAEA: Safety Assessments for Near Surface Disposal of Radioactive Waste, IAEA Safety Standards Series No. WS-G-1.1. IAEA, Vienna, Austria, 1999.
- /IAE 00/ IAEA: Application of Safety Assessment Methodologies for Near Surface Waste Disposal Facilities (ASAM), IAEA, Vienna, Austria, 2000.
- /IAE 03a/ IAEA: Safety Indicators for the Safety Assessment of Radioactive Waste Disposal, Sixth report of the INWAC Subgroup on Principles and Criteria for Radioactive Waste Disposal. , IAEA-TECDOC-1372. IAEA, Vienna, Austria, 2003.
- /IAE 03b/ IAEA: "Reference Biospheres" for solid radioactive waste disposal: Report of BIOMASS Theme 1 of the BIOSphere Modelling and ASSESSment (BIOMASS) Programme. Vienna, Austria, 2003.
- /IAE 04/ IAEA: Safety Assessment Methodologies for Near Surface Disposal Facilities (ISAM), Vol. I – Review and enhancement of safety assessment approaches and tools; Vol. II – Tests Cases, IAEA, Vienna, Austria, 2004.
- /IAE 06/ IAEA: Geological Disposal of Radioactive Waste. Safety Requirements. IAEA SAFETY STANDARDS SERIES No. WS-R-4, Wien, 2006, http://www-pub.iaea.org/MTCD/publications/PDF/Pub1231_web.pdf
- /IAE 10/ IAEA: Handbook of parameter values for the prediction of radionuclide transfer in terrestrial and freshwater environments, Technical Reports Series No. 472, Vienna, Austria 2010.
- /ICR 98a/ ICRP: Radiological Protection Policy for the Disposal of Radioactive Waste. International Commission on Radiological Protection Publication 77, Annals of the ICRP, 27 Supplement, ISBN 0080427499.

- /ICR 98b/ ICRP: Radiation Protection Recommendations as Applied to the Disposal of Long-Lived Solid Radioactive Waste. International Commission on Radiological Protection Publication 81, Annals of the ICRP, 28 (4), 1-25, ISBN 0080438598, 1998.
- /ICR 07/ ICRP: The 2007 Recommendations of the International Commission on Radiological Protection. ICRP (International Commission on Radiological Protection), Publication 103. Annals of the ICRP, 37:2-4, 2007.
- /IGD 09/ IGD-TP: Implementing Geological Disposal of Radioactive Waste Technology Platform, Vision Report, published as EC special report EUR 24160 EN, 2009.
- IGD-11/ IGD-TP: Implementing Geological Disposal of Radioactive Waste Technology Platform, Final Draft Deployment Plan (for public consultation). 2011.
- /ING 98/ Ingram, C.: Palaeoecology and geochemistry of shallow marine ostracoda from the Sand Hole Formation, Inner Silver Pit, southern North Sea. *Quat. Sci. Rev.* 17, 913-929, 1998.
- /JOE 10/ Jörg, G.; Bühnemann, R.; Hollas, S.; Kivel, N.; Kossert, K.; Van Winckel, S.; Lierse v. Gostomski, C.: Preparation of radiochemically pure ⁷⁹Se and highly precise determination of its half-life. *Applied Radiation and Isotopes* 68, 2339–2351, 2010.
- /KAP 61/ Kappelmeier, O.: Geothermik. in: Bentz, A. [Ed.], *Lehrbuch der Angewandten Geologie*, Vol. 1. Enke: Stuttgart (1961) 863-889.
- /KIM 04/ Kim, J.; Dong, H.; Seabaugh, J.; Newell, S. W.; Eberl, D.D.: Role of Microbes in the smectite-to-illite reaction. *Science* 303, 830–832, 2004.
- /KLI 07/ Klinge, H.; Boehme, J.; Grisseemann, C.; Houben, G.; Ludwig, R.; Rübel, A.; Schelkes, K.; Schildknecht, F.; Suckow, A.: Standortbeschreibung Gorleben, Teil 1: Die Hydrogeologie des Deckgebirges des Salzstocks Gorleben, *Geol. Jb.*, C 71 (2007) 199.

- /KLI 02/ Klinge, H.; Köthe, A.; Ludwig, R.; Zwirner, R.: Geologie und Hydrogeologie des Deckgebirges über dem Salzstock Gorleben, Z. Angew. Geol., 2 7-15 (2002).
- /KOE 00/ Kösters, E.; Vogel, P.; Schelkes, K.: 2D-Modellierung der paläohydrogeologischen Entwicklung des Grundwassersystems im Elberaum zwischen Burg und Boitzenburg, BGR, Hannover 2000.
- /KOE 07/ Köthe, A.; Hoffmann, N.; Krull, P.; Zirngast, M.; Zwirner, R.: Standortbeschreibung Gorleben, Teil 2: Die Geologie des Deck- und Nebengebirges des Salzstocks Gorleben, Geol. Jb. C 72 (2007) 147.
- /KRI 07/ Kristensson, O.; Börgesson, L.: CRT – Canister Retrieval Test; EBS Task Force Assignments. Clay Technology, 2007.
- /KRÖ 04/ Kröhn, K.-P.: Modelling the re-saturation of bentonite in final repositories in crystalline rock. Final report, FKZ 02 E 9430 (BMWA), Gesellschaft für Anlagen- und Reaktorsicherheit (GRS) mbH, GRS-199, Köln, 2004.
- /KRÖ 11/ Kröhn, K.-P.: Code VIPER Theory and Current Status. Status report, FKZ 02 E 10548 (BMWi), Gesellschaft für Anlagen- und Reaktorsicherheit (GRS) mbH, GRS-269, Köln, 2011.
- /KUR 04/ Kursten, B.: Results from corrosion studies on metallic components and instrumentation installed in the OPHELIE mock-up. Presentation on EIG EURIDICE' OPHELIE Day, June 10, 2004 (retrieved on May 25, 2011 from <http://www.euridice.be/eng/06publicaties2004agendaO.shtml>).
- /LAN 97/ Langmuir, D.: Aqueous environmental geochemistry. Prentice Hall, Upper Saddle River, New York, p. 600, 1997.

- /LEG 04/ Legarth, B.; Tischer, T.; Huenges, E.: Stimulating for productivity: Hydraulic Proppant Fracturing Treatments in Rotliegend Sandstones. In: Huenges, E., Wolfgramm, M. [Eds]: Sandsteine im In-situ-Geothermieslabor Groß Schönebeck – Reservoir-Charakterisierung, Stimulation, Hydraulik und Nutzungskonzepte, Scientific Technical Report STR04/03. Potsdam (Geoforschungszentrum Potsdam (GFZ)) (2004) 93-106. Download at: <http://www.gfz-potsdam.de/bib/zbstr.htm> (date of access: February 2008).
- /LIB 98/ Liberge, R.; Desvaux, J.-L.; Pageron, D.; Saliceti, C.: Industrial experience of HLW vitrification at La Hague and Marcoule. Proceedings of the annual Waste Management 1998 Symposium, Session 14 – HLW Vitrification, 1998.
- /LUD 02/ Ludwig, R.; Kösters, E.: Hydrogeologisches Modell Gorleben – Entwicklung bis zum paläohydrogeologischen Ansatz, Hydrogeologische Modelle – Ein Leitfaden mit Fallbeispielen. Arbeitskreis “Hydrogeologische Modelle und Grundwassermanagement” der Fachsektion Hydrogeologie der Deutschen Geologischen Gesellschaft (eds), Schriftenreihe der Deutschen Geologischen Gesellschaft, 24 (2002) 69-77.
- /MAD 95/ Madic, C.; Bourges, J.; Dozol, J.-F.: Overview of the long-lived radionuclide separation processes developed in connection with the CEA’s SPIN programme. Proceedings of the Third International Information Exchange Meeting on Actinide and Fission Product Partitioning and Transmutation, 381–393, 1995.
- /MAG 06/ Magill, J., and Pfennig, G., Galy, J., Karlsruhe Nuklidkarte, European Communities (2006).
- /MIL 12/ Miller, B.; Noseck, U.; Becker, D; Grupa, J.; Marivout, J.; Wolf, J.: Indicators in the Safety Case. An NEA Status Report. OECD/NEA, Paris, 2012.
- /NAG 02/ Nagra: Projekt Opalinus Clay: The long-term safety of a repository for spent fuel, vitrified high-level waste and long-lived intermediate-level waste sited in the Opalinus Clay of the Züricher Weinland. - Nagra, NTB 02-05; Wettlingen 2002.

- /NAG 08/ Nagra: Modellhaftes Inventar für radioaktive Materialien MIRAM 08. Technischer Bericht NTB 08-06, Nagra, Wettingen, Schweiz, 2008.
- /NEA 91/ NEA: Disposal of Radioactive Waste: Review of Safety Assessment Methods. A Report of the Performance Assessment Advisory Group of the Radioactive Waste management Committee. OECD Nuclear Energy Agency. Paris, 1991.
- /NEA 97/ NEA: Lessons Learnt from Ten Performance Assessment Studies (IPAG), OECD Nuclear Energy Agency, Paris, France, 1997.
- /NEA 99/ NEA: Confidence in the Long-term Safety of Deep Geological Repositories: Its Development and Communication, OECD Nuclear Energy Agency, Paris, France, 1999.
- /NEA 04a/ NEA: Post-closure Safety Case for Geological Repositories: Nature and Purpose, NEA Report No. 3679, OECD/NEA, Paris, France, 2004.
- NEA 04b/ NEA: Safety of disposal of spent fuel, HLW and long-lived ILW in Switzerland. An international peer review of the post-closure radiological safety assessment for disposal in the Opalinus Clay of the Zürcher Weinland. NEA No. 5568, OECD, 2004.
- /NEA 08a/ NEA: Safety Cases for Deep Geological Disposal of Radioactive Waste: Where Do We Stand? Symposium Proceedings, Paris, France, 23-25 January 2007, OECD NEA, NEA No. 6319, 2008.
- /NEA 08b/ NEA: Moving Forward with Geological Disposal of Radioactive waste – a collective Statement by the OECD/NEA Radioactive Waste Management Committee (RWMC), OECD/NEA No. 6433, Paris 2008.
- /NEA 09/ NEA: International Experiences in Safety Case for Geological Repositories (INTESC) NEA Report No. 6417, OECD/NEA, Paris, France, 2009.
- /NEA 11a/ NEA: Strategic Plan 2011-2016 for the Radioactive Waste Management Committee, NEA/RWM(2011)12, Paris, 28 July 2011.

- /NEA 11b/ NEA: <http://www.oecd-nea.org/rwm/rkm/documents/rkm-collective-statement-en.pdf>.
- /NEA 11c/ NEA <http://www.oecd-nea.org/rwm/docs/2011/rwm2011-6.pdf>.
- /NEA 11d/ NEA: Reversibility and retrievability (R&R) for the Deep Disposal of High-Level Radioactive Waste and Spent Fuel, Final Report of the NEA R&R Project (2007 2011), Paris, December 2011.
- /NEA 12a/ NEA: <http://www.oecd-nea.org/rwm/clayclub/>
- /NEA 12b/ NEA: <http://www.oecd-nea.org/rwm/saltclub/>
- /NEA 12c/ NEA: <http://www.oecd-nea.org/rwm/docs/2012/rwm-r2012-2.pdf>
- /NEA 12d/ NEA: Cementitious Materials in Safety Cases for Geological Repositories for Radioactive Waste: Role, Evolution and Interactions. OECD/NEA, Paris, March 2012.
- /NEA 12e/ NEA: The long-term Radiological Safety of a Surface Disposal Facility for Low-level Waste in Belgium. An International Peer Review of Key Aspects of ONDRAF/NIRAS´Safety Report of November 2011 in Preparation for the License Application. OECD/NEA, Paris 2012.
- /NEA 12f/ NEA: The Post-Closure Radiological Safety Case for a Spent Fuel Repository in Sweden. An international peer review of the SKB license-application study of March 2011 (Final report). OECD/NEA, Paris 2012.
- /NOS 06/ Noseck, U.; Brassler, Th.: Radionuclide transport and retention in natural rock formations – Ruprechtov site. FKZ 02 E 9 (BMW), Gesellschaft für Anlagen- und Reaktorsicherheit, GRS-218, Köln. 2006.
- /NOS 08a/ Noseck, U., Becker, D., Fahrenholz, C., Fein, E., Flügge, J., Kröhn, K.-P., Mönig, J., Müller-Lyda, I., Rothfuchs, T., Rübel, A., Wolf, J.: Scientific basis for the assessment of the long-term safety of repositories. Final report, FKZ-02 E 9954 (BMW), Gesellschaft für Anlagen- und Reaktorsicherheit (GRS) mbH, GRS-237, Braunschweig, 2008.

- /NOS 08b/ Noseck, U., Fahrenholz, C., Flügge, J., Fein, E., Schneider, A., Pröhl, G., 2008. Impact of climate change on far-field and biosphere processes for a HLW repository in rock salt. FKZ-02 E 9954 (BMW), Gesellschaft für Anlagen und Reaktorsicherheit, (GRS) mbH, GRS-241. Braunschweig 2008.
- //NOS 08c/ Noseck, U.; Brassler, Th.; Suksi, J.; Havlova, V.; Hercik, M.; Denecke, M.A.; Förster, H.J.: Identification of uranium enrichment scenarios by multi-method characterization of immobile U phases. *J. Phys. Chem. Earth*, 33, 969-977, 2008.
- /NOS 09/ Noseck U, Rozanski K, Dulinski M, Havlova V, Sracek O, Brassler Th, Hercik M, Buckau G: Carbon chemistry and groundwater dynamics at natural analogue site Ruprechtov, Czech Republic: insights from environmental isotopes. *Appl. Geochem.* 24, 1765-1776., 2008.
- /NOS 10/ Noseck, U., Havlova, V., Suksi, J., Cervinka, R., Brassler, Th.: Geochemical behaviour of uranium in sedimentary formations: insights from a natural analogue study. *Proceedings of The 2009 12th International Conference on Environmental Remediation and Radioactive Waste Management. ICM2009*, October 11-15, 2009, Liverpool, UK.
- /OBE 99/ Oberli, F.; Gartenmann, P.; Meier, M.; Kutschera, W.; Suter, M.; Winkler, G.: The half-life of ¹²⁶Sn refined by thermal ionization mass spectrometry measurements. *International Journal of Mass Spectrometry* 184, 145–152, 1999.
- /OLI 96/ Olivella, S.; Gens, A.; Carrera, J.; Alonso, E. E.: "Numerical formulation for a simulator (CODE_BRIGTH) for the coupled analysis of saline media. *Engineering Computations*, Vol. 13 No. 7, pp. 87 – 112, MCB University Press, 1996.
- /OLY 05/ Olyslaegers, G.; Zeevaert, T.; Pinedo, P.; Simon, I.; Proehl, G.; Kowe, R.; Chen, Q.; Mobbs, S.; Bergstroem, U.; Hallberg, B.; Katona, T.; Eged, K.; Kanyar, B.: A comparative radiological assessment of five European biosphere systems in the context of potential contamination of well water from the hypothetical disposal of radioactive waste. *J. Radiol. Prot.* 25, 375-391, 2005.

- /OND 08/ Ondraf: Evolution of the Near-Field of the Ondraf/Niras repository concept for Category C Wastes. – Ondraf/Niras report NIROND-TR 2007-07E, Brussels, Belgium.
- /PAT 09/ Patterson, D. J.: Seeing the big picture on microbe distribution. *Science* 325, 1506–1507, 2009.
- /PED 05/ Pedersen, K.: Microorganisms and their influence on radionuclide migration in igneous rock environments. *Journal of Nuclear and Radiochemical Sciences* 6, 11–15, 2005.
- /PHI 80/ Phillips, J.R.; Halbig, J.K.; Lee, D.M.; Beach, S.E.; Bement, T.R.; Dermendjiev, E.; Hatcher, C.R.; Kaieda, K.; Medina, E.G.: Application of non-destructive gamma-ray and neutron techniques for the safeguarding of irradiated fuel materials. LA-8212, Los Alamos National Laboratory, USA, 1980.
- /POL 93/ Pollastro, R. M.: Considerations and applications of the illite/smectite geothermometer in hydrocarbon-bearing rocks of miocene to mississippian age. *Clays and Clay Minerals* 41, 119–133, 1993.
- /POS 09/ Posiva: TKS-2009. Nuclear Waste Management at Olkiluoto and Loviisa Power Plants. Review of Current Status and Future Plans for 2010 –2012, Posiva, Eurajoki, Finland, 2009.
- /RES 10/ Resele, G.; Brommundt, J.; Holocher, J.; Kämpfer, Th.; Mayer, G.; Niemeyer, M.; Mönig, J.; Rübél, A.: WS2044- VerSi: Methode für den quantitativen Vergleich von Endlagersystemen. AF-Colenco / Gesellschaft für Anlagen- und Reaktorsicherheit (GRS) mbH. AF-Colenco 1313/27 und GRS-A-3545. Baden, Braunschweig, 2010.
- /RUE 07/ Rübél, A.; Becker, D.-A.; Fein E.: Radionuclide transport modelling to assess the safety of repositories in clays. FKZ 02 E 9813 (BMW), Gesellschaft für Anlagen und Reaktorsicherheit (GRS) mbH, GRS 228; Braunschweig, 2007.

- /RUE 10/ Rübél A.; Becker D.-A.; Fein E.; Ionescu, A.; Lauke, T.; Mönig, J.; Noseck, U.; Schneider, A.; Spießl, S.; Wolf, J.: Development of Performance Assessment Methodologies. FKZ 02 E 10276 (BMW), Gesellschaft für Anlagen und Reaktorsicherheit (GRS) mbH, GRS-259; Braunschweig, 2010.
- /SAN 96/ Sanzharova, N.I.; Kotik, V.A.; Arkhipov, A.N.; Sokolik, G.A.; Ivanov, Y.A.; Fesenko, S.V.; Levchuk S.E.: The quantitative parameters of the vertical migration of radionuclides in the soils in different types of meadows. Radiation Biology. Radiology, vol. 36 (4), 488 – 496 (1996).
- /SAN 06/ Sánchez, M.; Gens, A.: FEBEX Project. Final report on thermo-hydro-mechanical modelling. Technischer Bericht, 05-2/2006, ENRESA, 2006.
- /SAN 02/ Sander, W.; Herbert, H.-J.: Wirksamkeit der Abdichtung von Versatzmaterialien. – Geochemische Untersuchungen zum Langzeitverhalten von Salzversatz mit Zuschlagstoffen. FKZ 02 E 9430 (BMW), Gesellschaft für Anlagen und Reaktorsicherheit (GRS) mbH, GRS-180, ISBN 3-931995-48-8, Cologne, 2002.
- /SAN 09/ Sanz-Montero, M.E.; Rodríguez-Aranda, J.P.; Pérez-Soba, C.: Microbial weathering of Fe-rich phyllosilicates and formation of pyrite in the dolomite precipitating environment of a Miocene lacustrine system. European Journal of Mineralogy 21, 163–175, 2009.
- /SCH 01/ Schneider, M.; Coeytaux, X.; Faïd, Y. B.; Marignac, Y.; Rouy, E.; Thompson, G.; Fairlie, I.; Lowry, D.; Sumner, D.: Possible toxic effects from the nuclear reprocessing plants at Sellafield and Cap de La Hague. A working document prepared by WISE-Paris for the STOA Panel, Directorate A, Directorate General for Research, European Parliament, 2001.
- /SEM 12/ Semioshkina, N.; Staudt, Ch.; Kaiser, Ch.; Fahrenholz, Ch., Noseck, U.: Impact of different climates and climate transitions on biosphere modelling in long-term safety assessment. Gesellschaft für Anlagen- und Reaktorsicherheit (GRS) mbH. FKZ-02 E 10548 (BMW), GRS-299, Braunschweig, September 2012.

- /SKB 10/ Svensk Kärnbränslehantering AB: Climate and climate-related issues for the safety assessment SR-Site, Technical Report, TR-10-49, December 2010.
- /SKB 11/ SKB: Long-term safety for the final repository for spent nuclear fuel at Forsmark. Main report of the SR-Site project. Technical Report TR-11-01, Svensk Kärnbränslehantering AB, 2011.
- /STR 11/ Stroes-Gascoyne, S.; Schippers, C.; Sergeant, A.; Hamon, C. J.; Neble, S.; Vesvres, M.-H.; Barsotti, V.; Poulain, S.; Le Marrec, C.: Biogeochemical processes in a clay formation in situ experiment: Part D – microbial analyses – synthesis of results. Applied Geochemistry 26, 980–989, 2011.
- /SUT 98/ Suter, D., Biehler, D., Blaser, P., Hollmann, A., Derivation of a sorption data set for the Gorleben overburden, Proceedings DisTec 98, International Conference on Radioactive Waste Disposal, Hamburg (1998) 581-584.
- /THE 09/ THERESA: <http://www.theresaproject.com/web/page.aspx?sid=6954>.
- /TIM 09/ TIMODAZ: <http://www.timodaz.eu/conference09/> .
- /VIG 07/ Vigfusson, J.; Maudoux, J.; Raimbault, P.; Röhlig, K.-J.; Smith R. E.: European Pilot Study on The Regulatory Review of the Safety Case for Geological Disposal of Radioactive Waste Case Study: Uncertainties and their Management. Paris, 2007.
- /VIL 05/ Villar, M.V.; Martín, P.L.; Barcala, J.M.: Infiltration test at isothermal conditions and under thermal gradient. Technical report CIEMAT/DMA/M2140/1/05, CIEMAT, Madrid, 2005.
- /WEA 86/ Weast. C.W.: CRC Handbook of Chemistry and Physics. 67th edition. CRC Press. Inc.. Boca Raton. Florida. 1986.
- /WHO 11/ World Health Organisation: Guidelines for Drinking Water Quality. Fourth Edition. World Health Organisation, Geneva, Switzerland, 2011.

- /WOL 08/ Wolf, J.; Becker, D.-A.; Rübeler, A.; Noseck, U: Safety and performance indicators for repositories in salt and clay formations. FKZ 02 E 10548 (BMW), Gesellschaft für Anlagen- und Reaktorsicherheit (GRS) mbH, GRS-240; Braunschweig, 2008.
- /WER 11/ Wersin, P.; Leupin, O. X.; Mettler, S.; Gaucher, E. C.; Mäder, U.; De Canièrè, P.; Vinsot, A.; Gabler, H. E.; Kunimaro, T.; Kiho, K.; Eichinger, L.: Biogeochemical processes in a clay formation in situ experiment: Part A – Overview, experimental design and water data of an experiment in the Opalinus Clay at the Mont Terri Underground Research Laboratory, Switzerland. *Applied Geochemistry* 26, 931–953, 2011.
- /WIL 06/ Willman, C.; Håkansson, A.; Osifo, O.; Bäcklin, A.; Svärd, S. J.: Non-destructive assay of spent nuclear fuel with gamma-ray spectroscopy. *Annals of Nuclear Energy* 335, 427–438, 2006.
- /ZIN 65/ Zinken, C.: Mitteilung an Prof. H. B. Geinitz vom 18. März 1865 [Über ein neues Mineral, Kainit].- *Neues Jahrbuch für Mineralogie, Geologie und Paläontologie*, 310. 1865.

List of figures

Fig. 2.1	Example of a high-level generic safety case flowchart, showing the key elements and linkages	13
Fig. 2.2	Detailed generic flowchart of the safety assessment component which is included in the compilation of a safety case of the upper level generic flowchart.....	14
Fig. 2.3	High-level Long-lived Vitrified Waste Modules – Chronological evolution of the THMCGRB processes during the post-closure period /AND 05/.....	18
Fig. 2.4	Story boards representing the transverse (top) and longitudinal (bottom) cross section of a disposal tunnel /OND 08/	20
Fig. 2.5	Iterative management of uncertainties (adapted from Figure 6-9 of /POS 09/).....	27
Fig. 2.6	Example of a high-level generic flowchart, showing in red the feedback loop elaborated in Fig. 2.5 (adapted from Fig. 2.1).....	28
Fig. 2.7	Schematic illustration for the release of radionuclides out of the CRZ for a repository in clay and rock salt, respectively	49
Fig. 2.8	Compartments of the generic repository system and the locations of the CRZ and the indicator assessment (I1-I6).....	50
Fig. 2.9	The cumulative released quantities from the CRZ.....	59
Fig. 2.10	The contribution to power density in porewater at the CRZ boundary	60
Fig. 2.11	The contribution to radiotoxicity at the CRZ	61
Fig. 2.12	The effective individual dose in the biosphere.....	62
Fig. 2.13	Compartments of the generic repository system and the locations of the CRZ and the indicator assessment (I1-I6).....	64
Fig. 2.14	Plane view of the repository concept.....	66
Fig. 2.15	Elemental concentrations of released uranium from the repository	71
Fig. 2.16	Elemental concentrations of released thorium from the repository	72
Fig. 2.17	The contribution to power density in groundwater at the CRZ.....	73
Fig. 2.18	The contribution to radiotoxicity at the CRZ	74

Fig. 2.19	Naturally-occurring radionuclide concentrations in the near-surface water.....	75
Fig. 2.20	Effective individual dose [Sv/a], and main contributors to dose.....	76
Fig. 3.1:	The organization of the Technology Platform IGD-TP.....	109
Fig. 4.1	Schematic summary of sources of electron donors and acceptors for microbial activity in a DGR in clay as well as of microbial metabolism products of major importance for its long-term performance	114
Fig. 4.2	(A) Scanning electron microscopy micrograph of bacteria-shaped, iron-rich sulphides (arrowed) arranged between the exfoliation planes of biotite (denoted by B) grains (see inset with a width of 20 µm for higher magnification) /SAN 09/. (B) Transmission electron microscopy micrograph of the microbially reduced smectite sample with a ~40-nm-thick packet of 1.0-nm illite layers embedded in the matrix of 1.3-nm smectite layers /KIM 04/.....	116
Fig. 4.3	Locations indicative of microbially influenced corrosion on the lining (A) and the heat-generating tube (D) after the five-year-long contact with backfill consisting to 60 % of clay and with sand, respectively. Scanning electron microscopy micrograph (B) and energy-dispersive X-ray spectroscopy map of sulphur (C) across the interface between a stainless steel and the deposit from (A). Energy-dispersive X-ray spectroscopy maps of iron (E) and sulphur (F) in the deposit from (D) /KUR 04/.....	119
Fig. 4.4	Inventories of neodymium (at the time of vitrification) in CSD-V canisters delivered by AREVA to Germany.....	127
Fig. 4.5	(A) Dry kainite layers in the mine Brefeld, Germany indicate a natural sealing of brine pathways (Foto /BRO 01/); (B) due to mining activities reactivated brine pathways in layers of kainite, bloedite and epsomite...	137
Fig. 4.6	Schematic diagram of the equipment for crystallization pressure measurements (from /HER 07/)	138
Fig. 4.7	Schematic diagram of the development of fluid pressure, crystallization pressure and volume changes during the flooding of SVV with brines (from /HER 07/)	139

Fig. 4.8	Laboratory experiments with SVV at different scales: (left) in pressure cells of different sizes and geometries, (right) in large pressure tubes (from /HER 07/)	139
Fig. 4.9	Example of permeability measurements on samples from an experiment in a pressure tube of 3 m length and 20 cm in diameter with pure MgSO ₄ flooded at 8 MPa with tachyhydrite brine (figure from /HER 07/)	140
Fig. 4.10	Porosity-permeability relationship of SVV samples with IP21 brine compared to data for dry and wet crushed rock salt (from /HER 07/)	141
Fig. 4.11	Geotechnical data of SVV compared to data of rock salt, uniaxial measurements (no confining pressure) and triaxial measurements (confining pressure between 1 and 10 MPa)	141
Fig. 4.12	Concept and instrumentation of a SVV seal of pure anhydrous MgSO ₄ flooded with tachyhydrite brine in a vertical borehole (about 6 m deep, 1 m in diameter) in the potash formation carnallite in the Asse mine	143
Fig. 4.13	Concept and instrumentation of a SVV seal of pure anhydrous MgSO ₄ flooded with tachyhydrite brine in a horizontal borehole (1.2 m in diameter, 7.2 m length) in the potash formation tachyhydrite in the mine Teutschenthal	144
Fig. 4.14	Development of brine pressures during the flooding of the SVV element in a vertical borehole in the Asse mine in October / November 2007	145
Fig. 4.15	Development of total pressure (brine pressure and crystallization pressure) at different locations in the SVV element in a vertical borehole in the Asse mine	147
Fig. 4.16	Development of crystallization pressures in the SVV element in a horizontal borehole in tachyhydrite potash rocks in the mine Teutschenthal after flooding with tachyhydrite brine and after the three subsequent injection tests	149
Fig. 4.17	Development of temperatures in the SVV element in a horizontal borehole in tachyhydrite potash rocks in the mine Teutschenthal after flooding with tachyhydrite brine and after subsequent injection tests	150

Fig. 4.18	Set-up of ITT and location of the psychrometric sensors IBX<number>; (A) from /GUO06/, (B) from /ÅKE08/.....	154
Fig. 4.19	Results from in-situ measurements and from model calculations for the ITT including interlayer diffusion; from /KRÖ 11/.....	155
Fig. 4.20	Sketch of the Canister Retrieval Test; from /KRI07/.....	157
Fig. 4.21	Location of the model domain (A) and dimensions (B) ; from /KRI07/....	158
Fig. 4.22	Measured and calculated relative humidity/suction for the CRT; from /KRÖ 11/.....	160
Fig. 4.23	Physical interaction in the CRT-model; from /KRÖ 11/.....	161
Fig. 4.24	Principle of the test set-up	163
Fig. 4.25	Evolution of the water content distribution in the tested bentonite specimen	164
Fig. 4.26	Position of the value of 0.25 in the water content distributions over time.....	165
Fig. 4.27	Accumulated water inflow	166
Fig. 4.28	Climate during the reference glacial cycle in Forsmark (Sweden) /SKB 10/	172
Fig. 4.29	Climate during the moderate global warming scenario in Forsmark (Sweden) /SKB 10/	173
Fig. 4.30	Climate of Olkiluoto up to 125,000 years after present for scenario A and B and up to 225,000 years after present for scenarios C, D, E /CED 04/.....	174
Fig. 4.31	Atmospheric CO ₂ concentration assumed in scenarios C, D and E /CED 04/.....	175
Fig. 4.32	Graph of the surface temperature with regard to the CO ₂ concentration /CED 04/.....	177
Fig. 4.33	Summary of future climate cases analyzed in the safety assessments SR-Site (top) and for Olkiluoto (bottom) /SKB 10/, /CED 04/.....	179
Fig. 4.34	Calculated permafrost thickness during Weichselian in Northern Germany /KLI 07/.....	181

Fig. 4.35	Schematic cross section of the hydrogeological system at the reference site Gorleben (modified from /KLI 02/)	183
Fig. 4.36	In the model assumed development of permafrost and groundwater flow velocity in two different climate cycles	185
Fig. 4.37	Geometry of the groundwater flow and transport model, vertical exaggeration: factor 10	187
Fig. 4.38	Flow field and isoline for $c_{rel} = 0.0375$ (TDS = 10 g L ⁻¹) during a period with 100 m permafrost (190,000 a model time)	190
Fig. 4.39	Relative salt concentrations and velocity field for the present state (11,500 a model time)	193
Fig. 4.40	Relative salt concentrations and velocity field after a sea water inundation for steady-state conditions at 600,000 a model time /FLU 09/	194
Fig. 4.41	Relative salt concentrations and velocity field after a sea water inundation of 15,000 a (31,500 a model time)	194
Fig. 4.42	Relative salt concentrations and velocity field after permafrost conditions for steady-state conditions at 600,000 a model time /FLU 09/	198
Fig. 4.43	Relative salt concentrations and velocity field at the end of the second cycle at 251,500 a model time	198
Fig. 4.44	Relative salt concentrations and velocity field in the middle of a period with 50 m permafrost thickness at 146,500 a model time	198
Fig. 4.45	Relative salt concentrations and velocity field at the end of a period with 150 m permafrost thickness at 240,500 a model time	198
Fig. 4.46	Logarithmic plot of the Cs-135 concentration distribution at 251,500 a model time /FLU 09/, based on the present state flow field	201
Fig. 4.47	Logarithmic plot of the C-14 concentration distribution at 251,500 a model time /FLU 09/, based on the present state flow field	201
Fig. 4.48	Logarithmic plot of the I-129 concentration distribution at 251,500 a model time /FLU 09/, based on the present state flow field	201
Fig. 4.49	Logarithmic plot of the U-238 concentration distribution at 251,500 a model time /FLU 09/, based on the present state flow field	201

Fig. 4.50	Logarithmic plot of the Cs-135 concentration distribution at 251,500 a model time /FLU 09/, based on the steady-state permafrost flow field ...	204
Fig. 4.51	Logarithmic plot of the C-14 concentration distribution at 251,500 a model time /FLU 09/, based on the steady-state permafrost flow field ...	204
Fig. 4.52	Logarithmic plot of the I-129 concentration distribution at 251,500 a model time /FLU 09/, based on the steady-state permafrost flow field ...	204
Fig. 4.53	Logarithmic plot of the U-238 concentration distribution at 251,500 a model time /FLU 09/, based on the steady-state permafrost flow field ...	204
Fig. 4.54	Logarithmic plot of the Cs-135 concentration distribution at the end of the second cycle at 251,500 a model time	207
Fig. 4.55	Logarithmic plot of the C-14 concentration distribution at the end of the second cycle at 251,500 a model time	207
Fig. 4.56	Logarithmic plot of the I-129 concentration distribution at the end of the second cycle at 251,500 a model time	207
Fig. 4.57	Logarithmic plot of the U-238 concentration distribution at the end of the second cycle at 251,500 a model time	207
Fig. 4.58	Selection of discrete reference climate regions.....	210
Fig. 4.59	Comparison of the contribution of food types on the ingestion BDCF of selected radionuclides for (A) the Magdeburg and (B) Rome reference climate region and sand soil	211
Fig. 4.60	Tornado chart for the sensitivity analysis of Tc-99 for sand soil and the A) Magdeburg and B) Rome reference climate region	214
Fig. 4.61	Conceptual model for estimating the radiation exposure to man in case of agricultural use of dry lake sediment.....	216
Fig. 4.62	influence of transition time on the behaviour of activity concentration of Se-79 (top) and Tc-99 (bottom) in pasture grass under full irrigation condition	217
Fig. 4.63	BDCF calculated for the time before (Temperate), during (Transition), and after transition (Mediterranean).....	219
Fig. 4.64	Location of all investigation boreholes at Ruprechtov site	221
Fig. 4.65	Evolution of groundwater levels in the boreholes between the years 2005 and 2012.....	223

Fig. 4.66	Comparison of uranium concentrations (in mg/L) in groundwater in monitoring wells before mining (1999 – 2005) and after mining (2009 – 2012) at Ruprechtov locality	223
Fig. 4.67	(A) Eh/pH diagram with the new boreholes NAR2, NAR3 and NAR4 (green dots). (B) Measured Eh-values compared to potential redox pairs.....	225
Fig. 4.68	Saturation indices of various U(IV) minerals calculated for groundwater from old and new boreholes.....	226
Fig. 4.69	Manual drilling of material from a clay/lignite layer exposed to the surface (A). Uranium content analyzed by ICP-MS (B) and α -spectrometry (C) in the sub-samples of the open pit from core OC-A	227
Fig. 4.70	Activity ratios $^{234}\text{U}/^{238}\text{U}$ against $^{230}\text{Th}/^{238}\text{U}$ measured for individual samples	228
Fig. 4.71	$^{234}\text{U}/^{238}\text{U}$ activity ratios in leachates from sequential extraction in different sections of the outcrop core (A) and in leachates as well as in U(IV)/U(VI) separation fractions of an undisturbed clay/lignite sample from borehole NA13 (B).....	229
Fig. 4.72	(A) Grains of anhydrite (medium bright) intensively transformed into gypsum (dark), OC2-2; (B) systematically organised grains of pyrite with grey rim enriched by As (up to 5 wt.%), OC3-4.....	229
Fig. 4.73	Schematic geological cross section of Ruprechtov investigation area with main geological units	230
Fig. 4.74	Aerial view of Ruprechtov site during first years of NA investigations.....	232
Fig. 4.75	Space view of Ruprechtov site after beginning of kaolin open pit mining	232
Fig. 4.76	Detailed geological map of Ruprechtov site based on geological mapping 1:10 000. In the lower right Velký rybník pond is located	233
Fig. 4.77	Central outcrop of kaolin open pit at Ruprechtov site showing inclined sediments of do-called hanging strata including coal lens on top of kaolin (right edge of the photograph)	234
Fig. 4.78	Marginal outcrop of kaolin open pit at Ruprechtov site close to NAR3 borehole	234

Fig. 4.79	Coal seam in the upper level of open pit's outcrop at Ruprechtov site; results of gamma measurements as well as position of sampling is indicated	235
Fig. 4.80	Isolated coal lens as well as coal seam with different gamma radiation.....	235
Fig. 4.81	Outcrop in kaolin part of the Ruprechtov open pit	236
Fig. 4.82	NAR3 drill hole after progress of mining activities in this area	237
Fig. 4.83	Position of installed suction cups along the eastern margin of Ruprechtov open pit – in the background the ore mountains	238
Fig. 4.84	Position of installed suction cup 2 the cartridge is digged in at app. 100 cm depth.....	239
Fig. 4.85	Presentation of a salt dome imported from the openGEO software.....	242
Fig. 4.86	View into the geological structures of a salt dome. Different geological strata are displayed in different colours. The mine layout can be seen in the background	243
Fig. 4.87	Section through a geological model imported from openGEO.....	243
Fig. 4.88	Visualisation of the temperature distribution in and around two disposal drifts containing waste containers with disposed spent fuel	244
Fig. 4.89	Temperature distribution visualised in form of iso-surfaces.....	245
Fig. 4.90	Temperature distribution displayed in two orthogonal arranged cuts.....	245

List of tables

Tab. 2.1	Countries and organisations represented in MeSA	7
Tab. 2.2	Primary and secondary purposes for indicators	25
Tab. 2.3	Transport lengths [m] in the repository system and EMOS module applied for calculation	51
Tab. 2.4	BSK container data.....	52
Tab. 2.5	Mobilisation rates for different fuel components	53
Tab. 2.6	Relative inventory in the different fuel fractions.....	53
Tab. 2.7	Solubility limits in [mol/l], “high” denotes no solubility limit.....	53
Tab. 2.8	Sorption values [m ³ /kg] for the bentonite.....	54
Tab. 2.9	Sorption values [m ³ /kg] for the clay formations	54
Tab. 2.10	Transport parameters in the overburden.....	55
Tab. 2.11	Sorption values in [m ³ /kg] for the overburden.....	55
Tab. 2.12	Dose conversion factors and decay energies.....	56
Tab. 2.13	Inventory data years after end of operational phase and the released quantities after 10 ⁶ years	58
Tab. 2.14	Radionuclide inventory /BUH 08b/	67
Tab. 2.15	General data for the modelling of the repository	68
Tab. 2.16	Solubility limits in the emplacement areas [mol/m ³].....	68
Tab. 2.17	Inventory data after end of operational phase and released quantities after 10 ⁶ years	70
Tab. 3.1	Listing of Joint Activities /IGD 11/.....	112
Tab. 4.1	Research agenda for future work aimed at estimating effects of microbial activity on long-term performance of radioactive waste repositories in clays	121
Tab. 4.2	Composition of the solutions in SVV experiments.....	138
Tab. 4.3	Crystallization pressures from measurements in pressure cells of different sizes with pure MgSO ₄ and three brines at different solid-fluid ratios.....	140

Tab. 4.4	Climate during the first 120,000 years a.p. with regard of a moderate CO ₂ -concentration during the first 50,000 years.....	182
Tab. 4.5	Climate after the first 120,000 years a.p. with regard to the Weichselian ice age concerning /KLI 07/	182
Tab. 4.6	Model-Parameter	185
Tab. 4.7	Half-lives (HL) /MAG 06/ and K _d values /SUT 98/ of the considered radionuclides	190
Tab. 4.8	Matrix for the assignment of the K _d -values for the transport calculations in the two studies, derived from the flow fields and salt concentrations of the flow calculations (Fig. 4.38).....	191
Tab. 4.9	Köppen/Geiger climate classification and climate data for the reference climate regions	210
Tab. 4.10	BDCF for reference regions for the “Well” scenario and organic soil. The BDCF are in Sv/a per 1 Bq/l in near surface ground water.....	213
Tab. 4.11	Specific groundwater data for selected boreholes.....	224
Tab. 4.12	Summary of results from soil waters measurement.....	240

**Gesellschaft für Anlagen-
und Reaktorsicherheit
(GRS) mbH**

Schwertnergasse 1
50667 Köln

Telefon +49 221 2068-0

Telefax +49 221 2068-888

Forschungszentrum

85748 Garching b. München

Telefon +49 89 32004-0

Telefax +49 89 32004-300

Kurfürstendamm 200

10719 Berlin

Telefon +49 30 88589-0

Telefax +49 30 88589-111

Theodor-Heuss-Straße 4

38122 Braunschweig

Telefon +49 531 8012-0

Telefax +49 531 8012-200

www.grs.de